Hypertension-induced inflammation: from cellular mechanisms to disease

Danielle Lisa Michell

BSc, MSc

Vascular Pharmacology Laboratory,
Baker IDI Heart and Diabetes Institute
&
Department of Medicine (Alfred Hospital),
Central Clinical School, Monash University

January 2014

Submitted in total fulfilment of the requirements of the degree of
Doctor of Philosophy

"Your work is going to fill a large part of your life, and the only way to be truly satisfied is to do what you believe is great work. And the only way to do great work is to love what you do."

- Steve Jobs

TABLE OF CONTENTS

CHAPTER 1

CHAPTER 2

CHAPTER 3

CHAPTER 4

CHAPTER 5

CHAPTER 6

DEVELOPMENT OF A HYPERTENSIVE ATHEROSCLEROTIC MOUSE MODEL: HYPERTENSION PROVOKES PLAQUE INSTABILITY 143

CHAPTER 7

CHAPTER 8

CHAPTER 9

Summary

The work presented in this thesis focused on high intraluminal pressure and its role in vascular inflammation. This was done in the context of hypertension and its contribution to the progression of atherosclerosis, the major underlying pathology in coronary artery disease. While a large body of work have explored the role of immune cells in the pathogenesis of hypertension, very few studies have investigated the opposite; whether hypertension plays a role in the aetiology of inflammation.

Studies which have previously attempted to investigate the effect of high blood pressure and inflammation have been thwarted by the difficulty of trying to separate the consequences of the various neurohumoral factors associated with hypertension compared to those induced by the increase in pressure itself. This is particularly true of *in vivo* protocols. To address this, we developed a customised *ex vivo* vessel chamber that enabled the recording of leukocyte adhesion to the endothelium in real time, in intact vessels under various pressures. Using this technique, vessels exposed to high intraluminal pressure demonstrated greater leukocyte adhesion, adhesion molecule gene expression and endothelial microparticle production. Interestingly, we found this to be independent of the renin-angiotensin system. Several mechanisms involved in this process are presented in Chapters 4 & 5.

In Chapter 4, the production of reactive oxygen species (ROS), endothelial nitric oxide synthase (eNOS), arginase, and the transcription factor, nuclear factor κB (NFκB), all known to be implicated in both hypertension and vascular inflammation, were explored as possible mechanisms. High intraluminal pressure was shown to increase ROS production, arginase II expression and activity as well as NFκB expression, while eNOS was unaltered by acute increases in pressure. Furthermore, functional studies indicated a possible role for NADPH oxidase and the mitochondria as the sources of the ROS mediating response.

To tease out the mechanical forces responsible for the pressure-induced response, in Chapter 5, we observed the effect of different shear rates on leukocyte adhesion in pressurised vessels. High intraluminal pressure (circumferential stretch) together with low shear stress produced the greatest response, while high stress reduced the effect of high

pressure. Caveolae, membrane invaginations that have been shown to mediate many intracellular signalling pathways, were explored as possible mechanosensors involved in pressure-induced inflammatory response. *Cav1*$^{-/-}$ (Caveolin-1) mice and Cav1 KD cells had reduced leukocyte adhesion and adhesion molecule gene expression in response to TNFα stimulation. These results suggest caveolae play an important role in the inflammatory response. Furthermore, when the effect of pressure on caveolae structure was further explored, we showed, for the first time, that high intraluminal pressure reduced caveolae number. We speculate this may be due to the dissociation of the caveolae proteins Cav1 and cavin-1.

In Chapter 6, we examined the effect of hypertension on atherosclerosis in an *in vivo* setting. Hypertensive atherosclerotic prone BPHx*Apoe*$^{-/-}$ placed on a high fat diet for 12 weeks demonstrated no change in plaque size. However, detrimental changes in plaque morphology with increased lipid and macrophage content and reduced collagen were observed suggestive of reduced plaque stability. We also demonstrated that blockade of P-selectin, which mediates recruitment of leukocytes to the endothelium, partially improved this stability.

In conclusion, the studies described in this thesis provide evidence that high intraluminal pressure induces vascular inflammation. We demonstrated that the mechanical forces exerted by high pressure promote caveolae flattening, NADPH oxidase dependent ROS production, arginase II activation and NFκB translocation, which all contribute to endothelial activation, adhesion molecule expression and enhanced leukocyte adhesion, all hallmarks of inflammation. We also showed *in vivo* that hypertension may result in atherosclerotic plaque instability, which may be partially improved by blocking leukocyte recruitment. Therefore, this thesis has established fundamental concepts on how high intraluminal pressure can alter cellular biological responses that may lead to new paradigms in the management of the increased risk of cardiovascular complications seen in hypertensive individuals.

General Declaration/Copyright

Declaration for thesis based or partially based on conjointly published or unpublished work

In accordance with Monash University Doctorate Regulation 17.2 Doctor of Philosophy and Research Master's regulations the following declarations are made:

I hereby declare that this thesis contains no material which has been accepted for the award of any other degree or diploma at any university or equivalent institution and that, to the best of my knowledge and belief, this thesis contains no material previously published or written by another person, except where due reference is made in the text of the thesis.

This thesis includes 2 original papers published in peer-reviewed journals and 3 unpublished publications. The core theme of the thesis is the role of hypertension in cardiovascular disease. The ideas, development and writing up of all the papers in the thesis were the principal responsibility of myself, the candidate, working within the Baker IDI Heart and Diabetes Institute under the supervision of Professor Jaye Chin-Dusting and Dr Karen Andrews.

The inclusion of co-authors reflects the fact that the work came from active collaboration between researchers and acknowledges input into team-based research.

In the case of Chapter 3 my contribution to the work involved the following:
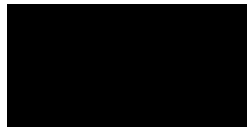
Thesis chapter	Publication title	Publication status*	Nature and extent of candidate's contribution
3	Imaging leukocyte adhesion to the vascular endothelium at high intraluminal pressure	Published	80%

I have renumbered sections of submitted or published papers in order to generate a consistent presentation within the thesis.

Under the Copyright Act 1968, this thesis must be used only under the normal conditions of scholarly fair dealing. In particular no results or conclusions should be extracted from it, nor should it be copied or closely paraphrased in whole or in part without the written consent of the author. Proper written acknowledgement should be made for any assistance obtained from this thesis.

I certify that I have made all reasonable efforts to secure copyright permissions for third-party content included in this thesis and have not knowingly added copyright content to my work without the owner's permission.

Signed: ████████████

Date: 12/01/2014

Acknowledgements

The work that has culminated in this PhD would not have been possible without many key people that have helped me in many different ways.

Words cannot express my appreciation for the support, guidance, patience, and motivation that my supervisors **Professor Jaye Chin-Dusting** and **Dr Karen Andrews** have given me throughout this PhD. **Jaye**, thank you for taking me in all those years ago, I will be forever indebted to you for helping me realise my true passion. Your optimism, ability to see the greater picture and the sheer knack for making my writing and presentations sound exciting is something I will be forever striving for. **Karen**, I have been truly lucky to also have you as a supervisor. Thank you for all your encouragement, technical expertise, and for every little day-to-day thing that you do that has got me through this and made it an enjoyable experience.

My time spent during this PhD would not have been nearly as rewarding or motivating if it were not for the past and present lab members of the Vascular Pharmacology laboratory. A special thank you to **Mandy**, **Nat**, **Olivier** and **Shirley** for all your advice and input to the body of work described in this thesis. Thank you to **Mandy**, for being a fantastic colleague with whom I can bounce ideas off, have those Friday afternoon discussions with, and approach for all life and work advice. To **Jen**, **Nat** and **Ann-Maree**, I don't think I will find an office as warm and caring as you guys have made it feel. Thanks for your conversations of work and life, your assistance in all those little things, the hugs when I needed them and the laughs that always followed. To **Murph**, thank you for being one of the first people to welcome me into the lab, you have been someone I can always turn to for advice, help and of course a place to stay! To **Andrea**, thank you for your friendship and all your help when you were in the lab. **Olivier**, thank you for teaching me about all things ROS and letting me use your cell chamber. Massive thanks must also go to **Murph**, **Mandy**, **Jen** and **Nat** for proof reading my chapters. To fellow students at the Baker IDI, **Dave**, **Sacha**, and many many more, suffice it to say life, as a PhD student, would not have been nearly as enjoyable if it were not for you guys.

Publications

Original Publications

- XL Moore, **D Michell**, S Lee, MR Skilton, R Nair, JB Dixon, AM Dart, J Chin-Dusting. Increased carotid intima-media thickness and reduced distensibility in human class III obesity: independent and differential influences of adiposity and blood pressure on the vasculature (2013). *Plos One* **8**:e53972

- S Khong, K Andrews, N Huynh, K Venardos, A Aprico, **D Michell**, M Zarei, K Moe, G Dusting, D Kaye, J Chin-Dusting (2012). Arginase II inhibition prevents nitrate tolerance. *British Journal of Pharmacology* **166**: 2015-23.

- **DL Michell**, KL Andrews, KJ Woollard, JPF Chin-Dusting (2011). Imaging leukocyte adhesion to the endothelium at high intraluminal pressure. *Journal of Visualized Experiments* **54**

Review

- **DL Michell**, KL Andrews, and JPF Chin-Dusting. Endothelial dysfunction in hypertension: The role of arginase (2011). *Frontiers in Bioscience (Scholars Edition)* **3**: 946-60.

Published Abstracts

- P Assemat, G Hannema, J Carberry, **D Michell**, K Andrews, A Dart, J Chin-Dusting, K Hourigan. Numerical and in vitro experimental study of arterial deformation and buckling under hypertension and atherosclerotic conditions. *Proceedings of the 18th Australasian Fluid Mechanics Conference,* 3 December 2012 to 7 December 2012, Australasian Fluid Mechanics Society, Parkville VIC Australia, pp. 1-4

- **D Michell**, KL Andrews, O Huet, KJ Woollard, XL Moore, JPF Chin-Dusting (2012). High intraluminal pressure induces vascular inflammation. *Hypertension* **60**: 491-491

- **D Michell**, K Andrews, XL Moore, O Huet, K Woollard, J Chin-Dusting (2011). Increases in pressure induces leukocyte adhesion in the endothelium. *Hypertension* **58:** 114-132

- JPF Chin-Dusting, **D Michell**, MR Skilton, J Dixon, A Dart, XL Moore (2010). Endothelial progenitor cells and carotid intima-media thickness in the morbidly obese. *Cardiovascular Research* **87**: S58-S58

- **D Michell**, XL Moore, M Skilton, R Nair, P Hadi, E Harris, J Dixon, A Dart, J Chin-Dusting (2010). Endothelial progenitor cells and the carotid intima-media thickness in severe obesity. *Hypertension*. **55**: 1504-05

- XL Moore, M Skilton, R Nair, P Hadi, E Harris, **D Michell**, J Dixon, A Dart, J Chin-Dusting (2009). Endothelial progenitor cells in obesity and weight loss. *Annals of Nutrition and Metabolism* **55**: 145-145

- XL Moore, **D Michell**, M Skilton, R Nair, P Hadi, E Harris, J Dixon, A Dart, J Chin-Dusting (2009). Endothelial Progenitor Cells are Up-regulated in the Severely Obese. *Circulation* 120:S492.

Abbreviations

α	Alpha		EMP	Endothelial microparticle production
ACE	Angiotensin converting enzyme		eNOS	Endothelial nitric oxide synthase
ADMA	Aymmetic dimethylarginine		FAD	Flavin adenine dinucleotide
Ang	Angiotensin		FBS	Foetal bovine serum
ANOVA	Analysis of variance		FMN	Flavin mononucleotide
$Apoe^{-/-}$	Apolipoprotein E knockout		FSG	Fish skin gelatin
ARB	Angiotensin receptor blocker		H_2SO_4	Sulfuric acid
AT1R	Angiotensin II type 1 receptor		H_3PO_4	Phosphoric acid
			H5V Cav1 KD	H5V cells with shRNA to caveolin-1
AT2R	Angiotensin II type 2 receptor		H5V Scr	H5V cells with scrambled control shRNA
β	Beta			
BEC	S-(2-boronoethyl)-L-cysteine		HDL	High density lipoprotein
BH_4	Tetrahydrobiopterin		HFD	High fat rodent diet
BSA	Bovine serum albumin		HR	Heart rate
Ca^{2+}	Calcium		hr	Hour
$CaCl_2$	Calcium chloride		HSS	High shear stress
CAD	Coronary artery disease		HUVEC	Human umbilical vein endothelial cells
Cav	Caveolin			
$Cav1^{-/-}$	Caveolin-1 knockout		i.p.	Intraperitoneal injection
Cl^-	Chloride		ICAM	Intracellular adhesion molecule
CO_2	Carbon dioxide			
CSF	Colony stimulating factor		IFN	Interferon
CVD	Cardiovascular disease		IL^-	Interleukins
DAPI	4',6-diamidino-2-phenylindole		iNOS	Inducible nitric oxide synthase
DASH	Dietary approaches to stop hypertension		JAM	Junctional adhesion molecule
DCFH	2,7-dichlorofluorescein		κ	Kappa
DNA	Deoxyribonucleic acid		K^+	Potassium
dNTP	Deoxyribonucleotide triphosphate		KCl	Potassium chloride
			KH_2PO_4	Monopotassium phosphate
DOCA	Deoxycorticosterone		LDL	Low-density lipoprotein
EDTA	Ethylenediaminetetraacetic acid		$Ldlr^{-/-}$	Low-density lipoprotein receptor knockout
EGTA	Ethylene glycol tetraacetic acid		LFA	Lymphocyte function-associated antigen
ELISA	Enzyme-linked immunosorbent assay		LPS	Lipopolysaccharides
			LSS	Low shear stress

μ	Micro	PBS	Phosphate buffered saline
M	Molar	PCR	Polymerase chain reaction
m	Milli	PF6-AM	Peroxyfluor-6 acetoxymethyl ester
m^2	Metre squared		
MAC	Macrophage antigen	PLA	Proximity ligation assay
MAP	Mean arterial blood pressure	PTRF	Polymerase I and transcript release factor
MβCD	Methyl-B-cylcodextrin		
MCP	Monocyte chemoattractant protein	RAS	Renin-angiotensin system
		RCA	Rat carotid arteries
$MgSO_4$	Magnesium sulphate	RNA	Ribonucleic acid
mon:dim	Monomer:dimer	ROS	Reactive oxygen species
Na^+	Sodium	RPM	Revolutions per minute
Na_4PO_7	Sodium Pyrophosphate	SEM	Standard error of the mean
NaCl	Sodium chloride	SNS	Sympathetic nervous system
NADPH	Nicotinamide adenine dinucleotide phosphate	SRs	Scavenger receptors
		TBS	Tris buffered saline
$NaHCO_3$	Sodium hydrogen carbonate	TBST	Tris buffered saline + 0.1% tween20
NFκB	Nuclear factor kB		
ng	Nanogram	TGF	Transforming growth factor
NGS	Normal goat serum	Th	T helper cell
NHA	N^G-hydroxy-$_L$-arginine	THP-1	Human monocytic cell line
nNOS	Neuronal nitric oxide synthase	TNF	Tumor necrosis factor
		VCAM	Vascular cell-adhesion molecule
NO	Nitric oxide		
NOS	Nitric oxide synthase	VEGF	Vascular endothelial growth factor
Nox	nicotinamide adenine dinucleotide phosphate oxidase		
		VLA	Very late antigen
		vWF	von Willebrand Factor
O_2	Oxygen	WPBs	Weibel palade bodies
OSS	Oscillatory shear stress		

Chapter 1

General introduction

Declaration for Chapter 1

Declaration by candidate

In the case of Chapter 1, the nature and extent of my contribution to the work was the following:

Nature of contribution	Extent of contribution (%)
Drafted and prepared the manuscript	90%

The following co-authors contributed to the work. If co-authors are students at Monash University, the extent of their contribution in percentage terms must be stated:

Name	Nature of contribution	Extent of contribution (%) for student co-authors only
Karen Andrews	Provided intellectual input and editing of manuscript	N/A
Jaye Chin-Dusting	Provided intellectual input and editing of manuscript	N/A

The undersigned hereby certify that the above declaration correctly reflects the nature and extent of the candidate's and co-authors' contributions to this work*.

Candidate's Signature	████	**Date** 12/01/2014

Main Supervisor's Signature		**Date**

*Note: Where the responsible author is not the candidate's main supervisor, the main supervisor should consult with the responsible author to agree on the respective contributions of the authors.

1.1 Coronary Artery Disease

Noncommunicable diseases such as cancers, diabetes, cardiovascular disease (CVD), digestive diseases and chronic respiratory diseases are the leading cause of death worldwide. Of these conditions CVD was the biggest killer, with 17.3 million deaths or 30% of all deaths in 2008 (Alwan, 2011). The prevalence and impact of this disease continues to grow. In those under the age of 70 years, CVD contributes to 39% of total deaths, a number that is even greater in lower-middle income countries where the rate of CVD associated deaths has doubled in the past few decades (Medls *et al.*, 2011). CVDs include ischaemic heart disease, cerebrovascular disease, inflammatory heart disease, hypertensive heart disease, cardiomyopathies, cardiac arrhythmias and rheumatic heart disease. Of these, coronary artery disease (CAD), underlies the most common cause of death worldwide, i.e. ischaemic heart disease.

Atherosclerosis, a complex inflammatory disease of blood vessels, is the underlying basis of CAD and many other CVDs. *Athero* is derived from the Greek language meaning 'porridge' or 'gruel' where *sclerosis* means 'hard', describing the lipid-laden section of the plaque and the collagen or fibrous dense sections, respectively. Clinically, the first manifestation of atherosclerosis is the 'fatty streak', which can start as early as childhood (Berenson *et al.*, 1998; Napoli *et al.*, 1999) or in foetal life as a result of maternal hypercholesterolaemia (Napoli *et al.*, 1997). Fatty streaks consist of lipids, inflammatory cells and vascular cells. As atherosclerosis progresses from a chronic asymptomatic disease, plaques can either occlude the blood vessel or rupture, resulting in thrombosis or a blood clot followed by ischaemia (Fig 1.1). If this process develops in the arteries of the heart it can lead to myocardial ischaemia or a heart attack, whereas if it forms in cerebral blood vessels it can lead to a stroke.
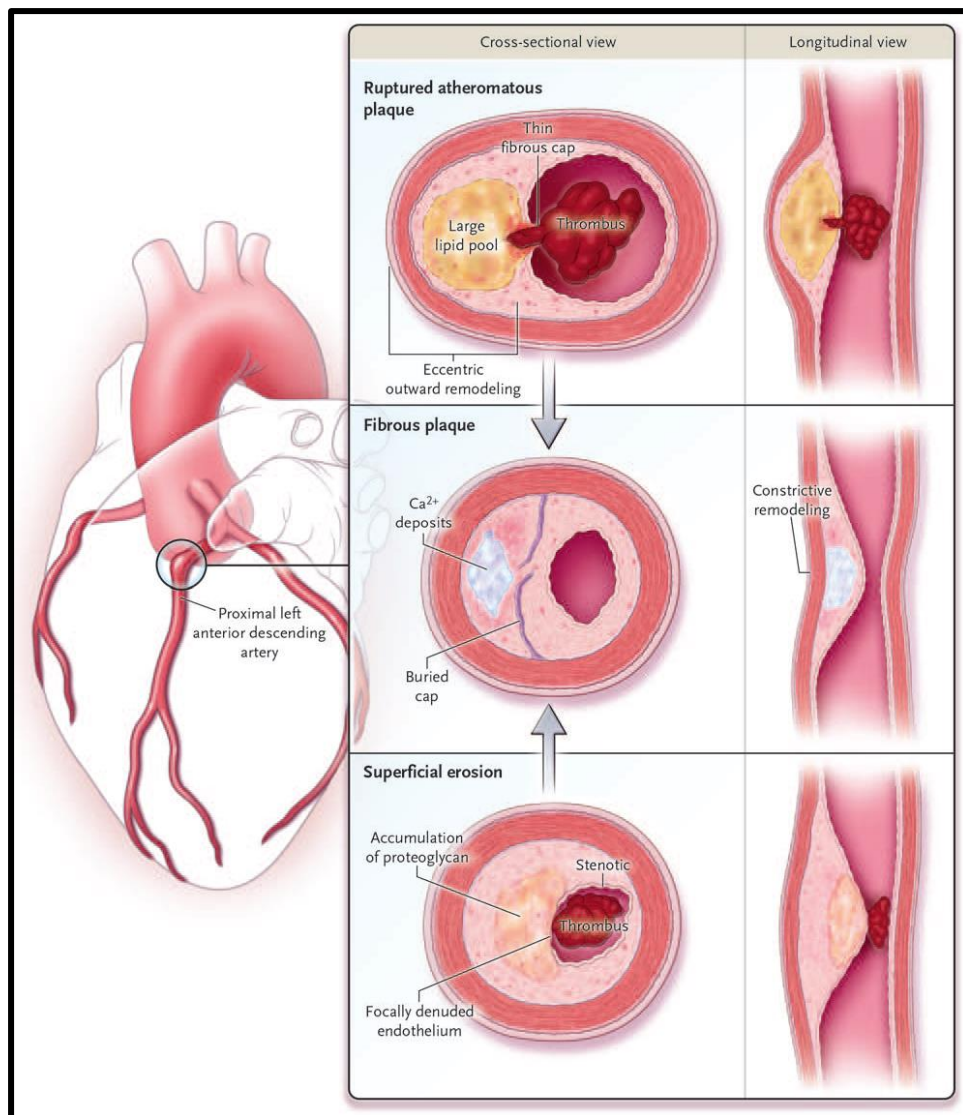
Figure 1.1   Atherosclerotic plaques associated with CAD (adapted from Libby, 2013).

Developing therapies to treat CAD and other CVDs relies heavily on identifying and understanding the risk factors associated. As atherosclerosis occurs in a large number of the population, many risk factors have been identified including behavioural, metabolic and social risk factors. Increased blood pressure or hypertension remains the largest contributing risk factor followed by tobacco, high blood glucose and physical inactivity (Fig 1.2).
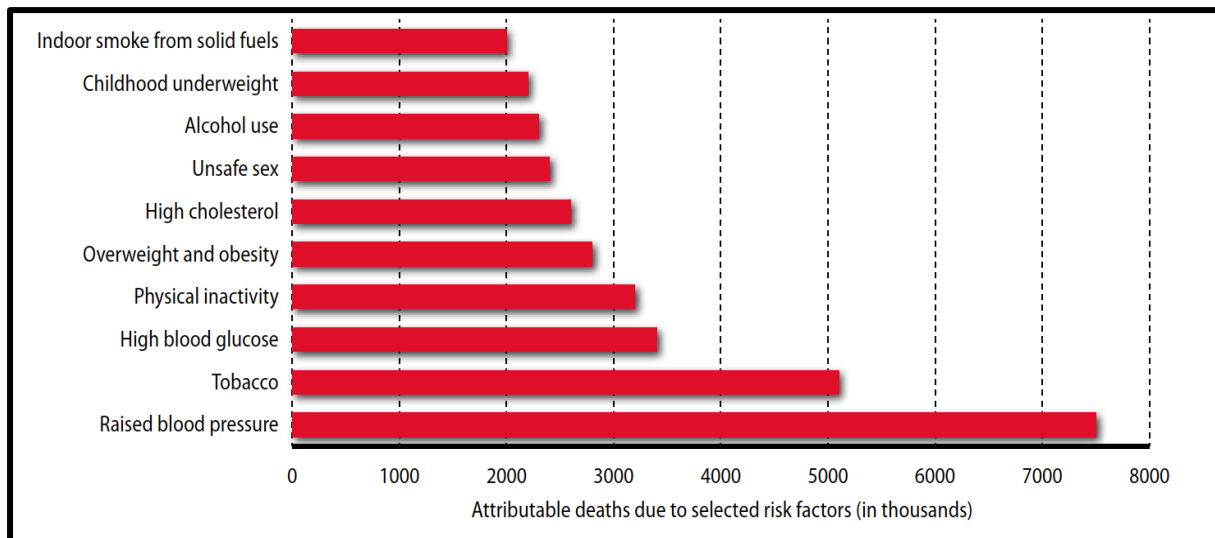
Fig 1.2 Selected risk factors attributable to cause of death (adapted from Medls *et al.*, 2011).

The progression of atherosclerosis to an unstable life threatening condition can take many years or even decades to develop. While the inflammatory progression of atherosclerosis to an unstable plaque is discussed later (Section 1.4.3), the clinical manifestations are reviewed here. Generally, when these life-threatening conditions transpire there is very little warning. Collectively termed acute coronary syndromes, these unstable plaques can clinically present as unstable angina, non-ST segment elevation myocardial infarction, ST elevation myocardial infarction, or a sudden cardiac arrest (Meier *et al.*, 2013a). Classic signs of acute coronary syndromes according to the National Heart Attack Alert Program (Cannon *et al.*, 2002) include chest pain, pressure, tightness or heaviness, shortness of breath, weakness, dizziness and loss of consciousness. If a heart attack is suspected, an electrocardiograph is taken and a non-ST segment elevation myocardial infarction versus an ST elevation myocardial infarction is determined based on the electrical impulses from the activity of the heart. An ST elevation myocardial infarction involves complete blockage of a coronary artery resulting in severe damage to the heart,

while a non-ST segment elevation myocardial infarction is only partial blockage of an artery and causes less damage. Unstable angina presents as a non-ST segment elevation myocardial infarction but does not result in permanent damage to the heart.

Blood assessment is also carried out to determine the presence of biomarkers. These include: cardiac troponin, a marker of myocardial damage; cystatin C, a marker of renal dysfunction; ischaemia modified albumin, a marker of myocardial ischaemia; B-type natriuretic peptide, a marker of left ventricular dysfunction; and C-reactive protein, a marker of inflammation (Lindahl, 2013). Further tests also include chest x-rays for determination of the presence of air or fluid in the lungs, echocardiograms to determine the location of damage on the heart and coronary angiographies to determine the site or sites of the vessel blockage. Interventions can include either coronary artery bypass grafts or percutaneous coronary intervention. As not all acute coronary syndrome patients present the same upon admission there are detailed practice guidelines in place to stratify the most urgent cases and reduce costs (Anderson *et al.*, 2011; Hamm *et al.*, 2011)

Percutaneous coronary intervention, also commonly known as coronary angioplasty, involves inserting a balloon via a catheter to inflate the occluded artery prior to placing a stent or wire mesh in an attempt to keep the artery open. As percutaneous coronary intervention is an invasive procedure, various anticoagulant therapies are administered to avoid clotting and to reduce the thrombus formed. Glycoprotein IIb/IIIa and thrombin inhibitors are commonly used as well as aspirin and the common $P2Y_{12}$ receptor blocker, clopidogrel (Meier *et al.*, 2013c). Due to these therapies as well as possible trauma from insertion of the stent, retroperitoneal hematomas can be a common complication during percutaneous coronary intervention. Various clinical management strategies to prevent bleeding including the use of the radial artery instead of the femoral, administration of bivalirudin, fluoroscopy or ultrasound-guided puncture and vascular closure devices, have all been discussed widely and are often implemented (Meier *et al.*, 2013b). Coronary artery

bypass graft is another revascularisation method that involves the usage of arteries obtained elsewhere in the body to bypass the affected arteries.

Regardless of the success or otherwise of these interventions, prevention by lowering modifiable risk factors such as hypertension, cholesterol, alcohol and tobacco use are key in reducing the occurrence of vascular inflammation, atherosclerosis, and ultimately CAD.

1.2 Hypertension*

Hypertension is defined as persistently elevated systolic blood pressure over 140 mmHg and diastolic blood pressure over 90 mmHg. Worldwide, the prevalence of elevated blood pressure is estimated to be in ~23% of the adult population and by 2025 this global burden is predicted to increase to 29% (Kearney *et al.*, 2005). With age and obesity identified as two major risk factors for hypertension, it will continue to be an even greater risk as the longevity and weight gain of populations increase. Other risk factors include genetic and environmental-related maladies involving the central nervous system, cardiac, renal, gastrointestinal and endocrine factors. With its strong association with inheritability, genome-wide association studies have been conducted to assess the role of genetics and several single-nucleotide polymorphisms, and various genes have found to be associated with an increased systolic blood pressure (chromosomes 10, 11, 12), diastolic blood pressure (chromosomes 10, 12, 15) as well as hypertension (chromosome 12) (Levy *et al.*, 2009).

Co-morbidities such as diabetes mellitus, dyslipidaemia, coronary heart disease, and hypercholesterolaemia all correlate with increases in blood pressure. Other factors such as stress and increased sympathetic nervous system activity stimulate the cardiovascular and renal systems to increase heart rate, cardiac output, insulin resistance, platelet activation, sodium retention, and augment vascular reactivity and vascular function leading to elevations in blood pressure and the progression of atherosclerosis.

Hypertension involves increased peripheral resistance to blood flow particularly in small resistance arteries. In these arteries vascular remodelling can occur and changes in structural, functional and mechanical mechanisms can lead to reduced lumen diameter and

---

* Adapted from Michell *et al.*, 2011a

increased intimal thickening. This hypertrophic phenotype, coupled with altered myogenic tone, results in cardiovascular complications and damaging effects to target organs. Therefore it is not surprising that hypertension is the single biggest risk factor for the incidence, development and progression of coronary heart disease, stroke, chronic heart failure and chronic kidney disease (Levy *et al.*, 1996; Lopez *et al.*, 2006). Furthermore, with each 10 mmHg increment in blood pressure, the risk for developing a cardiovascular event increases (Van den Hoogen *et al.*, 2000).

Several lifestyle and drug treatments provide excellent therapy in the management of hypertension. Lifestyle recommendations include physical exercise, healthy body weight, and reduced alcohol consumption. In DASH study (Dietary Approaches to Stop Hypertension) (Appel *et al.*, 1997) dietary recommendations involving reducing sodium intake and increasing grains, vegetables, fruits and nuts, have all been found to lower blood pressure. In obese patients on the DASH diet, blood pressure was lower compared to those taking potassium, magnesium and fibre supplements (Al-Solaiman *et al.*, 2010). First-line pharmaceutical treatments include thiazide diuretics, beta-blockers, ACE (angiotensin converting enzyme) inhibitors, long-acting calcium channel blockers, or angiotensin receptor blockers (ARB) (Khan *et al.*, 2009). Ideally, these drugs are used individually but when optimal blood pressure levels are not reached these agents are used concomitantly. While no one class of antihypertensive treatment appears superior in reducing the risk of CVD (Kono *et al.*, 2005), some agents are more suitable in certain cardiovascular complications. For example, ACE inhibitors and ARBs are recommended in chronic renal disease to control hypertension (Chobanian, 2009).

Despite many effective antihypertensive agents and the recent development of vaccines (particularly targeting the renin-angiotensin aldosterone system) (Do *et al.*, 2010), uncontrolled blood pressure and its severe effects remain an ongoing issue. Furthermore, while some antihypertensive treatments are effective in lowering blood pressure they may

not be sufficient in helping target the vascular dysfunction or remodelling (Bravo *et al.*, 2001). Therefore targeting another aspect in the progression of hypertension may help to reduce cardiovascular morbidity, particularly for patients that are difficult to treat with current antihypertensive treatments.

1.3 Inflammation

The deleterious effects of inflammation have been known since the ancient Greeks, with the definitions from the Latin terminology still used today. Upon injury or infection inflammation is associated with four characteristic ailments, including *rubor* or redness due to increased vasodilatation and local blood flow to the affected site, *calor* or heat, *dolor* or pain due to increased inflammatory factors that stimulate peripheral nerve fibres, and *tumor* that involves swelling from tissue oedema.

1.3.1 Phagocytosis

While the symptomatic properties of inflammation have been known for over a millennia the cellular processes involved first came to light in the early 1800s. Today, we know the inflammatory response to be an essential physiological response by the body to defend against injury or infection. The body houses an immune system that involves various organs and cells to combat and repair the site of damage. White blood cells known as phagocytes are the body's first line of defence. Originally observed and described by Metchnikoff in 1883 (Chernyak & Tauber, 1988), phagocytes engulf or internalise and consequently destroy unfavourable products such as bacteria, parasites, harmful molecules or cellular debris via a common process known as phagocytosis. Once thought of simply as ingestion, phagocytosis actually involves complex signalling pathways for the production, mobilisation, degranulation, consumption and destruction of foreign material.

Polymorphonuclear leukocytes or neutrophils, blood monocytes and tissue macrophages or histocytes are known as the 'professional phagocytes' (Stossel, 1974). Neutrophils, derived from the bone marrow, are the first to respond. They undergo maturation where they are then released into the blood stream and survive for about 10

hours (Tofts *et al.*, 2011). These cells mobilise to the site of injury by the trigger of various receptors to secretagogues such as chemotactic cytokines and lipopolysaccharides (LPS). Cytokines play a key role in inflammation and immune responses and include released factors that can be categorised into interleukins (IL-), tumor necrosis factor (TNF), interferon (IFN), colony stimulating factor (CSF), transforming growth factor (TGF), and chemokines. Various cell types such as leukocytes, endothelial cells and smooth muscle cells all release and react to cytokines making them an essential component in haemostasis.

Neutrophils then dock at the pathogen, and when they start engulfing they release various microbacteriacidal granules that aid in destruction. Some of these granules contain myeloperoxidase as well as Nox (nicotinamide adenine dinucleotide phosphate (NADPH) oxidase), which consequently generate a respiratory burst leading to superoxide, hydrogen peroxide and hypochlorous acid production. While there are many other granules it is thought that reactive oxygen species (ROS) and hypochlorous acid are the key molecules involved in this destruction (Reeves *et al.*, 2003). Another function of neutrophil degranulation is to signal to other phagocytes by releasing factors such as IL-8, TNFα and leukotriene B4 (Ramos *et al.*, 2005; Silva, 2010).

Unlike neutrophils, monocytes survive much longer and have proliferative and differentiation capabilities by which they develop into macrophages that can form even larger phagocytes by fusion. Due to their increased size macrophages can combat much larger areas by releasing an even greater amount of cytokines. While they do act a lot slower than neutrophils, they persist for longer and also release proteases involved in tissue remodelling (Chapman *et al.*, 1994). These are some of the features that make mononuclear phagocytes ideal in chronic infections such as tuberculosis, but also a hindrance in pathological conditions by perpetuating chronic inflammatory responses such as atherosclerosis. This is discussed later (Section 1.4).

1.3.2 Innate Immunity

The pathways discussed above generally come under the broader immune response known as *innate immunity*, which is distinguished from *acquired or antigen-specific immunity*, in that previous exposure to the invader is not required. Innate or 'ready-made' immunity is a rapid response that doesn't require the generation of antibodies, but instead relies on receptors that recognise certain morphological characteristics of pathogens. Scavenger receptors (SRs) and toll-like receptors are the two main receptors in innate immunity and are also known as germline-encoded pattern recognition receptors that enable specificity in cell recognition.

SRs are cell surface proteins found on macrophages, endothelial cells, and smooth muscle cells. Their ligand specificity allows them to take up foreign particles. The original and most classical example of SRs were first proposed in 1979 by Brown and Goldstein (Brown & Goldstein, 1979). They demonstrated that macrophages specifically engulfed modified low-density lipoproteins (LDL), such as oxidised LDL or acetylated LDL, but not native LDL, a key process in atherosclerotic plaque development. SRs also aid toll-like receptors, which are transmembrane proteins with ectodomains that mediate recognition of foreign pathogens and intracellular domains that are involved in downstream signalling. Their downstream signalling is via the MyD88- or TRIF-dependent pathways that lead NFκB (nuclear factor κB) activation (Medzhitov, 2001; Carmody & Chen, 2007) and production of inflammatory cytokines, chemokines and Type I IFN. It also leads to the induction of genes CD40, 80 and 86 that signal the acquired immunity T cell immunogenic response.

The complement system is another key process in innate and acquired immunity. Complement proteins are produced by the liver, where they enter the bloodstream, and once activated, can help destroy pathogens. They either coat the pathogen by a process known as opsonisation (Greenberg & Grinstein, 2002), priming it for attack, or they can form

membrane attack complexes (Rus *et al.*, 2005) that effectively punch holes in the pathogen causing abnormal homeostasis and ultimately cell lysis.

1.3.3 Acquired Immunity

While innate immunity is the first, rapid line of defence it is also the more primitive with acquired or adaptive immunity demonstrating a much more complex, multifaceted process that aides in long-term survival. Where neutrophils, monocytes and macrophages are important players in innate immunity, lymphocytes are critical in acquired immunity. All blood cells originate from haematopoietic stem cells in the bone marrow. These cells then differentiate into various progenitor cells depending on their lineage; either common myeloid progenitor cells (erythrocytes, neutrophils, monocytes, macrophages etc.) or common lymphoid progenitors (natural killer cells, T cells, B cells). Once T lymphoid progenitors are formed they migrate to the thymus and develop into mature T cells, and when activated these differentiate into cytotoxic T cells (CD8+) and T helper cells (CD4+). Alternatively, B cells differentiate into either plasma cells (CD20-) or memory B cells (CD20+). The specificity of acquired immunity in combating pathogens is accredited to its ability to detect antigens and produce specific antibodies to those particular antigens. During innate immunity phagocytes break down pathogens and while most are killed some are used to develop epitopes or receptor binding sites specific to that antigen. Dendritic cells are the most efficient at this process (Thery & Amigorena, 2001). They migrate to the thymus and present the antigen via their major histocompatibility Class II receptors to the T cell receptors, activating the T cells causing proliferation and differentiation.

T helper (Th) cells propagate the immune response by promoting both the humoral (Th2 cells) and cellular responses (Th1). In the cellular response CD8+ cells are activated by the secretion of IL-2 from CD4+ cells and act on the pathogen by secreting perforin (Kägi *et*

al., 1994) and activating the Fas pathway (Rouvier *et al.*, 1993) that instigates cell death. Th2 cells work on the humoral response by presenting the antigen to B cells where they can also proliferate and differentiate into plasma cells. The plasma cells develop antibodies or immunoglobulins to aid in destruction of the pathogen via either neutralisation of the pathogen, assisting in opsonisation or activating the complement system. The B cells can also differentiate into memory cells so that when a second insult occurs it can be quickly resolved. More recently, Th17 cells have also been put forward as regulators of immune responses, which also release inflammatory cytokines (Langrish *et al.*, 2005; Korn *et al.*, 2007).

1.4 Atherosclerosis: An Inflammatory Disease

Dysregulation of the inflammatory response can lead to damaging results. These include the acute pathology septic shock, in which the innate immune response gets amplified and dysregulated. This leads to an excessive release of chemokines causing fever, tachycardia and increased nitric oxide (NO), in turn leading to vasodilatation and hypotension and ultimately multiple organ failure (Lolis & Bucala, 2003). Examples of dysfunction of the adaptive immune system include autoimmune diseases such as rheumatoid arthritis and systemic lupus erythematosis in which self-antigens are recognised as foreign. Conversely, atherosclerosis, a chronic inflammatory disease of the blood vessels, is thought to involve both innate and adaptive immunity.

Initiation of atherosclerosis begins with the immune system's recognition of LDL as a 'foreign body'. The main function of LDL as a lipoprotein is to transport cholesterol around the body. However, with excessive cholesterol in the bloodstream (hypercholesterolaemia) resulting from over consumption or hereditary factors (Hobbs *et al.*, 1987; Lye *et al.*, 2013), circulating LDL can migrate and accumulate under the endothelium and into the intima. It is here that atheroprone LDL molecules are retained by the binding of their apoprotein B100 site to the proteoglycans in the intima (Skålén *et al.*, 2002). Once trapped in the intima, LDL is oxidised by various enzymes such as myeloperoxidase and lipoxygenases or by hypochlorous acid. Advanced glycation end products are also known to trap LDL and are commonly formed in those with hyperglycaemia (Goh & Cooper, 2008).

1.4.1 Leukocyte adhesion cascade

It is widely accepted that once LDL is oxidised it becomes pro-inflammatory, toxic, and recognised as 'non-self'. These molecules and surrounding cells start to release factors

that signal damage has occurred and to also induce an inflammatory response. This results in mobilisation of cell adhesion molecules, selectins and chemoattractants to the endothelial surface in order to signal to leukocytes and start the process known as the leukocyte adhesion cascade (Figure 1.3). This recruitment process involves the adhesion or tethering, rolling, activation, and arresting of leukocytes on the endothelial membrane and their subsequent transmigration through the endothelium.
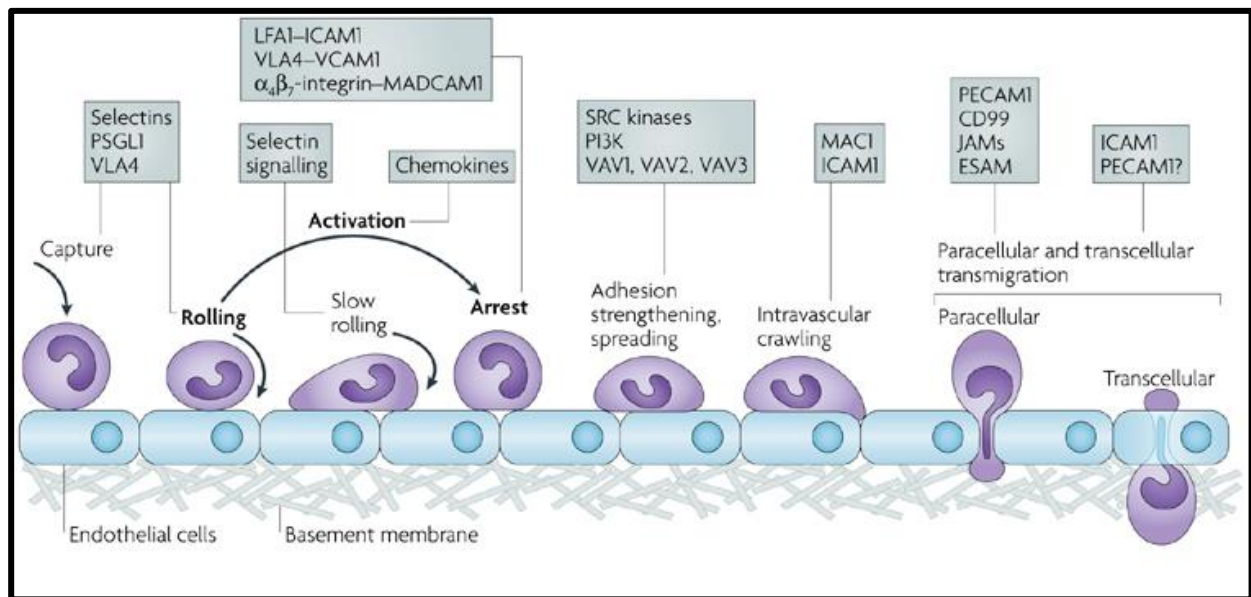
Figure 1.3. Leukocyte adhesion cascade. PSGL1: P-selectin glycoprotein ligand 1; VLA4: very late antigen 4; LFA1: lymphocyte function-associated antigen 1; ICAM1: intracellular adhesion molecule 1; VCAM1: vascular cell-adhesion molecule 1; MADCAM1: mucosal vascular addressin cell-adhesion molecule 1; PI3K: phosphoinositide 3-kinase; MAC1: macrophage antigen 1; PECAM1: platelet/endothelial-cell adhesion molecule; JAM: junctional adhesion molecule; ESAM: endothelial cell-selective adhesion molecule (adapted from Ley *et al.*, 2007).

The first phase, in which leukocytes start to slow down and roll along the vessel wall, is mediated by E-, L- and P-selectins binding to their carbohydrate ligands. Integrins found on monocytes and lymphocytes also bind to the cell adhesion molecules on the endothelium. During this time chemoattractants such as MCP-1 (monocyte chemoattractant protein - 1) and chemokines (CC, CXC, CX3C or C types) that bind particularly to G-protein coupled receptors (Kuang *et al.*, 1996; Aragay *et al.*, 1998) are presented on the endothelial cell surface. Rolling leukocytes sense these receptors and trigger the activation of integrins, which results in activation of the leukocytes (Ley *et al.*, 2007; Langer & Chavakis, 2009). The leukocytes then firmly adhere, or arrest, onto the endothelial membrane where they undergo a conformational change, spreading out due to ligand-induced post adhesion strengthening (Lefort *et al.*, 2009)

Following adhesion, macrophage-1 antigen and ICAM-1 (intracellular adhesion molecule) (Sumagin *et al.*, 2010) mediate the crawling along of leukocytes on the endothelial surface until they start to transmigrate through the endothelium, a process also known as diapedesis. Leukocytes can migrate via the paracellular or transcellular pathway. The paracellular pathway between endothelial cells requires vascular endothelial cadherins, adhesion molecules including platelet/endothelial cell adhesion molecule and integrins to assist in overcoming the adherens and tight junctions that bind the endothelial cells. The transcellular route occurs near the thinnest parts of the endothelial cell and involves migration through the cell via ICAM-1 coated caveolae that internalise and act as vesicles that form channels together with cytoskeletal proteins providing structural support (Carman & Springer, 2004; Dejana, 2006). Once through the endothelial barrier, the leukocytes then migrate via chemoattractants such as MCP-1 through o the basement membrane comprised of laminins and collagens and then into the intima.

1.4.2 Formation of a stable plaque

Once in the intima, monocytes differentiate into macrophages that rapidly engulf oxidised LDL via SR in an attempt to dispose of them. At the same time macrophages release chemokines and cytokines to dispose of other toxic molecules. However, when there are excessive levels of oxidised LDL the macrophages become lipid dense and are commonly referred to as foam cells. Foam cell accumulation forms a fatty streak, the beginning of atherosclerosis. In parallel with this process, dendritic cells and T cells also transmigrate to the infected area, resulting in the production of even more cytokines, chemokines, ROS, and matrix metalloproteinases. This in turn leads to an increased inflammatory response and lesion progression and plaque formation. Dendritic cells can act as antigen presenting cells, presenting the oxidised LDL fragments to the Th1 cells and activating the adaptive immune response which releases more pro-inflammatory factors. B cells and mast cells are also present in some atheroma but are generally localised on the adventitia just outside the lesion site (Figure 1.4). These cells aid in the recruitment of more inflammatory cells and the progression of the plaque.

Following macrophage and immune cell response smooth muscle cells, collagen, proteoglycans and elastin start to form under the endothelial layer, trapped in the atheroma under a fibrous cap (Lacolley *et al.*, 2012). It is here that the plaque is stable, and if contained, may be able to be cleared. Further inflammatory reactions can lead to advanced atherosclerosis with increased apoptosis of healthy cells, increased cholesterol and cholesterol crystals, and formation of a necrotic core with microvessels that feed the plaque keeping it thriving. During this time the plaque protrudes into the lumen and can slow down blood flow, creating a greater opportunity for immune cells to attach and further augment plaque size.
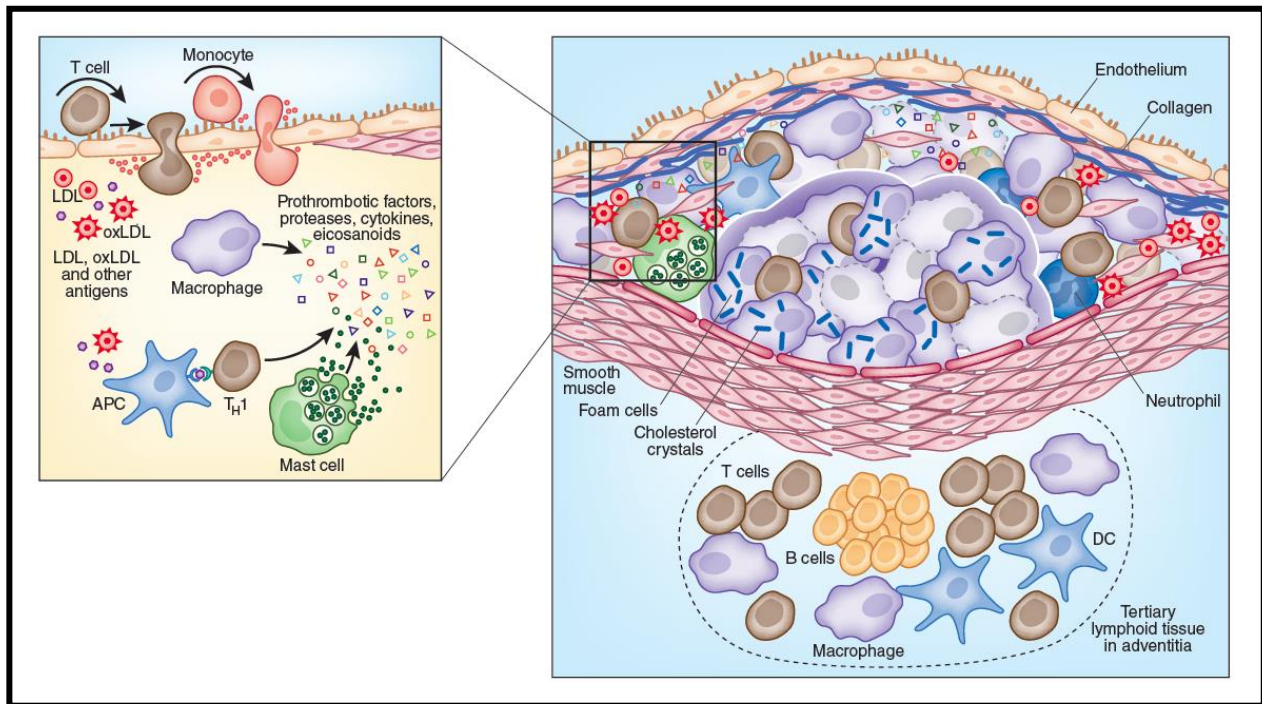
Figure 1.4. Pathology of a stable plaque (adapted from Hansson & Hermansson, 2011).

1.4.3 Progression to unstable plaque

Excessive plaque protrusion can obstruct blood flow causing infarction in downstream tissues and target end organ damage. Plaques can also become unstable due to a severe inflammatory response, leading to the destruction of the fibrous cap and overlying endothelial cells, and resulting in the recruitment of platelets to the area to initiate coagulation. The increase in platelet recruitment and fibrous cap rupture results in thrombus formation. If large enough, the thrombus can impede blood flow or dislodge into the blood stream where it can proceed to block flow to the heart (myocardial infarction), brain (stroke) or lungs (pulmonary embolism).

1.5 Endothelium – Contribution to Hypertension, Inflammation and Atherosclerosis†

Endothelial cells line the vasculature to form the endothelium, which acts as a semi-permeable monolayer between the lumen and the vessel wall. Endothelial cell structure and integrity are essential in maintaining vascular tone and haemostasis. Prenatally these cells originate from the same precursor as haematopoietic cells, the haemangioblast ($CD34^+$), which can differentiate into endothelial precursor cells ($VEGFR3^+$; vascular endothelial growth factor) to become vascular endothelial cells ($VEGF-R3^+$, $podoplanin^-$, $PAL-E^+$). Recent studies have shown that vasculogenesis also occurs postnatal with endothelial progenitor cells found to mobilize from the bone marrow (Asahara, 1997) and other sites in the body including the peripheral blood, liver (Aicher *et al.*, 2007), and adipose tissue (Miranville, 2004) to help repair and regenerate vessel walls in adults.

Despite the total mass of the endothelium only weighing between 100 – 500 g in humans the amount of surface area exposed to blood flow is thought to be highly active and up to 350 m^2 (Pries *et al.*, 2000). Through its paracrine, endocrine and autocrine functions the endothelium helps to regulate various cardiovascular processes. Blood wall exchanges occur through the abundant ion channels (K^+, Ca^{2+}, Na^+, Cl^-), G-proteins, caveolae and tyrosine kinase receptors in the plasma membrane lipid bilayer of the endothelium. Such exchanges include the release of vasomotor factors such as NO or prostacyclin that inhibit platelet aggregation and cause relaxation as well as the release of endothelium-derived hyperpolarizing factor, which elicits the activation of outward K^+ currents causing vascular smooth muscle cell hyperpolarization (McGuire *et al.*, 2001). These responses result from stimuli such as thrombin, bradykinin, adenosine diphosphate or changes in blood flow or

---

† Adapted from Michell *et al.*, 2011a

pressure. Conversely, vasoconstriction factors such as thromboxane A_2, endothelin-1, angiotensin II, prostaglandins, ROS, free radicals, pro-coagulant, pro-thrombotic factors and pro-inflammatory mediators are stimulated during disease states leading to impaired endothelium-derived vasodilatation or endothelial dysfunction.

1.5.1 Endothelium Function - Characteristics and measurements

Under physiological conditions, damage to the vasculature leads to several haemostatic processes signalled by the endothelium to reduce blood flow. These include vasoconstriction, formation of a haemostatic plug, initiation of the coagulation cascade, repair of the damaged site via endothelial progenitor cells, local endothelial cells and smooth muscle cells and finally fibrinolysis. However, pathological conditions such as hypertension, atherosclerosis, diabetes, and coronary heart disease are characterised by endothelial dysfunction, when the endothelium is unable to regulate these processes.

In their 1980 seminal paper, Furchgott and Zawadzki (1980) demonstrated that damage to the integrity of the endothelium led to impaired vasorelaxation following stimulation with acetylcholine, compared to vessels where the endothelium was preserved. They further demonstrated that the vasorelaxation observed was mediated by the release of an endothelium derived relaxing factor, later identified by Ignarro and colleagues as NO (1987). In 1998, Furchgott, Ignarro and Murad were all recognized with the Nobel Prize as having made substantial contributions towards the discovery of this gaseous molecule (SoRelle, 1998). Endothelial dysfunction is generally defined as impaired endothelium-dependent vasodilatation to specific stimuli and characterised by an imbalance between vasoconstriction and vasodilatation factors, predominantly NO. However, there is growing literature to support the notion that endothelial dysfunction is also involved in pro-inflammatory states, which will be discussed later. Endothelial dysfunction is regarded as

the initial and reversible step in the pathological process of CVDs such as hypertension and diabetes mellitus but is also thought to be essential in the progression of many infections and autoimmune diseases due to its angiogenic properties in the pathogenesis of certain cancers (Nikitenko, 2008).

The assessment of endothelial dysfunction can be based on a variety of biomarkers, including cellular markers, and gross vasoreactivity techniques. Serum concentrations of ICAM, VCAM (vascular cell adhesion molecule), E-selectin, P-selectin, as well as von Willebrand Factor (vWF) and microalbuminuria, have been used as biomarkers due to their expression on vascular endothelial cells during dysfunction and their consequent release into the bloodstream. Despite the current controversy in determining specific surface markers for endothelial progenitor cells, typically CD34+/KDR+/CD133+, a vast amount of literature demonstrate that these cells are found to inversely correlate with endothelial dysfunction in patients with CAD, diabetes and other CVD risk factors and co-morbidities. Increases in mature circulating endothelial cells, which are products of endothelial wall turnover and apoptosis during endothelial damage, are another cellular marker implicated in CVDs. Emerging evidence also suggests endothelial microparticles, which are continually shed blebbings of endothelial cells into the bloodstream, are elevated in CVD (Boulanger, 2006).

Non-invasive tests of endothelial function include flow-mediated dilatation of the brachial artery, which measures change in diameter of the brachial artery via an ultrasound, laser Doppler examination, pulse wave analysis, and pulse amplitude tonometry. More invasive techniques include venous occlusion plethysmography, which is used to assess change in forearm blood flow and arterial stiffness via infusion of various vasorelaxants into the brachial artery. Cardiac catheterization is the most invasive and expensive technique and it assesses changes in epicardial diameter and blood flow.

Despite the various techniques available it is still unclear whether endothelial dysfunction is a cause or a consequence of hypertension. In hypertensive animal models, rats fed on a fructose-rich diet were found to have impaired endothelial-mediated vasodilatation 10 days before the rats were shown to have increased blood pressure (Katakam *et al.*, 1998), a similar result is also seen in endothelial NOS (nitric oxide synthase; eNOS) knockout mice. However, many other models demonstrate chronic hypertension can lead to damaging effects on the endothelium (Kunes *et al.*, 2004; Torok, 2008).

Clinical studies also show confounding results; a study conducted by Rossi and colleagues (Rossi *et al.*, 2004) using 952 normotensive post-menopausal women demonstrated that each decrease in flow-mediated dilation predicted an increased risk in the development of hypertension during a 3.5 year follow-up even when adjusted for multiple factors. This finding suggests that impaired endothelial-mediated vasodilatation precedes future development of hypertension in this cohort. In a recent report from the Multi Ethnic Study of Atherosclerosis looking at flow-mediated dilatation and hypertension in 3500 participants the opposite finding over a 4.8 year follow-up was reported (Shimbo *et al.*, 2010). While at baseline, reduced flow-mediated dilatation correlated with increased prevalence in blood pressure, but this association was lost when results were adjusted for various factors such as age, sex, ethnicity, body mass index, cholesterol levels and other metabolic factors leading the authors suggest that endothelial dysfunction is a consequence, and not a cause, of hypertension.

1.5.2 Impaired NO

The most widely studied biological mechanism of endothelial dysfunction in hypertension is the decreased bioavailability of NO. NO is not only a potent vasodilator and essential in regulating vascular tone and blood pressure, but it also contributes to the

regulation of haemostasis and to platelet and leukocyte adhesion, as well as vascular smooth muscle cell proliferation. NO is a very small lipid soluble molecule with a half-life of just a few seconds before it is converted into nitrates and nitrites that are ultimately excreted. Within the body NO can act in many ways such as a neurotransmitter (nervous system), a vasodilator (cardiovascular system) and an inhibitor of viral replication (immune system).

1.5.3 Endothelial nitric oxide synthase (eNOS)

Nitric oxide synthase, a family of P450 mono-oxygenase-like enzymes, catalyses the production of NO and exists in three distinct isoforms; NOS-1, NOS-2, NOS-3. They differ not only in their genetic origin (Huang *et al.*, 1996) (Alderton *et al.*, 2001) but also in their location. NOS-1 or neuronal NOS (nNOS) is predominantly found in the central and peripheral nervous system but also in the skeletal muscle, pancreas and endometrium and has a role in neurotransmission and glomerular interactions (Mungrue, 2004). NOS-2 or inducible NOS (iNOS) is found in the heart and liver and in activated macrophages, smooth muscle and endothelial cells and has a role in inflammation (Aktan, 2004; Li & Forstermann, 2009). Finally NOS-3 or eNOS is found predominantly in the endothelium but also in the brain and epithelial cells. eNOS is involved in vascular relaxation, regulating platelet adhesion/aggregation and in angiogenesis (Shaul, 2002; Cirino *et al.*, 2003).

The process of NO synthesis involves firstly the oxidation of arginine to N^G-hydroxy-$_L$-arginine (NHA) using NADPH and oxygen catalysed by the NOS (Woodward *et al.*, 2009). The second step is when NHA is subsequently converted to $_L$-citrulline via NOS, resulting in the production of NO. Actions of NOS are accelerated by the cofactors flavin adenine dinucleotide (FAD), flavin mononucleotide (FMN) and tetrahydrobiopterin (BH_4).

In the endothelium eNOS is localized to highly rich lipid invaginations or caveolae of the plasma membrane (Shaul *et al.*, 1996b) where it is bound in an 'inactive' state to the

coat protein caveolin-1. Activation of eNOS also involves heat shock protein 90, calmodulin binding, phosphorylation of Ser1179 and dephosphorylation of Thr497 domains and subcellular localization. Under normal shear flow there is an influx of Ca^{2+} causing calmodulin to bind to eNOS, causing its subcellular localization to either the cytosol or the Golgi (Sanchez, 2006) or possibly to the mitochondria (Gao, 2004), which ultimately results in activation. Once NO is produced it can then stimulate soluble guanylate cyclase in vascular smooth muscle cells to increase cyclic guanosine monophosphate which in turn leads to relaxation and reduced Ca^{2+}. Impaired NO bioavailability, commonly seen in various CVDs including hypertension can be due to either impaired production or increased degradation of NO. With regards to the established pathway of its synthesis, impaired NO production may be a result of reduced eNOS activity, substrate and cofactor availability and the localization of eNOS or the presence of endogenous inhibitors. Sanchez *et al.,* (2006) suggest that eNOS translocation from the caveolae to the Golgi via acetylcholine may correspond to a vasodilation pathway, whereas they show that platelet-activating factor, an inflammatory marker and vasoconstrictor, causes eNOS to locate to the cytosol. Therefore cytosolic relocation of eNOS, and particularly mitochondrial bound eNOS (Gao, 2004) may relate to an inflammatory response.

Since the works of Huang and colleagues (1996) and Shesely and colleagues (1996) demonstrating a hypertensive phenotype in eNOS knockout mice, studies have been utilizing these models extensively and have demonstrated an essential role of eNOS in the vasculature. In animal models, supplementation with the eNOS substrate L-arginine leads to enhanced NO synthesis in diabetic (Kohli *et al.*, 2004) and pulmonary hypertensive rats (Goret *et al.*, 2008; Ou *et al.*, 2010), as well as reduced atherosclerotic lesions in rabbits (Nematbakhsh *et al.*, 2008) and cerebral infarcts in various experimental models of stroke (Willmot *et al.*, 2005). More importantly, clinical studies have also shown L-arginine supplementation increases NO synthesis and enhances vascular reactivity. Indeed,

hypertensive patients have paradoxically high levels of L-arginine in their plasma (Perticone *et al.*, 2005) yet display impaired L-arginine transport in platelets, red blood cells (Moss *et al.*, 2004) and endothelial cells, and are therefore unable to adequately produce optimum NO. Consequently, L-arginine activity may be rate-limiting for NO production and this is seen even in normotensive patients with a family history of hypertension (Schlaich, 2004). Increased L-arginine transport can be seen in various studies to improve vascular function; De Meirelles and collegues (2008) demonstrated hypertensive patients undergoing 12 weeks of aerobic exercise had significantly improved L-arginine transport and NOS activity, as well as reductions in fibrinogen and C-reactive protein.

1.5.4 L-arginine

Against this backdrop, it is thus of little surprise that L-arginine supplementation has been reported to improve endothelial function. Indeed, supplementation of L-arginine in humans has been delivered via several modes, including intra-arterially, intravenously and orally and in high risk patients it has been shown to both increase NO production and decrease leukocyte adhesion, platelet aggregation and hyperplasia of the intimal layer (Tousoulis *et al.*, 2007). Despite this, owing to the diverse role of L-arginine, its supplementation is likely to result in increased stimulation of metabolism via pathways other than NO synthesis, such as those that increase ornithine, polyamines, creatine, proline and spermine (Beaumier *et al.*, 1995). It is thus important to note that although L-arginine therapy can produce its effects via NO dependent mechanisms, effects independent of NO may also play a functional role.

L-arginine is also a potent hormone secretagogue. It has long been used for the assessment of growth hormone release by the pituitary gland (Merimee *et al.*, 1967) and L-arginine administration results in an approximate two fold increase in plasma growth

hormone, insulin and glucagon release (Bode-Boger *et al.*, 1996; Giugliano *et al.*, 1997). L-arginine also releases prolactin (MacAllister *et al.*, 1995) and insulin either directly or indirectly (by the release of other endothelium dependent agents such as muscarinic agonists (Giugliano *et al.*, 1997). The mechanisms regulating the endocrine secretagogue effect on various hormones in response to L-arginine remains largely unknown. However, the secretagogue effect is of important consideration when evaluating the role of L-arginine on the vasculature, since many of these resultant hormones have been independently reported to act on vascular smooth muscle cells. Apart from its complex metabolism and potent secretagogue effects, dietary L-arginine supplementation is also less than ideal since it is an amino acid that undergoes considerable first pass metabolism. Indeed, ingestion of L-arginine may not have large physiological effects due to its low bioavailability, reported to be as low as 21% through to 67% (Boger *et al.*, 1998; Tangphao *et al.*, 1999).

The eNOS inhibitor ADMA (asymmetric dimethylarginine), which is an endogenous analogue of L-arginine and a competitive inhibitor for L-arginine metabolism can also reduce its availability for NO production. ADMA is not only increased in essential hypertension but also inversely correlated with forearm blood flow (Perticone *et al.*, 2005). The enzyme arginase (discussed later) may also be another determinant of reduced cytosolic L-arginine and impaired NO production.

Reduced L-arginine, increased ADMA or BH_4 deficiency can also lead to uncoupling or dysfunction of eNOS and other NOS isoforms. eNOS contains two dimers; an N-terminal oxygenase domain that binds BH_4, L-arginine, iron, and calmodulin ions, as well as a C-terminal reductase domain that binds FAD, FMN and NADPH. In the pathological setting, BH_4 is oxidised to BH_2 causing altered electron flow from FMN and FAD to L-arginine and the uncoupling of eNOS dimers. This in turn results in free radical production, particularly superoxide, in place of NO. Studies in hypertension have demonstrated a down regulation of BH_4 and in an animal nephrectomised model, BH_4 supplementation normalises systolic

blood pressure levels (Podjarny, 2004). Other mechanisms causing uncoupling of eNOS include impaired Akt kinase phosphorylation of the serine[1179] domain (Dimmeler *et al.*, 1999; Fulton *et al.*, 1999) or increased phosphorylation of the theronine[497] domain via protein kinase C (Harris *et al.*, 2001; Church & Fulton, 2006). Additionally, arginase II is known to compete with eNOS for L-arginine and consequently may regulate eNOS activity (Lim *et al.*, 2007b).

1.5.5 Arginase

Arginase is a fundamental manganese metalloenzyme in the hepatic urea cycle that hydrolyses L-arginine to urea and L-ornithine. Arginase exists in two distinct isoforms (I and II) in which they differ in intracellular, gene and tissue expression, gene transcription and transduction regulators as well as metabolism. While both enzymes are found throughout the body, arginase I or hepatic arginase is a cytosolic enzyme found abundantly in the liver but also in red blood cells, whereas arginase II or extra-hepatic arginase is a mitochondrial enzyme expressed more widely and which is seen in the kidney, brain, gastrointestinal tract, prostate and the vasculature. Vascular endothelial cells and smooth muscle cells express both isoforms, but it appears that the distribution is vessel and species dependent (Bachetti *et al.*, 2004; Ming *et al.*, 2004; Zhang *et al.*, 2004). In particular, arginase II appears to be the predominant arginase isoform in human endothelial cells (Ming *et al.*, 2004). Arginase isoforms share ~59% homology, with arginase I composed of 322 amino acid residues, 11.5 kbp long and 8 exons on chromosome 6q23, whereas arginase II appears to have 344 amino acid residues and 8 exons but is on chromosome 14q24.1-q24.3. Products of arginine hydrolysis involve increased urea production and L-ornithine leading to increases in polyamines, proline, and glutamate (involved in cell growth and proliferation), as well as a reduction in NO.

Initially, the role of arginase in the body was mainly thought of as disposing excess nitrogen via amino acid and nucleotide metabolism. Studies recently, however, suggest an important role for arginase in the vasculature. In the endothelium, arginase is now regarded to help regulate NO levels by competing with eNOS for L-arginine. Arginase is also thought to modulate eNOS (Berkowitz *et al.*, 2003) and this is most likely to occur when eNOS is translocated from the caveolae to the cytosol and perhaps even the mitochondria under pro-inflammatory states. As such, increased arginase activity/expression has been implicated in many vascular pathologies including hypertension (Xu *et al.*, 2004; Demougeot *et al.*, 2005), ischaemia-reperfusion (Hein *et al.*, 2003), uraemia (Thuraisingham *et al.*, 2002), aging (Berkowitz *et al.*, 2003), sexual arousal (Kim *et al.*, 2003; Masuda, 2008), diabetes (Kashyap *et al.*, 2008; Romero *et al.*, 2008a) and atherosclerosis (Ming *et al.*, 2004; Ryoo *et al.*, 2008). In hypertension, an arginase activity and expression study demonstrated that increased arginase activity reduces NO mediated dilation in hypertensive pigs, which was then normalized using an arginase inhibitor (Zhang *et al.*, 2004).

These results are also seen in other models of hypertension, including Dahl rats with salt-induced hypertension (Johnson *et al.*, 2005) and in bovine pulmonary arterial endothelial cells in which NO production was increased and urea was decreased when both L-arginine and L-valine were used to inhibit arginase activity (Chicoine *et al.*, 2004). Moreover in a model of chronic hypertension, treatment with an arginase inhibitor for 10 weeks in older aged spontaneously hypertensive rats, elicited a decrease in blood pressure and cardiac fibrosis and improved vascular function (Bagnost *et al.*, 2010). In one small clinical study assessing attenuated reflex cutaneous vasodilatation in essential hypertension, increased NO-dependent vasodilatation was observed when arginase was inhibited but not following L-arginine supplementation (Holowatz & Kenney, 2007). Interestingly, it has also been reported that arginase expression of both isoforms is increased in spontaneously

hypertensive rats even before overt hypertension develops and that it is positively correlated to systolic blood pressure in these rats (Demougeot *et al.*, 2007b).

Therefore, these results suggest that in genetic hypertension, vessels have the propensity to develop endothelial dysfunction before established hypertension is even developed. This dysfunction may also occur before inflammatory mechanisms take place, as increased inflammatory markers are not seen until these rats are adults (Sanz-Rosa *et al.*, 2005; Demougeot *et al.*, 2007b), suggesting underlying molecular/transcriptional mechanisms, possibly via NFκB.

Despite these recent findings it is still unclear the exact mechanisms/pathways that induces arginase upregulation in hypertension. Several studies have examined a possible association with ROS production that may help link hypertension-induced endothelial dysfunction and inflammation. Ryoo and colleagues (2008) demonstrate in atherogenic prone *Apoe*$^{-/-}$, that when arginase II activity is reduced via either inhibition or gene deletion NO bioavailability is increased and ROS production is reduced, resulting in improved endothelial function and reduced vascular stiffness. They also show that plaque area, thickness and foam cells are all reduced in the thoracic aorta treated with the arginase inhibitor S-(2-boronoethyl)-L-cysteine (BEC). The ROS/arginase link may also be reciprocal; where intraluminal hydrogen peroxide is found to upregulate arginase expression and impair NO-mediated dilation in porcine coronary arteries and these effects are attenuated when arginase inhibitors alpha-difluoromethylornithine or nor-Nω-hydroxy-L-arginine reduced hydrogen peroxide and increased vascular function (Thengchaisri *et al.*, 2006). The inflammatory cytokine TNFα has also been shown to upregulate arginase in ischaemia-reperfusion resulting in reduced bioavailability of L-arginine and the uncoupling of eNOS, and ensuring increased superoxide production (Gao *et al.*, 2007). This action may be via Nox, as alveolar macrophages treated with the Nox inhibitor, apocynin, demonstrate a concomitant decrease in arginase (Matthiesen *et al.*, 2008).

1.5.6 Reactive oxygen species

ROS are a class of molecules that may result from and cause eNOS uncoupling, decreased NO production and increased NO degradation. Although essential for cell metabolism and signalling, when there is an imbalance in the production of oxidants or ROS to antioxidants in blood vessels, this leads to a pro-oxidant state and the pathogenesis of oxidative stress causing endothelial dysfunction, increased contractility, vascular smooth muscle cell growth and apoptosis, monocyte migration, lipid peroxidation, inflammation and increased deposition of extracellular matrix proteins. Furthermore, ROS have been shown to activate signal transduction pathways and induce gene expression and growth factors (Allen & Tresini, 2000; Sauer *et al.*, 2001). As is reviewed extensively, endothelial dysfunction in hypertension and many CVDs is due in part to an increase in ROS production (Kunes *et al.*, 2004; Schiffrin, 2004; Thomas *et al.*, 2008). ROS are produced from the mitochondria and subcellular sources such as the mitochondrial electron transport chain, NADPH oxidase, xanthine oxidase, cytochrome P450, cyclooxygenase, lipoxygenase, and uncoupled eNOS. Initial formation begins with the reduction in one electron of molecular oxygen causing formation of ·superoxide. Superoxide can then go on to produce hydroxyl radical, hydrogen peroxide via superoxide dismutase, and peroxynitrite from scavenging NO.

Experimental models of hypertension including DOCA-salt (deoxycorticosterone acetate) rats (Viel *et al.*, 2008), spontaneously hypertensive rats (Zhou *et al.*, 2008), L-NAME hypertensive rats (Bauersachs *et al.*, 1998), and hypertriglyceridaemic rats (Kunes *et al.*, 2002) all demonstrate increases in ROS production. In some models, increases in ROS are found to precede hypertension suggesting that production of ROS may contribute to the initiation and the progression of hypertension (Houston, 2005). Furthermore, treatment with antioxidants improves vascular function and structure, prevents target-organ damage, and reduces blood pressure in animal models of hypertension (Chen *et al.*, 2001b; Houston,

2005). Yet clinical studies have been less conclusive. Indeed, ROS levels are enhanced in hypertensive patients with reports of increased levels of hydrogen peroxide (Lacy *et al.*, 2000) and upregulation of vascular NADPH (Fortuno *et al.*, 2004). However, most clinical trials demonstrate no beneficial effects of antioxidants on blood pressure (Paravicini & Touyz, 2008a). Indeed, in some clinical trials, antioxidants have even shown detrimental effects including increased risk of angina pectoris (Myung *et al.*, 2013) and an increase in mortality and cardiovascular death (Vivekananthan *et al.*, 2003). A major hurdle in determining the efficacy of antioxidants is the lack of appropriate techniques to distinguish the degree of oxidative stress in humans (Halliwell *et al.*, 2004). Other potential reasons include the use of inappropriate antioxidants, the incorrect targeting, timing and dose of supplements and that ROS are indeed essential to normal physiological processes. Despite this, excessive ROS is well documented in several cardiovascular diseases. Therefore, until future studies focus on 'more disease specific, target-directed, highly bioavailable antioxidants' as opposed to vitamin supplementation, the potential benefit of antioxidants in human diseases cannot be discounted (Firuzi *et al.*, 2011).

Of the many toxic effects excess ROS has on the vasculature, inflammation appears to be the greatest and is involved in the initiation and development of atherosclerotic plaques commonly associated with hypertension and various CVDs.

1.6 Renin-Angiotensin System (RAS) – Contribution to Hypertension, Inflammation and Atherosclerosis

The renin-angiotensin system (RAS) or renin-angiotensin-aldosterone system is a hormonal cascade that regulates blood pressure by modifying renal sodium and water reabsorption. While this is the classical role of the RAS, it also plays fundamental roles in the pathogenesis of CVDs.

1.6.1 Components of the RAS

In 1898, Tigerstedt and Bergman first discovered renin in kidney extracts and demonstrated that when injected into the jugular vein of rabbits, renin has a pressor effect (as reviewed in (Phillips & Schmidt-Ott, 1999). It was not until decades later that renin was discovered to be responsible for the production of the powerful vasoconstrictor, angiotensin (Ang) II (Goldblatt *et al.*, 1934; Braun-Menendez & Page, 1958). The RAS pathway, as we now understand it, is schematically depicted in Fig 1.5. Renin is secreted mainly by the juxtaglomerular cells in the kidney but can also be produced in the brain, adrenal gland, ovary and adipose tissue (Atlas, 2007). Renin then cleaves angiotensinogen from the liver to form the inactive decapeptide Ang I (Ang 1-10) that is then hydrolysed by ACE to form Ang II (Ang 1-8).

Figure 1.5. The renin-angiotensin system cascade. Demonstrating the classical (in bold) and extended pathways (adapted from Atlas, 2007).

While other metabolites for Ang, such as Ang III (Ang 2-8), Ang IV (Ang 3-8) and Ang (1-7) are formed in this cascade, most of the research involving RAS in inflammation and hypertension has focussed on the role of Ang II and its main receptors: Ang II type 1 (AT1R) and Ang II type 2 (AT2R). Stimulation of the AT1R induces vasoconstriction, increased blood pressure, sodium retention in the renal tubules, aldosterone synthesis in the adrenal cortex and pro-inflammatory pathways (Phillips & Kagiyama, 2002; Schmeisser *et al.*, 2004). Alternately, AT2R stimulation induces counter-regulatory effects such as vasodilatation and induction of anti-inflammatory (Rompe *et al.*, 2010), and anti-proliferative pathways (Widdop *et al.*, 2003). However, this concept it still somewhat controversial since AT2R stimulation has been shown to induce vasoconstriction in aged hypertensive rats (Pinaud *et al.*, 2007). Indeed, the RAS is a complex pathway but with the use of knockout animals,

transgenic overexpression and pharmacological inhibitors we now have a greater understanding of its role in hypertension, inflammation and atherosclerosis.

1.6.2 RAS in hypertension and atherosclerosis

The RAS was classically considered to be an endocrine system where Ang II production is blood-borne and involved in targeting certain tissues. There is now ample evidence, however, to show that the RAS has autocrine and paracrine functions whereby generation of local Ang II can influence blood pressure, inflammation and atherosclerosis. Unsurprisingly, the RAS has therefore long been a key pharmacological target for the treatment of hypertension and other CVDs. Inhibition of renin is currently being evaluated in clinical trials (Gheorghiade *et al.*, 2011; Krum *et al.*, 2011). Alternatively, 17 types of ACE inhibitors have been developed for the treatment of CVD since the first major trial CONSENSUS (1987) and most have demonstrably beneficial effects on cardiac function in heart failure. In addition, ACE inhibitors have been reported to reduce the incidence of stroke (30%), CAD (20%) and major cardiovascular events (21%) (Neal *et al.*, 2000), and chronic treatment with ACE inhibitors is very successful in maintaining blood pressure in hypertensive patients (Zaman *et al.*, 2002). However, ACE inhibitors can have major side effects including coughing and angioedema (von Lueder & Krum, 2013) and are therefore not tolerated by all patients. ARBs are another class of drug that are cardioprotective (Dahlof *et al.*, 2002) through their reduction of stroke risk. Other inhibitors include aldosterone receptor antagonists, neutral endopeptidase inhibition and angiotensin receptor neprilysin inhibitors that combine ARBs with neutral endopeptidase inhibition show promising results (Solomon *et al.*, 2012).
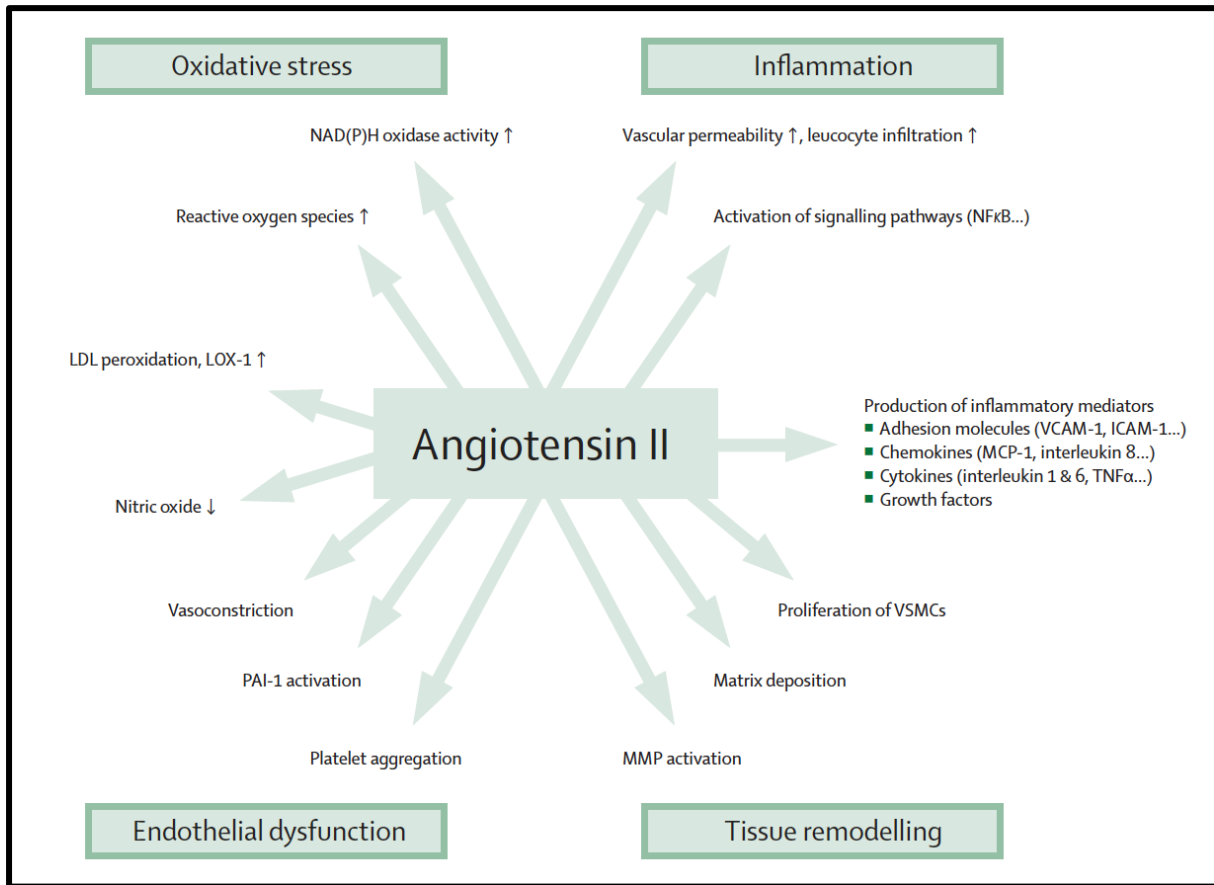
Figure 1.6. Mechanisms affected by Ang II (adapted from Schmieder *et al.*, 2007).

Since Ang II can affect various cellular mechanisms such as oxidative stress (Dikalov & Nazarewicz, 2013), vascular inflammation (Marchesi *et al.*, 2008), endothelial dysfunction (Pueyo *et al.*, 2000) and tissue remodelling (Fig 1.6), it is unsurprising that blocking its effects may affect other systems besides blood pressure. Indeed, it is via these mechanisms that over-production of Ang II can contribute to end-organ damage. Certainly, in vascular inflammation the RAS is involved in vascular permeability, inflammatory cell recruitment and activation and vascular repair (for review see (Brasier *et al.*, 2002; Marchesi *et al.*, 2008). Oxidative stress is also increased with Ang II via Nox; Ang II infusion has been shown to increase superoxide two-fold and this can, in turn, lead to endothelial dysfunction (Rajagopalan *et al.*, 1996).

The actions of Ang II can have profound effects on hypertension and vascular inflammation and can enhance the progression of atherosclerosis. In apolipoprotein E deficient (*Apoe*$^{-/-}$) mice on a high fat diet, Ang II-induced hypertension increases atherosclerotic lesions as well as aneurysms (Daugherty *et al.*, 2000; Weiss *et al.*, 2001). Furthermore, local generation of Ang II, as shown in DOCA salt-induced hypertension in *Apoe*$^{-/-}$ mice, generates an increase in lesions within the aorta (Weiss & Taylor, 2008). ACE2 is thought to have a protective effect in converting Ang II to Ang (1-7), and when deficient, not only increases circulating Ang II but also increases atherosclerosis in *Ldlr*$^{-/-}$ (low density lipoprotein receptor knockout; Thatcher *et al.*, 2011) and *Apoe*$^{-/-}$ mice (Thomas *et al.*, 2010). It is argued that the atherosclerosis derived from Ang II-induced hypertension is mainly due to the increase in Ang II itself, and not the increase in blood pressure *per se*, as a lesser atherogenic effect is seen with noradrenaline administration (Weiss *et al.*, 2001). Recent studies, however, demonstrate that RAS-independent mechanisms may exist for hypertension-induced inflammation, as is discussed later (Section 1.12). Ang II infusion also increases AT1R in the rostral ventrolateral medulla (Allen, 1998; Nunes & Braga, 2011), which is essential in hypertension and may also play a role in atherosclerosis.

1.7 Sympathetic Nervous System – Contribution to Hypertension, Inflammation and Atherosclerosis

Under physiological conditions the sympathetic nervous system (SNS) is involved in mediating the body's fight-or-flight response. Indeed, stress and arousal both have a significant correlation with CAD and cardiovascular events. For instance, an analysis of cardiovascular events during the FIFA World Cup in 2006 demonstrated that the risk of an acute cardiovascular event was doubled during match days, particularly during the first two hours of the match (Wilbert-Lampen *et al.*, 2008). Events such as earthquakes (Suzuki *et al.*, 1995) and wars (Meisel *et al.*, 1991), both undoubtedly high stress events, are associated with a greater likelihood of cardiovascular events.

Exerting a potent effect on vasomotor tone, the SNS was initially thought to be involved in acute blood pressure control. However, it is now understood that the SNS can act in a very dynamic way by influencing the development of essential hypertension, uncomplicated hypertension, end-organ damage and complicated hypertension with cardiovascular events (Grassi, 2010). Therefore, SNS activation is involved in the amplification of blood pressure increases, since even those with blood pressure that are in the higher range of normal, demonstrate increased SNS activity (Seravalle *et al.*, 1993). As such, various pharmacological agents are used clinically to reduce SNS and consequently, hypertension. These include α-blockers, central sympatholytics (Grassi *et al.*, 2000), β-blockers (Wallin *et al.*, 1984), long-acting calcium antagonists (Grassi *et al.*, 2003), ACE inhibitors and ARBs. More recently, alternative methods have been utilised to lower blood pressure such as renal denervation. The seminal work conducted by Esler and colleagues (Krum *et al.*, 2009; Schlaich *et al.*, 2009) demonstrated that in those with resistant hypertension, sympathetic renal denervation can markedly reduce blood pressure, and

noradrenaline spillover (a marker of sympathetic drive), in addition to attenuated sympathetic activity. It is still unknown whether denervation reduces cardiovascular risk; however, Brandt *et al.*, (2012) demonstrated that denervation resulted in improved arterial stiffness as well as improved systolic pressure load. Additionally, studies performed by Hu *et al.*, (2012) in Wistar rats found that renal denervation performed either before or after myocardial infarction is useful both therapeutically and preventatively with respect to cardiac function post myocardial infarction. It is exciting to consider this intervention may reduce other cardiovascular complications associated with increased SNS activity (Fig 1.7).
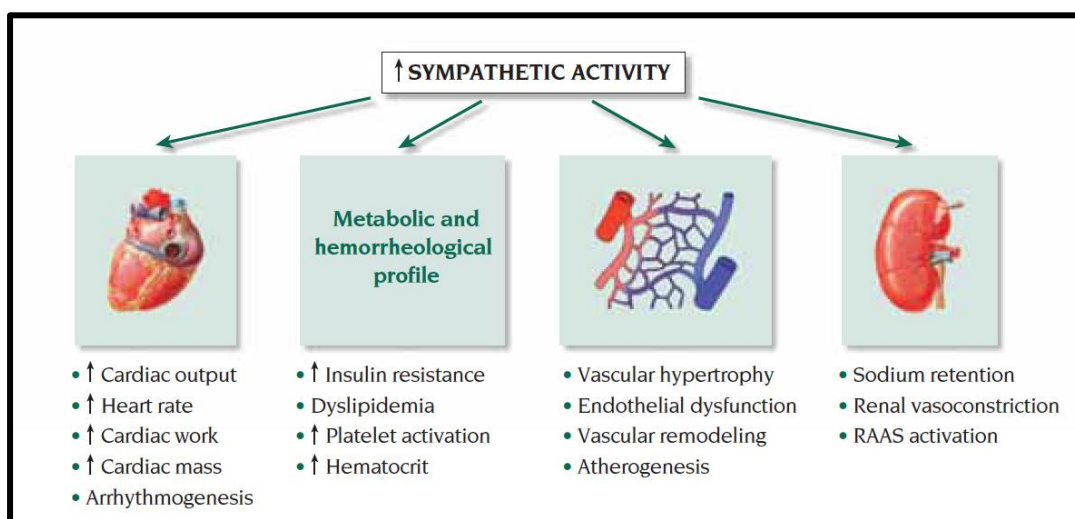
Figure 1.7. Effects of increased sympathetic activation (adapted from Grassi, 2007).

Since activation of the SNS leads to various complications, it is thought to act as a promoter of end-organ damage (Grassi, 2010). Indeed, evidence suggests a correlation exists between noradrenaline spillover and cardiac hypertrophy, increased left ventricular mass and left ventricular dysfunction (Greenwood *et al.*, 2001; Schlaich *et al.*, 2003; Burns *et al.*, 2007). Furthermore, platelet activation, increased clotting factors and increased vWF is seen with increased adrenergic activity and catecholamines (von Kanel & Dimsdale, 2000). Increased catecholamines are also known to damage the endothelium and consequently

lead to local oedema and necrosis (Makhmudov *et al.*, 1985; Johansson & Ostrowski, 2010). Moreover, circulating adrenaline and noradrenaline, both secreted by the SNS, are correlated with endothelial glycocalyx and cell damage in acute myocardial infarction (Ostrowski *et al.*, 2013). Spontaneously hypertensive rats are shown to have increased adhesion molecules in the nucleus of the solitary tract (brain stem) compared to Wistar controls (Waki *et al.*, 2007) that may result in increased cell transmigration and inflammation. From this study and others, it has been proposed that cytokine production in the brain may regulate neuronal activity (Zubcevic *et al.*, 2011). Similar to their role in endothelial cells, it is thought cytokines can regulate neuronal activation via the production of ROS and iNOS and the reduction of NO, which may lead to neuroinflammatory processes. Indeed, receptors for cytokines can be found in various brain cell types (Utsuyama & Hirokawa, 2002), and an increase in cytokine production in the brain is seen in both animal models of hypertension (Shi *et al.*, 2010) and heart failure (Felder, 2010). While there are some studies that link sympathetic nerve activity, hypertension and vascular inflammation, the mechanisms still remain largely unexplored.

1.8 Haemodynamic Forces – Contribution to Hypertension, Inflammation and Atherosclerosis

Under basal conditions, fluid shear stress and circumferential stretch results in continuous release of compensatory vasoactive substances. Circumferential wall stretch is due to the pulsatile luminal pressure exerted on the vascular smooth muscle cells whereas shear stress is an effect of the frictional force created by the flow of blood along the endothelial cells. While there are studies demonstrating the influence of stretch on endothelial cells (von Offenberg Sweeney *et al.*, 2004), shear flow is thought to be the prominent mechanical force exerted. The magnitude of endothelial shear flow in vessels is dependent on the velocity of blood flow, direction, and obstructions along the vessel, as well as the location of flow in the vascular tree.

Under physiological conditions, the flow of blood along straight vessels, also known as undisturbed laminar flow, results in high shear stress (HSS) values ($15 - 70$ dyn/cm^2) and several cardioprotective properties. Indeed, cultured endothelial cells from different human vessels demonstrate reduced inflammation following exposure to HSS compared to static conditions (Luu *et al.*, 2010a). Physiological shear stress conditions have also been shown to lead to anti-inflammatory effects, with reduced TNFα-induced adhesion molecule expression (Yamawaki *et al.*, 2003). Yet conflicting reports exist. A study using MRI technology has shown that one patient was found to develop plaque ulceration at the location with the highest shear stress (Groen *et al.*, 2008). This finding suggests that HSS may not be protective in areas of vulnerable plaques. However, it is well established that sites in the vascular tree most vulnerable to atherosclerotic plaques include the inner curve of vessels, as well as vessel bifurcations and branches. At these sites, disturbed laminar flow is at its most prominent (Chatzizis *et al.*, 2007; Chiu *et al.*, 2009) and presents in two forms:

unidirectional, which results in low shear stress (LSS) values (<12 dyn/cm^2) or bidirectional, leading to oscillatory shear stress (OSS) or turbulent flow. LSS and OSS have been found to be associated with decreased NO bioavailability, upregulation of LDL, degradation of the extracellular matrix, apoptosis, promotion of oxidative stress, and inflammation as well as vascular and plaque remodelling (Dardik *et al.*, 2005).

1.8.1 Mechanosensors

As endothelial cells serve as a barrier between blood flow and vascular smooth muscle cells, it has been suggested that they act as mechanosensors that transform the mechanical stimuli into intracellular biochemical signals in order to cause changes in cell morphology, cell function and gene expression. Several membrane-associated complexes have been proposed, including ion channels, tyrosine kinase receptors, G-protein-coupled receptors, caveolae, adhesion proteins, cytoskeleton, glycocalyx, and primary cilia (Figure 1.8). Of these, the current thesis focuses on the lipid rafts or caveolae.
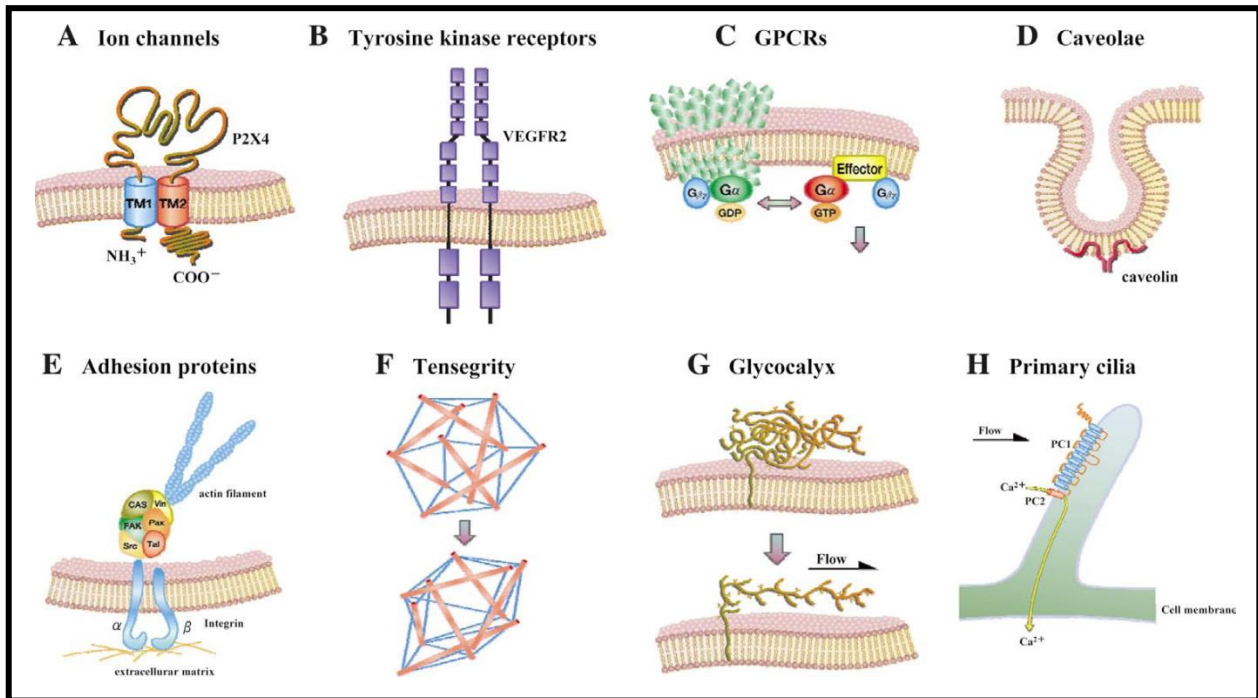
Figure 1.8. Proposed endothelial mechanosensors (adapted from Ando & Yamamoto, 2009).

1.9 Caveolae – Contribution to Hypertension, Inflammation and Atherosclerosis

Caveolae are structural microdomains or invaginations found along the plasma membrane and are implicated in endocytosis, cellular signalling and cholesterol and lipid metabolism. Caveolae are of a particular interest in the scope of this thesis as their proteins, caveolins and cavins, have been implicated as mechanosensors and in intracellular signalling for vascular inflammation.

1.9.1 Morphology

George Palade, a pioneer in electron microscopy, first identified caveolae in capillaries (Palade, 1953). Today, caveolae are commonly defined as invaginations and specialised lipid rafts of the plasma membrane that are 60-80 nm in diameter. Schlormann *et al.*, (2010) demonstrate that after glutaraldehyde fixation, caveolae exhibit the typical omega (Ω) shape whereas after cryofixation, the morphology is more cup-like in appearance. In any case, caveolae can present with varying degrees of invagination depending on the cell type, biogenesis of the caveolae and its function.

Caveolae are found on many cell types including vascular endothelial cells, epithelial cells, adipocytes, fibroblasts, smooth muscle cells and striated muscle cells but not on neuronal cells or lymphocytes. The density of caveolae along the plasma membrane also appears to be cell dependent, with caveolae spanning from about 50% of the plasma membrane on adipocytes (Thorn *et al.*, 2003) to 5% on fibroblasts (Guillot *et al.*, 1990). Furthermore, Gabella (1978) reported that caveolae density in the rat myocardium was 6.1 caveolae/μm^2 in cardiac muscle cells compared to 67.5 caveolae/μm^2 in the endothelial cells of intramuscular capillaries and arterioles. Apart from membrane association, various other

morphologies are now recognised as caveolae including grape clusters, tubular forms, or intracellular domains (Figure 1.9). Due to their membrane location, caveolae are often mistaken for clathrin-coated pits because of the cholesterol and glyosphingolipid-rich membrane domains, but their distinguishing feature is the lack of the clathrin coat and the
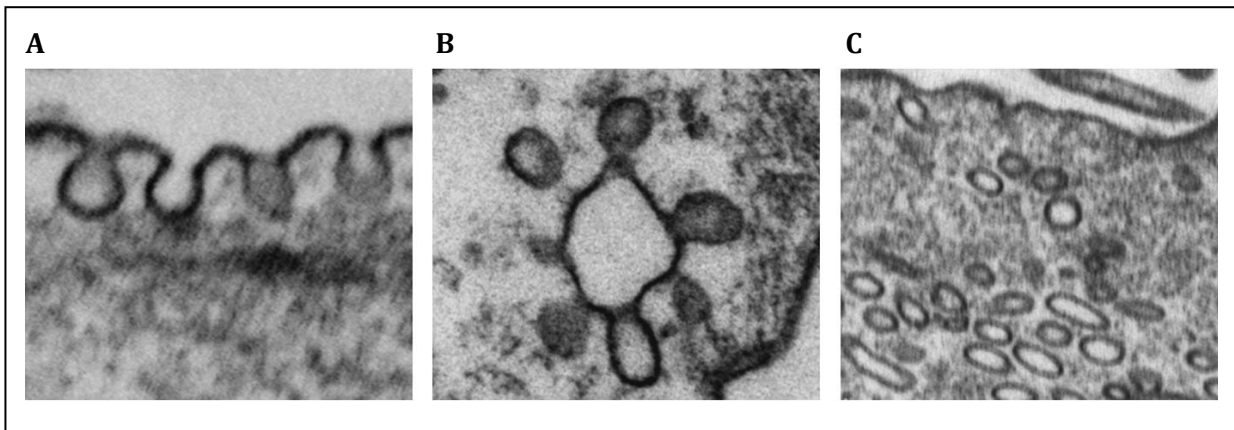
presence of the integral membrane protein caveolin.

Figure 1.9. Caveolae structures. Electron microscopy of the classic caveolae (**A**) on the plasma membrane, (**B**) grape-like clusters and (**C**) intracellular domains (adapted from Patel & Insel, 2009).

1.9.2 Caveolins

First identified in 1989 (1989), caveolins (Cav) are 22-24 kDa proteins with a hairpin configuration in which the N- and C-termini are both located in the cytoplasm (Monier *et al.*, 1995). Cav1 and Cav2 isoforms are expressed in non-muscle and smooth muscle cells, whereas Cav3 is predominantly found in striated muscle cells.

Synthesized in the rough endoplasmic reticulum, caveolin forms a 12-18 oligomer complex with cholesterol (Smart *et al.*, 1994; Monier *et al.*, 1995). These complexes are then transported via the secretory pathway to the Golgi complex, where they are oligomerised

again into hetero-oligomeric forms with Cav1 and Cav2 binding. During this time, caveolin has been reported to change from being detergent-soluble to detergent-resistant molecules (Pol *et al.*, 2005). About 100-200 caveolin next assemble and coat the golgi that are cholesterol rich before they exit the golgi and fuse with the plasma membrane (Tagawa *et al.*, 2005), where they form mature caveolae containing sphingolipids, cholesterol, and phosphatidylinositol (4,5)-biphosphate. The exact mechanisms involved in the transport of caveolae to the membrane still remain unclear. In endothelial cells, and while at the plasma membrane, Cav1 is also found to bind directly to filamin, an F-actin cross-linking protein, suggesting cytoskeleton support (Stahlhut & van Deurs, 2000; Sverdlov *et al.*, 2009).

From the plasma membrane, caveolins are then endocytosed, fused with endosomes, and subsequently degraded in lysosomes (Hayer *et al.*, 2010b). While the knockout of caveolins reduces the number of caveolae, overexpression does not increase the number in the endothelium (Bauer *et al.*, 2005), suggesting that other proteins may play a role in biosynthesis. Along with these coat proteins, various supporting proteins, called cavins, have recently been identified as essential to caveolae formation and function. The location and function of cavins 1-4 as well as the caveolins are summarised in Table 1.2.

1.9.3 Cavins

Cavin-1, a soluble cytosolic protein, has been shown to be present in caveolae in a 1:1 ratio with Cav1 and is only recruited to the cell surface once caveolae are present in their mature form. Hill *et al.*, (2008) first identified Cavin-1 or PTRF (polymerase I and transcript release factor) and demonstrated that Cav1 requires the assistance of cavin-1 for the stabilisation and the formation of caveolae. In support of this supposition, Cav1 alone has been found along the membrane disassociated with caveolae suggesting that Cav1 has a function outside caveolae. Such roles have been proposed, particularly in those cells that

lack caveolae but present with Cav1. For example, all three caveolins are expressed in neuronal cells and are thought to act as scaffolds for signalling, while in lymphocytes they are thought to be involved in T cell activation (Head & Insel, 2007). When cavin-1 does localise with Cav1 it is only nanometres apart, but rather than directly binding they are both associated with the cholesterol phosphatidylserine and can thus be readily dissociated with cholesterol depletion.

Cavin-2 has similar properties to cavin-1 in that it is involved in caveolae formation, and has been shown to recruit cavin-1 to caveolae. Thus the knockdown of cavin-2 reduces caveolae number (Hansen *et al.*, 2009). It has also been reported that over expressing cavin-2 leads to morphological changes and elongation of caveolae, as such cavin-2 is essential for the curvature seen in caveolae. By contrast, cavin-3 is thought to regulate caveolae function and has been associated with caveolins away from the plasma membrane. Induction of cavin-3 in lung cancer cells that lack cavin-3 protein demonstrated an increase in budding of caveolae in the cytosol and movement of caveolae along microtubules (McMahon *et al.*, 2009). Cavin-1 to -3 are expressed in both non-muscle and muscle cells whereas cavin-4 is thought to be only expressed in muscle cells and is involved in sarcolemmal caveolae and muscle myogenesis (Tagawa *et al.*, 2008). In summary, cavins are essential for caveolae formation and function and are thought to bind together as a complex of 60-80 cavin molecules (Hayer *et al.*, 2010a).

Table 1.1. Caveolins and Cavins

	Alternative names	Tissue expression	Function	Knockout/knockdown effect	Ref
Caveolins					
Caveolin-1	Cav1; VIP 21	Non-muscle cells, smooth muscle cells	Formation of caveolae, regulates NO production via eNOS, microvascular permeability, Ca2+ influx, vascular remodelling , angiogensis, mitosis, insulin signalling	Reduced caveolae density, increased microvascular permeability, cardiac hypertrophy, dilated cardiomyopathy, pulmonary hypertension, impaired angiogenesis, neointimal hyperplasia	(Griffoni *et al.*, 2000; Miyawaki-Shimizu *et al.*, 2006)
Caveolin-2	Cav2;	Non-muscle cells, smooth muscle cells	Supports Cav1, regulates the density of caveolae, mitosis	Pulmonary dysfunction, alveolae septal thickening, EC hyperproliferation, exercise intolerance	(Razani *et al.*, 2002)
Caveolin-3	Cav3;	Striated muscle	Formation of caveolae, eNOS regulation	Loss of caveolae, cardiomyopathy, cardiac hypertrophy,	(Woodman *et al.*, 2002)
Cavins					
Cavin-1	PTRF; BBP; Cav-p60; Cavin	Muscle & non-muscle cells	Scaffolding and formation of caveolae at the membrane	Loss of caveolae, dyslipidemia, reduced adipose tissue, glucose intolerance	(Hill *et al.*, 2008; Liu *et al.*, 2008)
Cavin-2	SDPR; SDR; PS-p68	Muscle & non-muscle cells	Curvature of the membrane, deformation of caveolae	Loss of caveolae, overexpression induces caveolae deformation and membrane tabulation	(Hansen *et al.*, 2009)
Cavin-3	SRBC; PRKCDBP	Muscle & non-muscle cells	Budding of caveolae, intracellular transport, aid in signalling	Reduced Cav1 trafficking	(McMahon *et al.*, 2009)
Cavin-4	MURC	Muscle cells	Muscle specific, structural function	Cav3 dysfunction	(Bastiani *et al.*, 2009)

VIP: Vesicular integral membrane protein; PTRF: Polymerase I and transcript release factor; BBP: BFCOL1-binding protein; SDPR: serum deprivation protein response; SDR: serum deprivation response; SRBC: sdr-reulated gene product that binds to c-kinase; PRKCDBP: protein kinase c, delta binding protein; MURC: muscle restricted/related coiled-coil protein. Adapted from (Insel & Patel, 2007; Bastiani & Parton, 2010; Hansen & Nichols, 2010).

1.9.4 Caveolae function in endothelial cells

Caveolae are enriched with various signalling proteins (Fig 1.10), which help to shed light onto the various functions caveolae and their coat proteins have in endothelial cells. These functions include cholesterol transport, eNOS and vascular reactivity, reduction/oxidation signalling, and mechanotransduction.
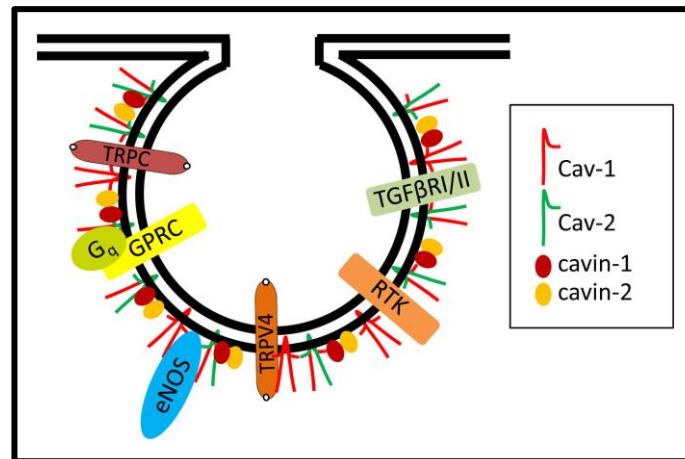
Figure 1.10. Signalling proteins enriched in endothelial caveolae. Cav-1: caveolin-1; Cav-2: caveolin-2; TRPC: transient receptor potential channel; GPRC: G-protein-coupled-receptors; G_q: heterotrimeric G protein; TRPV4: TRP cation channel subfamily V member 4; RTK: receptor tyrosine kinase; TGFβRI/II: transforming growth factor-beta type I and II receptors (adapted from (Sowa, 2012).

1.9.4.1   Cholesterol transport

Caveolae have been shown to be involved in the transcytosis of various macromolecules including albumin (Ghitescu *et al.*, 1986), iron transferrin (Soda & Tavassoli, 1984), chemokines (Ge *et al.*, 2008), insulin (King & Johnson, 1985) and LDL (Ghitescu *et al.*, 1986). Using cholesterol disrupting agents, Zhang *et al.*, (2008) demonstrated that the oxidised LDL scavenger receptors CD36 and SR-B1 are localised in the caveolae. In addition, *Cav1*$^{-/-}$ (caveolin-1 knockout) mice display an increase in plasma triglycerides along with reduced LDL secretion and increased HDL levels (high density lipoprotein) (Frank *et al.*, 2008). This was reported to be due to reduced LDL transcytosis, suggesting caveolae play a crucial role in both the uptake and the regulation of LDL transport. The transport and

entrapment of LDL to the sub endothelium is thought to be one of the first steps in the development of atherosclerosis. Indeed, double $Cav1^{-/-}/Apoe^{-/-}$ mice demonstrate reduced adhesion molecule expression (Frank *et al.*, 2004), leukocyte adhesion (Engel *et al.*, 2011) and atherogenesis compared to $Apoe^{-/-}$ mice. All of which is only reversed when endothelial *Cav1* is re-expressed (Fernandez-Hernando *et al.*, 2010). The development and consequences of atherosclerosis are discussed in Section 1.4.

1.9.4.2   eNOS and vascular reactivity

As previously discussed in Section 1.5.3, the binding of Cav1 is generally shown to suppress eNOS activity, since $Cav1^{-/-}$ mice exhibit increased basal NO release and cyclic guanosine monophosphate production (Drab *et al.*, 2001; Razani *et al.*, 2001). Interestingly, Yu *et al.*, (2006) demonstrated that $Cav1^{-/-}$ mice presented with reduced blood flow in response to vascular shear stress, but displayed no change in lumen diameter. They also showed an increase in vessel wall thickness and cellular proliferation compared to controls. The reconstitution of Cav1 into the vessels ablated the response, suggesting that eNOS is unable to localize in the caveolae, resulting in impaired response to shear stress. Therefore, not only is Cav1 important in the regulation of eNOS but its location in the caveolae is essential.

Despite their increased eNOS activity and NO production, and reports of reduced myogenic tone (Albinsson *et al.*, 2007), $Cav1^{-/-}$ mice seem to have no change in mean arterial blood pressure (Desjardins *et al.*, 2008; Rahman & Sward, 2009). Insel and Patel (Insel *et al.*, 2007) suggest this may be due to compensatory mechanisms from the long-term loss of Cav1 or due to the plasticity of the vasculature. They suggest that knockout mice may not be overly physiologically relevant in this context and suggest alternative methods such as siRNA. Recently, Bernatchez *et al.*, (2011) knocked down Cav1 with the peptide cavnoxin that targets the scaffolding domain of Cav1 that binds to eNOS, and demonstrated reduced vascular tone and blood pressure in control mice but not in $Cav1^{-/-}$ or $eNOS^{-/-}$ mice. Conversely, there have been reports of $Cav1^{-/-}$ mice with pulmonary hypertension (Zhao *et al.*, 2009), in which an over active eNOS leads to the reduction of protein kinase G (PKG) activity. Interestingly, this reduction was abrogated in the double $Cav1^{-/-}/eNOS^{-/-}$ mice, demonstrating the unique regulation of eNOS by Cav1.

1.9.4.3   REDOX signalling

Nox, known to be the predominant source of ROS (Griendling *et al.*, 2000; Touyz, 2004; Ray & Shah, 2005), has seven isoforms; Nox-1, -2 and -4 are the most well described in the vasculature. In 2007, Yang and Rizzo (Yang & Rizzo, 2007) demonstrated that Nox subunits may be preassembled and functional in caveolae. Via western blotting, they demonstrated that Nox subunits are localized in the same light buoyant density membrane factions as Cav1. Using both the crude method of depletion of membrane cholesterol with methyl-β-cyclodextrin (MβCD) and an isoluminol assay, they demonstrated that via TNFα or Ang II stimulation ROS production was increased in raft membranes. Milovanova *et al.*, (2008) have also shown that cessation of shear flow in order to mimic ischaemia, increased ROS production via Nox-2 in lungs and endothelial cells and that this was reduced in *Cav1$^{-/-}$* mice. However, *Cav1$^{-/-}$* mice also demonstrate similar production of ROS via Nox-2, compared to wild type mice following thrombin treatment. This suggests that in this setting caveolae serve as a sensor of altered shear and that reduced Nox activity may be due to reduced membrane depolarization. Along with regulating eNOS, which is also a ROS generating enzyme, these studies suggest caveolae may in addition regulate ROS production through Nox.

1.9.4.4   Mechanotransduction

Differing mechanical forces are shown to have varying impacts on caveolae. Laminar or HSS has been shown to increase caveolae number in cultured bovine aortic endothelial cells exposed 10 dyn/cm^2 for 1 hr (Park *et al.*, 1998) and 1 & 3 days at 19 dyn/ cm^2 (Boyd *et al.*, 2003), compared to static conditions. Conversely, Sinha et al., (2011) showed that endothelial cells exposed to stretch via osmotic swelling demonstrate a significant reduction in the number of caveolae at the cell surface. Interestingly, they demonstrated that this was not due to an increase in endocytosis but rather a flattening and disassembling of caveolae (Sinha *et al.*, 2011). Conversely, Albinsson *et al.*, (2007) demonstrated that Cav1 initiates downstream signalling in response to shear but not pressure or stretch. Perhaps in endothelial cells, caveolae act as mechanosensors to shear flow in order to elicit a cascade of events that promote NO production and vasodilation, but in response to stretch they

instead elicit a structural response. As flattening is such an inherent property of caveolae, it has been proposed that this is a quick cell survival mechanism, creating a greater cell surface area (Parton & del Pozo, 2013). This is in line with other reports highlighting caveolae as membrane reservoirs (Sens & Turner, 2006; Sinha *et al.*, 2011).

It has been shown that upon flattening, caveolar scaffolding proteins are disassembled and released into the plasma membrane (caveolin) and cytosol (cavin) (Sinha *et al.*, 2011). However, it is still unclear the purpose of disassembling, aside from the conformational change. Whether this leads to compensatory signals to promote caveolae biogenesis due to their reduced number remain to be seen.

1.10 Inflammation-Induced Hypertension

Alterations in the immune system have long been implicated in the genesis of hypertension (White & Grollman, 1964), and more recently studies from David Harrison's laboratory (Guzik *et al.*, 2007; Marvar *et al.*, 2010) using genetically modified mice have strengthened the concept that hypertension has an immunologic basis. They demonstrate mice lacking lymphocytes (*Rag1$^{-/-}$*; recombination activating protein) are resistant to hypertension induced by Ang II, DOCA-salt, or noradrenaline. They also show that after the adoptive transfer of T cells but not B cells, Ang II-induced hypertension in *Rag1$^{-/-}$* mice was completely restored. Furthermore, they subsequently show that Ang II, DOCA-salt, or noradrenaline also promote T cell activation and accumulation. Since these seminal papers, other studies have moved this concept forward and shown that immune deficient mice are protected against hypertension (Crowley *et al.*, 2010) and that T regulatory cells prevent Ang II- (Barhoumi *et al.*, 2011; Matrougui *et al.*, 2011) and aldosterone- (Kasal *et al.*, 2012) induced hypertension.

Monocytes have also been shown to take part in Ang II-induced hypertension (Wenzel *et al.*, 2011). Via selective ablation, studies have demonstrated a loss of lysozyme M-positive monocytes reduced not only the number but their infiltration into the vascular wall. In addition, *M-CSF$^{-/-}$* mice have not only reduced Ang II-induced high blood pressure but also reduced endothelial dysfunction, vascular remodelling and oxidative stress (De Ciuceis *et al.*, 2005). Neutrophils have also been shown to regulate blood pressure, where Morton *et al.*, (2008) show that neutropenia resulted in hypotension via regulating vascular tone. While there is much focus on the role of immune cells and inflammatory cells in the pathogenesis of hypertension this thesis focuses on whether conversely, hypertension plays a role in the aetiology of inflammation.

1.11   Hypertension-Induced Inflammation

Recent reports suggest that hypertension-induced endothelial dysfunction involves low-grade inflammation that can progress into hypertension-induced atherosclerosis and several cardiovascular complications. This comes as no surprise as these conditions are commonly co-correlated and have similar risk factors (i.e. age, obesity, diet, diabetes, smoking) resulting in vascular remodelling and dysfunction. Indeed, inflammatory markers that are reportedly upregulated in hypertensive patients such as TNFα, C-reactive protein (Schillaci *et al.*, 2003), IL-6, IL-1b and Ang II (Boos & Lip, 2006; Savoia & Schiffrin, 2006; Androulakis *et al.*, 2009) are also involved in the initial stages of atherosclerotic plaque development and the adhesion cascade (see Section 1.4.1).

By contrast, other animal studies have shown a relationship to exist between high intraluminal pressure and plaque development. Indeed, in *Apoe*$^{-/-}$ mice with eNOS ablation induced hypertension (Knowles *et al.*, 2000b), enhanced atherosclerotic plaque size is observed compared to control *Apoe*$^{-/-}$ mice. The authors have suggested that this finding may be due to the increased pulse pressure, turbulent flow and stretch exerted on the vessels as well as the reduced NO production. Using *Apoe*$^{-/-}$ mice with high blood pressure induced via renal artery clamping, Mazzolai *et al*., (2004) demonstrated that an endogenous increase in Ang II elicited an increase in unstable plaques, as evidenced by thinning of the fibrous cap, an increased lipid or necrotic core, elastic lamina fragmentation and media atrophy. Furthermore, they show this process was greatly mediated by activation of proinflammatory lymphocytes. Wu *et al*., (2002) also show that *Apoe*$^{-/-}$ mice with aortic constriction induced-hypertension also develop cardiac dysfunction. In particular, the atherosclerotic plaque forms proximal to the constriction and is independent of the RAS.

This effect is also seen in clinical studies in which essential hypertensive patients demonstrate increases in ICAM-1, VCAM-1 and E-selectin in their serum following a cold pressor test (Buemi *et al.*, 1997). Furthermore, studies show that with stenosis of rabbit aorta, the induction of hypertension causes monocyte adhesion to be increased only in the region proximal to the stenosis (Tropea *et al.*, 1996), which is where the highest oscillatory shear stress occurs. While it is clear that high intraluminal pressure results in leukocyte adhesion and atherosclerotic development, the exact mechanisms and pathways are still

unclear although various studies have implicated all the factors described above including ROS production, NFκB activation, endothelin-1, and the RAS.

1.12   Summary

The aetiology and progression of hypertension involves various endogenous systems, namely the endothelium, the RAS and the SNS. More recently great interest has focussed around the role of immune cells. Interestingly, many studies suggest that it is these systems that cause the progression of essential hypertension to CAD. However, there is increasing interest that high blood pressure in itself may play a role, exerting downstream signalling in the endothelium. Haemodynamic forces, caveolae, arginase, eNOS, and ROS and NFκB are all suggested signalling mechanisms involved in hypertension-induced inflammation and are explored in this thesis.

1.13   Scope of Thesis

To test the hypothesis that high pressure *per se* can induce inflammation, I have used a customised perfusion vessel chamber (Michell *et al.,* 2011b) to assess, in real time, leukocyte adhesion to the endothelium at differing pressures under flow conditions, in endothelium intact vessels and using whole blood. I have also evaluated intracellular signalling pathways in the endothelium that contribute to this process, and show that caveolae play a critical role in this process, producing ROS and activating NFκB. Finally, I have demonstrated that high blood pressure increases plaque instability in a newly developed hypertensive atherosclerotic mouse model.

Chapter 2

General methods and materials

2.1 *In Vitro* Techniques

2.1.1 Cell culture

2.1.1.1 HUVECs:

Human umbilical vein endothelial cells (HUVECs; Lonza, #C2517A) were cultured in EGM-2 media (Lonza, #CC-3162) with antibiotics-antimycotics (0.1x; Gibco, #15240) and maintained in tissue culture polystyrene flasks; passages 3-6 were used.

2.1.1.2 Transformed H5V:

Transformed H5V cells (a gift from Dr Marie-Odile Parat, University of Queensland), derived from mouse embryonic heart endothelium, contained either a lentivirus with shRNA to caveolin 1 (H5V Cav1 KD) or scrambled shRNA (H5V Scr). These cells were maintained in DMEM/F12 media with 5% foetal bovine serum (FBS) and 2 μg/ml puromyocin dihydrochloride (Sigma, #P8833).

2.1.1.3 THP-1:

The human acute monocytic leukaemia cell line THP-1 (ATCC, TIB-202) was cultured in RPMI growth medium (Invitrogen, #21870-076) with 10% FBS, 1% penicillin/streptomycin (2x), 1% sodium pyruvate (100x; Gibco, #11360), 1% non essential amino acids (100x; Gibco, #1140-050), and 55 μM β-mercaptoethanol (Gibco, #21985-023). To determine total number per flask the non-adherent cells were spun down at 22°C, 1400 RPM for 5 min, they were then resuspended in 1 ml of media and counted using a haemocytometer. Cells were counted according to the following: *Cells/ml = # cells counted/# large squares counted x 10^4 x dilution factor.* All cells were kept at 37°C with 5% CO_2 where media was replenished every 48 hr.

2.1.2 Pressurising endothelial cells

This methodology was developed and optimised as part of this candidature. A monolayer of HUVECs or transformed H5V cells were plated on 25 mm round glass coverslips (Warner Instruments Inc., #64-0705) coated with Collagen I (BD Biosciences, #354236). Once confluent, they were placed in a stainless steel sealed chamber (Penn Century Co.) connected to pressure transducers and a pressure servo controller (Living Systems). The chamber was placed on a temperature controlled platform maintained at 37°C with Krebs modified buffer (NaCl 119, KCl 4.7, $MgSO_4 \bullet 7H_2O$ 1.17, $NaHCO_3$ 25, KH_2PO_4 1.18, $CaCl_2$ 2.5, glucose 11 and EDTA 0.03 mmol/L) maintained at physiological pH by infusing carbogen gas (95% O_2; 5% CO_2) at 37°C: and pressurised. Cells were either unpressurised (control), pressurised at 0, 60, 80 or 120 mmHg for 1 hr and used for assessment of reactive oxygen species production (section 2.1.3), or snap frozen for nucleic acid or protein extraction (section 2.3). Controls (no pressure) were used in the cell setup as the cells pressurised at 0 mmHg occasionally demonstrated varying 'activated' responses therefore it was necessary to have completely 'no intervention' controls for comparison.

2.1.3 Measurement of reactive oxygen species in pressurised endothelial cells

HUVECs were setup in the pressurised sealed chamber as described (section 2.1.2). The chamber was placed under a fluorescent upright Olympus microscope (BX51) coupled to a digital camera. Production of ROS was determined using either 2,7-dichlorofluorescein (DCFH; Sigma, #D6883) or the more sensitive hydrogen peroxide indicator Peroxyfluor-6 acetoxymethyl ester (PF6-AM; a gift from Christopher Chang; Dickinson *et al.*, 2011). Cells were perfused with Krebs modified buffer (1 ml/min) with either DCFH (5 µM) or PF6-AM (5 µM) for 30-60 min for stabilisation. Following stabilisation, pressure (0 – 120 mmHg) was applied for 1 hr followed by 30 min of no pressure. From the start of perfusion, images were acquired every 10 min using the Zeiss Axiovision software and stored for offline analysis. Fluorescence intensity was determined using ImageJ 1.47g and data was expressed as % change in intensity compared to the average of the last three images during the stabilisation period.

2.1.4 Adhesion assay under static conditions

Confluent H5V transformed cells on glass coverslips were either untreated (control), or stimulated with mTNFα (4hrs, 5ng/ml). Following treatment, 3 x 10^5 per 2 cm^2 surface area of THP-1 cells were added to the endothelial cells and incubated at 37°C with 5% CO_2 for 2 hrs. Coverslips containing endothelial cells and adhered THP-1 cells were then placed into 4% formaldehyde overnight at 4°C. Coverslips were mounted face down onto slides with a drop of mounting media (Dako), slides were then allowed to set overnight at room temperature. A minimum of three images were taken per slide using 4x magnification on a FSX100 Olympus microscope with accompanying software. Analysis was done using ImageJ 1.47g. Results were expressed as the % of adhered THP-1 cells per field compared to H5V Scr controls.

2.2 Experimental procedures involving animals

All experiments involving humans and animals were approved by the Alfred Hospital Ethics Committee and the Alfred Medical Research and Education Precinct Animal Ethics Committee, which adhere to the National Health and Medical Research Council (NHMRC) Australian Code of Practice for the Care and Use of Animals for Scientific Purposes. Ethics approval numbers for this thesis are: E/1062/2011/B, E/1111/2011/B, E/1315/2013/B, E/1265/2012/B, 397/09. All animals were housed at AMREP Animal Services Pty Ltd located at the AMREP precinct with a 12-hour light cycle and unrestricted access to water and standard chow. Male 10 week old Sprague Dawley rats, 8-10 week old C57BL/6 and caveolin-1 knockout (*Cav1$^{-/-}$*), 8-10 week old *Apoe$^{-/-}$* and BPHx *Apoe$^{-/-}$* mice were used in the studies described within this thesis. *Cav1$^{-/-}$* mice were backcrossed to a C57BL/6 genetic background as previously described (Fu *et al.*, 2012).

2.2.1 Pressurising carotid arteries

This methodology was developed and optimised as part of this candidature and has been published (Michell et al., 2011b); Chapter 3). This methodology describes vessels that were pressurized under no flow during incubation. The purpose of these experiments was

to observe the effect of pressure alone on leukocyte adhesion. As such standard flow rate (1 ml/min) was used for both pressure values. The effect of different shears was then observed later in vessels exposed to the same pressure.

10-week-old Sprague Dawley rats were euthanized via 100% CO_2 asphyxiation. Left and right common carotid arteries, aorta and heart were excised and placed in ice-cold Krebs buffer.

2.2.1.1   Shear stress in rat carotid arteries

This technique was developed and optimised as part of this candidature. The shear stress exerted on the vessels was mathematically estimated using Hagen-Poiseuille's equation: $\tau = 4\eta Q/\pi r^3$; τ = shear stress (dyn/cm^2); η = viscosity (poise); Q = flow (ml/sec); and r = radius (cm). Viscosity of the labelled whole blood was assumed to be 0.035 poise (Ibrahim *et al.*, 2003). To determine the radius of a vessel, snap shot images of carotids pressurised to 120 mmHg were acquired using the Zeiss Axiovision software at 160x magnification followed by a scale captured at the same magnification. At the standard flow rate (100 µl/min) shear stress was calculated at 1.67 dyn/cm^2, equivalent to LSS. The vessels were then subjected to LSS during incubation and perfusion of the blood. In order to subject vessels exposed to the same pressure to HSS the flow was increased to 1 ml/min (16.7 dyn/cm^2) during both incubation and perfusion of blood.

2.2.2 Stimulated mouse aorta for *ex vivo* vessel chamber

8-10 week old mice were euthanized via 100% CO_2 asphyxiation. Aorta and heart were gently excised and placed in ice-cold Krebs buffer. The aorta was cleaned, placed in 2 ml Krebs buffer with or without mTNFα (5ng/ml) and incubated for 4 hours at 37°C, in 5% CO_2. Following incubation, vessels were mounted on the vessel chamber primed with Krebs buffer maintained at physiological pH by infusing carbogen gas (95% O_2; 5% CO_2) at 37°C.

2.2.3 Leukocyte adhesion in *ex vivo* vessel chamber

Following 1 hr pressure incubation or 4 hr TNFα stimulation, heparinised (30 units) human whole blood was fluorescently labelled with DiI (1:1000; Invitrogen, #V-22885) and perfused (100 µl/min) through mounted vessels for 10 mins. Two separate fields were visualised at 1, 3, 5, 7.5 and 10 min, and 15 second recordings were acquired using the Zeiss SteREO Discovery V.20 fluorescent microscope coupled to a digital camera and controller (Hamamatsu Corp) and Zeiss Axiovision Rel. 4.8. Leukocyte adhesion was quantified by the number of cell to vessel wall interactions per field of view. Previous experiments in the lab demonstrate no changes in adhesion comparing blood from different species or donors (Woollard *et al.*, 2008).

2.3 Extraction of nucleic acids and protein

2.3.1 Homogenizing vessels for RNA

This technique was developed and optimised as part of this candidature. Using the Micro-Dismembrator S (Sartorius, BBI-8531722), vessels were placed in shaking flasks with a grinding ball kept on liquid nitrogen. 300 µl of an acid phenol guanidine isothiocyanate solution (TRIzol; Invitrogen, #15596) was added to each vessel and the flasks sealed. The flasks were shaken at 2,000 RPM for 30 sec. Homogenized vessel powder was stored at -80°C until RNA isolation.

2.3.2 Homogenizing cells for RNA

Following washing with cold PBS (phosphate buffered saline), cells were lysed when 300 µl of TRIzol was added per 10 cm^2 surface area of cells. Cells were then resuspended several times and stored at -80°C until RNA isolation.

2.3.3 RNA isolation

RNA was isolated with TRIzol according the method by Chomczynski and Sacchi in 1987 (Chomczynski & Sacchi, 1987). The RNA was separated using a chloroform phase

separation method in which RNA is found in the aqueous phase, and proteins and DNA in the organic and interphase, respectively. RNA was then precipitated with isopropanol.

Samples in 300 µl TRIzol were thawed on ice and incubated for 5 min at room temperature to dissociate the nucleoprotein complexes. Chloroform (60 µl) was added and samples were vigorously shaken for 15 sec and then incubated at room temperature for 3 min. Samples were spun at 12,000 g for 15 min at 4°C to separate the phases. 150 µl of isopropanol was added to the aqueous phase and the samples were mixed and incubated at room temperature for 10 min. After centrifugation at 12,000 g for 10 min at 4°C the supernatant was removed and 75 % ethanol was added to the pellet. Samples were vortexed and centrifuged again at 7,500 g for 5 min at 4°C. The supernatant was removed and the pellets left to air dry for 10 min. RNA was then dissolved in 20 µl of warm (60°C) ultra-pure water and heated at 60°C for 10 min. Samples were spun down and measured for total RNA quantity and purity using the NanoDrop 2000 spectrophotometer (Thermo Scientific).

2.3.4 DNase treatment of RNA

To remove any remaining genomic DNA in the total RNA, the sample (2 µg made up to a final volume of 16 µl with RNase free water) was treated with 2 µl of DNase (Promega, #M610A) and 2 µl DNase 10 x reaction buffer (Promega, #M198A). Following 45 min incubation at 37°C, 2 µl of DNase stop solution (Promega, #M199A) was added to each sample to stop the reaction. Samples were incubated at 65°C for 10 min to inactivate the DNase.

2.3.5 First-strand cDNA synthesis from RNA

1 µl of random primer (Promega, #C1181) was added to the total DNase treated RNA (16 µl). Samples were mixed and spun down, heated at 70°C for 5 min and then chilled on ice for a minimum of 5 min. A reaction mix containing 8 µl 5x first strand buffer (Promega, #M531A), 2 µl dNTP mix (Promega, #U1511), 1 µl RNase (Promega, #N2111), 5 µl ultra-pure water and 1 µl M-MLV reverse transcriptase (Promega, #M1705) was added to each sample.

The contents were mixed and collected by brief centrifugation and then incubated at 37°C for 60 min. cDNA (40 ng/μl) was stored at -20°C.

2.3.6 Protein extraction from tissue

Tissues were manually ground in a hand-held tissue grinder (Kimble Chase, 885480-0020) over liquid nitrogen. Lysis buffer (100 μl): 10 mM Tris pH 7.4, 0.1 M NaCl, 1 mM EDTA, 1 mM EGTA, 20 mM Na_4PO_7, 2 mM Na_3VO_4, 0.1% SDS, 0.5% sodium deoxcholate, 1% triton x 100, 10% glycerol, with one complete mini EDTA-free tablet (Roche, #04693159001), and 1 mM of PMSF (phenylmethylsulfonyl fluoride; Sigma, #P7626) was added to each sample. Samples were vortexed and sonicated on ice at 20% intensity for 3 sec. Following 30 min incubation on ice, samples were spun at at 12,000 g at 4°C for 20 min. The supernatant was collected and stored at -20°C.

2.3.7 Protein extraction from cultured cells

After washing with cold PBS, 70 μl of lysis buffer was added per 10 cm^2 surface area of cells. Cells were scraped, vortexed, and sonicated at 14% intensity for 3 sec on ice. They were incubated on ice for 30 min and centrifuged at 12,000 g for 20 min at 4°C. The supernatant was collected and stored at 20°C.

2.3.8 Protein determination

To determine the total protein in each sample a colourimetric assay (Bio-Rad, 500-0007), based on the Lowry assay (Lowry *et al.*, 1951), was used. An alkaline copper tartrate solution (25 μl) was added to each sample and bovine serum albumin (BSA) dilution standards (5 μl) in a 96-well plate. A dilute Folin reagent was then added (200 μl) and the plate was incubated for 15 min at room temperature. Absorbance was read at 750 nm on a spectrophotometer. Sample protein concentration was then determined from a standard curve. Lysates were then used for eNOS monomer:dimer expression (section 2.5.1) or arginase activity (section 2.6).

2.4 Real time quantitative PCR

Reverse transcribed cDNA from each sample was used for PCR (polymerase chain reaction) amplification with specific primer pairs for certain genes (Table 2.1). Reaction volume for each sample consisted of 2 µl cDNA, 0.045 µl forward primer, 0.045 µl reverse primer, 5.41 µl ultra-pure water, and 7.5 µl SYBR mix (Roche, #14551800). Samples were then run for the gene of interest and the housekeeper (mouse and human: 18s, rat: RpIp1) under the following cycling conditions: holding stage 95°C for 10 min; cycling stage 95°C for 10 sec, 60°C for 30 sec; continuous melt curve stage 95°C for 15 sec, 60°C for 1 min, 95°C for 15 sec, 60°C for 15 sec. Expression of the gene of interest was calculated using comparative C_T ($\Delta\Delta C_T$) method normalised to the housekeeper.

Table 2.1. Primers for PCR

Species	Target	Primer sequences (5' – 3')	
Human	18s	Fwd:	GCCGCTAGAGGTGAAATTCTTG
		Rev:	CATTCTTGGCAAATGCTTTCG
Human	ICAM-1	Fwd:	GCTGGAGCTGTTTGAGAACAC
		Rev:	CAAGTTGTGGGGGGAGTCG
Human	MCP-1	Fwd:	TTCTGTGCCTGCTGCTCAT
		Rev:	GGGGCATTGATTGCATCT
Rat	RplpI	Fwd:	CTGGTGGTCCTGCTCCAT
		Rev:	TGTCATCCTCGGATTCTTCA
Rat	ICAM-1	Fwd:	GCAGACCACTGTGCTTTGAG
		Rev:	TCCAGCTCCACTCGCTCT
Rat	MCP-1	Fwd:	AGCATCCACGTGCTGTCTC
		Rev:	ATCATCTTGCCAGTGAATGAG
Rat	eNOS	Fwd:	TGACCCTCACCGATACAACA
		Rev:	ATGAGGTTGTCCGGGTGTC
Rat	Arginase I	Fwd:	CCGCAGCATTAAGGAAAGC
		Rev:	CCCGTGGTCTCTCACATTG
Rat	Arginase II	Fwd:	CTAGTGAAGCTGCGAACGTG
		Rev:	GCCCTAGCAGAAGCAGCTC
Rat	P-selectin	Fwd:	AATCCCCCGCAGTGTAAAG
		Rev:	GGGTGTGTACAGTCCATGGTT
Mouse	18s	Fwd:	TTGACGGAAGGGCACCACCAG
		Rev:	GCACCACCACCCACGGAATCG
Mouse	ICAM-1	Fwd:	CCCACGCTACCTCTGCTC
		Rev:	GATGGATACCTGAGCATCACC
Mouse	MCP-1	Fwd:	TCTTACCTGTGCGCTGTGAC
		Rev:	ACTGGATCTTCAGGGAATGAGT

2.5 SDS-PAGE and Western blotting

For separation of the proteins, samples were run on a cold SDS-PAGE gel at 0.02 amps at 4°C. They were then transferred onto a PVDF membrane overnight at 15 volts at 4°C. Following washing with TBS (tris buffered saline) and blocking with 3% skim milk for 1 hr, the membrane was incubated with either the primary antibody or the housekeeper antibody and incubated on a shaker (20 rpm) overnight at 4°C. The primary antibody was then washed off with TBST (TBS and 0.1% tween20; Sigma, #P5927) 4 times (10 min each) and the membranes were incubated with the secondary antibody on the shaker (60 rpm) for 1 hr at room temperature. The secondary antibody was removed via washing with TBST 4 times (10 min each). Luminol and oxidising chemilumescence solutions (VWR International, #RPN2106) were added (1:1 ratio) and incubated at room temperature in the dark for 1 min. Chemiluminescence was detected by exposure to Amersham Hyperfilm ECL chemiluminescence films (GE Healthcare, #28906839). Bands were then quantified using densitometry by ImageJ 1.47g

2.5.1 eNOS monomer:dimer

To separate any weak disulfide bonds, samples (20-30 µg protein) were thawed on ice prior to incubation at room temperature for 5 min. Samples were run on a 6% SDS-PAGE gel. Membranes were incubated with the primary antibody with either eNOS (1:10,000; BD Transduction, #610297) or β-actin antibody (1:2000; Cell Signaling Technology, #4970) in 1% BSA. Samples were then incubated with the secondary antibody for either eNOS (anti-mouse; 1:2000; Biorad, #170-6516) or β-actin (anti-rabbit; 1:1000; Biorad, #170-6515) in 3% skim milk. Results were expressed as a ratio of monomer to dimer.

2.6 Arginase Activity Assay

This assay was developed and optimised as part of this candidature. Arginase catalyses L-arginine to L-ornithine and urea. This colourimetric assay measures the amount of urea produced as directly proportional to arginase activity.

Arginase activity was determined by measuring the arginase dependent production of urea by spectrophotometry as previously described (Corraliza *et al.*, 1994; Demougeot *et al.*, 2005). Briefly, rat carotid lysates were added to Tris HCl (50 mM, pH 7.4) and 10 mM MnCl$_2$. Arginase was activated by heating the samples for 10 min at 56°C. 100 µl of L-arginine (0.5 M, pH 9.7) was added to the samples for 60 min with shaking at 37°C to hydrolyse the substrate. The reaction was stopped with the addition of 800 µl of acidic solution (H2SO4:H3PO4:H2O = 1:3:7). 50 µl of α-Isonitrosopropiophenone (Sigma, #220094; 9% absolute ethanol) was added and samples were incubated 45 min at 100°C to colourimetrically determine the urea production. Samples were placed in the dark for 10 min and read on a spectrophometer at 540 nm. Arginase activity was determined by the amount of urea production using a urea standard curve and expressed as nmol of urea/mg of protein/min.

2.7 Histology

Following one hour of continuous pressure, rat carotids were perfused with paraformaldehyde (4%) under pressure. Vessels were then removed from the chamber and cut into two-three segments and frozen in optimal cutting temperature embedding compound in liquid nitrogen and stored at -80°C. The ends of the vessels attached to the cannula were discarded. Using a cryostat (Zeiss 102717 Microm HM 550) 6 µm sections were cut and 3 sections (30 µm apart) were placed on the slide with 10 slides per vessel. Slides were then processed for Duolink staining (section 2.7.1) or immunofluorescence of Cav1 and cavin-1 (section 2.7.2.1).

2.7.1 Duolink

This technique was developed and optimised as part of this candidature in collaboration with Rob Parton and Harriet Lo (Institute for Molecular Bioscience, University of Queensland). Duolink® is an *in situ* proximity ligation assay (PLA) that detects endogenous protein interactions, in which a pair of highly specific target secondary antibodies (PLA probes) bind to proteins in close proximity as described previously (Thymiakou & Episkopou, 2011).

Slides containing 6 μm sections of rat carotid arteries were soaked in PBS. Once dry, paraffin circles were drawn around each section. One drop of blocking solution (0.2% BSA, 0.2% fish skin gelatine; FSG) was added for 15 min to cover each frozen section. Blocking solution was aspirated and samples were incubated in a pre-heated humidity chamber for 30 min at 37°C following the addition of the following primary antibodies: Cav1 (1:200; BD, #610407) and Cavin 1 (1:150; made in Parton laboratory) for Duo positive slides, and Cav1 (1:200) only for Duo negative slides. Sections were then placed back in the humidity chamber overnight. Slides were aspirated and washed twice for 5 min with TBST. Secondary antibodies conjugated with the PLA probes (Olink Bioscience, minus: 82024, plus: 82022) were added (1:5) and slides were incubated in the humidity chamber for 1 hr at 37°C. The secondary antibody was then tapped off and slides were washed again twice for 5 min with TBST under gentle agitation. To join PLA probes in close proximity, a ligase solution (Olink Bioscience, 92007-0100) containing two oligonucleotides was added to each section and incubated for 30 min at 37°C. The ligase solution was then tapped off and slides were washed twice for 2 min with TBST under gentle agitation. To fluorescently assess the binding of the PLA probes, an amplification/polymerase solution was added to each section and incubated in the humidity chamber for 100 min at 37°C. Slides were washed in TBS twice for 10 min followed by 1 min in 0.01x TBST. Slides were then left to dry at room temperature in the dark. All slides were aspirated and DAPI stain (4',6-diamidino-2-phenylindole; 1:500, Invitrogen, #D21490) was added and incubated for 10 min. Slides were then rinsed in distilled water and coverslips were mounted in mowiol (Sigma, #D2522) mounting medium. Slides were dried overnight at room temperature and then stored at 4°C before imaging.

2.7.2 Immunofluorescence

2.7.2.1   *Caveolin 1 and Cavin 1*

Slides were soaked in PBS and once dry, paraffin outlines were drawn around each section. Blocking buffer (0.2% BSA, 0.2% FSG in PBS) was added to each section and incubated at room temperature for 15 min. One section from each slide was aspirated and the primary antibody mix (30 μl) consisting of Cav1 (1:200), Cavin1 (1:150) and the blocking solution was added. After incubating overnight at 4°C, slides were washed 3 times for 5 min

with PBS. Secondary antibody mix (30 μl) was added to all sections consisting of alexa fluor®

anti-mouse 488 (1:500; Invitrogen, #A11029), alexa fluor® anti-rabbit 555 (1:500; Invitrogen,

#A21429) and blocking solution. Following 30 min incubation at room temperature, sections

were then washed 3 times for 5 min in PBS. All slides were aspirated and DAPI stain (1:500;

Invitrogen, #D21490) was added and incubated for 10 min. Slides were then rinsed in

distilled water and coverslips were mounted. Slides were dried overnight at room

temperature and then stored at 4°C before imaging.

2.7.2.2   NFκB

This technique was developed and optimized as part of this candidature. HUVECs

were treated for 30 mins with either TNFα (5 ng/ml) or pressurised to 0, 120 mmHg and

then fixed in 4% formaldehyde for 15 min at room temperature. Cells were blocked for 1 hr

in PBS (0.3% TritonX100, 5% normal rabbit serum) at room temperature and then incubated

overnight at 4°C with the primary antibody (1:50; NFκB; Cell Signaling Technology, #8242) in

PBS (0.1% tween20, 0.1% BSA). Cells were washed with PBS 3 times for 5 min and incubated

for 1 hr at room temperature with the secondary antibody alexa fluor® 546 (1:500;

Invitrogen, #A11035) in PBS (0.1% tween20, 0.1% BSA). After three further 5 min washes in

PBS, cells were counterstained and mounted in DAPI mounting medium (5 μl; Invitrogen,

P36935). Using a Nikon AR1 confocal microscope (Monash Microimaging) a z-stack image

was recorded from three separate fields of view for each sample. Analysis of both cytosolic

and nuclear fluorescence, were conducted by thresholding each z-stack for each slice using

Fiji 1.47t and measured according to the following equation: *(integrated density/area)-*

background.

2.8 Electron microscopy of rat carotid arteries

Pressurised rat carotids were fixed with 100 mM cacodylate buffer pH 7.4 containing

2.5% glutaraldehyde. They were cut into 1 mm thick segments and washed 3 times for 10

min in 100 mM of fresh cacodylate buffer and stored at 4°C. Segments attached to the

vessel chamber cannulas were discarded. Samples were fixed in a biowave at 150 watts (20

seconds on, 1 min off, 1 min on), rinsed in 100 mM sodium cacodylate and fixed with 1% osmium tetroxide in 100 mM cacodylate buffer (2 mins on, 2 min off, 2 min on and 80 watts). Following a water rinse samples were dehydrated in acetone followed by epon resin infiltration at 250 watts. Samples were incubated overnight at 60°C to polymerize the resin.

Sectioning was undertaken on a Rechert Ultracut S ultramicrotome at Monash Micro Imaging BioEM facility, Monash University. The epon block was trimmed and 70 – 90 nm sections were cut using a Diatome 45° diamond knife. Sections were collected on 200 square mesh Copper-Paladium grids. Sections were stained with 2% uranyl acetate, washed with distilled water and then stained with Reynold's Lead Citrate solution for 5 min and washed again. Sections were allowed to dry at room temperature.

2.8.1 Imaging caveolae

Using a transmission electron microscope (Hitachi H7500) (Monash Micro Imaging BioEM, Monash University) images were captured at 60,000x magnification. Caveolae were defined as 60-100 nm invaginations of the luminal membrane. Two fields from each cell were counted using ImageJ with an average taken from a minimum of 25 cells per vessel. Length of the plasma membrane was also quantified and results were expressed as the number (#) of caveolae/length of luminal membrane (μm).

2.8.2 Ruthenium red staining of caveolae

Pressurised rat carotids were fixed with 100 mM cacodylate buffer pH 7.4 containing 2.5% glutaraldehyde and 1 mg/ml of ruthenium red. Vessels were cut into 1 mm thick segments with the ends discarded and the samples were washed 3 times for 10 min in 100 mM cacodylate buffer. Samples were osmicated for 3 hr in 100 mM cacodylate buffer pH 7.4 containing 15 osmium tetroxide and 1 mg/ml ruthenium red. Samples were washed 3 times for 10 min with 100 mM cacodylate buffer and stored at 4°C. Professor Rob Parton (University of Queensland) then conducted the sectioning, imaging and analysis.

Chapter 3

Imaging leukocyte adhesion to the vascular endothelium at high intraluminal pressure

Declaration for Chapter 3

Declaration by candidate

In the case of Chapter 3, the nature and extent of my contribution to the work was the following:
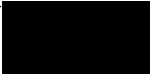
Nature of contribution	Extent of contribution (%)
Performed 95% of the experiments, data and statistical analysis and the preparation of the manuscript and video	80%

The following co-authors contributed to the work. If co-authors are students at Monash University, the extent of their contribution in percentage terms must be stated:

Name	Nature of contribution	Extent of contribution (%) for student co-authors only
Karen Andrews	Provided technical expertise, intellectual input and editing of manuscript	N/A
Kevin Woollard	Provided intellectual input and editing of manuscript	N/A
Jaye Chin-Dusting	Provided intellectual input and editing of manuscript	N/A

The undersigned hereby certify that the above declaration correctly reflects the nature and extent of the candidate's and co-authors' contributions to this work*.

Candidate's Signature	███████	Date 12/01/2014

Main Supervisor's Signature		Date

*Note: Where the responsible author is not the candidate's main supervisor, the main supervisor should consult with the responsible author to agree on the respective contributions of the authors.

Preface

Hypertension remains the leading biomedical risk factor for CAD. Interestingly, the majority of research has focused on the causes of hypertension and their role in the progression of atherosclerosis, the underlying cause of CAD. Animal models that have investigated the effects of hypertension in atherosclerosis development and progression (Tropea *et al.*, 1996; Knowles *et al.*, 2000b; Weiss *et al.*, 2001; Mazzolai *et al.*, 2004) have shown that hypertension enhances atherosclerosis. However, these *in vivo* models are, by their nature, influenced by all the systemic factors involved including various neurohumoral signals (e.g. angiotensin II) that also stimulate inflammation. As a result, it is difficult to determine what role, if any, pressure *per se* plays. While some studies have assessed the effect of high intraluminal pressure *per se* on vascular inflammation *in vitro* (Riou *et al.*, 2007), these experiments also had limitations, such as the injection of cultured monocytes instead of the perfusion of whole blood, in addition to studying the systems under static rather than real time, perfusion conditions. Therefore, in order to observe the direct effect of pressure on vascular inflammation we developed an *ex vivo* vessel perfusion method that enables visualisation of leukocyte adhesion in intact vessels under pressure in real time. This method allows the examination of the direct role of high intraluminal pressure on vascular inflammation in a physiological setting. This chapter forms a manuscript accepted for publication by the Journal of Visualized Experiments entitled "Imaging leukocyte adhesion to the vascular endothelium at high intraluminal pressure".

Video Article

Imaging Leukocyte Adhesion to the Vascular Endothelium at High Intraluminal Pressure

Danielle L. Michell, Karen L. Andrews, Kevin J. Woollard, Jaye P.F. Chin-Dusting

Vascular Pharmacology Laboratory, Baker IDI Heart and Diabetes Institute, Monash University

Correspondence to: Jaye P.F. Chin-Dusting at ▮▮▮▮▮▮▮▮▮▮▮▮▮▮

Abstract

Worldwide, hypertension is reported to be in approximately a quarter of the population and is the leading biomedical risk factor for mortality worldwide. In the vasculature hypertension is associated with endothelial dysfunction and increased inflammation leading to atherosclerosis and various disease states such as chronic kidney disease[2], stroke[3] and heart failure[4]. An initial step in vascular inflammation leading to atherogenesis is the adhesion cascade which involves the rolling, tethering, adherence and subsequent transmigration of leukocytes through the endothelium. Recruitment and accumulation of leukocytes to the endothelium is mediated by an upregulation of adhesion molecules such as vascular cell adhesion molecule-1 (VCAM-1), intracellular cell adhesion molecule-1 (ICAM-1) and E-selectin as well as increases in cytokine and chemokine release and an upregulation of reactive oxygen species[5]. *In vitro* methods such as static adhesion assays help to determine mechanisms involved in cell-to-cell adhesion as well as the analysis of cell adhesion molecules. Methods employed in previous *in vitro* studies have demonstrated that acute increases in pressure on the endothelium can lead to monocyte adhesion, an upregulation of adhesion molecules and inflammatory markers[6] however, similar to many *in vitro* assays, these findings have not been performed in real time under physiological flow conditions, nor with whole blood. Therefore, *in vivo* assays are increasingly utilised in animal models to demonstrate vascular inflammation and plaque development. Intravital microscopy is now widely used to assess leukocyte adhesion, rolling, migration and transmigration[7-9]. When combining the effects of pressure on leukocyte to endothelial adhesion the *in vivo* studies are less extensive. One such study examines the real time effects of flow and shear on arterial growth and remodelling but inflammatory markers were only assessed via immunohistochemistry[10]. Here we present a model for recording leukocyte adhesion in real time in intact pressurised blood vessels using whole blood perfusion. The methodology is a modification of an *ex vivo* vessel chamber perfusion model[9] which enables real-time analysis of leukocyte -endothelial adhesive interactions in intact vessels. Our modification enables the manipulation of the intraluminal pressure up to 200 mmHg allowing for study not only under physiological flow conditions but also pressure conditions. While pressure myography systems have been previously demonstrated to observe vessel wall and lumen diameter[11] as well as vessel contraction this is the first time demonstrating leukocyte-endothelial interactions in real time. Here we demonstrate the technique using carotid arteries harvested from rats and cannulated to a custom-made flow chamber coupled to a fluorescent microscope. The vessel chamber is equipped with a large bottom coverglass allowing a large diameter objective lens with short working distance to image the vessel. Furthermore, selected agonist and/or antagonists can be utilized to further investigate the mechanisms controlling cell adhesion. Advantages of this method over intravital microscopy include no involvement of invasive surgery and therefore a higher throughput can be obtained. This method also enables the use of localised inhibitor treatment to the desired vessel whereas intravital only enables systemic inhibitor treatment.

Video Link

The video component of this article can be found at http://www.jove.com/details.php?id=3221

Protocol

1. Isolating carotid arteries

1. Euthanase10 week old Sprague Dawley rats via CO_2/O_2 asphyxiation.
2. Excise left and right common carotid arteries with aorta and heart ensuring minimal stretching of the vessels.
3. In ice cold Krebs buffer separate the carotid arteries from the aorta and heart and perform close dissection.
4. Keep isolated vessels in Krebs on ice before mounting.

Approx. time = 45 mins

2. Priming the vessel chamber

1. At the proximal and distal connectors of the vessel chamber flush Krebs buffer maintained at physiological pH by infusing carbogen gas (95% O_2; 5% CO_2) through the buffer at 37°C.

2. Ensure tubing and cannulas are flushed completely and are aligned.
3. Flush Kreb buffer through the P1 (proximal) and P2 (distal) transducers. Close taps to ensure no air bubbles in the transducers.
4. Connect the transducers to the corresponding connectors and again flush more Krebs buffer ensuring no air bubbles. Close off taps to the chamber.

Approx. time = 15 mins

3. Pressurizing the vessel chamber

1. Turn on pressure equipment: pressure servo, pressure monitor, peristaltic pump (Figure 1).
2. With the peristaltic pump on pressure and the pressure servo on automatic run Krebs buffer through the tubing at 20 mmHg (dial at 1), ensuring no air bubbles.
3. Connect tubing to the closed P2 transducer. Pressure will become stable.
4. Open P2 tap to the vessel chamber to flush out any bubbles then close off.
5. Fill the bath with Krebs buffer (5 - 7 mL).

Approx. time = 10 mins

4. Mounting the vessel

1. Under a dissecting microscope place black polyester ties onto each cannula (Figure 2).
2. Move cannulas and cannula holders apart and mount ¼ vessel (aortic arch end) onto the P1 cannula. Ensure not to tear the vessel.
3. Using a syringe filled with Krebs buffer gently flush excess blood out of the vessel via P1 transducer. Close off P1 to chamber.
4. Secure vessel to the P1 cannula with the polyester tie.
5. Move cannulas/cannula holders closer for mounting onto the P2 cannula.
6. Mount distal end of the vessel (~¼ of the length) onto distal cannula. Secure with polyester tie.

Approx. time = 20 mins

5. Pressurizing the vessel

1. Adjust the cannula holders to ensure no bend or stretch in the vessel.
2. With P1 and P2 closed to the chamber switch the pressure servo from automatic to manual. Check on the pressure servo there is no continual decrease in pressure within 10 seconds. If there is, a leak is occurring and the connections and transducers need to be secured in place.
3. Adjust the pressure servo back to automatic then open P2 to the chamber. Under the microscope observe the vessel dilate when the tap is opened to the chamber.
4. Switch the pressure servo to manual. Again check for continual decrease in pressure within 10 seconds. If there is a leak then the system is not pressure tight and there is likely to be a hole in the vessel.
5. Switch back to automatic open P1 to the chamber. On the manual setting check that the pressure remains stable.
6. If no leak, on manual setting increase dial to 2 (40 mmHg).
7. Adjust to automatic and observe the vessel under the microscope. If necessary, adjust the cannula holder to ensure no bend in the vessel. Check for leaks on manual setting.
8. Repeat steps 5.6 - 5.7 increasing the dial to 3 (60 mmHg), 4 (80 mmHg) and so on until desired pressure is reached.

Approx. time = 15 - 30 mins

6. Incubating the pressurized vessel

1. Connect the temperature controller set to 37°C.
2. With a second peristaltic pump perfuse Krebs buffer (1 mL/min) into the vessel chamber bath.
3. Connect aspirator to chamber ensuring only the top layer of the bath is removed.
4. Incubate pressurized vessel at 37°C for 1 hour with the pressure set to automatic.
5. Check the pressure is not leaking (switching to manual) periodically.
6. The effects of various pharmacological interventions can be observed by simply adding the compound to the bath during incubation.

Approx. time = 1 hour

7. Perfusing the pressurized vessel with whole blood

1. During incubation obtain at least 7.5 mL human whole blood/vessel collected in 40 U heparin/mL blood. Incubate in a 50 ml falcon at 37°C.
2. 10 minutes before the end of the incubation label blood with VybrantDil (1:1000) for 10 minutes at 37°C in dark.
3. After 10 minutes, collect blood in a syringe clearing any bubbles and attach onto a syringe pump with a heat jacket set at 37°C.
4. Close off P1 transducer to the chamber/vessel and connect syringe and waste tubing.
5. Purge blood at 1000 µL/min through the waste tubing to remove any bubbles.
6. Open P1 to the chamber. The pressure servo will adjust automatically to maintain desired pressure.
7. Perfuse blood at 100 µL/min.
8. Using a fluorescent microscope coupled to a digital camera record two fields of the perfused vessel for 15 seconds at 1, 3, 5, 7.5 and 10 minutes.
9. Post perfusion endothelial integrity and function can be assessed via pharmacological techniques such as myograph and adhesion molecule expression can be determined by immunohistochemistry to further validate the inflammatory response.

Approx. time = 15 mins

8. Representative Results:

A schematic diagram of the pressure chamber setup is shown in **Figure 1**. With a digital camera coupled to a fluorescent microscope results can be visualised instantly via live video recordings. Representative video images are seen in **Figure 3** where leukocytes are considered to be adherent to the endothelium if they remained stationary for 10 seconds. With video recordings on continuous loop adhered cells can be counted as an average per field. While both low (**Figure 3A**) and high (**Figure 3B**) pressure will cause some amount of adhesion a significant increase in leukocyte adhesion at the higher intraluminal pressure is seen and this is also demonstrated quantitatively (**Figure 4**).
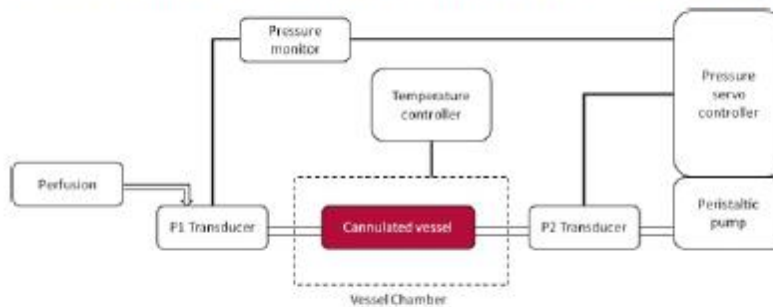
Figure 1. Pressurised ex vivo vessel chamber schematic. A cannulated vessel connected to a proximal (P1) transducer and a distal (P2) transducers that enables blood pressure to be manipulated within the vessel. Perfusion is through the P1 transducer and pressure is maintained via P2 transducer.
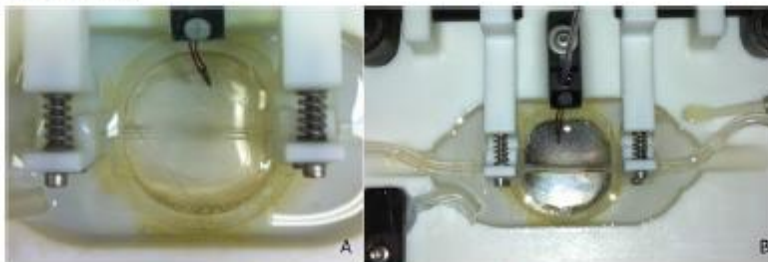
Figure 2. Cannuala with ties. Black polyester ties are attached to each cannula.
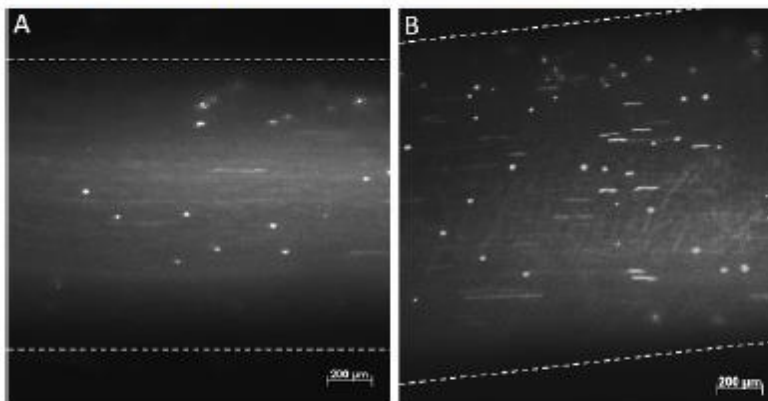
Figure 3. Representative video images. Dynamic cell adhesion (red arrow) under fluorescence at 80 mmHg (A) and 120 mmHg (B) after 10 minutes of perfusion.
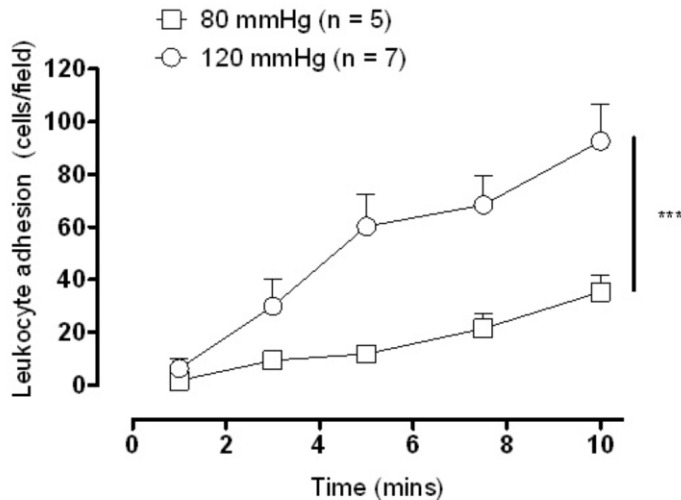
Figure 4. Leukocyte adhesion in Sprague Dawley carotid arteries after 1 hour incubation at low (80 mmHg) and high pressure (120 mmHg). ***$P<0.001$, as analysed by 2-way repeated measures ANOVA using Bonferroni post hoc test.

Discussion

This is a modified method to study leukocyte adhesion to the endothelium in intact isolated blood vessels under pressurised conditions in real time. Perfusion of the vessel chamber alone enables a quick validation of pro-inflammatory strains of large mice and rat vessels. Enabling pressure manipulation allows dynamic cell interactions to be observed from low to very high intraluminal pressures, thus better mimic-ing physiological and pathophysiological conditions. Diameter of vessels can also be measured using a sufficient cell-imaging program and therefore shear flow and rate can be determined and therefore manipulated.

With its myograph capabilities, pharmacological interventions placed in the bath add another dimension to the experimental conditions possible with this model enabling studies of mechanistic and signalling pathways. While endothelial preservation cannot be confirmed during pressure manipulation, responses to ACh and PE can be conducted post perfusion[9].

It should be noted that this setup demonstrates the effects of intraluminal pressure on cell-to-cell interactions not the effects of pulsatile blood flow nor systolic or diastolic pressures. Furthermore, while acute pressure changes on leukocyte adhesion were observed, this setup can be also utilised to look at chronic pressure effects (ie increasing incubation times and using a chronic pressure animal model). Sprague Dawley common carotid arteries are demonstrated in this set up but other strains and species may be used with appropriate adjustments to the cannula size. Indeed, it is important to note that the age and weight of animals affect vessel size and thus that the set up needs to be individualised for each vessel. Close and careful dissection of the connective tissue can improve visualisation of leukocytes immensely.

Disclosures

The study protocol was approved by the Alfred Medical Research and Education Precinct Animal Ethics Committee and the Alfred Hospital Ethics Committee.

Acknowledgements

References

1. Lopez, A.D., Mathers, C.D., Ezzati, M., Jamison, D.T., & Murray, C.J. Global and regional burden of disease and risk factors, 2001: systematic analysis of population health data. *Lancet.* **367** (9524), 1747-1757 (2006).
2. Szczech, L.A. *et al.* Acute kidney injury and cardiovascular outcomes in acute severe hypertension. *Circulation.* **121** (20), 2183-2191.
3. Rodriguez-Garcia, J.L., Botia, E., de La Sierra, A., Villanueva, M.A., & Gonzalez-Spinola, J. Significance of elevated blood pressure and its management on the short-term outcome of patients with acute ischemic stroke. *Am J Hypertens.* **18** (3), 379-384 (2005).
4. Levy, D., Larson, M.G., Vasan, R.S., Kannel, W.B., & Ho, K.K. The progression from hypertension to congestive heart failure. *JAMA.* **275** (20), 1557-1562 (1996).
5. Ley, K., Laudanna, C., Cybulsky, M.I., & Nourshargh, S. Getting to the site of inflammation: the leukocyte adhesion cascade updated. *Nat Rev Immunol.* **7** (9), 678-689 (2007).
6. Riou, S. *et al.* High pressure promotes monocyte adhesion to the vascular wall. *Circ Res.* **100** (8), 1226-1233 (2007).
7. Ley, K. & Gaehtgens, P. Endothelial, not hemodynamic, differences are responsible for preferential leukocyte rolling in rat mesenteric venules. *Circ Res.* **69** (4), 1034-1041 (1991).

8. Bernhagen, J. *et al.* MIF is a noncognate ligand of CXC chemokine receptors in inflammatory and atherogenic cell recruitment. *Nat Med.* **13** (5), 587-596 (2007).
9. Woollard, K.J. *et al.* Pathophysiological levels of soluble P-selectin mediate adhesion of leukocytes to the endothelium through Mac-1 activation. *Circ Res.* **103** (10), 1128-1138 (2008).
10. Eberth, J.F. *et al.* Importance of pulsatility in hypertensive carotid artery growth and remodeling. *J Hypertens.* **27** (10), 2010-2021 (2009).
11. Cooke, J.P., Rossitch, E., Jr., Andon, N.A., Loscalzo, J., & Dzau, V.J. Flow activates an endothelial potassium channel to release an endogenous nitrovasodilator. *J Clin Invest.* **88** (5), 1663-1671 (1991).

Chapter 4

Intracellular signalling in pressure-induced inflammation

4.1 Introduction

Hypertension is a major global health burden and recognised as a key risk factor for CAD. However, the exact mechanism by which hypertension contributes to the development of CAD, remains unknown. Atherosclerosis, the underlying cause of CAD, is a progressive inflammatory disease characterised by the accumulation of lipids and fibrous tissue in conduit arteries. Often silent for decades, atherosclerotic lesions can become unstable, leading to plaque rupture and the associated thrombotic events often result in stroke or myocardial infarction (Libby *et al.*, 2011; Tuttolomondo *et al.*, 2012).

Inflammation, and the associated innate and adaptive immune response, is a necessary and beneficial defence mechanism against pathogens, tissue damage or injury. In essence, inflammation localises and eliminates the irritants while repairing surrounding tissue. However, in the vascular bed this defence mechanism can be an initiating event leading to atherosclerosis. The adhesion cascade involving the capture, adhesion and slow rolling of leukocytes on the activated endothelium and transmigration into the smooth muscle intima are all features of atherogenesis (Libby *et al.*, 2011). The activation of the endothelium is generally characterised by the increased expression of adhesion molecules such as VCAM-1, ICAM-1 and P- and E-selectin (Watanabe & Fan, 1998; Cybulsky *et al.*, 2001) as well as cytokines and chemokines such as MCP-1, resulting in the recruitment of leukocytes to the endothelium. Endothelial activation can be triggered by such diverse disturbances as LDL cholesterol, endotoxins and physical trauma, all of which are important in the setting of atherosclerosis. In this context, weibel palade bodies (WPBs), endothelial granules that store vWF, P-selectin, and other vascular modulators, play a critical role as endothelial cells secrete WPBs in response to vascular injury. WPBs release vWF, which triggers platelet rolling and externalisation of P-selectin, which subsequently activates leukocyte trafficking. Endothelial exocytosis is one of the earliest responses to vascular damage and plays a pivotal role in thrombosis and inflammation. Furthermore, many genes that control cellular adhesion molecules expression are under the control of the transcription factor, NFκB. Activation of NFκB relies on the degradation of its cytoplasmic inhibitor, IκB-α, which enables the unbound NFκB to translocate to the nucleus where it induces adhesion molecule expression.

Recent studies, particularly from the Harrison laboratory (Guzik *et al.*, 2007; Marvar *et al.*, 2010), implicate the immune system, in particular the role of T-cells, as having a central role in the development of hypertension. Importantly, very few studies have explored the converse; whether high blood pressure causes inflammation and how this influences the progression of atherosclerosis. Indeed, the only evidence to date investigating a direct effect of pressure on vascular inflammation suggested that high pressure does promote monocyte adhesion to the vascular wall, albeit in a static adhesion setting (Riou *et al.*, 2007).

Neurohumoral signals such as noradrenaline, catecholamines and the RAS play substantial roles in the pathogenesis of hypertension. The RAS in particular is implicated as a major regulator of blood pressure control and salt handling (Griendling *et al.*, 1997). Since Ang II also stimulates vascular smooth muscle cell proliferation, hypertrophy and inflammation, the ability to dissect the causative mechanism between high intraluminal pressure *per se* and non-pressure RAS effects in the exacerbation of atherosclerosis has proven particularly challenging. Past evidence obtained from animal models of hypertension-induced in the atherosclerotic susceptible *Apoe*$^{-/-}$ mouse suggests that the progression of atherosclerosis is primarily due to RAS activation, independent of hypertension (Weiss *et al.*, 2001). Interestingly, even in the setting of RAS-independent hypertension, local generation of Ang II in response to local inflammation has significant pathophysiological relevance to the development of plaques (Weiss *et al.*, 2008). Interestingly, Chen *et al.*, (2001a) report that the accelerated atherosclerosis observed in the *Apoe*$^{-/-}$/*eNOS*$^{-/-}$ mouse is independent of hypertension *per se*, suggesting that the progression to disease is greatly influenced by nitric oxide bioavailability. However, other studies have clearly highlighted a contribution of hypertension in atherosclerosis, in which aortic constriction or stenosis, increased expression of adhesion molecules were observed only in proximal segments where pressure was increased but not distal segments where pressure was normal, effects which were RAS independent (Tropea *et al.*, 1996; Wang *et al.*, 2004). To further complicate matters, *in vitro* experiments assessing high intraluminal pressure on mouse carotid arteries followed by injection of U937 monocytic cells found that Ang II stimulation did not enhance adhesion to the endothelium at either normal or high pressure (Riou *et al.*, 2007). Even if it were true that pressure *per se* plays an important role

in vascular inflammation, the exact mechanisms underlying the effect of pressure remain to be determined.

In this study we have used a customised *ex vivo* vessel chamber ((Michell *et al.*, 2011b); Chapter 3) to assess leukocyte adhesion under pressure in real time in intact vessels using whole blood to test the hypothesis that high intraluminal pressure *per se* induces inflammation. In addition, we aimed to elucidate the intracellular signalling pathways involved.

4.2 Methods

4.2.1 Animals

10-12 week old male Sprague Dawley rats were used in this study. Animals were housed at the Precinct Animal Centre in a room with a 12 hour light:12 hour dark cycle and access to food and water *ad libitum*. Animal experimentation was approved by the AMREP Animal Ethics Committee (Approval No: E/0886/2009/B), which adheres to the National Health and Medical Research Council (NHMRC) Australian Code of Practice for the Care and Use of Animals for Scientific Purposes.

4.2.2 Ex vivo pressure myography

To observe the direct effect of pressure on vascular inflammation, carotid arteries isolated from Sprague Dawley rats (RCA) were pressurised at 60, 80 and 120 mmHg for 1 hr. Vessels were pressurised as previously described in Chapter 3 and either perfused to assess leukocyte adhesion (Section 4.3.3) or snap frozen for gene expression (Section 4.3.4) or eNOS (4.3.5) and arginase (Section 4.3.6) protein quantification.

4.2.2.1 Pharmacological interventions in pressurised arteries

To investigate the intracellular signalling pathways activated in response to high intraluminal pressure we used specific pharmacological blockade of known intracellular inflammatory pathways. RCA were pressurised at 120 mmHg for 1 hr and incubated with the following compounds: AT1R antagonist (candesartan; 100 nM), Nox antagonist (apocynin; 3 µM), cytochrome P450 antagonist (miconazole; 30 µM), xanthine oxidase antagonist (allopurinol; 100 µM), mitochondrial ROS antagonist (cyclosporin A; 2 µM), nitric oxide synthase antagonist (L-NAME; 100 µM), arginase antagonist (BEC; 100 µM). Treated and pressurised vessels were then perfused to assess leukocyte adhesion (Section 4.3.3).

4.2.3 Leukocyte adhesion ex vivo

Following pressurisation, RCA were perfused with human whole blood fluorescently labelled with DiI for 10 min (Alfred Ethics Committee project no. 397/09) and the number of leukocytes adhering to the endothelium were quantified as previously described in Chapter 2, section 2.2.3.

4.2.4 Gene expression analysis with real time quantitative real time PCR

Gene expression analysis of rat and human ICAM-1, MCP-1, eNOS, ArgI, ArgII, human 18S and rat RpIp1 mRNA was performed as previously described in Chapter 2, section 2.3 and 2.4.

4.2.5 Detection of eNOS monomer dimer protein

eNOS monomer and dimer protein was assessed in pressurised HUVECs and RCA. Aorta and endothelial cell lysates were homogenised and analysed by western blot as previously described in Chapter 2, section 2.3 and 2.5, respectively.

4.2.6 Determination of arginase activity by urea production

Arginase activity in pressurised RCA was determined as previously described in Chapter 2, section 2.3.6 and 2.6.

4.2.7 Pressurising endothelial cells

To investigate the influence of pressure on the endothelium we examined human umbilical vein endothelial cells (HUVECs) that were seeded onto collagen coated coverslips, grown to confluence and pressurised at 0, 60 and 120 mmHg as previously described in Chapter 2, section 2.1.2. Cells were assessed for enodothelial microparticle production (section 4.3.8), production of ROS (section 4.3.9), vWF release (section 4.3.10) and NFκB expression (section 4.3.11).

4.2.8 Endothelial microparticle production

Following pressurisation, HUVECs were incubated overnight in 1 ml DMEM at 37°C with 5% CO_2. As an indicator of cell number, total protein concentration was determined in cells by the Lowry assay as previously described in Chapter 2.3.8. Endothelial microparticles (EMP) were isolated using ultracentrifugation. Briefly, the harvested cells were centrifuged at 5,000 g for 10 min at 4°C and the pellet (which largely comprised cell debris) was discarded. The top 95% of supernatant was further spun at 16,000 g for 60 min at 4°C. The bottom 60% was discarded and remaining 40% was used to quantify microparticles. Microparticles were assessed by FACS using a pre-defined microparticle gating strategy involving size selection comparisons with commercial beads sized 0.1, 0.5, 1 and 10 nM (Sigma and BD).

4.2.9 Determination of ROS

The production of reactive oxygen species (ROS) was determined in HUVECs pressurised to 0, 60 and 120 mmHg with DCFH (5 μM) and the more sensitive hydrogen peroxide indicator PF6-AM (5 μM) along with the cell mortality dye propidium iodide (PI; 5 μM) as previously described in Chapter 2, section 2.1.3. In a separate set of experiments L-NAME (100 μM) was added to cells pressurised at 120 mmHg and compared to cells without L-NAME. Unfortunately due to the design of the experiment the effect of L-NAME on basal fluorescence could not be determined. The fluorescence can be triggered very rapidly by a number of factors (i.e. handling, light exposure), as such, a 1-1.5 hour baseline was recorded to ensure a stable basal signal for a minimum of 3 time points. As basal fluorescence can be different for each experiment a % change in baseline was represented to see any actual changes between treatments.

4.2.10   Endothelial von Willebrand Factor release

HUVECs were seeded onto collagen coated coverslips, grown to confluence and unpressurised, pressurised at 80 and 120 mmHg for 1 hr (section 4.4.7), or stimulated with

TNFα (5 ng/ml; 4 hr). The supernatant was used to determine the release of vWF by ELISA (Imubind vWF ELISA kit; American Diagnostica, #828). Briefly, 100 µL of each sample was added to a microwell, covered and incubated for 1 hr. Following washing with 250 µL of wash buffer (PBS, 0.05% Tween 20, pH 7.4; 4 times) 100 µL of substrate (perborate/3,3',5,5' – tetramethylbenzidine) was added to each well to initiate a reaction with the horseradish peroxidise conjugated in the microwells. Following 20 min incubation at room temperature, 50 µL of 0.5 M H_2SO_4 was added to stop the reaction. Samples were read at 450 nm on a spectrophotometer, a standard curve was generated and the vWF release in the samples was determined from the standard curve.

4.2.11   Nuclear Factor κB production by immunofluorescence

HUVECs were seeded onto glass slides and were either unpressurised, pressurised (120 mmHg), pressurised with apocynin, or pressurised with BEC for 30 min. Cells were then fixed, blocked, probed with a primary antibody (1:50; NFκB goat purified) overnight followed by a secondary antibody (1:500; alexa fluor 546 anti-goat) for 1 hr and mounted with DAPI as previously described in Chapter 2, section 2.7.2.2.

4.2.12   Statistics

Data are expressed as mean ± SEM and were analysed using GraphPad Prism version 6.00 software (GraphPad Software, La Jolla, California, USA). Assessment of leukocyte adhesion and ROS production were measured using a two-way repeated measures analysis of variance (ANOVA) with the factors pressure (0 mmHg, 80 mmHg or 120 mmHg) or treatment (presence of absence of pharmacological pathway inhibitors). Gene expression with greater than two groups, eNOS protein expression, urea production, and NFκB expression were analysed using a one-way ANOVA with the factor pressure. Where there were significant differences in analysis of variance, a Bonferroni post hoc analysis was performed to account for multiple comparisons. Endothelial microparticle production and gene expression (which compared two groups) were analysed using an unpaired Student's t-test. *P*<0.05 was considered statistically significant.

4.3 Results

4.3.1 Acute high intraluminal pressure induces endothelial inflammation

Leukocyte adhesion in RCA was greater in vessels pressurised to 120 mmHg compared to 80 mmHg (Fig 4.1A). Leukocyte adhesion following 1 hr of pressure in RCA was comparable between in vessels pressurised to 60 and 80 mmHg. However, RCA pressured to 120 mmHg had a significant 3-fold greater number of adhered leukocytes compared to RCA pressurised to either 60 or 80 mmHg (n=4-5; *P*<0.001; Fig 4.1B).

To determine if the increase in leukocyte adhesion in the vessels pressurised to 120 mmHg was paralleled by an increase in endothelial activation we examined the mRNA gene expression of ICAM-1 and MCP-1. RCA pressurised to 120 mmHg demonstrated a higher ICAM-1 (5.63±1.50) and MCP-1 (100.6±26.2) mRNA expression (n=5-7; *P*<0.05; Fig 4.2A&B) when compared to unpressurised vessels.

To confirm the role of the endothelium in pressure-induced vascular inflammation, we pressurised cultured HUVECs and measured markers of activation. The expression of ICAM-1 was significantly higher at 120 mmHg compared with control, 0 and 80 mmHg (n=5-6; *P*<0.05; Fig 4.3A). We also found a similar trend for one of the key cheomattractants, MCP-1 (n=5; *P*>0.05; Fig 4.3B) although this was not statistically significant. Furthermore, microparticle formation, which is indicative of endothelial activation, was assessed and was also increased in HUVECs following pressurisation to 120 mmHg for 1 hr. The EMP number in the media was increased when quantified 24 hrs after the 1 hr treatment period (n=3; *P*<0.05; Fig 4.4). These data indicate that acute high intraluminal pressure induces endothelial inflammation.
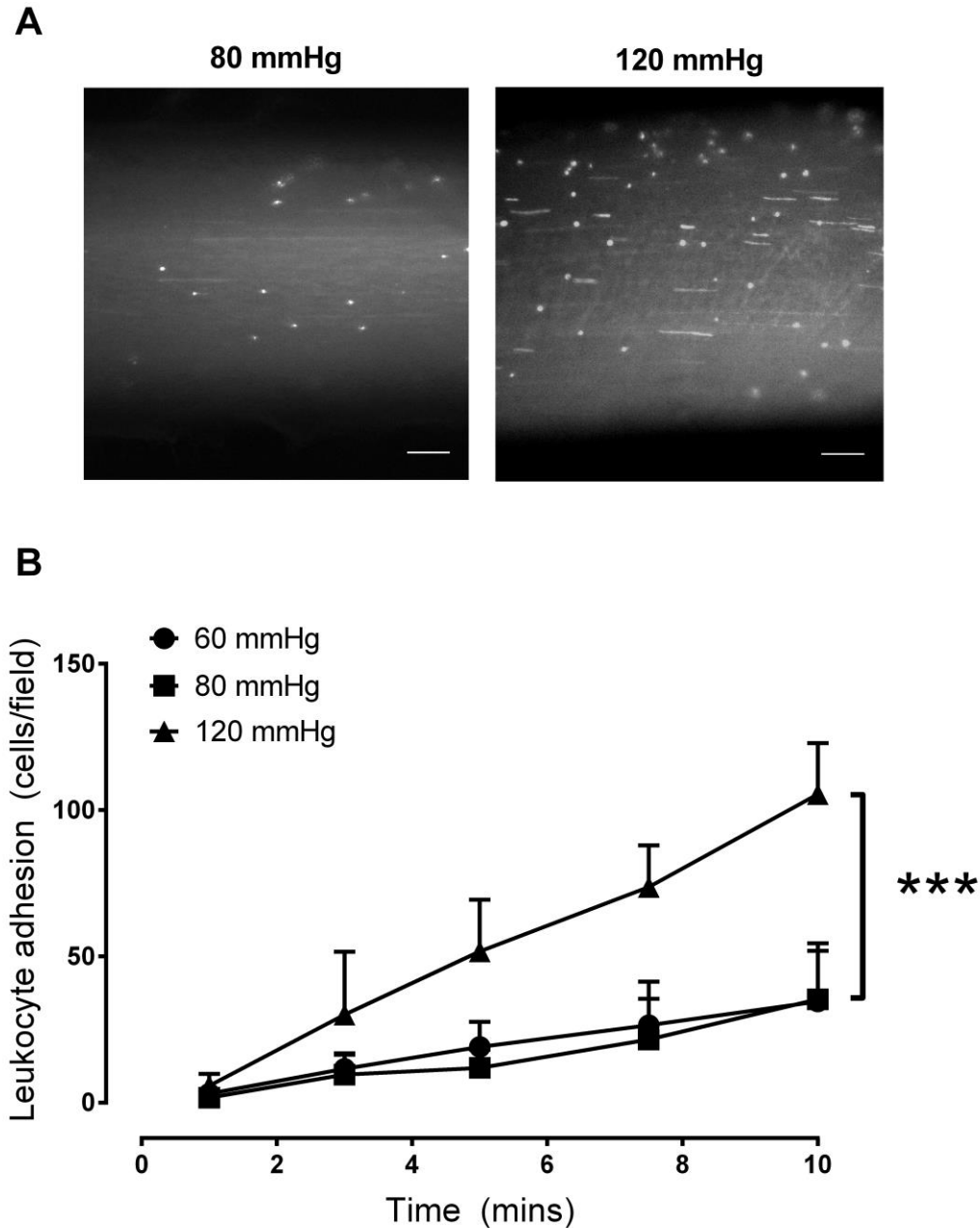
Figure 4.1 Effect of acute pressure on leukocyte adhesion in rat carotid arteries. Carotid arteries from 10 week old Sprague Dawley rats were excised and pressurised (60, 80, 120 mmHg) for 1 hr. (**A**) Representative images of dynamic cell adhesion under fluorescence at 80 and 120 mmHg after 10 min of perfusion. Bar = 200 μm. (**B**) Quantification of leukocytes adhered per field over 10 mins (n=4-5). Results are expressed as mean ± SEM. Data were analysed using a two-way ANOVA with Bonferroni post hoc test. ***P<0.01. vs. 60 mmHg & 80 mmHg.
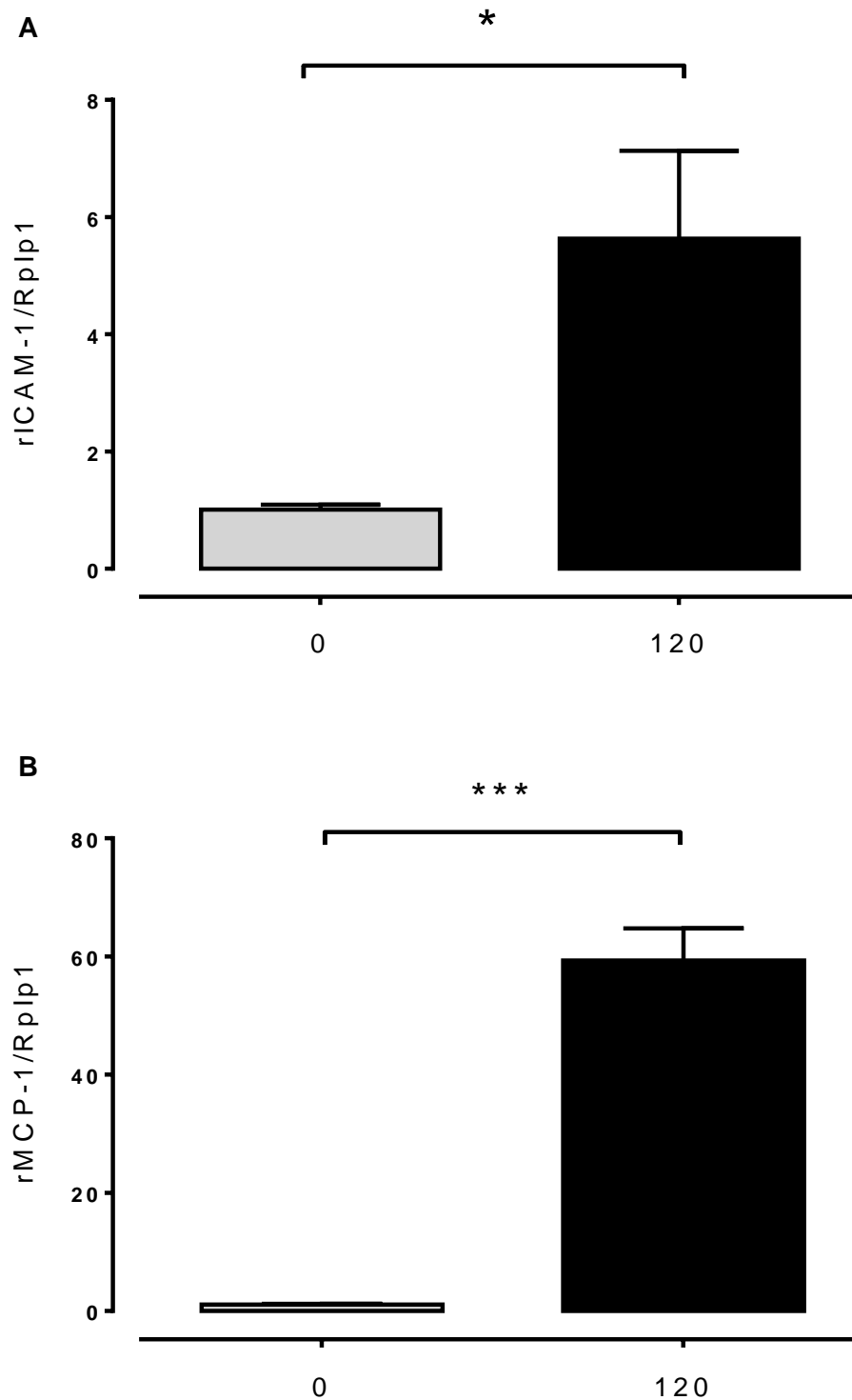
Figure 4.2. Effect of acute pressure on mRNA expression in rat carotid arteries. mRNA expression of ICAM-1 (**A**) and MCP-1 (**B**) relative to Rplp1 in rat carotid arteries pressurised at 0 and 120 mmHg for 1 hr normalised to 0 mmHg (n=5-6). Results are expressed as mean ± SEM. Data were analysed with a Student t-test where *$P<0.05$, ****$P<0.01$.
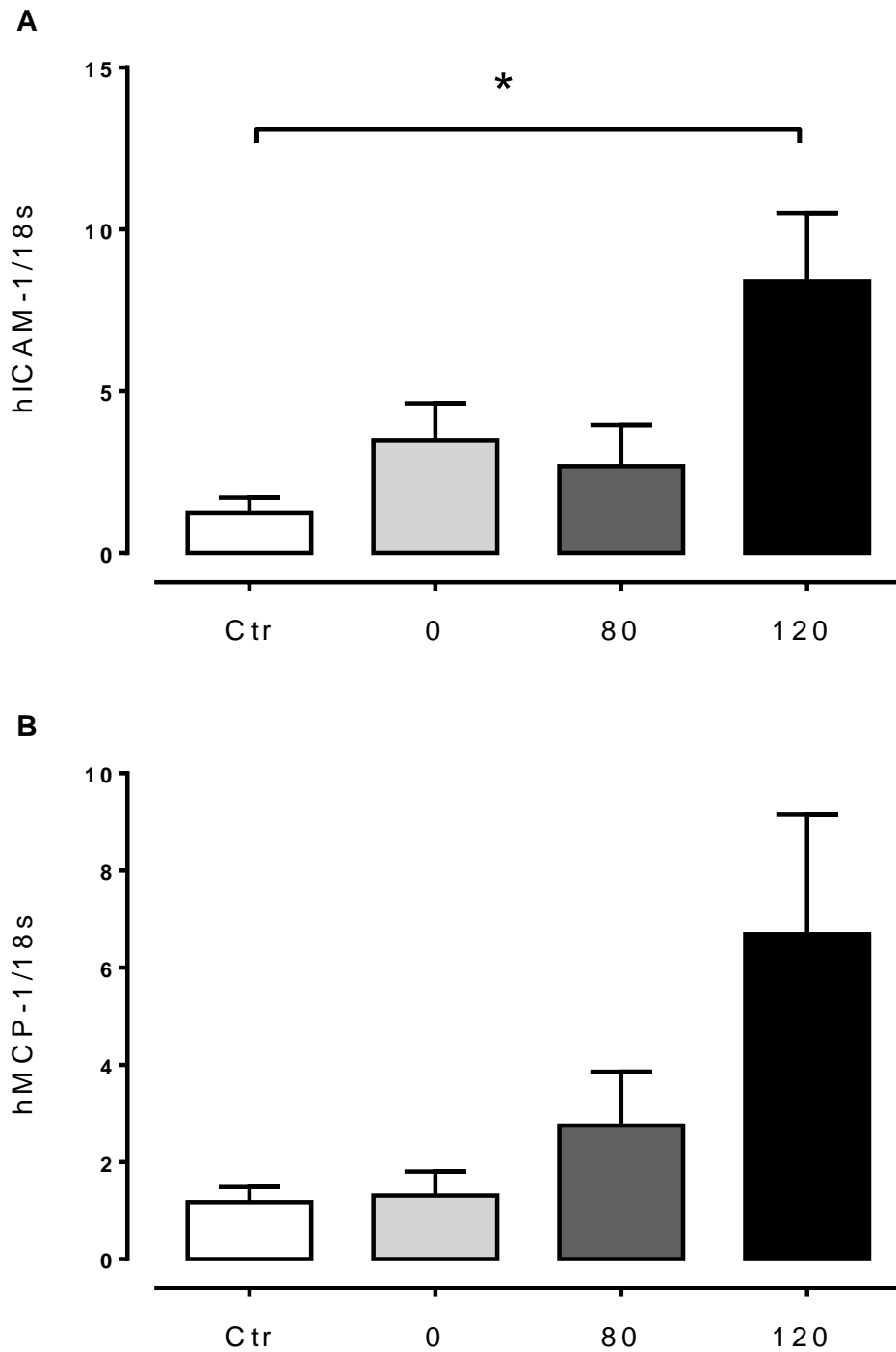
Figure 4.3. Effect of acute pressure on mRNA expression in HUVECs. mRNA expression of ICAM-1 (**A**) and MCP-1 (**B**) relative to 18S in HUVECs pressurised at 0, 80 and 120 mmHg for 1 hr normalised to control (ctr; n=5-6). Results are expressed as mean ± SEM. Data were analysed with a one-way ANOVA with Bonferroni post hoc test where *$P < 0.05$*.
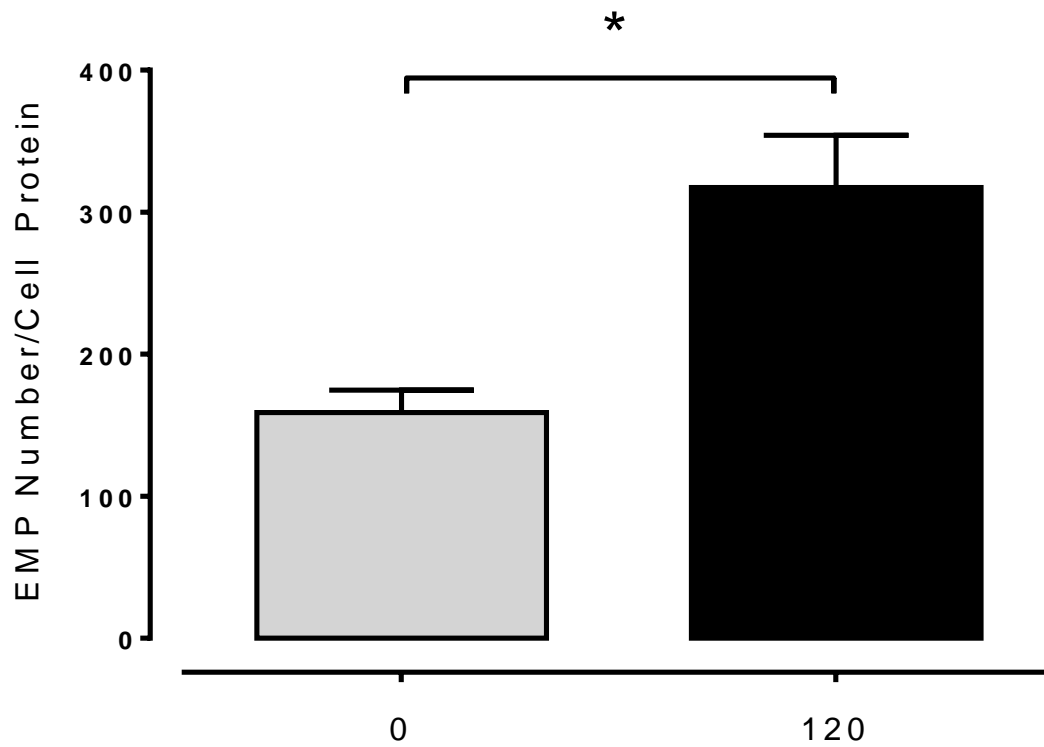
Figure 4.4. Effect of acute pressure on endothelial microparticle production in HUVECs. EMP number in HUVECs pressurised at 0 and 120 mmHg for 1 hr (n=3). Results are expressed as mean ± SEM. Data were analysed with a Student t-test where *P<0.05.

4.3.2 Pressure-induced inflammation is Angiotensin II type 1 receptor independent.

The majority of hypertensive animal models have enhanced signalling through the RAS (Schmieder *et al.*, 2007). Since Ang II is known to exacerbate vascular inflammation and atherosclerosis we sought to determine if AT1R activation was involved in the increase in leukocyte adhesion. To do this we used the AT1R antagonist, candesartan (100 nM). Leukocyte adhesion in RCA pressurised at 120 mmHg in the presence of candesartan was not different to adhesion in RCA pressurised at 120 mmHg (105±8 cells/field vs. 67±23 cells/field; n=4-5; *P*>0.05; Fig 4.5). These data suggest that pressure-induced adhesion is RAS independent.
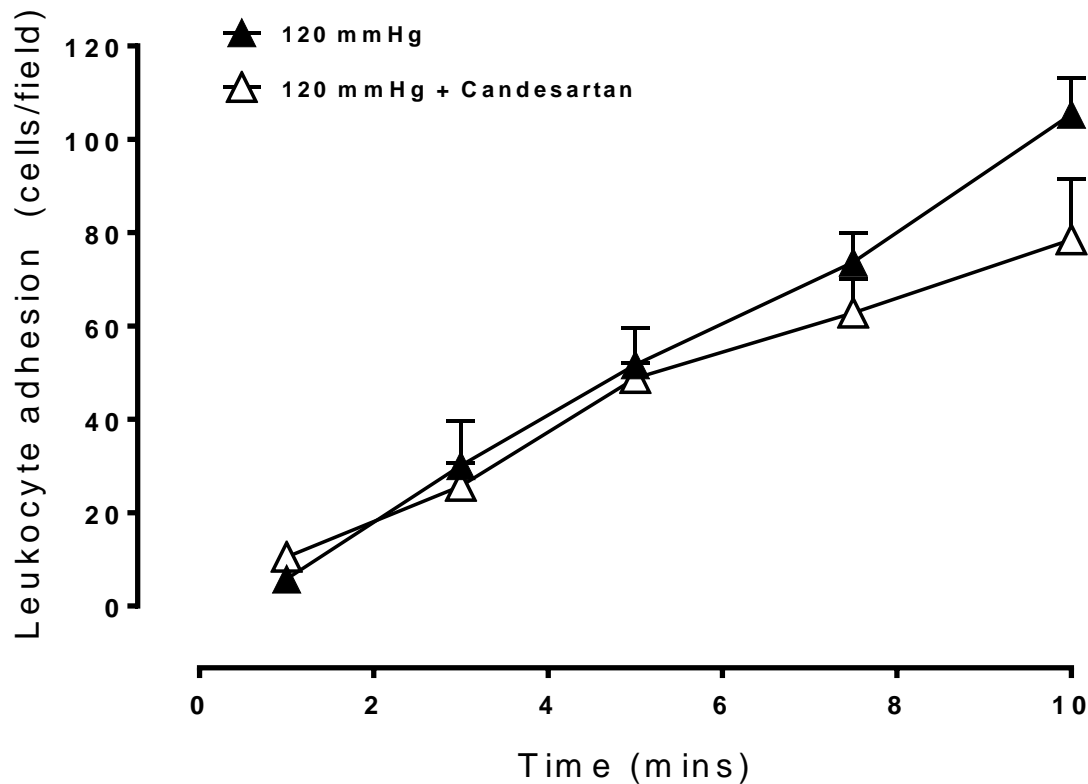
Figure 4.5 Effect of angiotensin receptor 1 blockade on leukocyte adhesion in rat carotid arteries. Leukocyte adhesion in rat carotid arteries under 120 mmHg in the presence and absence of the angiotensin receptor 1 antagonist candesartan (100 nM; n=5). Results are expressed as mean ± SEM. Data was analysed by a two-way ANOVA with *P*>0.05.

4.3.3 ROS plays a role in pressure-induced adhesion

ROS have been implicated to play an important role in both hypertension (Zalba *et al.*, 2001; Touyz & Schiffrin, 2004) and inflammation (Forstermann, 2008; Selemidis *et al.*, 2008). To determine whether pressure *per se* induces ROS production and subsequent inflammation, we examined if pressure-induced endothelial inflammation was dependent on intracellular ROS production via Nox, mitochondrial, xanthine oxidase and/or cytochrome P450). The non-specific Nox inhibitor, apocynin (3 µM) and the mitochondrial ROS inhibitor cyclosporin A (2 µM), both reduced adhesion (n=4-5, $P<0.05$; Fig 4.6A&B) of leukocytes in RCA pressurised to 120mmHg. ROS can be produced by the opening of the mitochondrial permeability transition pore (Batandier *et al.*, 2004) and cyclosporin A is a known blocker of the transition pores and thus can reduce ROS generation shown previously (Argaud *et al.*, 2004, Yuen *et al.*, 2011, Chen *et al.*, 2013). On the other hand, inhibition of xanthine oxidase with allopurinol (100 µM) or inhibition of cytochrome P450 with miconazole (30 µM) did not affect adhesion (4.6 C&D). Therefore, this data implicates a role for Nox and mitochondrial ROS formation in pressure-induced leukocyte adhesion.

To confirm that the pressure-induced ROS is mediated by local endothelial ROS production, we examined production of ROS in pressurised HUVECs (Fig 4.7A&B). We observed no change in global ROS production as measured by DCFH in HUVECs pressurised to 60 mmHg compared to baseline. However, cells pressured at 120 mmHg appeared to rapidly produce significantly higher levels of ROS, which began to subside over time. Importantly, there was no significant difference in cell mortality in response to pressure as determined by PI. Apocynin administration blunted production of ROS at 120 mmHg (5.8±1.2% change after 10 mins; n=6-12; $P<0.05$; Fig 4.7C). Using the more specific probe for hydrogen peroxide, PF6-AM, HUVECs pressurised to 120 mmHg induced a rapid sustained increase in ROS production, which was maintained for 60 mins (22.0±5.3% after 10 mins; n=7; $P<0.05$; Fig 4.7D). PF6-AM at 60 mmHg was initially observed but showed varying results and as PF6-AM was a gift from Christopher Chang (University of California, USA) and in limited quantity we were unable to reproduce consistent results. Thus fluorescence data at 0 mmHg compared to 120 mmHg is shown.

Collectively, these results suggest that increased intraluminal pressure induces local endothelial ROS production that promotes leukocyte adhesion.
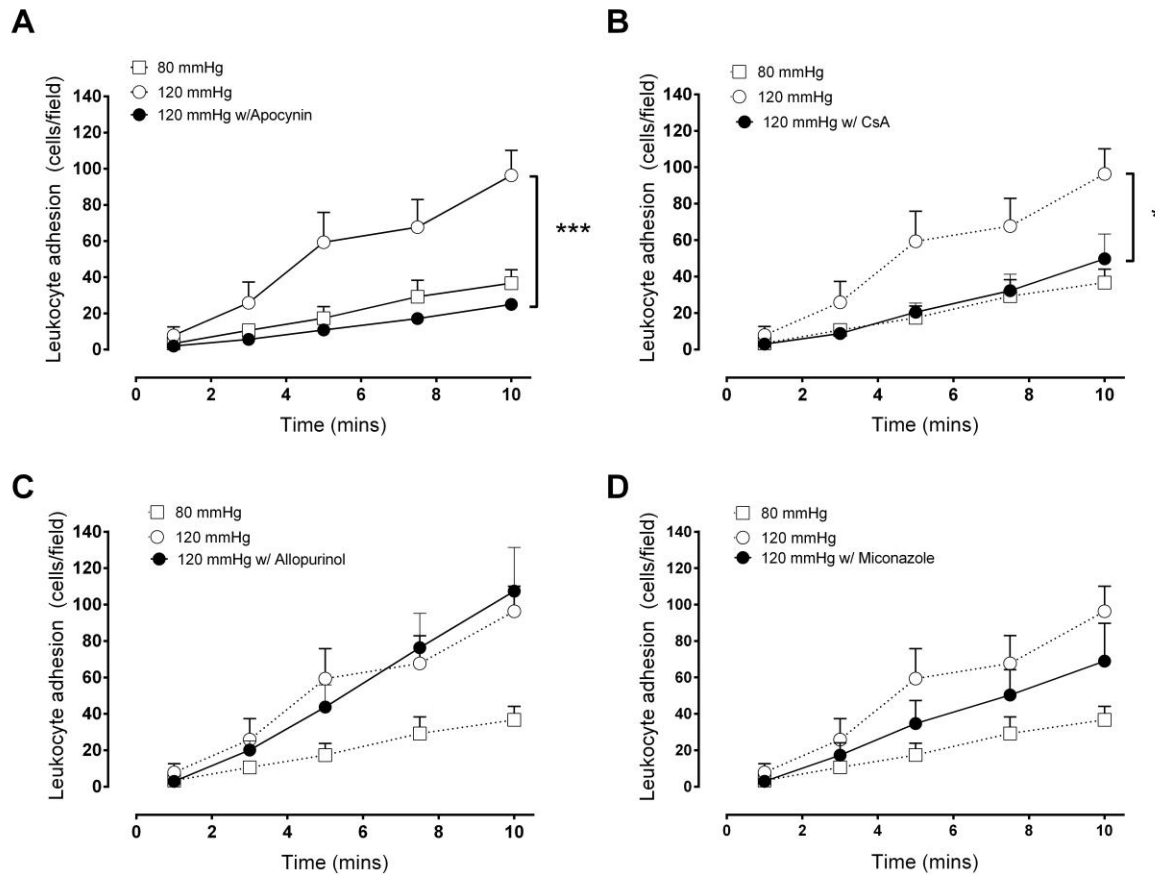
Figure 4.6 The role of local ROS production in pressure-induced inflammation in vessels. Assessment of ROS source was determined by the quantification of leukocyte adhesion in rat carotid arteries during high pressure (120 mmHg) in the presence of **(A)** Nox inhibition (apocynin: 3 µM), **(B)** mitochondrial ROS inhibition (cyclosporine A; CsA; 2 µM), **(C)** xanthine oxidase inhibition (allopurinol; 100 µM) or **(D)** cytochrome P450 inhibition (miconazole: 30 µM), (n=3-5). Results are expressed as mean ± SEM. Data was analysed using a two-way ANOVA with Bonferroni post hoc test where **$P<0.01$, ***$P<0.001$.
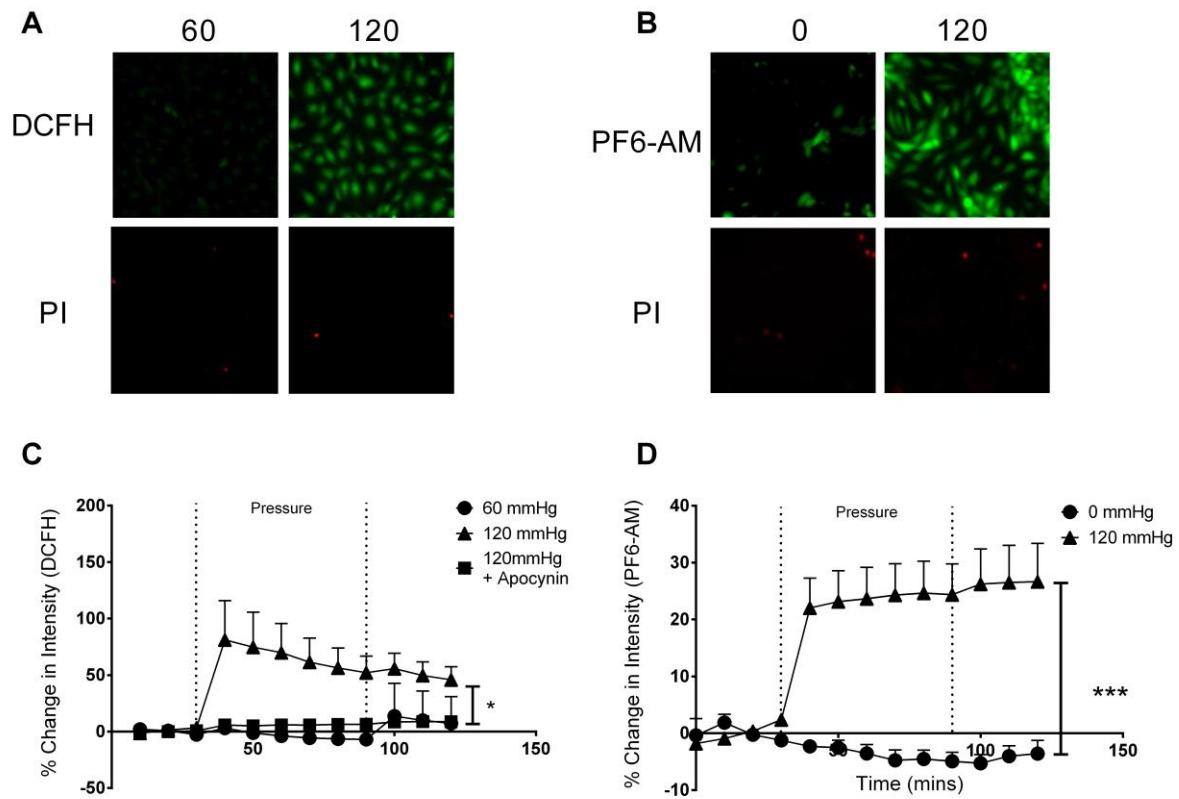
Figure 4.7 Effect of acute pressure on ROS production in HUVECs. (A) and **(B)** Representative images of cultured HUVECs pressurised (0, 60 or 120 mmHg) for 1 hr in a sealed cell chamber demonstrating an increase in intensity of DCFH (5 µM; a non-specific indicator of ROS production) and PF6-AM (5 µM; a chemo-selective fluorescent indicator for hydrogen peroxide) but no increase in propdium iodide (PI; 5 µM; a cell mortality marker). Data is quantified as % change in intensity of **(C)** DCFH or **(D)** PF6-AM (n=5-12 independent experiments). The increase in DCFH was abolished in the presence of the Nox inhibitor apocynin (3 µM). Results are expressed as mean ± SEM. Data were analysed using a two-way ANOVA with Bonferroni posthoc test where *$P<0.05$, ***$P<0.001$.

4.3.4 eNOS does not play a role in pressure-induced inflammation

NO derived from eNOS is a critical regulator of blood pressure, and the uncoupling of eNOS from its dimeric state can be a direct source of superoxide (Ozaki *et al.*, 2002; Takimoto *et al.*, 2005). Therefore, we examined the effect of pressure on eNOS gene expression in RCA (n=4-5; *P*>0.05; Fig 4.8) and monomer:dimer ratio by western blot in HUVECs and RCA (n=4-5; *P*>0.05; Fig 4.9A&B). There was no change in either mRNA levels of eNOS or monomer:dimer in cells or vessels pressurised to 80 and 120 mmHg compared to controls (Fig 4.8-9). To confirm these findings, we examined the effect of NOS inhibition on pressure-induced ROS production using L-NAME (100 µM). DCFH intensity was not different in cells pressurised to 120 mmHg with or without co-incubation with L-NAME (n=4; *P*>0.05; Fig 4.10). Taken together, these findings suggest that eNOS does not play a role in pressure-induced inflammation in this setting.
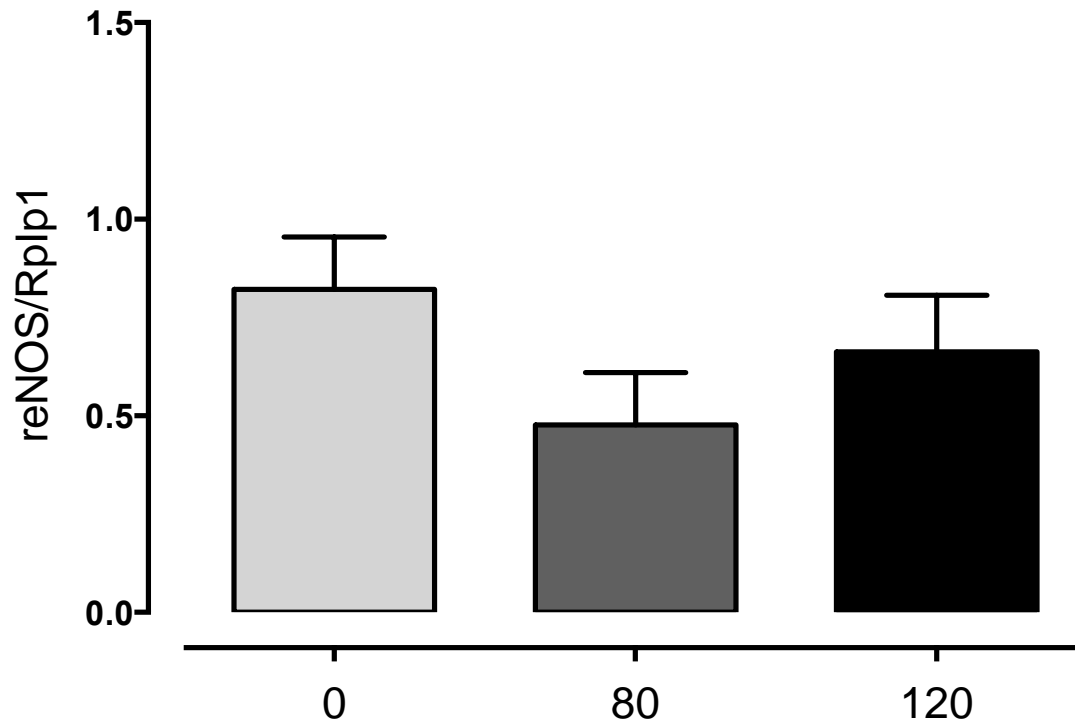
Figure 4.8 Effect of acute pressure on eNOS mRNA expression in rat carotid arteries. mRNA expression of eNOS relative to Rplp1 in carotid arteries pressurised at 0, 80 and 120 mmHg for 1 hr normalised to 0 mmHg (n=4-5). Results are expressed as mean ± SEM.

A

B
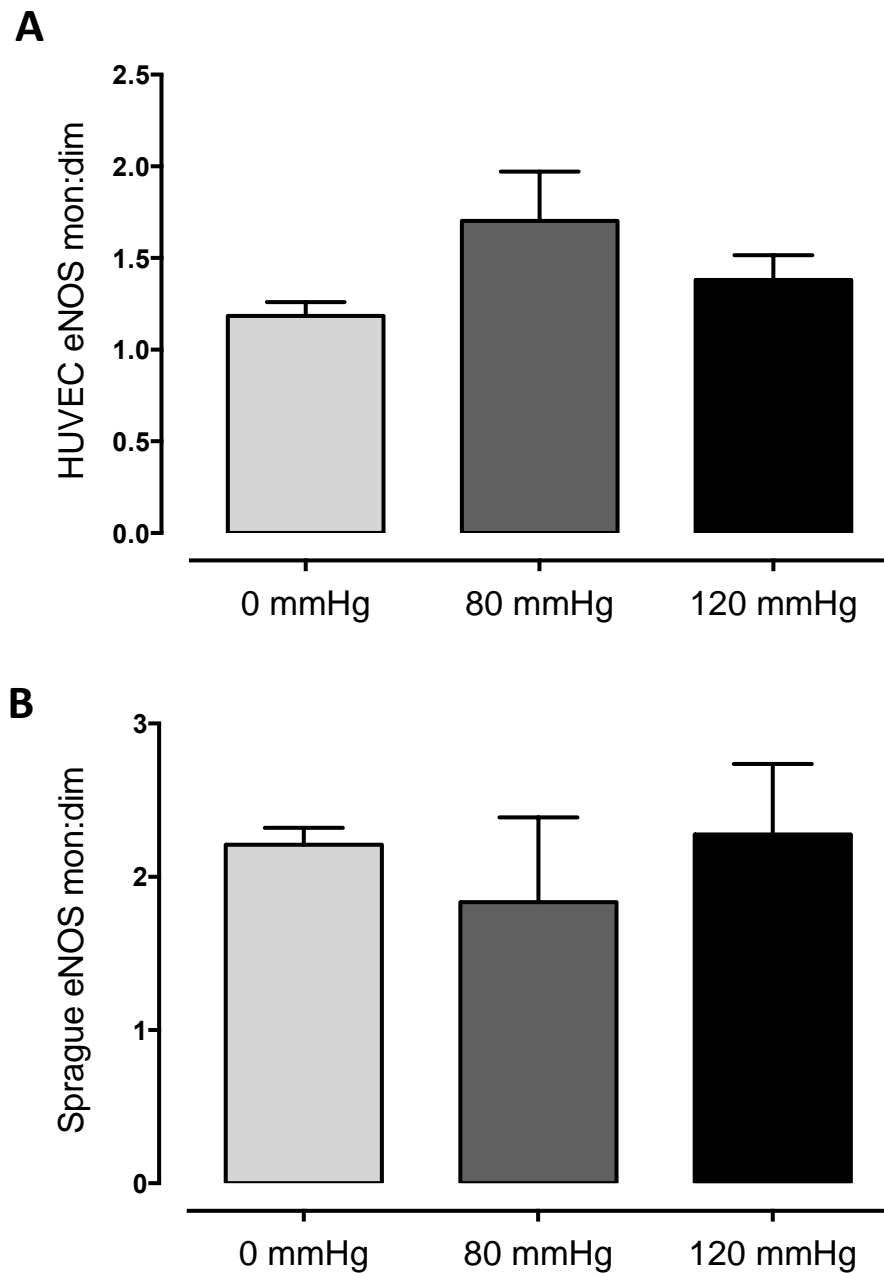
Figure 4.9 Effect of acute pressure on eNOS monomer:dimer ratio. Protein expression of eNOS monomer:dimer (mon:dim) ratio in lysates of **(A)** HUVECs and **(B)** rat carotid arteries pressurised at 0, 80 and 120 mmHg for 1 hr (n=4-6). Results are expressed as mean ± SEM.
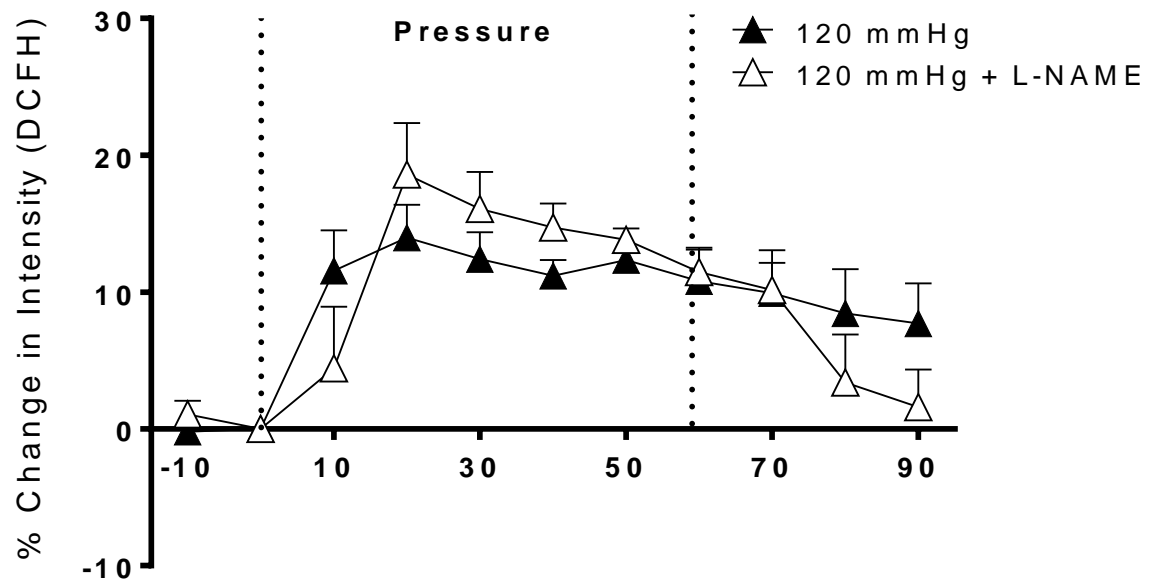
Figure 4.10 Effect of NOS inhibition on ROS production in HUVECs. % Change in intensity from baseline of DCFH (5 µM) a non-specific indicator of ROS in HUVECs pressurised to 120 mmHg in the presence and absence of the NOS inhibitor L-NAME (100 µM), n=4. Results are expressed as mean ± SEM.

4.3.5 Arginase II plays a key role in pressure-induced inflammation

The enzyme arginase (isoforms I & II) competes with eNOS for the substrate L-arginine. Since arginase activity and expression is enhanced in the setting of hypertension (Demougeot *et al.*, 2007a), we aimed to determine the contribution of arginase to pressure-induced inflammation. Leukocyte adhesion to the endothelium in RCA pressurised to 120 mmHg in the presence of the arginase inhibitor BEC (100 μM) was similar to vessels pressurised to 80mmHg (120 mmHg: 96.4±13.8 vs. 120 mmHg + BEC: 43.9±14.7 leukocytes/field; n=4-5; *P*<0.001; Fig 4.11). Gene expression of the ArgI isoform was unchanged with pressure (80 & 120 mmHg; n=3-4; *P*>0.05; Fig 4.12A) but expression of the ArgII isoform was greater in cells pressurised to 120 mmHg when compared to cells pressurised to 80 mmHg and 0 mmHg (0 mmHg: 1.0±0.1 vs. 120 mmHg: 2.0±0.5; n=4-7; *P*<0.05; Fig 4.12B). Similarly arginase activity was greater in vessels pressurised to 120 mmHg compared to 80 mmHg and the unpressurised control vessels (0 mmHg: 4.4±0.6, 80 mmHg: 3.7±1.8, 120 mmHg: 15.1±3.8; n=4-6; *P*<0.05; Fig 4.13). These data suggest that arginase contributes to pressure-induced inflammation and ArgII activity and expression is greater following pressure stimulation.
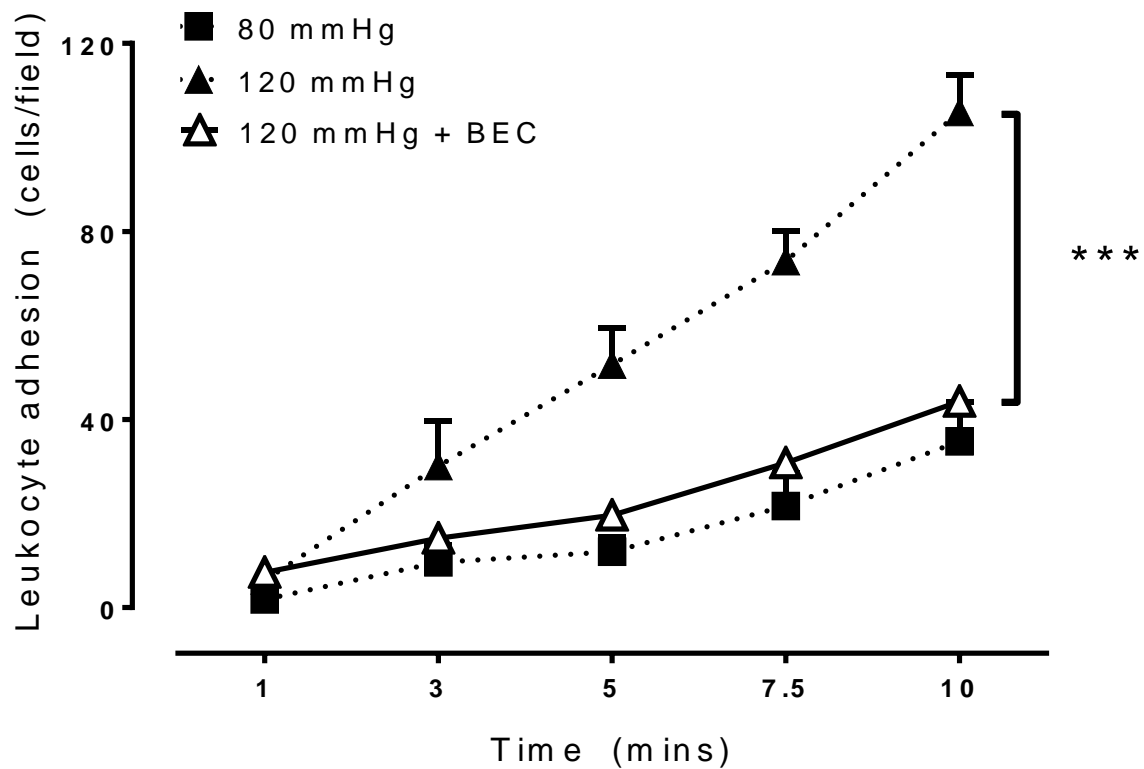
Figure 4.11. Effect of arginase inhibition on acute pressure-induced inflammation in rat carotid arteries. Leukocyte adhesion in RCA under pressure in the absence and presence of the arginase inhibitor BEC (100 µM), n=4-5. Results are expressed as mean ± SEM. Data were analysed using a two-way ANOVA with Bonferroni post hoc test where ***$P<0.001$ versus 120 mmHg.

A

B
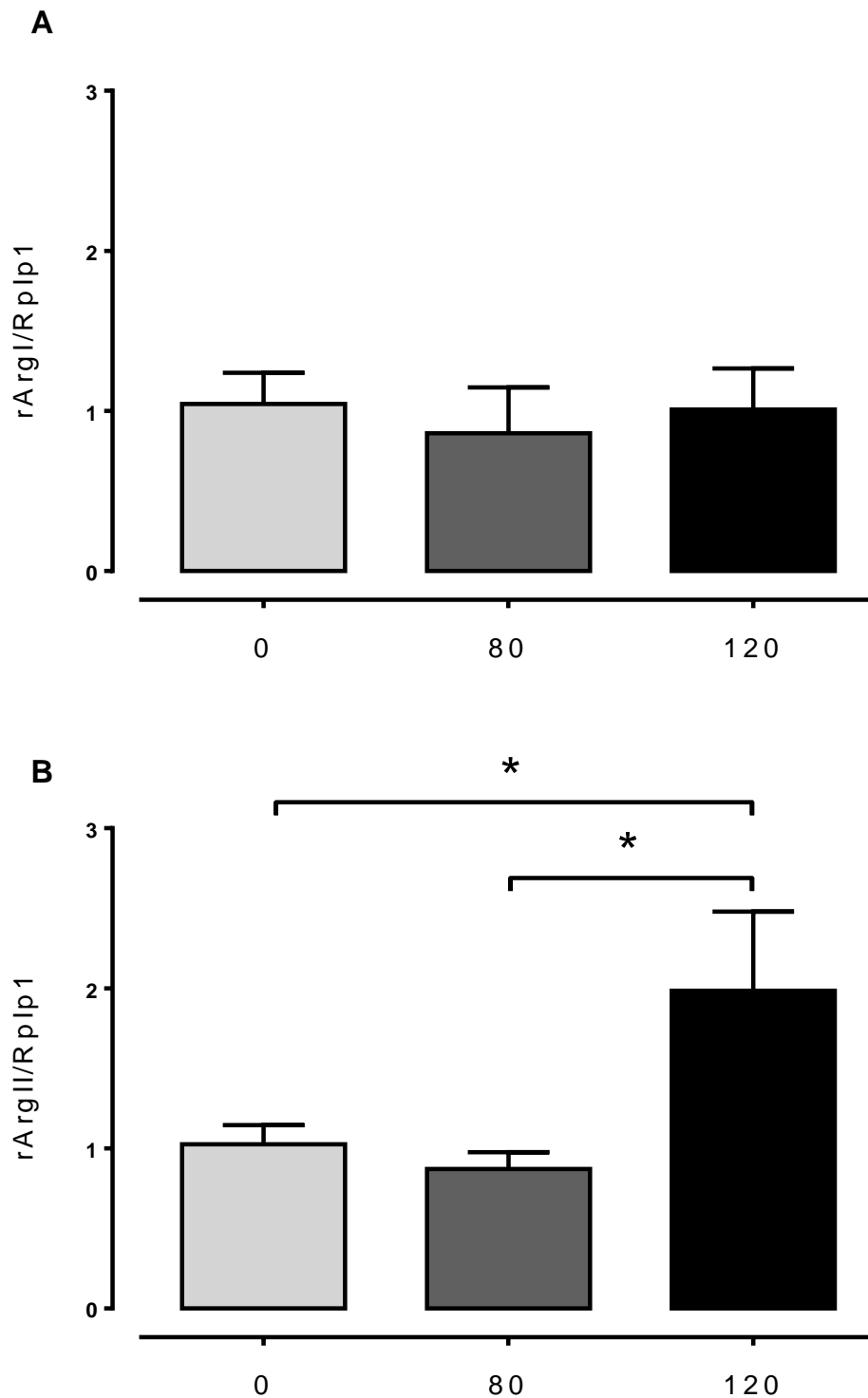
Figure 4.12 Effect of acute pressure on arginase I and II mRNA expression in rat carotid arteries. mRNA expression of arginase I **(A)** and II **(B)** (ArgI and II) relative to Rplp1 in RCA pressurised to 0, 80 and 120 mmHg for 1 hr normalised to 0 mmHg (n=3-7). Results are expressed as mean ± SEM. Data were analysed using a one-way ANOVA with Bonferroni post hoc test where *P<0.05.
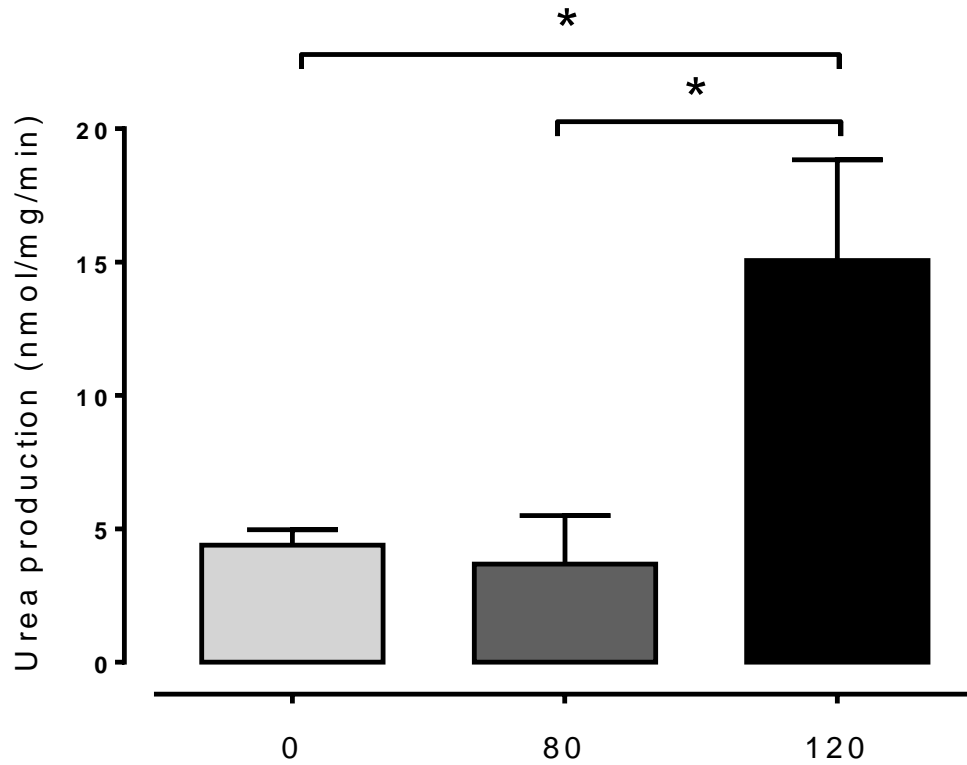
Figure 4.13 Effect of acute pressure on arginase activity in rat carotid arteries. Arginase activity measured by urea production in lysates of RCA pressurised at 0, 80 and 120 mmHg for 1 hr (n=4-6). Results are expressed as mean ± SEM. Data were analysed using a one-way ANOVA with Bonferroni post hoc test where *P<0.05.

## 4.3.6 Pressure does not induce exocytosis of vWF

It has recently been shown that stretch induces WPB exocytosis in HUVECs (Xiong et al., 2013). Therefore, we examined vWF release in HUVECs stimulated with pressure (0, 80 or 120 mmHg) or TNFα (5 ng/ml) for 5 min. We observed no difference in vWF release between any of the treatment groups compared to control (Fig 4.14A). HUVECs stimulated with TNFα for 4 hr released significantly more vWF compared to unstimulated HUVECs (Ctr: 0.72±0.14 vs. TNFα: 6.68±1.09; n=6; P<0.001; Fig 4.14B) but pressure-stimulated HUVECs at 80 and 120 mmHg for 1 hr did not alter vWF release. These findings suggest that vWF (and WPB exocytosis) is not involved in the inflammatory response to pressure.

4.3.7 Pressure induces NFκB expression

The transcription factor NFκB plays an important role in cytokine transcription; a hallmark of vascular inflammation and importantly NFκB signalling in response to pressure has been hypothesised (Riou *et al.*, 2007). To quantify both the nuclear and cytosolic expression of the NFκB p65 subunit, HUVECs were fluorescently probed and imaged using a confocal microscope (Fig 4.15). We observed increased nuclear and cytosolic NFκB fluorescence in HUVECs pressurised at 120 mmHg (30 mins) compared to control (n=10-11; *P*<0.001; Fig 4.16A & B). To investigate the role of ROS and arginase in the activation of NFκB we co-incubated pressurised HUVECs with the Nox inhibitor apocynin or the arginase inhibitor, BEC. Nuclear and cytosolic NFκB fluorescence was significantly lower in the presence of either apocynin or BEC when compared to 120 mmHg alone (n=5-11; *P*<0.05; Fig 4.15 & 4.16) suggesting a critical role for both arginase and ROS in adhesion molecule expression induced by pressure.

A

B
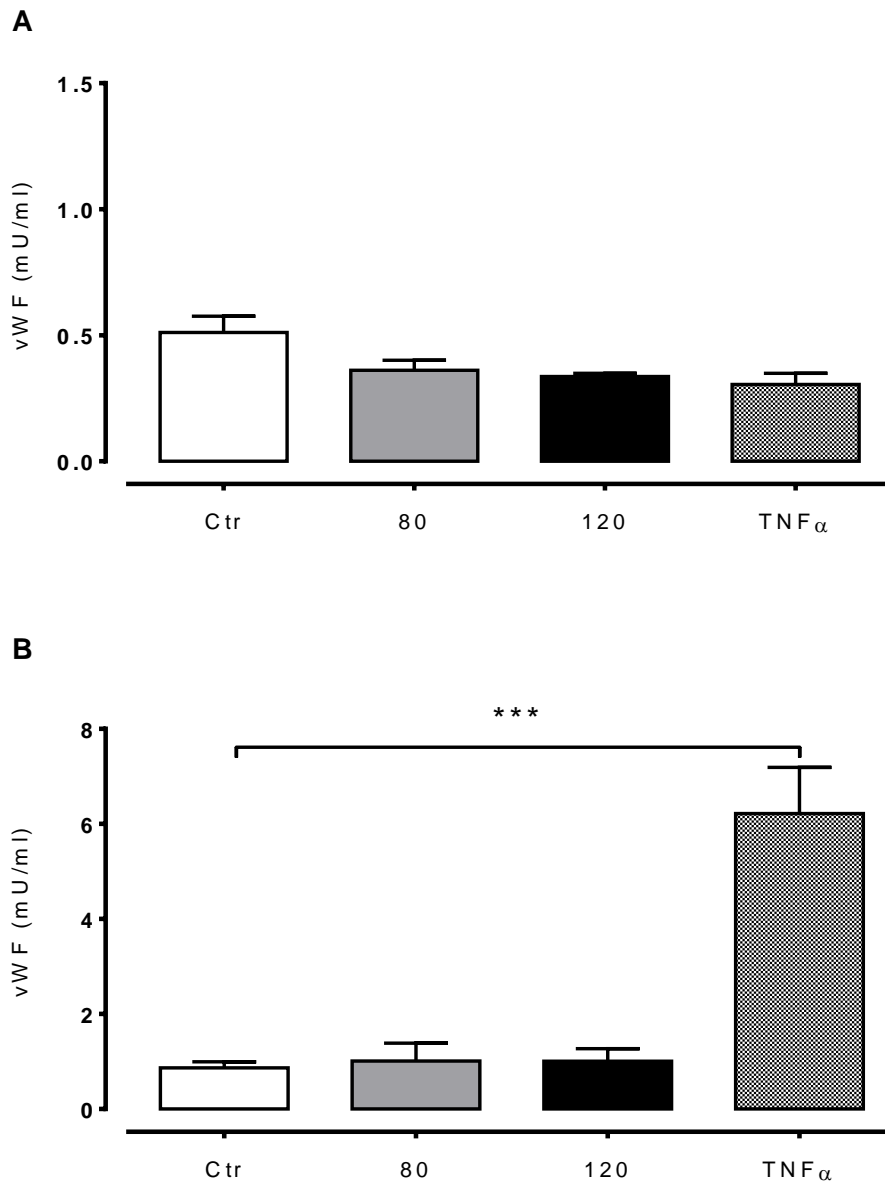
Figure 4.14 vWF exocytosis under pressure. HUVECs were either unpressurised, pressurised (80 or 120 mmHg, 1 hr) or TNFα stimulated (5ng/ml) for 5 min (**A**) or 1 hr pressure/4 hr TNFα stimulation (**B**). The supernatant was then analysed for vWF release by ELISA (n=4-6). Results are expressed as mean ± SEM. Data were analysed using a one-way ANOVA with Bonferroni post hoc test where ***$P<0.001$.
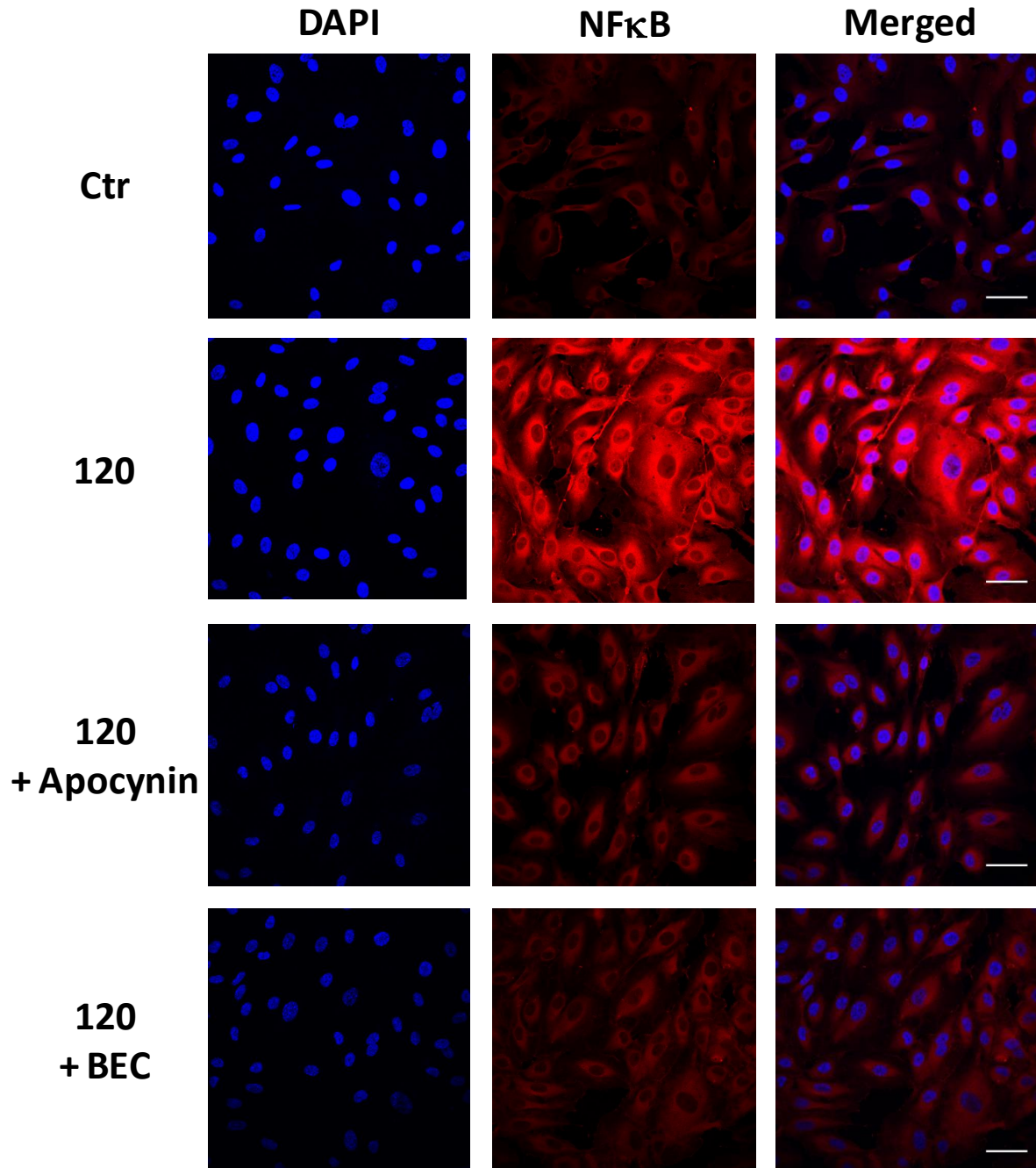
Figure 4.15 Effect of pressure on NFκB fluorescence. Representative confocal images of HUVEC NFκB staining (red) and nuclear staining (DAPI; blue) in unpressurised (Ctr), 120 mmHg or 120 mmHg in the presence of either the Nox inhibitor apocynin (3 μM) or the arginase inhibitor BEC (100 μM) for 30 min. Scale bar = 50 μm.
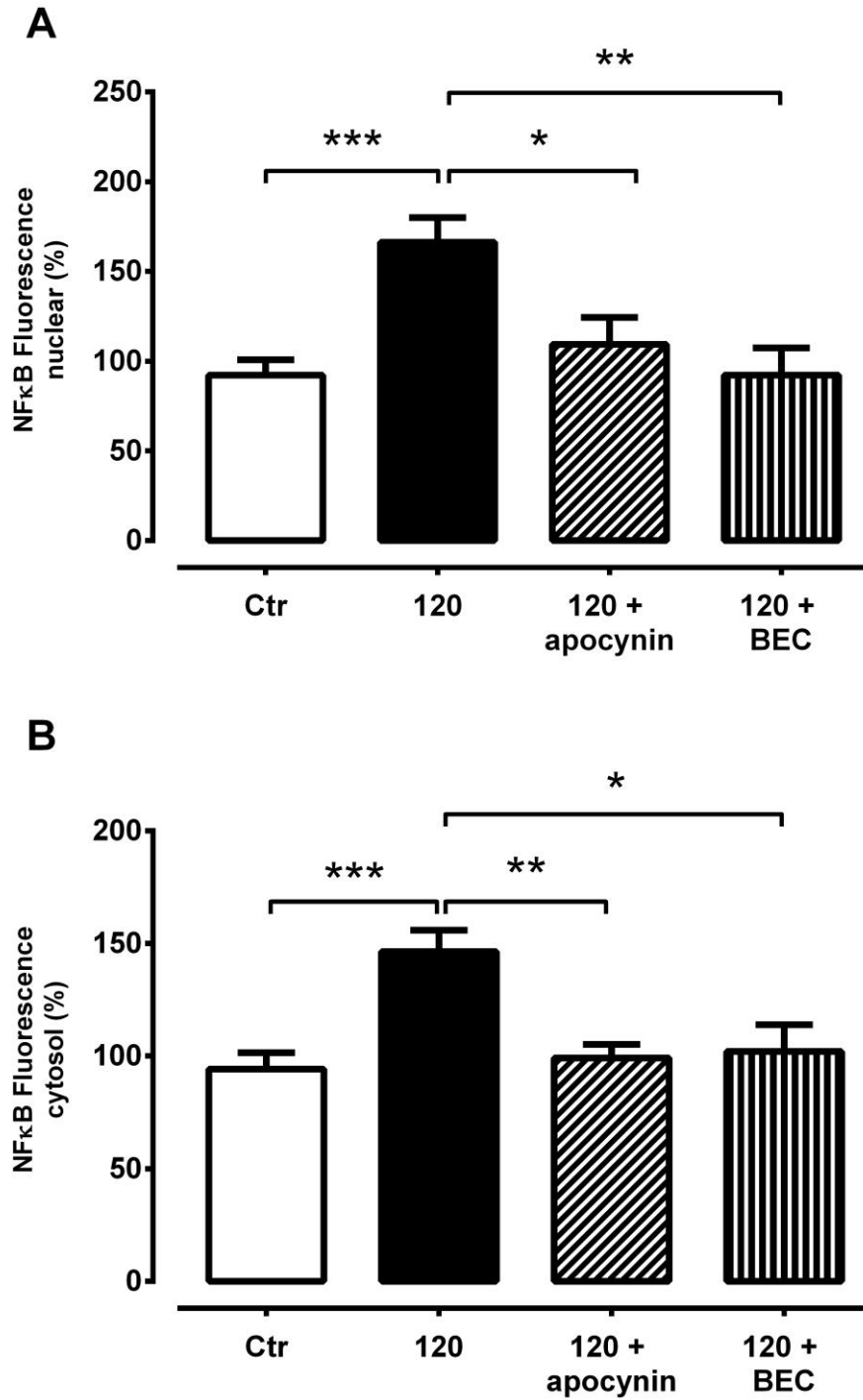
Figure 4.16 Effect of pressure on NFκB fluorescence. (**A**) Nuclear and (**B**) cytosolic NFκB in HUVECs unpressurised (Ctr) and pressurised at 120 mmHg or 120 mmHg in the presence of either the Nox inhibitor apocynin (3 μM) or the arginase inhibitor BEC (100 μM) for 30 min (n=5-11). Results are expressed as mean ± SEM. Data were analysed using a one-way ANOVA with Bonferroni post hoc test where *$P<0.05$, **$P<0.01$, ***$P<0.001$.

4.4 Discussion

The attachment of leukocytes to the endothelium is one of the first critical steps in the progression of atherosclerosis (Cybulsky *et al.*, 1999; Ley *et al.*, 2007; Libby *et al.*, 2011). In this chapter we explored the role of high intraluminal pressure in augmenting this critical process. We show that acute (1 hr) increases in intraluminal pressure (up to 120 mmHg) stimulates leukocyte to endothelial adhesion, ICAM-1 and MCP-1 expression in vessels, ICAM-1 expression in HUVECs and endothelial microparticle shedding. These data are consistent with increased endothelial activation. Furthermore, we demonstrate a pressure-induced signalling cascade whereby ROS generation, increased arginase II expression and activity promotes the nuclear translocation of NFκB, the rapid increase in adhesion molecule expression and ultimately leukocyte adhesion.

Indeed, increased inflammatory markers are seen in hypertensive patients (Chae *et al.*, 2001; Chrysohoou *et al.*, 2004) and the risk of pre-hypertensive patients developing hypertension has been attributed to the level of their inflammation (Engstrom *et al.*, 2002; Chrysohoou *et al.*, 2004). Furthermore, hypertensive patients show a positive correlation between the inflammatory marker C-reactive protein (Blake *et al.*, 2003) and carotid intima-media thickness, a surrogate measure of predisposition to atherosclerosis (Lakka *et al.*, 1999). More recently, Tadzic *et al.*, (2013) demonstrated that reducing high blood pressure with a calcium channel blocker, reduces endothelial ICAM-1 and VCAM-1 further supporting the hypothesis of pressure-induced stimulation of endothelial cytokines. Despite these correlations, few studies have assessed the effect of high blood pressure *per se* on endothelial cells and importantly, whether pressure in its own right can trigger inflammation. One such study showed that adhesion of fluorescently cultured monocytes injected into the lumen of previously pressurised mouse carotid arteries were increased at 150 mmHg compared to 80 mmHg after 12 and 24 hours (Riou *et al.*, 2007). Our findings support and extend these studies by using a customised *ex vivo* vessel chamber which enables us to study the direct effect of intraluminal pressure in real time with perfusion. We showed that pressure *per se* induces gene expression of the adhesion molecules ICAM-1 and MCP-1, endothelial activation and dysfunction and the accumulation of leukocytes to the endothelium in rat carotid arteries and cultured endothelial cells. Finally, levels of EMPs in the media of pressurised HUVECs were higher compared to unstimulated cells. EMPS are

microvesicles (<1.5µm) shed from the cell membrane during cellular activation, damage and apoptosis (Dignat-George & Boulanger, 2011). Plasma levels of EMPs are augmented in patients with chronic inflammatory diseases such as atherosclerosis (Koga *et al.*, 2005) and hypertension (Preston *et al.*, 2003).

Accumulating evidence suggests that hypertension is intrinsically linked to inflammation and the progression of atherosclerosis. However, it is difficult to know if this is due to the pressure *per se* or the neurohumoral influences such as noradrenaline, acetylcholine and the RAS, which are intimately involved in both the progression of hypertension as well as vascular inflammation. As previously mentioned, atherosclerosis is primarily dependent on the RAS in *Apoe$^{-/-}$* mice (Weiss *et al.*, 2001), and in *Apoe$^{-/-}$/eNOS$^{-/-}$* mice, the development of atherosclerosis is thought to be independent of hypertension (Chen *et al.*, 2001a). However, there is certainly evidence to suggest that hypertension does lead to atherosclerosis independent of the RAS (Wang *et al.*, 2004; Riou *et al.*, 2007). The mechanical force induced by pressure can activate the AT1R independently of Ang II (Zou *et al.*, 2004). Further, stretch has also been shown to induce local Ang II release from the endothelium, which in turn increases ROS production (Delli Gatti *et al.*, 2008). However, our studies determined that acute pressure-induced endothelial activation is independent of Ang II/ATR1 signalling since AT1R antagonism had no effect on pressure-induced adhesion. While the effect of candesartan at 100 nM on AT1Rs in this study was not confirmed; however, Shimizu *et al*. (1999) demonstrate 100 nM is effective in improving myocardial ischaemia/reperfusion injury in rat hearts and it can also reverse myogenic constriction in chronic heart failure (Gschwend *et al*., 2003). Therefore, our data indicates that there is an important role of RAS-independent ROS production in pressure-induced inflammation.

ROS, including superoxide, hydrogen peroxide, hydroxyl radical, and peroxynitrite are produced under healthy conditions in a controlled manner and are essential for cell signalling and metabolism (Thannickal & Fanburg, 2000). However, in many pathological states including hypertension (Paravicini & Touyz, 2008b), production of ROS is increased and production surpasses elimination by non-enzymatic and enzymatic anti-oxidant molecules, establishing a pro-oxidant state. In hypertensive patients, increased levels of hydrogen peroxide (Lacy *et al.*, 2000), upregulation of vascular Nox (Fortuno *et al.*, 2004) and other biomarkers of oxidative stress such as 8-epi-isoprostanes have been reported (Minuz *et al.*, 2002). In conditions of low shear stress, such as seen in hypertension, ROS

production via Nox is increased (Mohan *et al.*, 2007) and expression of antioxidants is decreased (Mowbray *et al.*, 2008). In pre-hypertensive spontaneously hypertensive rats, superoxide is involved in the progression of hypertension (Jameson *et al.*, 1993; Chabrashvili *et al.*, 2002), which can be prevented with the administration of antioxidants (Virdis *et al.*, 2004; Nabha *et al.*, 2005). Animal models of adult hypertension including; DOCA-salt-induced (Park *et al.*, 2002), Ang II-induced (Virdis *et al.*, 2004), and stroke-prone spontaneously hypertensive rats (Chen *et al.*, 2001b) all exhibit increased ROS largely attributable to the upregulation of Nox-induced ROS.

In the present study an increase in acute pressure (120 mmHg) increased ROS production via Nox and mitochondrial ROS pathways, which influenced leukocyte adhesion. Despite the fact that Nox is proposed to be the main source of ROS production (Griendling *et al.*, 2000; Touyz, 2004; Ray *et al.*, 2005), non-antioxidant actions of apocynin have been reported (Jiang & Dusting, 2003). Future work utilizing specific Nox isoform deficient mice in these experiments would allow us to confirm the current findings and to investigate the isoform responsible.

ROS can combine with NO to produce peroxynitrite, negating the well characterised anti-inflammatory actions of NO (Harrison *et al.*, 2006). A decrease in NO bioavailability leads to decreased vasodilatation, increased platelet aggregation, thrombosis, inflammation and leukocyte adhesion, all exacerbating vascular dysfunction and promoting vascular damage. The production of NO from ʟ-arginine is dependent on the distribution and stimulation of eNOS. However, despite a decrease in NO bioavailability, eNOS expression actually *increases* in hypertension. It is now well accepted that the scavenging of NO in hypertension is a consequence of an increase in oxidative stress (Hahn & Schwartz, 2009). Under chronic high blood pressure eNOS is 'uncoupled' and rather than producing NO, superoxide is preferably formed (Cheng *et al.*, 1996; Yun *et al.*, 1999). Increased leukocyte adhesion has been demonstrated in cat mesentery with eNOS blockade (Kubes *et al.*, 1991) and in *eNOS* deficient mice (Lefer *et al.*, 1999). Suppressing endogenous NO also increases endothelial ICAM-1 and VCAM-1 surface expression in HUVECs via the activation of NFκB. Therefore, our findings that pressure alone did not alter eNOS mRNA or protein expression, nor was eNOS uncoupled after 1 hr of increased pressure were unexpected. The effect of ʟ-NAME on leukocyte adhesion was also performed and actually decreased attachment under high pressure but as time did not permit further exploration of this phenomenon, this data

has not been included. Nevertheless, it is clear from our results presented that eNOS uncoupling does not contribute to pressure-induced endothelial inflammation.

NOS and the enzyme arginase share L-arginine as the parent substrate and increases in arginase can contribute to a diminished precursor environment thus inducing eNOS uncoupling (Lim *et al.*, 2007a) and the production of superoxide preferentially to NO (Munzel *et al.*, 2005). Although, we have shown that pressure-induced endothelial inflammation is not mediated by eNOS, previous reports demonstrating that increased expression and/or activity of arginase in hypertension (Xu *et al.*, 2004), diabetes (Romero *et al.*, 2008b) and atherosclerosis (Ryoo *et al.*, 2006) led us to hypothesise that arginase may be involved in pressure-induced inflammation. Indeed, we observed that arginase activity and arginase II expression is increased in vessels after 1 hr of pressure stimulation. This is consistent with findings in spontaneously hypertensive rats where both isoforms (arginase I and II) are increased prior to the development of overt hypertension (Demougeot *et al.*, 2007a), suggesting that arginase may be both a cause as well as a consequence of high blood pressure. Our findings advance these studies and demonstrate for the first time that arginase plays an important role in pressure-induced inflammation. Interestingly, evidence for the role of ROS in the regulation of endothelial arginase has been demonstrated. In pig coronary arterioles exogenous hydrogen peroxide mediates a reduction in NO-dependent relaxation by reducing L-arginine and increasing the expression of arginase after only 1 hr of treatment suggesting that arginase may be an early target of increased ROS (Thengchaisri, 2006). Furthermore, vascular injury via acute stimulation with TNFα and/or ischaemia-reperfusion, induced an increase in ROS which enhances arginase activity (Jung *et al.*, 2010). The interaction between ROS and arginase may also be reciprocal as inhibition of Nox in alveolar macrophages down regulates arginase activity (Matthiesen *et al.*, 2008).

The secretory organelles of endothelial cells, WPBs, can be rapidly triggered which results in their degranulation/exocytosis. WPBs house a number of inflammatory mediators including vWF, P-selectin, interleukin-8, angiopoiten-2 and vasoconstrictors such as endothelin (Rondaij *et al.*, 2006), all shown to increase the expression of adhesion molecules and recruit leukocytes to the surrounding endothelium (Kisucka *et al.*, 2008). Although such an inference has been made (Bertuglia *et al.*, 2007), it is unknown if high intraluminal pressure causes WPB degranulation. What is clear, is that patients with essential hypertension have increased levels of soluble P-selectin compared to

normotensives (Lip *et al.*, 1995) and Xiong *et al*., (2013) demonstrated in HUVECs that exposure to stretch for 5 mins can induce rapid exocytosis of vWF leading to P-selectin translocation and increased leukocyte adhesion. However, in pressurised HUVECs, we observed no difference in vWF release compare to unstimulated cells, suggesting under the current conditions pressure does not result in WPB release and is not involved in the pressure-induced inflammation examined in this chapter.

The endothelial adhesion molecules are under transcriptional control of NFκB. We observed that HUVECs exposed to increased pressure had enhanced nuclear NFκB expression. These results suggest NFκB transcription of inflammatory markers may be the dominant pathway in this pressure response. Consistent with this idea previous studies have shown that mouse carotid artery segments exposed to high pressure have enhanced degradation of the anchoring protein, IκBα, and increased nuclear translocation of NFκB (Lemarie *et al.*, 2003). Interestingly, this was shown to be RAS independent. There is evidence that ROS and arginase, which we have shown to be critical in pressure-induced inflammation, can induce the activation of NFκB (Levrand *et al.*, 2005; Ckless *et al.*, 2007). In addition, we found inhibition of Nox or arginase reduced pressure-induced NFκB expression. This is in line with previous reports where arginase inhibition reduced NFκB activation in lung epithelial cells (Ckless *et al.*, 2007). Increased hydrogen peroxide production was also shown to induce NFκB activation and endothelial cell apoptosis in rat models of hypertension (Ungvari *et al.*, 2007) and inhibition of ROS production reduces activation of NFκB in HUVECs (Ogata *et al.*, 2000). Our findings, and other studies as shown, provide evidence for a critical role for Nox and arginase in the activation of NFκB and the subsequent leukocyte adhesion in response to increased pressure.

This chapter provides compelling evidence that high intraluminal pressure causes adhesion molecule expression and leukocyte to endothelial adhesion, a hallmark of vascular inflammation and the initiating step in the development of atherosclerosis. The inflammation is dependent on the activation of arginase II, ROS and NFκB. These results suggest that therapeutic strategies that reduce inflammation in hypertensive patients may be beneficial in reducing the risk of atherosclerosis. The next chapter of this thesis explores the effects of circumferential stretch and shear and investigates possible mechanosensors involved in this process.

Chapter 5

Role of caveolae in pressure-induced inflammation

5.1 Introduction

In Chapter 4, we demonstrated that high intraluminal pressure directly induces leukocyte adhesion, endothelial inflammation and dysfunction. This was due to the activation of a number of intracellular signalling pathways, namely increased arginase II expression, ROS production and NFκB activation. However, exactly how the endothelial cell senses pressure and stimulates these pathways is still not known.

Large arteries are able to respond to large pulsatile changes in blood pressure created by contractions of the heart due to their elasticity. This adaptability enables blood pressure in smaller resistance arteries to stay relatively constant. Elevated systolic and/or diastolic blood pressure, resulting from increased systemic vascular resistance and/or cardiac output, exerts a complex and abnormal mechanical insult on the arterial wall. Mechanical forces generated at the endothelium by fluid shear stress (longitudinal) and vessel circumferential stretch (radial) can potently affect vascular tone resulting in the continuous release of vasoactive endothelial autacoids.

Prolonged increases in pressure can result in proliferation and remodelling of vascular smooth muscle cells (Touyz, 2005; Rizzoni & Agabiti-Rosei, 2012) and subsequent thickening of the vascular wall ultimately reducing the elasticity and ability of the arteries to respond to changes in pressure. Whilst vascular smooth muscle cells have been shown to be influenced by stretch (for review see Haga *et al.*, 2007) and endothelial cells to be mostly influenced by shear stress (Li *et al.*, 2005b), the impact of stretch on endothelial cells is less well defined.

Blood vessels can be subjected to various shear stress forces depending on blood flow. Uni-directional laminar flow along straight vessels results in HSS values, while bi or multi (turbulent) directional flow commonly observed at vessel bifurcations has relatively lower shear stress values (termed oscillatory shear stress; OSS). Laminar flow or pulsatile flow with HSS (>15 dyn/cm^2) is associated with endothelial quiescence (Berk *et al.*, 2002; Pan, 2009) and cardio protection as a consequence of a reduction in vascular tone mediated by an increase in NO and a reduction in vasoconstrictor production, adhesion expression, ROS production and AT1R expression (Pan, 2009; Ramkhelawon *et al.*, 2009). Areas subjected to OSS are more susceptible to endothelial damage and atherosclerosis due to increased endothelial cell proliferation and apoptosis, increased ROS production, reduced

NO bioavailability and increased expression of adhesion molecules. Many of these characteristics are also observed with LSS; < 4 dyn/cm^2 (Pan, 2009).

The haemodynamic forces present in hypertensive patients are less well defined. Hypertensive patients with reduced wall shear stress in carotid arteries (Jiang *et al.*, 1999; Lee *et al.*, 2009), pulmonary arteries (Tang *et al.*, 2012), and radial arteries (Khder *et al.*, 1998) have been reported and in some instances were positively correlated with atherosclerotic plaque development (Jiang *et al.*, 1999; Lee *et al.*, 2009). Interestingly, rats subjected to aortic constriction demonstrated increased vascular wall remodelling in the pre-stenotic hypertensive region where increased stretch was apparent along with laminar shear (Prado *et al.*, 2006). Lee *et al.*, (2008) also demonstrated a positive correlation between circumferential stretch and plaque burden in those with essential hypertension. These studies suggest both laminar shear and circumferential stretch may contribute to pressure-induced plaque production. Therefore, the experiments described in this chapter aim to determine which of these mechanical forces is involved in the pressure-induced inflammatory response.

Several different mechanosensors and signalling pathways have been proposed as regulators of the endothelium's response to shear. In particular, the mechanosensors involved in stretch on vascular smooth muscle cells have been widely studied with evidence that integrins, the cytoskeleton, ion channels and G proteins may be activated by stretch in vascular smooth muscle cells, for review see (Hahn *et al.*, 2009). In terms of endothelial cells, exertion of circumferential stretch results in increased ICAM-1 (Cheng *et al.*, 1996), VCAM-1 and E-selectin expression (Yun *et al.*, 1999).

More recently, caveolae, 50- to 100-nm flask-shaped invaginations of the plasma membrane, have been implicated as mechanosensors. Caveolae are major cellular structures mediating vesicular transport, including transcytosis and endocytosis, as well as housing many proteins relating to cholesterol metabolism and cell signalling. They also play a critical role in lipid homeostasis and signal transduction. Cav1, the main structural protein of endothelial caveolae, is involved in macrophage inflammation, adhesion and phagocytosis and negatively regulates eNOS activity (Li *et al.*, 2005a; Medina *et al.*, 2007; Wu *et al.*, 2009). Recently, the soluble cytosolic protein, polymerase I and transcript release factor (PTRF), also known as cavin-1, was reported to be essential for caveolae formation (Hill *et al.*, 2008) and is upregulated under oxidative stress conditions (Volonte & Galbiati,

2011). Importantly, in mouse lung endothelial cells, caveolae numbers are decreased in response to osmotic swelling and stretch along with a disassembly of cavin-1 from Cav1 (Sinha *et al.*, 2011). While *Cav1*$^{-/-}$*/Apoe*$^{-/-}$ mice demonstrate reductions in leukocyte adhesion, adhesion molecule expression, and plaque development (Fernandez-Hernando *et al.*, 2009; Engel *et al.*, 2011), the effect of pressure on caveolae and consequently its role in the pressure-induced inflammatory response is unclear. We hypothesized that caveolae are not only essential mechanosensors in this response but also play an important role in mechanotransduction.

5.2 Methods

5.2.1 Animals

10-12 week old male Sprague Dawley rats and 8-10 week old C57Bl/6 and *Cav1*$^{-/-}$ mice were used in this study. Animals were housed at the Precinct Animal Centre in a room with a 12-hour light/dark cycle and access to food and water *ad libitum*. Animal experimentation was approved by the AMREP Animal Ethics Committee (Approval No: E/0886/2009/B, E/1315/2013/B), which adhere to the National Health and Medical Research Council (NHMRC) Australian Code of Practice for the Care and Use of Animals for Scientific Purposes.

5.2.2 Ex vivo pressure myography

To observe the direct effect of pressure on inflammation isolated RCA from Sprague Dawley rats were pressurised at 0, 80 and 120 mmHg for 1 hr. Vessels were pressurised as previously described in Chapter 3. Following pressure vessels were either perfused with whole blood to assess leukocyte adhesion (section 5.2.4) or snap frozen for gene expression (section 5.2.5).

5.2.2.1 *Shear stress in pressurised carotid arteries*

During pressure incubation, RCA were subjected to static (no flow), LSS (1.67 dyn/cm^2; 100 µl/min) or HSS (16.7 dyn/cm^2; 1000 µl/min) as previously described in Chapter 2, section 2.2.4.

5.2.2.2 *Pharmacological interventions in pressurised arteries*

For pharmacological interventions RCA were pressurised at 120 mmHg for 1 hour with the cholesterol acceptor MβCD (10 mM). This compound was used to determine the importance of membrane integrity in sensing and transducing pressure. The endothelial membrane is lined with lipid rafts and MβCD is known to remove cholesterol. This result would help confirm if the membrane played an important role in pressure-induced inflammation.

5.2.3 Stimulated mouse aorta

Aorta from 8-10 week old C57Bl/6 and *Cav1$^{-/-}$* mice were excised, cleaned and incubated with TNFα (5ng/ml; 4 hr) at 37°C, 5% CO_2 as previously described in Chapter 2, section 2.2.2. In previous experiments in the laboratory leukocyte adhesion in unstimulated mouse aorta has shown little to no adhesion and was therefore not undertaken in these experiments. Furthermore, as the objective was to only observe the effect on leukocyte adhesion without pressure shear stresses were not calculated for these experiments.

5.2.4 Leukocyte adhesion ex vivo

Following pressurisation, RCA or mouse aorta were perfused with human whole blood (Alfred Ethics Committee project no. 397/09) fluorescently labelled with DiI for 10 min and the number of leukocytes adhered to the endothelium were quantified as previously described in Chapter 2, section 2.2.3.

5.2.5 TNFα stimulated endothelial cells

H5V cells derived from mouse embryonic heart endothelium (Garlanda *et al.*, 1994) were transformed with a lentivirus containing shRNA to caveolin 1 (H5V Cav1 KD) or scrambled shRNA (H5V Scr), a gift from Dr Marie-Odile Parat (University of Queensland). Once confluent, H5V Scr or H5V Cav1 KD cells were stimulated with mTNFα (4hrs, 5ng/ml). Following stimulation cells were either assessed for monocyte adhesion (section 5.2.7) or snap frozen for gene expression (section 5.2.8).

5.2.6 *In vitro* THP-1 adhesion

Following TNFα stimulation H5V Scr and Cav1 KD cells were incubated with the monocytic cell line THP-1 (3 x 10^5 per 2 cm^2 surface) and imaged as previously described in Chapter 2, section 2.1.4.

5.2.7 Pressurised endothelial cells

H5v Cav1 KD and H5V Scr cells were seeded onto collagen coated 25 mm round glass coverslips and pressurised in a stainless steel sealed chamber at 0 and 120 mmHg as previously described in Chapter 2, section 2.1.2. Following pressure, cells were snap frozen for gene expression (section 5.2.8).

5.2.8 Gene expression analysis with real time quantitative RT PCR

Gene expression analysis of rat and mouse ICAM-1, MCP-1, mouse 18S and rat RpIp1 mRNA was performed as previously described in Chapter 2, section 2.3 and 2.4.

5.2.9 Electron microscopy of caveolae in pressurised carotids

RCA pressurised at 0, 80 and 120 mmHg for 1 hr were fixed, dehydrated, sectioned, and imaged with a transmission electron microscope (Hitachi H7500; Monash Micro Imaging BioEM, Monash University) as previously described in Chapter 2, section 2.8. Caveolae (defined as 60-100 nm invaginations) were counted, non-blinded, in a minimum of 25 cells per vessel, with two fields per vessel.

5.2.9.1 Ruthenium red stained pressurised carotids

RCA were pressurised at 0, 80 and 120 mmHg for 1 hr and fixed in 100 mM cacodylate buffer ph 7.4 containing 2.5% glutaraldehyde and 1 mg/ml of ruthenium red. Samples were dehydrated, sectioned, and imaged with a transmission electron microscope by Professor Rob Parton at the University of Queensland.

5.2.10 Duolink™ in situ proximity ligation of Cav1 and cavin-1

6 μm sections of RCA pressurised at 0, 80 and 120 mmHg were incubated with Cav1 (1:200) and cavin-1 primary antibodies (1:200 and 1:150, respectively) followed by proximity ligation assay (PLA) secondary antibodies (1:5), hybridized and subjected to rolling-circle amplification, which was detected by fluorescence. Fluorescence was only observed when

there was close juxtaposition of the two proteins. For further detail refer to Chapter 2, section 2.7.1.

5.2.11 Immunofluorescence in pressurised carotids

6 µm sections of RCA pressurised at 0, 80 and 120 mmHg were stained for Cav1 and cavin-1 primary antibodies (1:200 and 1:150, respectively) along with fluorescent secondary antibodies (1:500) and imaged as previously described in Chapter 2, section 2.7.

5.2.12 Statistics

Data are expressed as mean ± SEM and were analysed using GraphPad Prism version 6.00 software (GraphPad Software, La Jolla, California, USA). Assessment of leukocyte adhesion, THP-1 adhesion and mouse gene expression were measured using two-way repeated measures ANOVA. Factors included different pressures, shear rates, inhibitors, cell line and time. Rat gene expression and caveolae number were analysed using a one-way ANOVA. Where there were significant differences in interaction, a Bonferroni post hoc analysis was performed. The interaction of Cav1 and cavin-1 at two pressures were analysed using an unpaired Student's t-test. $P<0.05$ was considered statistically significant.

5.3 Results

5.3.1 Circumferential stretch in pressure-induced inflammation

The haemodynamic forces blood vessels are subjected to include circumferential wall stretch and fluid shear stress. Increases in pressure directly induce circumferential stretch, which, as shown in the previous chapter, increases leukocyte to endothelial adhesion. In the experiments described in Chapter 4, RCA were subjected to increased pressure for 1 hr without flow (i.e. no shear) followed by 10 min low shear blood flow for imaging purposes. In the current chapter, to examine the effect of shear stress on RCA, vessels were subjected to either: static (no flow), LSS (1.67 dyn/cm^2; 0.1 ml/min) or HSS (16.7 dyn/cm^2; 1ml/min) according to the Hagen-Poiseuille equation (Malek *et al.*, 1999; Davies, 2009) for 1 hr and assessed for leukocyte adhesion and gene expression.

Leukocyte adhesion in unpressurised RCA incubated for 1 hr under static conditions or under flow with LSS were not different (7±3 and 5±2 respectively; n=5-6; Fig 5.2) suggesting LSS does not induce inflammation without pressure. Leukocyte adhesion responses in RCA subjected to 120 mmHg under flow with LSS were similar to those pressurised to 120 mmHg without flow (90±23 vs. 96±14 cells/field; n=5-6; *P*>0.05; Fig 4.4&5.2). However, adhesion in vessels under 120 mmHg and with HSS was reduced compared to 120 mmHg and LSS, supporting reports in the literature of the protective effects of HSS (Malek *et al.*, 1999; Tinken *et al.*, 2010).

To determine whether the levels of adhesion observed were due to endothelial activation, mRNA expression analysis of the genes involved in adhesion was assessed in RCA pressurised and subjected to various shear rates. MCP-1 expression in RCA exposed to 120 mmHg with LSS was significantly higher than unpressurised RCA (13.1±2.0 vs. 1.2±0.3; n=5; *P*<0.001; Fig 5.2). Consistent with function findings described above, RCA pressurised to 120 mmHg under HSS, while greater than unpressurised RCA, demonstrated a blunted response compared to pressurised RCA with LSS. MCP-1 expression at 0 mmHg with LSS trended to be higher than 0 mmHg (static) (1.3±0.3 and 5.4±1.4 respectively; *P*>0.05; n=5-6; Fig 5.2). These results suggest both circumferential stretch and LSS are important in endothelial activation and inflammation whereas HSS is cardio protective.
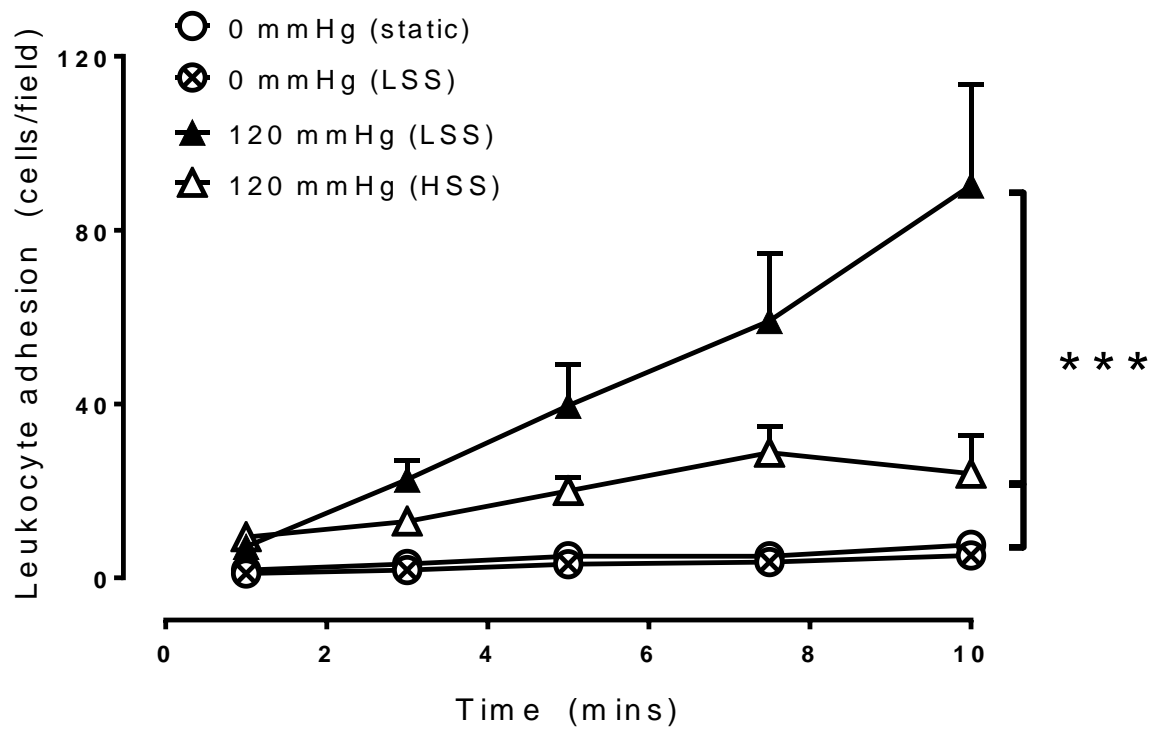
Figure 5.1. The effect of shear stress during acute pressure-induced inflammation in rat carotid arteries. Quantification of leukocyte adhesion in carotid arteries under pressure coupled with no flow (static), LSS (1.67 dyn/cm^2) or HSS (16.67 dyn/cm^2) conditions (n=5-6). Results are expressed as mean ± SEM. Values were compared with two-way ANOVA with Bonferroni post hoc where ***P<0.001 versus 120 mmHg (LSS).
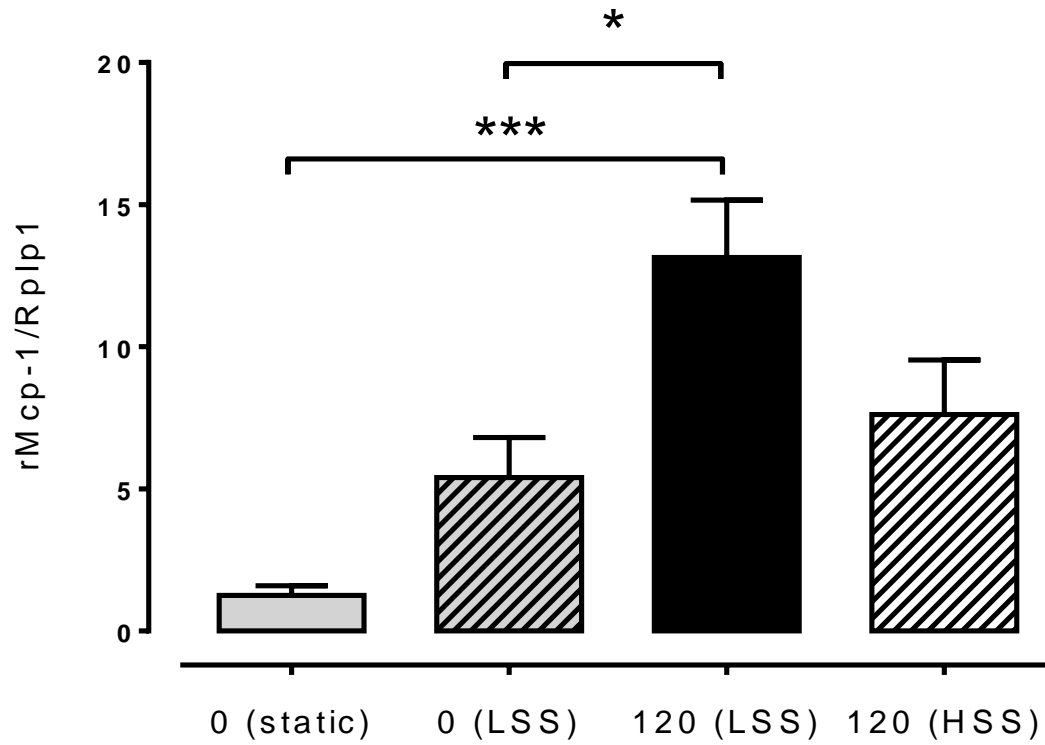
Figure 5.2. The effect of shear stress on *Mcp-1* mRNA expression in vessels. mRNA expression of MCP-1 relative to Rplp1 in rat carotid arteries under pressure (0 and 20 mmHg) with no flow (static), LSS (1.67 dyn/cm^2) or HSS (16.67 dyn/cm^2) conditions for 1 hr. All groups are expressed relative to 0 mmHg (static) (n=4-6). Results are expressed as mean ± SEM. Data were analysed with a one-way ANOVA with Bonferroni post hoc where *P<0.05, ***P<0.001.

5.3.2 Caveolae are involved in endothelial inflammation

To investigate the importance of membrane integrity in sensing pressure differences, the cholesterol acceptor MβCD, coupled with high pressure (120mmHg) in RCA was assessed. Leukocyte adhesion was lower in vessels treated with 120 mmHg + MβCD as compared to 120 mmHg pressure alone (47±13 vs.105±8 cells/field; n=4-5; P<0.001; Fig 5.3), highlighting the importance of the membrane-associated mechanosensors.

Of the various mechanosensors that line the plasma membrane the structural microdomains known as caveolae are associated with both pressure and inflammation. For instance, caveolae are closely linked with both eNOS (Bucci *et al.*, 2000) and Nox (Yang *et al.*, 2007). To assess the role of caveolae in pressure-induced inflammation we first examined the role of caveolae with TNFα stimulation as TNFα receptors are known to reside in caveolae (D'Alessio *et al.*, 2005). Aortas from 8-10 week old *Cav1$^{-/-}$* mice were stimulated with TNF-α for 4 hr (5ng/ml) and leukocyte adhesion was assessed. Adhesion was significantly reduced in aorta from *Cav1$^{-/-}$* mice compared to aorta from C57Bl/6 mice (20±4 vs. 8±3 cells/field; P<0.01; n=7; Fig 5.4).

Next, H5V Scr and H5V Cav1 KD cells were stimulated with TNFα to determine if endothelial cell activation was altered by caveolae expression. H5V Scr cells demonstrated increased gene expression of ICAM-1 and MCP-1 when stimulated with TNFα compared to unstimulated cells (n=4-6; *P*<0.05; Fig 5.5). However, TNFα stimulated H5V Cav1 KD cells had a lower response compared to H5V Scr (ICAM-1: 2.6±0.4 vs. 5.5±0.7; n=5; *P*<0.001; Fig 5.5A, MCP-1: 2.6±0. vs. 5.2±1.0; n=5; *P*<0.01; Fig 5.5B). Consistent with our gene expression analysis, we also observed a decrease in monocyte adhesion to H5V Cav1 KD cells following TNFα stimulation compared to scrambled controls (138±40 vs. 288±30%; n=3; *P*<0.01; Fig 5.6). These results demonstrate Cav1 and caveolae are essential for TNFα-induced endothelial activation and inflammation.
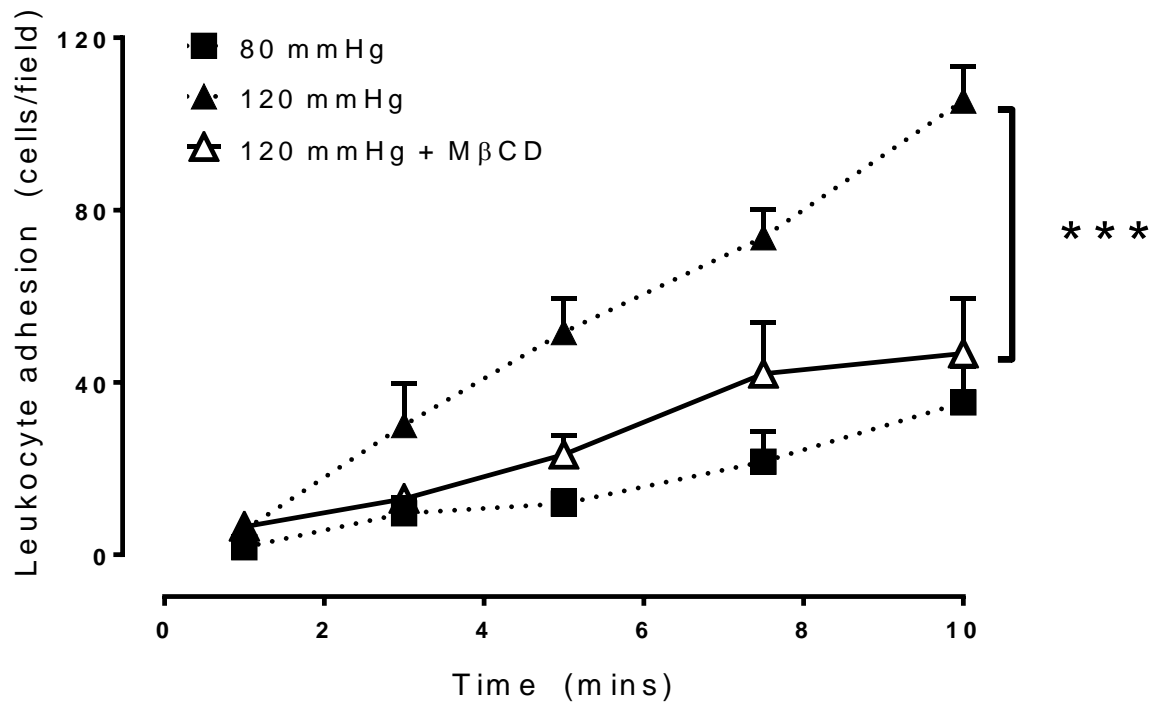
Figure 5.3. The effect of a cholesterol acceptor during acute pressure-induced inflammation in rat carotid arteries. Quantification of leukocyte adhesion in carotid arteries under pressure coupled with the cholesterol acceptor MβCD (10 mM; n=4-5). Results are expressed as mean ± SEM. Data were analysed using a two-way ANOVA with Bonferroni post hoc where ***P<0.001 versus 120 mmHg.
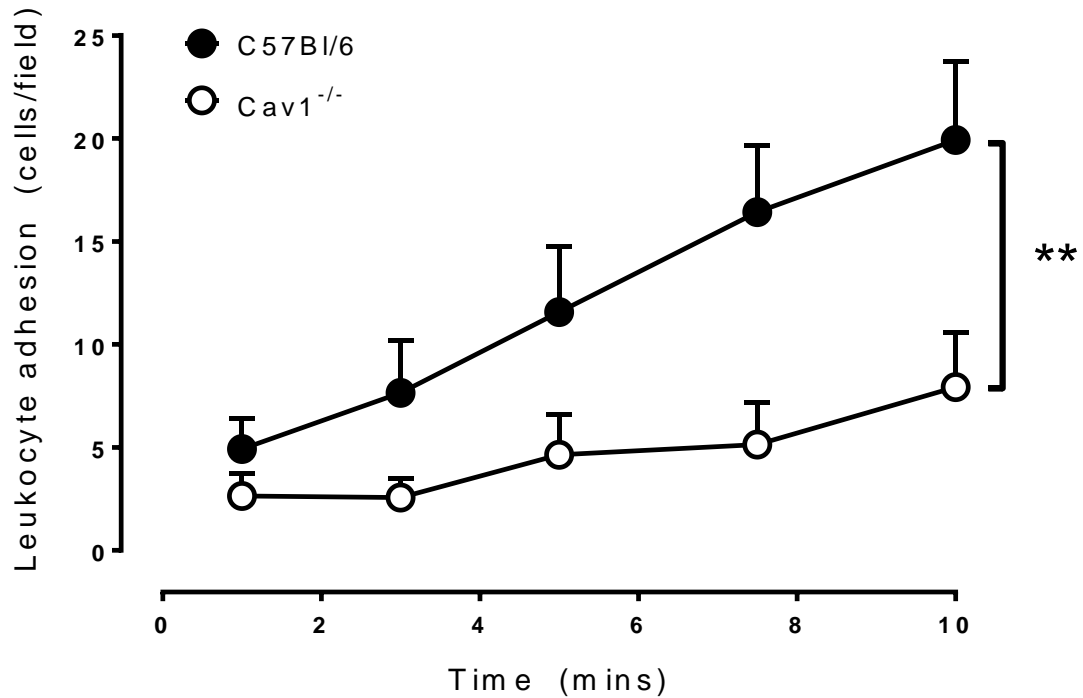
Figure 5.4. Leukocyte adhesion in stimulated *Cav1*^{-/-} aorta. Quantification of leukocyte adhesion in C57Bl/6 and *Cav1*^{-/-} mice following TNFα stimulation (4hrs; 5ng/ml; n=7). Results are expressed as mean ± SEM. Data were analysed using a two-way ANOVA with Bonferroni post hoc where **P<0.01.
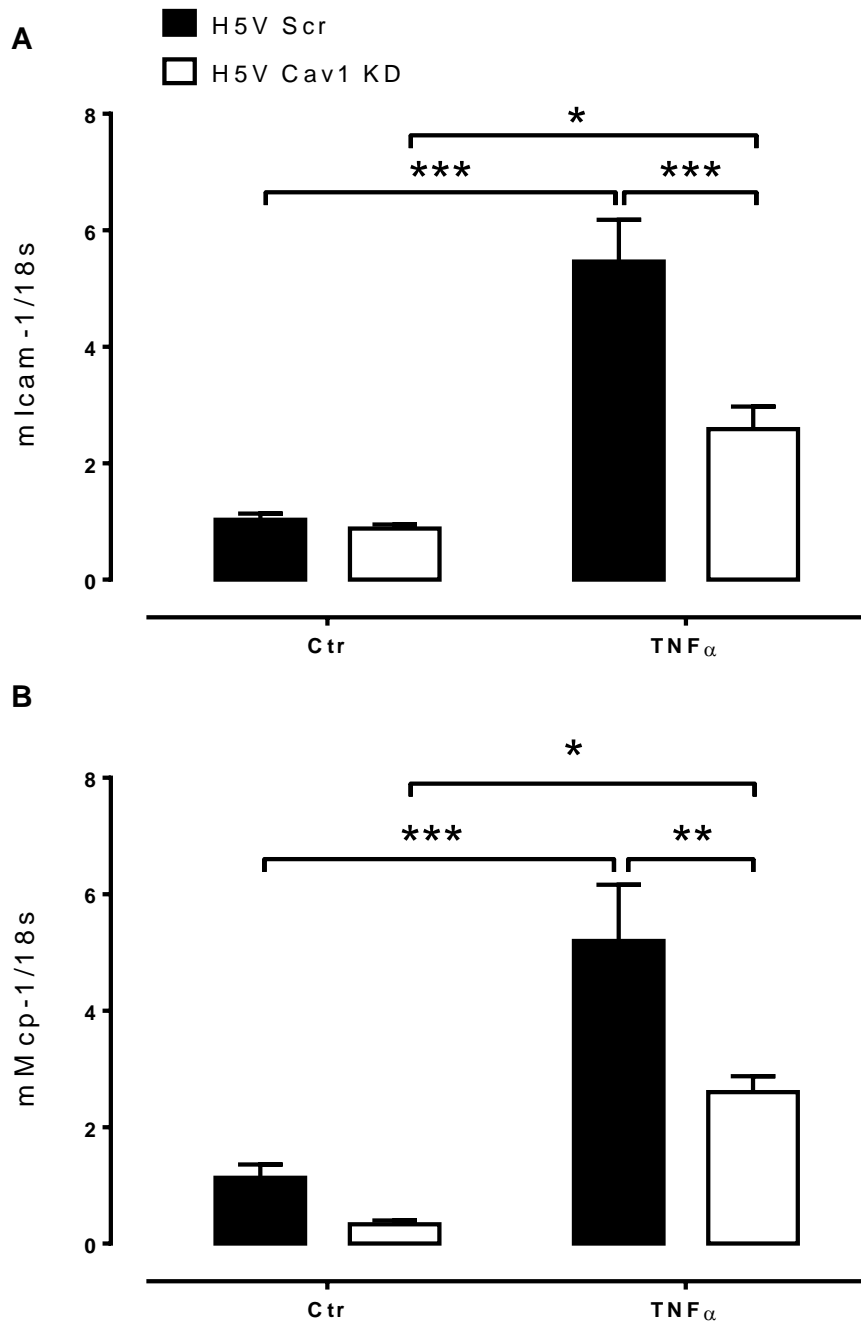
Figure 5.5. Effect of Cav1 KD on mRNA expression in endothelial cells. (**A**) ICAM-1 and (**B**) MCP-1 gene expression in transformed H5V cells with either scrambled shRNA (H5V Scr) or Caveolin-1 shRNA (H5V Cav1 KD) that were unstimulated (Ctr) or stimulated with TNFα for 4hrs (5ng/ml) (n=4-6). Results are expressed as mean ± SEM. Values were analysed using a two-way ANOVA with Bonferroni post hoc where *$P<0.05$, **$P<0.01$, ***$P<0.001$.

A
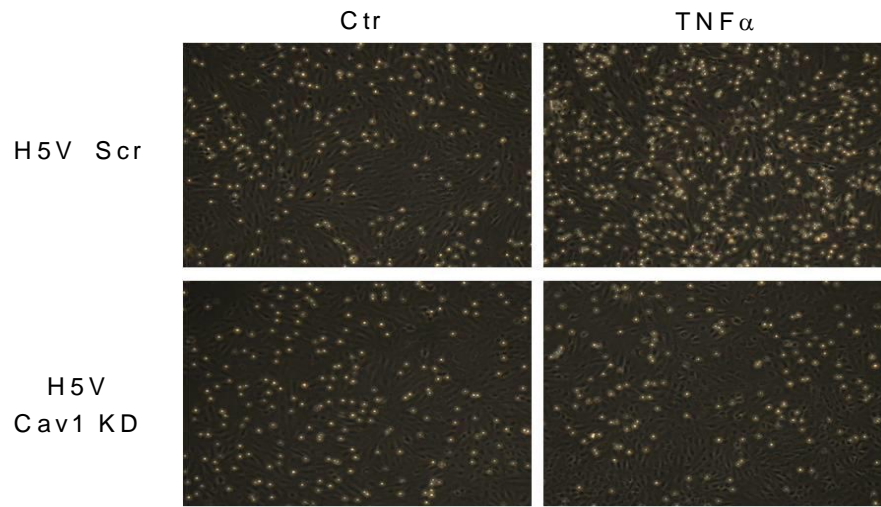
B
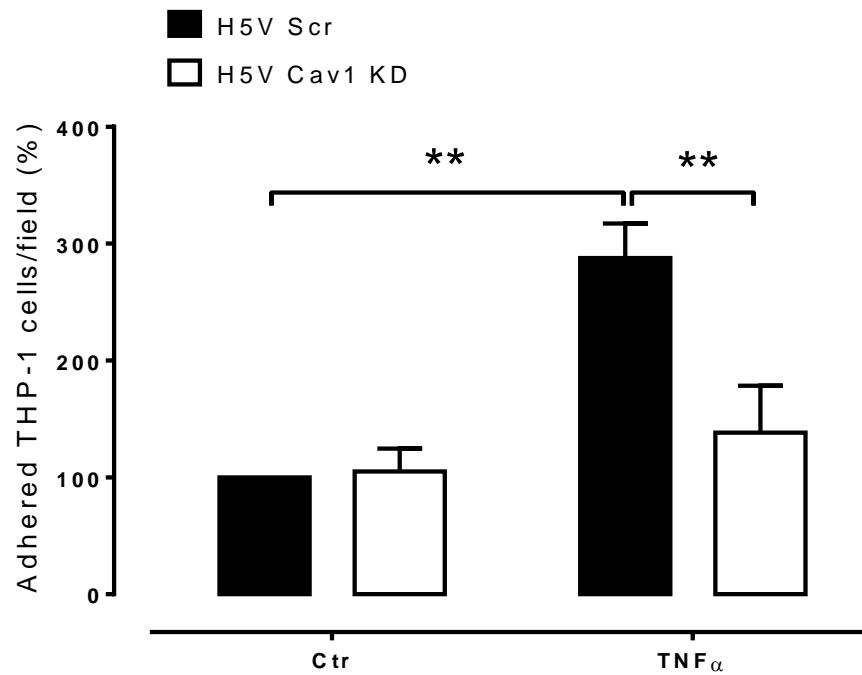
Figure 5.6. Effect of Cav1 KD on monocyte adhesion to endothelial cells. (**A**) Representative images of THP-1 (1×10^6/ml) adhesion to H5V Scr or Cav1 KD monolayer following TNFα stimulation (4 hrs; 5ng/ml). (**B**) Quantitative analysis of THP-1 adhesion as a percentage of H5V Scr control (n=3). Results are expressed as mean ± SEM. Values were analysed using a two-way ANOVA with Bonferroni post hoc where **$P<0.01$.

5.3.3 Pressure reduces caveolae number along the plasma membrane

To explore the possible effect of pressure on caveolae structure, pressurised RCA (0, 80 & 120mmHg) were imaged using an electron microscope (Fig 5.7A). For each vessel a minimum of 25 endothelial cells were counted with two fields imaged per cell. Elevated pressure (120 mmHg) reduced the number of caveolae per μm length of plasma membrane when compared to 0 and 80 mmHg (0 mmHg: 3.81±0.26 vs. 120 mmHg: 1.89±0.22; *P*<0.01; 80 mmHg: 3.08±0.22 vs. 120mmHg: 1.89±0.22; n=3; P<0.05; Fig 5.7B). Even though it may appear that Fig 5.7A represents the same number of caveolae between 80 mmHg and 120 mmHg, the surface area is increased at 120 mmHg and thus causing fewer caveolae/μm as depicted in Fig 5.7B. In addition, morphological changes were observed with a greater deformation of the endothelial layer at 120 mmHg (Fig 5.7A). The reduction in caveolae with pressure was also confirmed in RCA stained with the cell surface marker, ruthenium red (Fig 5.8; 0mmHg: 100% vs. 120mmHg: 43%).

A
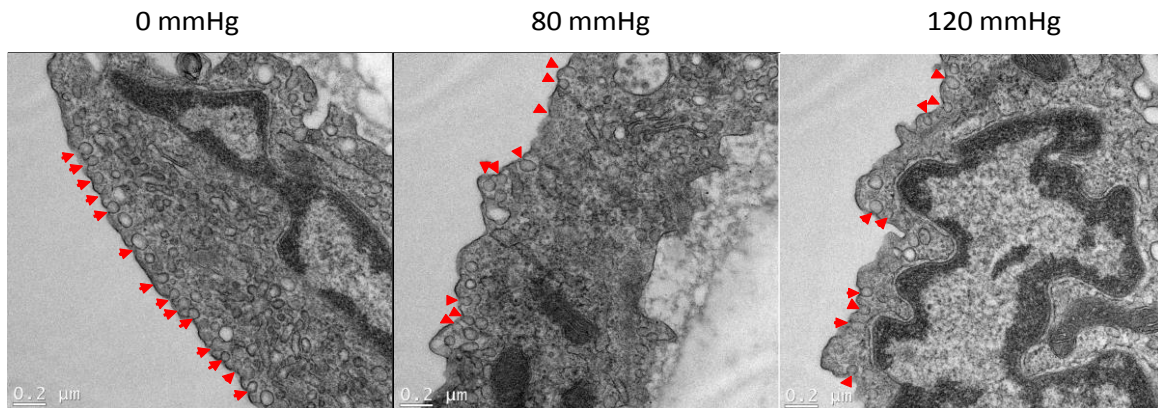
B
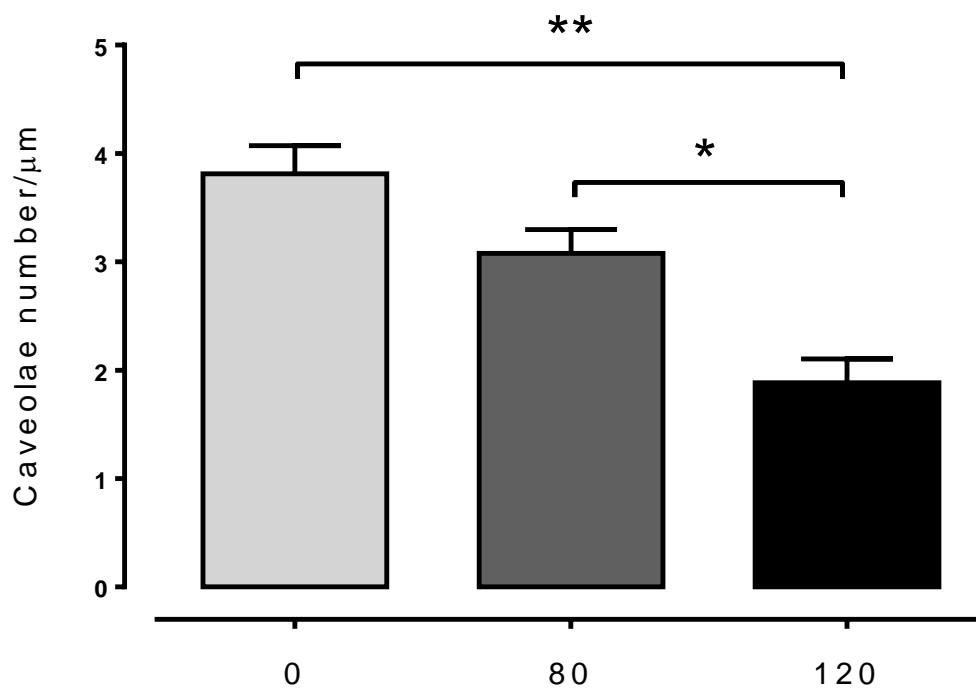
Figure 5.7. The effect of pressure on caveolae number in carotid arteries. (**A**) Representative ultrathin resin sections of the caveolae (red arrows) in rat carotid arteries after 1 hr of pressure (0, 80 and 120 mmHg) examined by electron microscopy. Scale bar=200 nm. (**B**) Quantification of caveolae detected per um of plasma membrane on ultrathin resin sections from carotid arteries after 1 hr of pressure (0, 80, 120 mmHg), n=3. Results are expressed as mean ± SEM. Values were analysed using a one-way ANOVA with Bonferroni post hoc where *$P<0.05$, **$P<0.01$.

0 mmHg
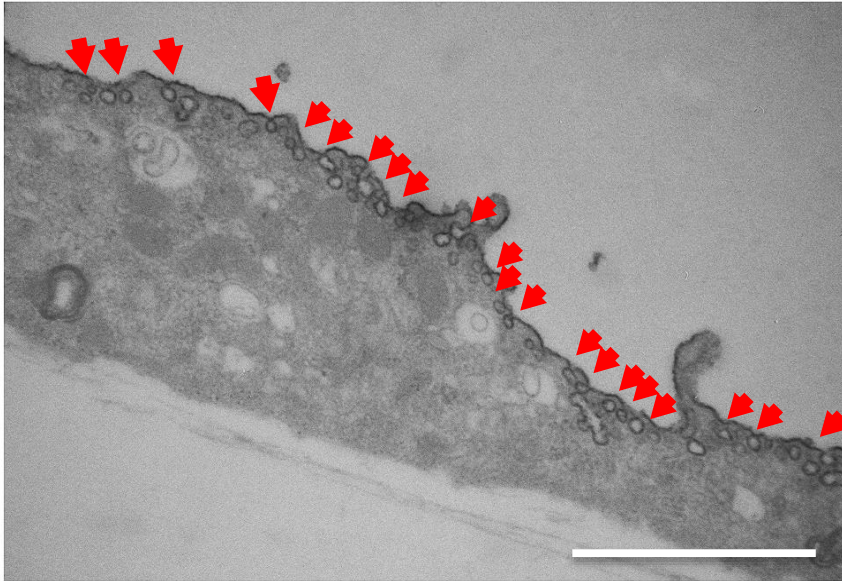
120 mmHg
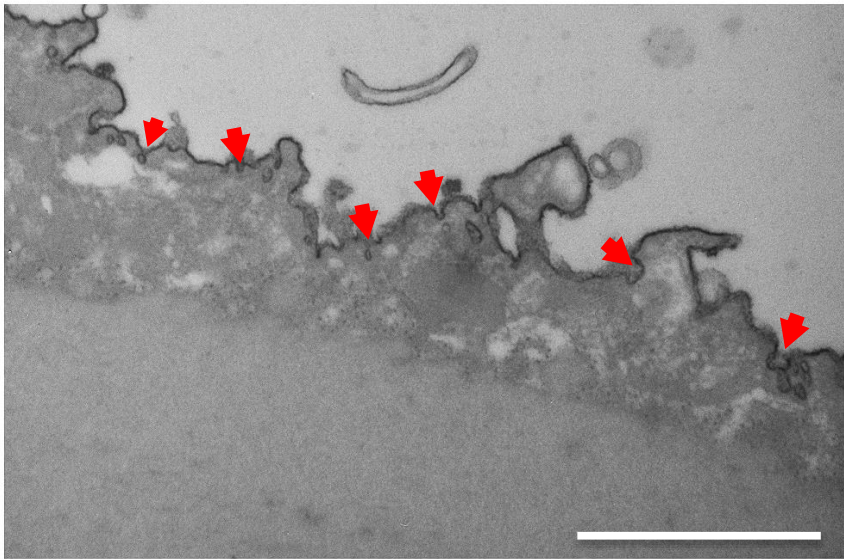
Figure 5.8. Ruthenium red stained caveolae in pressurised carotid arteries. Representative images of caveolae (red arrows) rat carotid arteries (0 and 120 mmHg) stained in the presence of the membrane marker ruthenium red. Scale bar=1000 nm.

5.3.4 Caveolae are important in pressure-induced inflammation.

To explore the possible role of caveolae in the pressure-induced inflammatory response gene expression of ICAM-1 and MCP-1 in pressurised H5V Scr and Cav1 KD cells were examined. ICAM-1 was significantly upregulated in H5V Scr cells pressurised to 120 mmHg compared to unpressurised (Ctr) and 0 mmHg (Ctr: 1.0±0.1, 0 mmHg: 0.6±0.1 vs. 120 mmHg: 2.0±0.3; n=4-6; $P<0.01$; Fig 5.9A) whereas in H5V Cav1 KD cells it was not. *MCP-1* gene expression in H5V Scr cells was also upregulated at 120 mmHg (Ctr: 1.1±0.2, 0 mmHg: 0.5±0.2 vs. 120 mmHg: 3.1±1.2; n=4-6; $P<0.05$; Fig 5.9B) while expression in H5V Cav1 KD cells at 120 mmHg was not different to unpressurised cells (n=3-6; $P>0.05$; Fig 5.9B).

5.3.5 Cav1 and cavin-1 may disassemble with pressure

A possible explanation for the reduction of caveolae number seen in pressurised vessels is the disassembling of caveolae structural proteins Cav1 and cavin-1, which have previously been shown to rapidly dissociate when caveolae flatten out in response to stress (Sinha *et al.*, 2011). Therefore, to examine the interaction of Cav1 and cavin-1 under pressure we used a Duolink™ *in situ* proximity ligation assay (PLA) in pressurised RCA with a fluorescent signal indicative of the close proximity of the two proteins. Preliminary results demonstrate no difference in fluorescence at the higher pressure (0 mmHg: 12.4±1.4 vs. 120 mmHg: 7.7±0.9; n=3; Fig 5.10). However, preliminary immunofluorescence staining of these proteins, suggest there is a reduction of total Cav1 and cavin-1 at 120 mmHg (Fig 5.11). Further work is required to validate these findings.
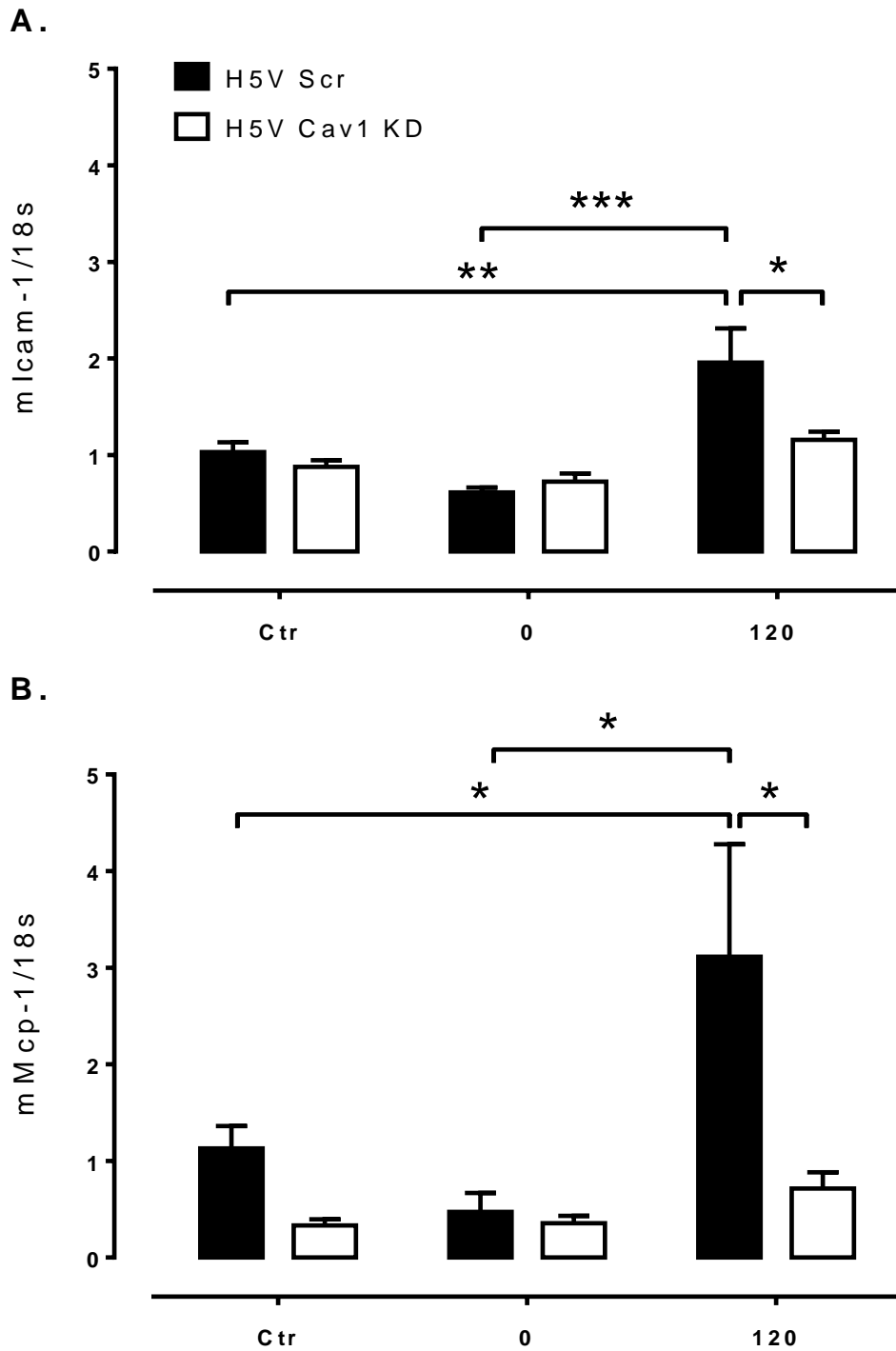
Figure 5.9. Effect of Cav1 KD on mRNA expression in pressurised endothelial cells. (**A**) ICAM-1 and (**B**) MCP-1 gene expression in transformed H5V cells with either scrambled shRNA (H5V Scr; black) or Caveolin-1 shRNA (H5V Cav1 KD; white). Cells were untreated, or pressurised at 0 and 120 mmHg, n=3-6. Results are expressed as mean ± SEM. Values were analysed using a two-way ANOVA with Bonferroni post hoc where *P<0.05.

A
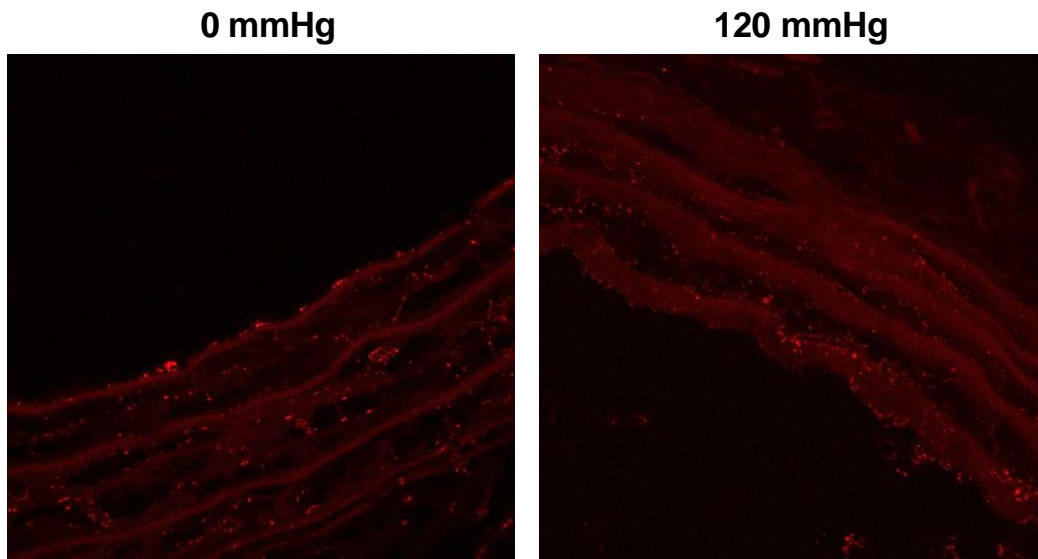
B
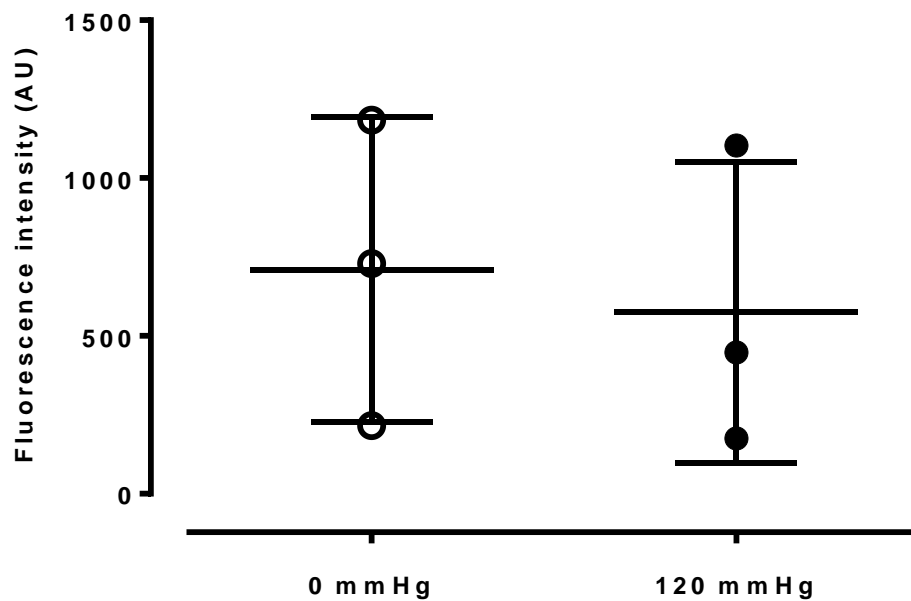
Figure 5.10. Interaction of caveolin-1 and cavin-1 in pressurised carotid arteries. (**A**) Representative confocal immunofluorescence images of the interaction of Cav1 and cavin-1 as detected by the Duolink™ PLA in RCA pressurised (0 and 120 mmHg) for 1 hour. (**B**) Preliminary quantification of PLA in carotid arteries (n=3). Results are expressed as mean ± SEM. Data were analysed with an unpaired Student t-test.
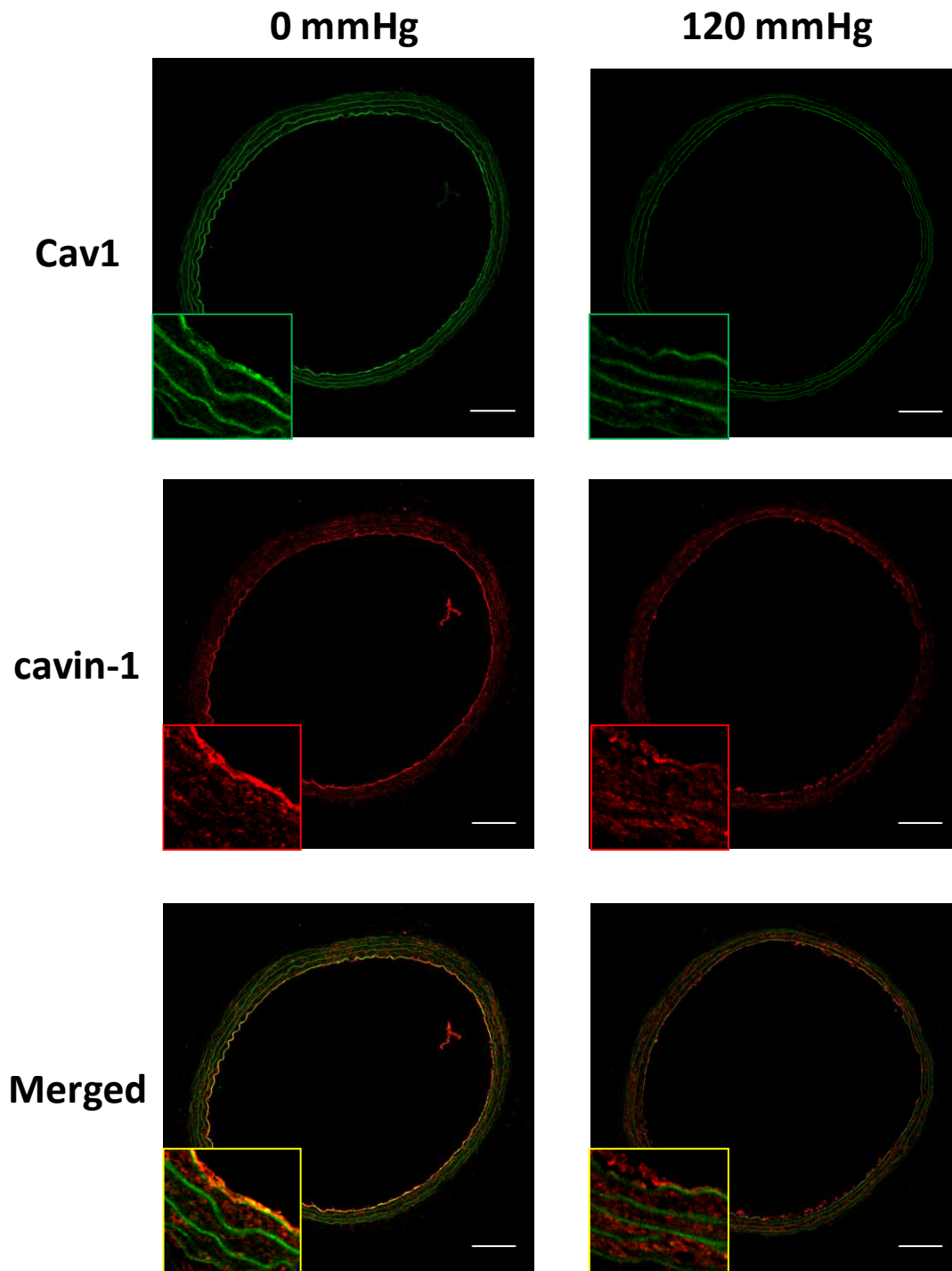
Figure 5.11 Distribution Cav1 and cavin-1 in carotid arteries. Representative confocal immunofluorescence images of Cav1 and cavin-1 in carotids arteries pressurised (0 and 120 mmHg) for 1 hour. Scale bar=20 μm with zoomed images x3.

5.4 Discussion

This chapter describes the role of mechanical forces and mechanosensors, particularly caveolae, in the pressure-induced inflammatory response. By controlling for discrete parameters of the *ex vivo* pressure myograph protocol it can be reasoned that circumferential stretch is the predominant mechanical force activating the inflammatory response. Furthermore, with the use of shRNA knockdown cells, knockout mice, and specific antibodies for Cav1 and cavin-1 we demonstrate that caveolae play an essential role in this process.

HSS actively suppresses inflammation by inducing a negative feedback mechanism causing release of local NO, preventing adhesion molecule expression (Walpola *et al.*, 1995), and reducing endothelial dysfunction and apoptosis (Chiu & Chien, 2011b). Indeed, reduced inflammation is seen in various cultured endothelial cells (Luu *et al.*, 2010b) as well as rabbit aorta exposed to HSS (Yamawaki *et al.*, 2003). HSS is the main underlying reason for the beneficial aspects of exercise training including improved flow-mediated vasodilation and vascular remodelling (Tinken *et al.*, 2010). Our study supports these findings by demonstrating that vessels subjected to high pressure coupled with HSS have both reduced leukocyte adhesion and adhesion molecule expression compared to those subjected to high pressure and LSS.

The consensus in the literature is that wall shear stress acts predominantly on endothelial cells whereas circumferential stretch acts on the intima, media and adventitia eliciting changes in smooth muscle cells (Li *et al.*, 2005b; Haga *et al.*, 2007). Therefore, less is known about the effect of stretch on endothelial cells particularly *in vivo*. Vessels exposed to high pressure coupled with LSS had the same amount of leukocyte adhesion as those exposed to static high pressure suggesting that perhaps stretch is the predominant force observed. Indeed, LSS alone did not induce vascular inflammation as opposed to increased pressure without shear (i.e. stretch), which was inflammatory. However, it should be noted that the experimental protocol did require that blood was flowed at a rate of LSS for the final 10 mins under both circumstances. In the clinical setting, untreated hypertensive patients have been shown to have reduced shear (Khder *et al.*, 1998; Lee *et al.*, 2009) as well as increased tension or stretch (Lee *et al.*, 2008). Importantly, this increased stretch is

positively correlated with the progression of atherosclerosis in carotid arteries (Lee *et al.*, 2008).

Mechanosensors that sense changes in shear and stretch are located on the endothelium and are involved in the activation of downstream signalling pathways. The lipid-rich invaginations along the plasma membrane, caveolae, are a prime candidate mechanosensor in the pressure-induced response as they are abundant in endothelial cells, house adhesion molecules (Millan *et al.*, 2006) and can directly regulate eNOS. The location of eNOS to plasmalemmal caveolae was first demonstrated in 1996 (Shaul *et al.*, 1996a). Since then it has been established that eNOS is inactive when bound to the primary protein of caveolae, Cav1 (Ju *et al.*, 1997; Michel *et al.*, 1997) and is activated by an increase in shear stress (Rizzo *et al.*, 1998). These studies demonstrate an important role of caveolae in blood pressure regulation. Indeed, *Cav1*$^{-/-}$ mice demonstrate impaired flow-mediated dilation and increased vascular remodelling, which is restored when endothelial Cav1 is reconstituted (Yu *et al.*, 2006). Interestingly, despite increased NO production, studies report that overall *Cav1*$^{-/-}$ mice do not demonstrate alterations in systemic blood pressure but rather demonstrate a pulmonary hypertensive phenotype (Zhao *et al.*, 2002).

Caveolae are also involved in signalling an inflammatory response. It has been shown that caveolae may regulate Nox-induced ROS production in endothelial cells as Nox subunits are heavily enriched in caveolae (Yang *et al.*, 2007) and are activated in the caveolae with angiotensin II stimulation (Lobysheva *et al.*, 2011). Furthermore, a major function of Cav1 is the transportation of LDL to the cytosol (Frank *et al.*, 2008) playing an important role in atherosclerosis. Indeed, in studies examining the role of caveolae in plaque formation it has been shown that *Cav1*$^{-/-}$*/ApoE KO*$^{-/-}$ mice are protected from atherosclerosis. Reductions in proatherogenic CD36 and adhesion molecules (Frank *et al.*, 2004) and inhibition of leukocyte adhesion *in vivo* (Engel *et al.*, 2011) have also been observed. The reduced plaque formation is also shown to be specifically dependent on endothelial caveolae, where re-expression of endothelial Cav1 in the *Cav1*$^{-/-}$*/Apoe*$^{-/-}$ mice results in a similar atherosclerotic phenotype to control *Apoe*$^{-/-}$ (Fernandez-Hernando *et al.*, 2010). Our findings with TNFα stimulation are consistent with these studies, in which leukocyte adhesion in *Cav1*$^{-/-}$ aorta was reduced compared to C57BL/6 controls. In addition, adhesion molecule gene expression and monocyte adhesion in TNFα-stimulated Cav1 KD cells were reduced compared to

scrambled controls further supporting the important role of caveolae in TNFα-induced inflammation.

In relation to pressure, we discovered an important role for caveolae in pressure-induced inflammation. Electron microscopy images of pressurised carotid arteries demonstrated a clear pressure dependent reduction in the number of caveolae. This was further confirmed by electron microscopy imaging of ruthenium red stained carotids. Due to its close association with eNOS Park *et al.*, (1998) and Boyd et al., (2003) have demonstrated an increased caveolae number in response to HSS compared to static conditions. Conversely, and more closely representing our conditions, Sinha *et al.*, (2011) showed that endothelial cells exposed to stretch via osmotic swelling demonstrate a significant reduction in the number of caveolae at the cell surface. Furthermore, they demonstrated that this was due to the flattening of caveolae and disassembling of cavin-1 from Cav1. Using a PLA in pressurised RCA we did not see a change in Cav1 and cavin-1 interaction; however, this is possibly due to an inadequate visualisation of the signal in the tissue, which we are currently investigating further in pressurised cells. Nevertheless, the immunofluorescence of cavin-1 in RCA was reduced with pressure, suggesting a reduction in caveolae number, which is consistent with our electron microscopy evidence, which showed a trend for increased membrane length at the higher pressure. It is suggested this is a quick cell survival mechanisms (Parton *et al.*, 2013) where caveolae have a role as membrane reservoirs (Sens *et al.*, 2006; Sinha *et al.*, 2011).

Aside from a change in membrane length, an increased deformity was also noted at the higher pressure. Whether these are the hypothesized projections formed to aide in leukocyte transmigration (Carman *et al.*, 2004; Dejana, 2006; Nieminen *et al.*, 2006) remains to be determined. Nevertheless, it seems that reduced caveolae number and their flattening is essential for pressure-induced inflammation. Our findings that Cav1 KD cells have blunted adhesion molecule gene expression, a similar response to TNFα stimulation, certainly is in support of this notion.

In summary, we have identified caveolae as key mechanosensors involved in the pressure-induced inflammatory response. Firstly, we provide evidence that increased pressure when coupled with increased circumferential stretch and LSS elicits a dramatic inflammatory response. Secondly, this response is reduced with HSS. Thirdly, we demonstrate that caveolae are not only important mechanosensors but are also involved in

mechanotransduction as evidenced by the reduction in adhesion molecule expression and leukocyte adhesion *ex vivo* and *in vitro* following Cav1 blockade. Finally, we demonstrate, for the first time, that high intraluminal pressure reduces caveolae number. Collectively these data suggest caveolae are an essential mediator between the effect of pressure and the downstream signalling pathways.

Chapter 6

Development of a hypertensive atherosclerotic mouse model: hypertension provokes plaque instability

6.1 Introduction

Uncontrolled blood pressure and its complications are an ongoing issue, despite the use of antihypertensive agents. Most antihypertensive treatments only treat the elevated blood pressure and do not have the ability to effectively repair vascular dysfunction or remodelling (Bravo *et al.*, 2001). Patients with resistant hypertension have a greater risk of target organ damage (Gaddam *et al.*, 2008) and plaque development (Cuspidi *et al.*, 2001). In the previous chapters, we showed that increased luminal pressure could induce vascular inflammation. We suggest that targeting this consequence of high blood pressure may be a useful combination therapy to address the complications associated with hypertension.

A hurdle in the development of appropriate pharmacological interventions for hypertension-induced vascular complications is the lack of appropriate mouse models that exhibit both hypertension and atherosclerosis. Of the models that have been used, many involved surgical interventions such as the 2 kidney-1 clip and 1 kidney-1 clip (Mazzolai *et al.*, 2004), aortic constriction (Tropea *et al.*, 1996) and carotid artery ligation (Nam *et al.*, 2009) to induce hypertension. Alternatively, chronic pharmacological stimulation with Ang II or noradrenaline is used to increase blood pressure but the doses used are not necessarily physiologically relevant. To overcome this, we aimed to create a spontaneous model of hypertension that was prone to atherosclerosis. With this model we are afforded the opportunity to investigate the effect of high blood pressure on leukocyte adhesion and plaque development.

BPH/2J (or Schlager) mice are a spontaneously hypertensive mouse model generated in the late 1970s. BPH/2J mice were originally derived from an 8-way cross of unrelated normotensive mice. These mice develop hypertension from 5 weeks of age and at 20 weeks have a MAP of 130 mmHg compared to control levels of 112 mmHg (Schlager & Sides, 1997). These mice have a neurogenic form of hypertension regulated by neurons located in the medial amygdala (Davern *et al.*, 2010), and demonstrate increased levels of oxidative stress (Uddin *et al.*, 2003). Importantly, their hypertension has been reported to be RAS independent (Palma-Rigo *et al.*, 2011) although recently, Jackson *et al.*, (2013) provided evidence that the RAS may play a role during the active period (night) in these mice. For the current study, we crossed BPH/2J mice with *Apoe*$^{-/-}$ mice to create a hypertensive atherosclerotic model (BPHx*Apoe*$^{-/-}$). Given the enormous role of the ROS in the intracellular

signalling pathway in pressure-induced endothelial activation observed in the previous chapters, we hypothesised that treatment with a ROS inhibitor would be beneficial. However, as ROS inhibitors decrease blood pressure (Mullan *et al.*, 2002; Park *et al.*, 2002; Unger & Patil, 2009) this would make the interpretation of the cause and consequence of vascular inflammation difficult. Therefore, we targeted leukocyte recruitment in this model, to discretely quantify the contribution of pressure-induced inflammation to atherosclerosis.

P-selectin is a promising target to control leukocyte recruitment to the activated endothelium. P-selectin is secreted from WPB in endothelial cells and platelets, and is a key adhesion molecule in the initial stages of leukocyte recruitment (Eriksson *et al.*, 2001). P-selectin is required for the movement of leukocytes into lesions and advancing the progression of the plaque in *Apoe$^{-/-}$* mice (Dong *et al.*, 2000). Inhibition of P-selectin with the human monoclonal antibody inclacumab in clinical trials in patients with atherosclerosis has shown promising results, with reduced myocardial damage after percutaneous coronary intervention (Tardif *et al.*, 2013). In *Apoe$^{-/-}$* mice, blocking P-selectin with the antibody RB40.34, reduces rolling and adhesion of monocytes in mice fed a high fat diet for 4-5 weeks (Ramos *et al.*, 1999). In a carotid artery wire injury model, one bolus injection (100 or 200 μg i.p.) reduced macrophage content in plaques and neointima formation 4 weeks following injury (Phillips *et al.*, 2003). Therefore, inhibition of P-selectin may enable a clear exploration of whether inhibition of the pressure-induced adhesion cascade, can reduce chronic plaque progression**.**

In this chapter we aimed to develop and characterize the BPHx*Apoe$^{-/-}$* mice, explore the chronic effect of high blood pressure on plaque progression, and examine whether blocking inflammation in the context of sustained high blood pressure can reduce plaque development in these mice. We hypothesized that the BPHx*Apoe$^{-/-}$* mice would have enhanced atherosclerosis as the increased blood pressure would promote leukocyte recruitment. We also reasoned that inhibiting leukocyte recruitment, via treatment with a P-selectin blocking antibody, would prevent the pressure-induced accelerated atherosclerosis.

6.2 Methods

6.2.1 Establishing BPHx*Apoe*$^{-/-}$ colony

To create a spontaneously hypertensive, diet-induced atherosclerotic mouse model, breeding pairs of either male or female *Apoe*$^{-/-}$ mice were crossed with male or female Schlager BPH/2J mice. Development of this model was approved by the AMREP Animal Ethics Committee (Approval No: E/1111/2011/B), which adheres to the National Health and Medical Research Council (NHMRC) Australian Code of Practice for the Care and Use of Animals for Scientific Purposes. The blood pressure of the offspring (F2) was determined via tail cuff at > 6 weeks and approximately one third of mice had systolic blood pressure above 135 mmHg. These hypertensive mice were heterozygous for *Apoe*$^{+/-}$, due to *Apoe*$^{-/-}$ male or female paired with BPH/2J (*Apoe*$^{+/+}$) mice, and were paired with their hypertensive *Apoe*$^{+/-}$ siblings (systolic blood pressure >135 mmHg). The offspring (F3) were screened for hypertension and the *Apoe* gene in the homozygous condition (-/-) and bred with a sibling of similar phenotype and genotype. This process resulted in a fixed line of mice with a deficiency of the *Apoe* gene and a propensity to develop hypertension (BPHx*Apoe*$^{-/-}$). Blood pressure was measured in all mice prior to study inclusion to confirm the presence of the hypertensive phenotype.

6.2.2 Genotyping for *Apoe*$^{-/-}$

Tail biopsies were taken at weaning and sent to Transnetyx (Cordova, TN) for commercial genotyping of the *Apoe* deficiency. The Transnetyx method involves a qPCR based probe hybridization to detect the presence of both the knockout and wild type alleles in the samples. Using target specific junction sequence within the mutant allele that consisted of endogenous *Apoe* and neomycin cassette sequence, the presence of the knockout allele was determined. The wild type genotype was determined by targeting the wild type sequence, which was deleted by the insertion of the neomycin resistance cassette.

6.2.3 Blood pressure telemetry

All telemetry experiments were performed in collaboration with Professor Geoff

Head's Neuropharmacology Laboratory (Baker IDI Heart and Diabetes Institute) with the assistance of Kristy Jackson and John-Luis Moretti.

6.2.3.1 *Measurement of BP, HR and locomotor activity*

Under isofluorane open circuit anaesthesia (1.5-2.5%) 8 – 10 week old BPHx*Apoe*$^{-/-}$ and *Apoe*$^{-/-}$ mice on normal chow diet were implanted with radiotelemetry devices weighing 1.4 g and approximately 10 mm in length (TA11PA-C10; DataSciences International (DSI), St Paul, USA) as previously described (Butz & Davisson, 2001; Davern *et al.*, 2010). Briefly, the catheter was inserted into the left carotid artery and the transmitter body was inserted subcutaneously along the right flank. Mice were housed individually and each cage was placed on a receiver plate (model RPC-1 Receiver, DSI, MN, USA) connected to a pressure output adapter (R11CPA) and an analogue converter (PR11A). Following 10-day recovery from surgery, 1 min averages of pulsatile arterial blood pressure readings and locomotor activity were recorded continuously over a 72-hour period sampled at 100 Hz as previously described (Jackson *et al.*, 2007). Mean arterial pressure and heart rate were analysed in the Neuropharmacology laboratory using an in-house program in Labview (Head *et al.*, 2001).

6.2.4 Study animals

8-week-old BPHx*Apoe*$^{-/-}$ or *Apoe*$^{-/-}$ were fed a high fat rodent diet (HFD) 21% fat and 0.15% cholesterol and water *ad libitum* for 12 weeks. BPHx*Apoe*$^{-/-}$ mice with a tail cuff reading of systolic blood pressure >135 mmHg and *Apoe*$^{-/-}$ mice with a reading of <120 mmHg were entered into the study. This study was approved by the AMREP Animal Ethics Committee (Approval No: E1265/2012/B), which adheres to the National Health and Medical Research Council (NHMRC) Australian Code of Practice for the Care and Use of Animals for Scientific Purposes.

6.2.5 P-selectin intervention

This study aimed to determine whether blocking vascular inflammation and the adhesion cascade, without lowering blood pressure, could reduce atherosclerotic plaque

progression in chronic hypertensive mice. BPHx*Apoe*$^{-/-}$ and *Apoe*$^{-/-}$ mice were fed a high fat diet (HFD) for 12 weeks and assessed for plaque area and morphology with and without treatment of one or two bolus injections of P-selectin blockade, RB40.34, (Phillips *et al.*, 2003). At Week 0 mice underwent tail cuff plethysmography for preliminary blood pressure determination. Phillips *et al.*, (2003) demonstrated that RB40.34 was present at least 7 days following administration and disappeared by 14 days. Since there are no reports of RB40.34 administration in a chronic atherosclerotic model, we investigated four treatment groups: saline treated (i.p.; intraperitoneal injection), isotype control (2 injections at week 1 and 3: Ctr; 2x100 µg i.p.; BD Pharmingen, #553995), one injection of the anti-P-selectin antibody RB40.34 (1 injection at weeks 1: 100 µg i.p.; BD Pharmingen, #553744), or two injections of RB40.34 (2 injections at week 1 and 3: 2x100 µg i.p.). Mice received either one injection of P-selectin at Week 1 (1x100 µg RB40.34) or two injections; one at Week 1 and again in Week 3 (2x100 µg RB40.34). Saline and isotype injections were delivered at Week 1 and Week 3 (Fig 6.1).

Figure 6.1 Study design of P selectin blockade in chronic hypertensive atherosclerotic mice.

6.2.6 Tissue collection

Mice were killed after the 12 week treatment period by 100% CO_2 asphyxiation. The arch, thoracic and abdominal aorta, lungs, liver, kidney, heart and spleen were excised and placed in ice-cold Krebs buffer. The aorta was cleaned for Sudan IV imaging, while the sinus of the heart was frozen in OCT for subsequent immunohistochemistry analysis.

6.2.7 Sudan IV staining in mouse aorta

The aorta was cleaned and placed into a labelled biopsy cassette between two sponges and stored in 10% formalin overnight. Cassettes were rinsed in 70% ethanol for 1 min and placed in Sudan-Herxheimers solution (5g Sudan IV, 500 ml 80% ethanol, 500 ml acetone) for 30 min. Cassettes were rinsed in 80% ethanol and placed in fresh 80% ethanol for 20 min, followed by 60 min under running tap water. Cassettes were then placed back into 10% formalin for up to two weeks before imaging. Sudan IV samples were further cleaned of any remaining connective tissue and fat from the outside. The whole aorta was dissected lengthwise to expose the internal vessel wall. The aorta was mounted onto a glass slide with glycerol gelatin (Sigma, #GG1). Images (3-5) were taken per vessel on a microscope fixed to a digital camera and computer and then stitched together using Fiji 1.47h software (Schindelin *et al.*, 2012). Plaque area was analysed and quantified in the arch, thoracic, abdominal and total aorta using Fiji 1.47h software.

6.2.8 Aortic Sinus staining

Immunohistochemistry was specifically determined in the aortic sinuses in the heart. This includes the left, right, and non-coronary aortic sinuses behind the aortic valve leaflets.

6.2.8.1 CD68

Thawed 6 µm sections were washed with PBS twice for 5 min and incubated in 3% hydrogen peroxide in methanol for 20 min. Sections were washed with PBS (2 x 5 min) again and blocked with 10% normal goat serum (NGS) for 30 min and incubated with avidin

blocking solution (Vector SP-2001) for 15 min. After a quick rinse in PBS, sections were incubated with Biotin blocking solution (Vector SP-2001) for 15 min and rinsed again with PBS. Sections were incubated overnight at 4°C with either the CD68 primary antibody (1:200; rat anti-mouse; Serotec, #MCA1957) in 5% NGS or 5% NGS only (negative control).

Sections were washed with PBS (2 x 5 min) and incubated with the secondary antibody (1:100; mouse anti-rat; BD Pharmingen, #550325) in 5% NGS for 30 min. After a wash in PBS (2 x 5 min) the ABC complex (Vectastain, #PK-6100) was added for 30 min followed by further washes in PBS (2 x 5 min). The DAB (3,3'-Diaminobenzidine) mix (Vector Laboratories Inc, #SK-4100) was added until the sections turned brown. Sections were then washed in ultra-pure water (2 x 5 min) and stained with Mayer's Haematoxylin (45 sec). Residual stain was removed with a rinse in running tap water until clear, 4 min in Scott's tap water and another rinse in tap water. Sections were dehydrated with 95% ethanol (3 min) followed by three changes in 100% ethanol (3 min each) and cleared in two changes of xylene (5 min each). Sections were then air dried and mounted with depex mounting medium and dried overnight. Sections were imaged at 20x using the FSX100 light microscope.

6.2.8.2   *Oil Red-O*

Thawed 6 μm sections were fixed in 10% neutral buffered formalin for 4 min and washed in PBS for 4 min. Sections were stained in Oil Red-O working solution (3 parts oil red-o stock (3% oil red-o in isopropanol; Sigma-Aldrich, #O0625): 2 parts ultra-pure water) for 2 hr. Excess stain was removed with 3 dips in 60% isopropanol and washed in ultra-pure water for 2 min. Sections were counterstained with Mayer's Haematoxylin for 4 min. Residual stain was removed with running tap water for 3 min followed by ultra-pure water for 3 min. Sections were then air dried and mounted with aqueous mounting media (Aquamount; Grale Scientific, #36226S). Sections were imaged at 20x using the FSX100 light microscope.

6.2.8.3   *Collagen staining via picrosirius red*

Thawed 6 μm sections were fixed in acetone for 15 min at 20°C and washed in PBS 2 x 5 min. Sections were stained in 0.1% Sirius Red F3BA (Sigma, #365548; made up in

saturated aqueous picric acid) for 1 hr and washed in 0.01 N HCl for 2 min. Following a rinse in dH_2O sections were dehydrated in 100% ethanol (2 x 5 min) and then cleared in xylene (2 x 5 min) before mounting with depex. Slides were imaged on a BX61 Olympus microscope under bright field and polarised light and images were analysed with ImageJ.

6.2.9 Statistics

Data are expressed as mean $\pm$ SEM and were analysed using GraphPad Prism version 6.00 software (GraphPad Software, La Jolla, California, USA). Heart rate, blood pressure, locomotor activity, bodyweight change, plaque area and sinus staining between the BPHx*Apoe*$^{-/-}$ and *Apoe*$^{-/-}$, as well as sinus staining with RB40.34 intervention (which compared two groups) were analysed using an unpaired Student's t-test. Body weight pre and post high fat diet in the BPHx*Apoe*$^{-/-}$ and *Apoe*$^{-/-}$ was analysed using a two-way repeated measures ANOVA with the factors strain and time. Weight change and plaque area with RB40.34 intervention were analysed using a one-way ANOVA with the factor treatment. Significant differences were analysed using a Bonferroni post hoc to account for multiple comparisons. *P*<0.05 was considered statistically significant.

6.3 Results

For strain comparative purposes, only animals injected with saline were analysed.

6.3.1 Blood pressure is greater in BPHx*Apoe$^{-/-}$* than *Apoe$^{-/-}$*

Blood pressure was measured using radiotelemetry in conscious BPHx*Apoe$^{-/-}$* and *Apoe$^{-/-}$* mice 10-12 weeks of age. 24-hour averages of SAP (systolic arterial pressure), DAP (diastolic arterial pressure), MAP (mean arterial pressure) and HR (heart rate) were greater in the BPHx*Apoe$^{-/-}$* compared to *Apoe$^{-/-}$* mice (n=5; *P*<0.05; Fig 6.2A-H). This result was particularly apparent during the day (inactive period) where SAP was 17% greater in BPHx*Apoe$^{-/-}$* than in *Apoe$^{-/-}$* (113±3 vs. 97±1 mmHg; n=5; *P*<0.05) and DAP was 22% greater (90±5 vs. 74±1 mmHg; n=5; *P*<0.05). There was no difference in activity units (n=5; *P*>0.05; Fig 6.2I&J).

6.3.2 Body weight increased after 12 weeks on high fat diet

Body weight in both BPHx*Apoe$^{-/-}$* and *Apoe$^{-/-}$* mice increased following 12 weeks on HFD (n=5-6; *P*<0.001; Fig 6.3A). Furthermore, BPHx*Apoe$^{-/-}$* mice showed a trend towards a greater weight gain in response to the HFD compared to *Apoe$^{-/-}$*; but this did not reach statistical significance (n=5-6; *P*=0.10; Fig 6.3B).

6.3.3 BPHx*Apoe$^{-/-}$* did not demonstrate greater plaque area

Total and regional plaque area was assessed using Sudan IV staining. There was no difference in total, aortic arch, thoracic, or abdominal plaque area in BPHx*Apoe$^{-/-}$* compared to *Apoe$^{-/-}$* mice (n=4-6; *P*>0.05; Fig 6.4; Fig 6.5A-D).
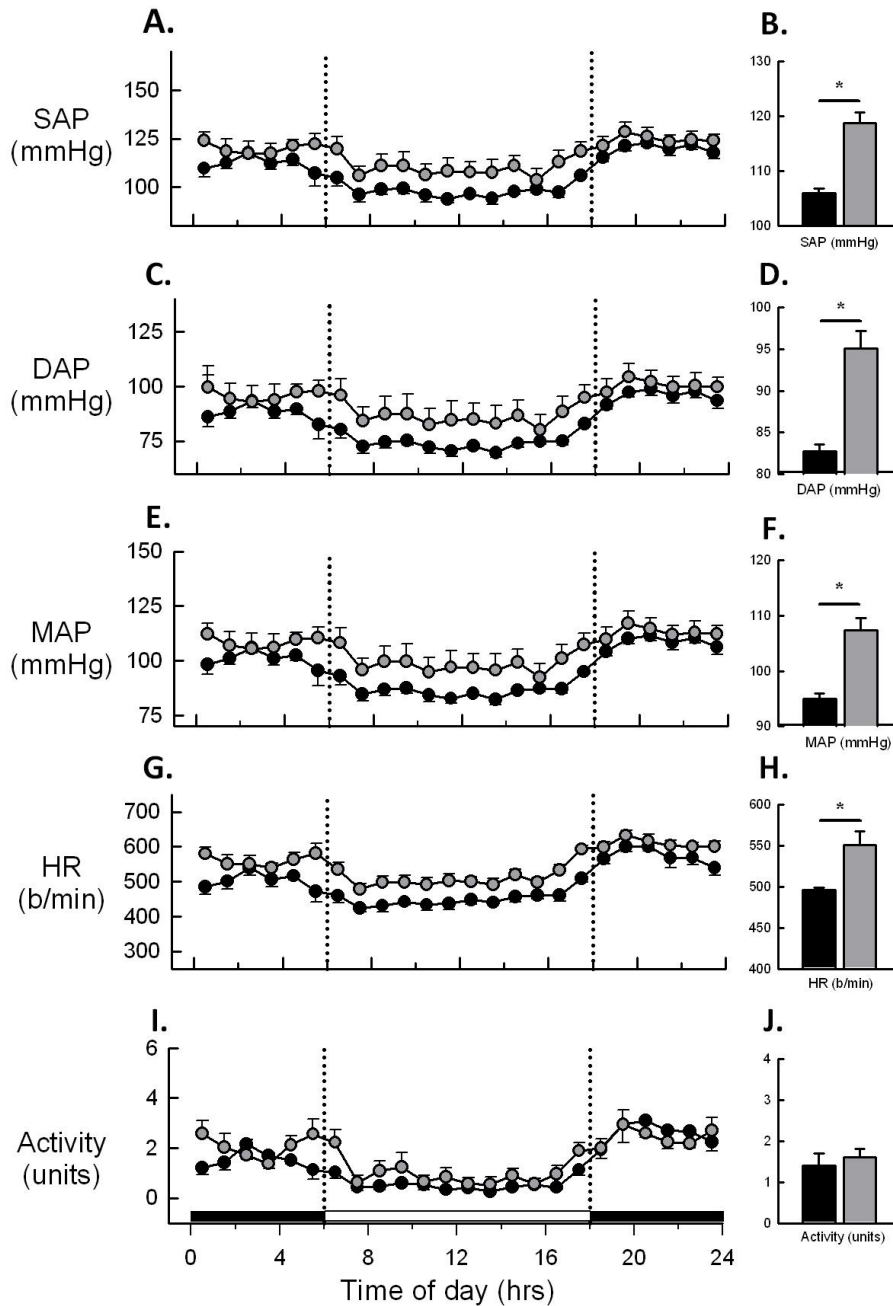
Figure 6.2 Heart rate, blood pressure and locomotor activity. Radiotelemetry measurements in *Apoe^-/-* (black) and BPHx*Apoe^-/-* (grey) mice of (**A**) hourly averages and (**B**) 24 hr mean of systolic arterial pressure (SAP; mmHg), diastolic arterial pressure (DAP; mmHg) (**C**) hourly averages and (**D**) 24 hr mean, mean arterial pressure (MAP; mmHg) (**E**) hourly averages and (**F**) 24 hr mean, heart rate (HR; in beats per min, b/min) (**G**) hourly averages and (**H**) 24 hr mean and locomotor activity (Activity; arbitrary units) (**I**) hourly averages and (**J**) 24 hr mean. Data are presented as mean ± SEM for 24 hour comparisons (**B, D, F, H, J**), n=5. Data were analysed with an unpaired Student t-test where **P*<0.05.
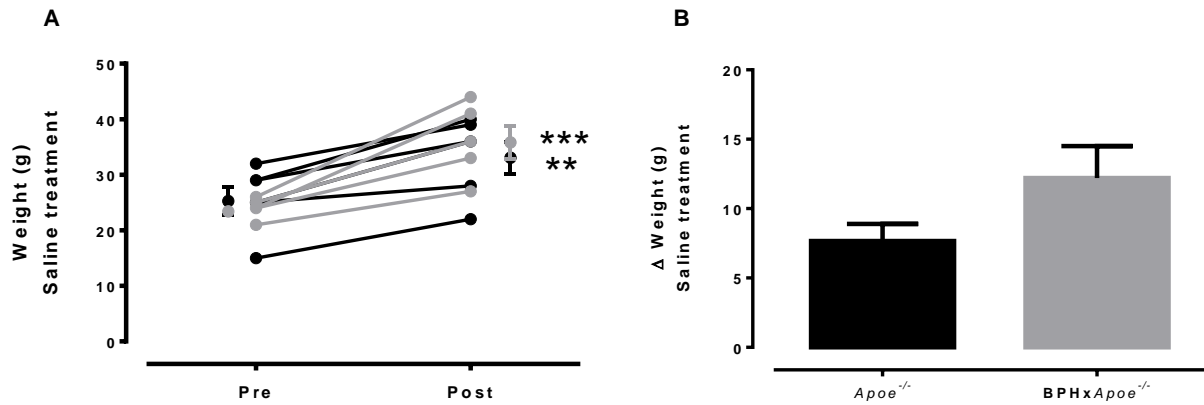
Figure 6.3 Effect of high fat diet on weight. (**A**) *Apoe*^-/- (black) and BPHx*Apoe*^-/- (grey) individual and mean ± SEM weight pre and post 12 weeks on high fat diet. (**B**) Change in weight after high fat diet, n=5-6. Data are presented as mean ± SEM. Data were analysed with a two-way ANOVA with a Bonferroni post hoc test where **P<0.01 *Apoe*^-/-, ***P<0.001 BPHx*Apoe*^-/- pre vs. post. Change in weight was analysed using an unpaired Student t-test.

A.

B.

Figure 6.4 Atherosclerotic plaque in aorta. Representative images of Sudan IV stained plaque in (**A**) *Apoe*$^{-/-}$ and (**B**) BPHx*Apoe*$^{-/-}$ aorta after 12 weeks on a high fat diet.
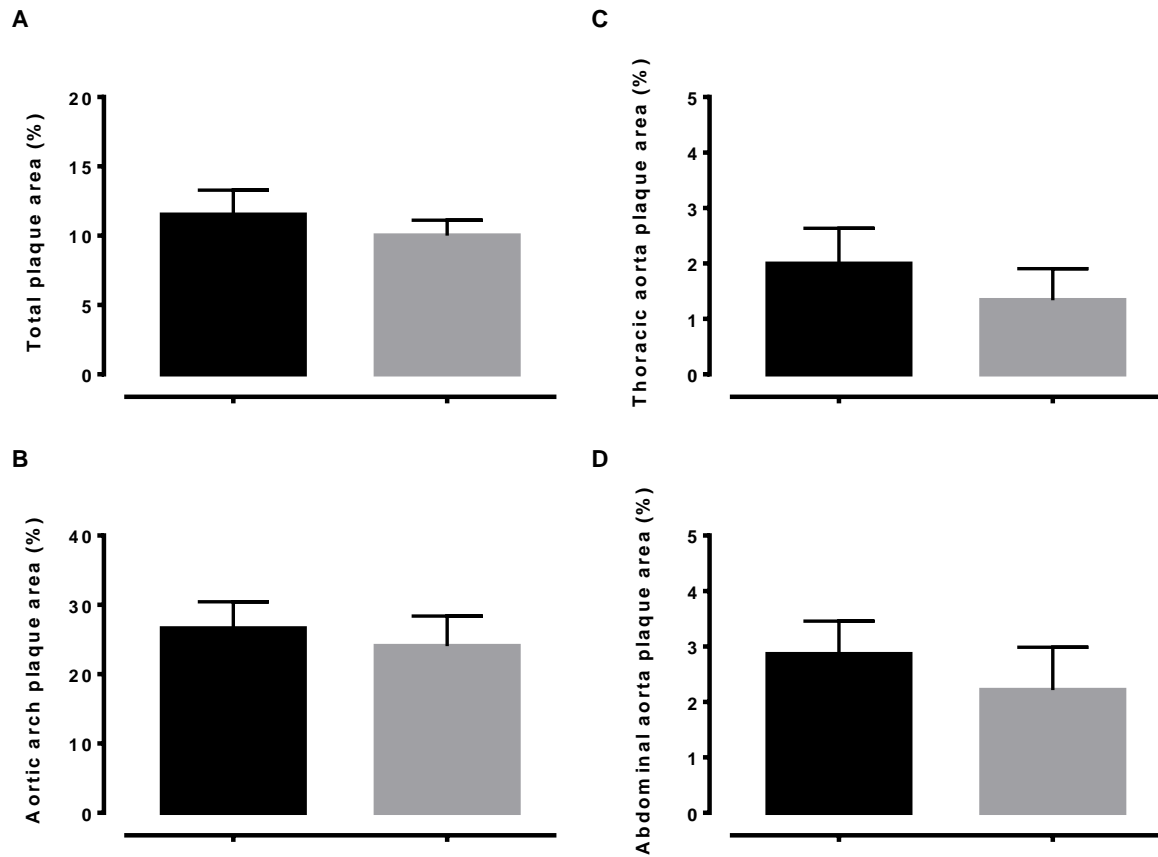
Figure 6.5 Atherosclerotic plaque in the aorta. Sudan IV stained plaque area (%) in the (**A**) total, (**B**) arch, (**C**) thoracic and (**D**) abdominal aorta in *Apoe*$^{-/-}$ (black) and BPHx*Apoe*$^{-/-}$ (grey) mice after 12 weeks on a HFD (n=4-6). Data are presented as mean ± SEM. Data were analysed using an unpaired Student's t-test.

6.3.4 BPHx*Apoe*^{-/-} mice demonstrate plaque instability

To examine plaque stability, the aortic sinus was sectioned and stained for lipid content using oil red O, macrophage accumulation via CD68 and collagen deposition with picrosirius red. Lesions from the BPHx*Apoe*^{-/-} mice had increased lipid deposition compared to *Apoe*^{-/-} mice (18.1±2.4% vs. 29.3±3.4%; n=4-5; *P*<0.05; Fig 6.6). Macrophage content was also increased in the BPHx*Apoe*^{-/-} mice compared to *Apoe*^{-/-} mice (13.9±2.0% vs. 31.4±4.6%; n=3-5; *P*<0.05; Fig 6.7). Collagen content was not significantly different in BPHxApoe^{-/-} mice compared to Apoe^{-/-} mice (11.7±2.4% vs. 6.1±1.2%; n=3-4; P=0.13; Fig 6.8). However, overall these results suggest BPHxApoe^{-/-} have reduced plaque stability. The collagen/lipid ratio, a measure of plaque stability (Naghavi et al., 2003; Zeibig et al., 2011) while not currently significantly reduced in BPHxApoe^{-/-} (Apoe^{-/-}: 0.76±0.29 vs. BPHxApoe^{-/-}: 0.24±0.10; n=3-4; P=0.21) may show statistical significance once the n numbers are increased.

A

B
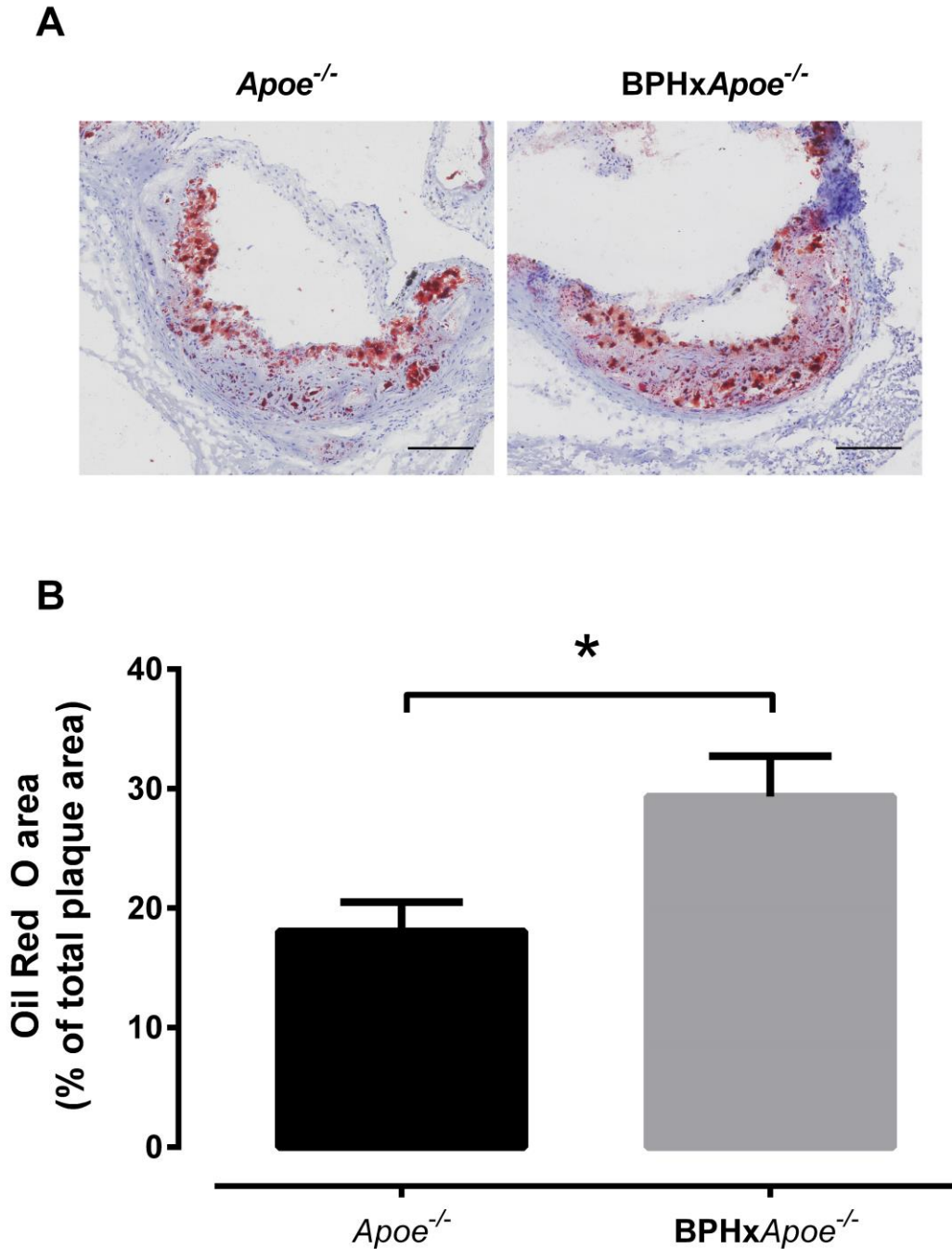
Figure 6.6 Oil Red O stained aortic sinus. (**A**) Representative images of Oil Red O stained aortic sinus atherosclerotic lesions from *Apoe*$^{-/-}$ (black) and BPHx*Apoe*$^{-/-}$ (grey) mice fed a HFD. Scale bar = 150 μm. (**B**) Group data demonstrating stained area (%) of Oil Red O (n=4-5). Data are presented as mean ± SEM. Data were analysed using an unpaired Student t-test where *P<0.05**.**
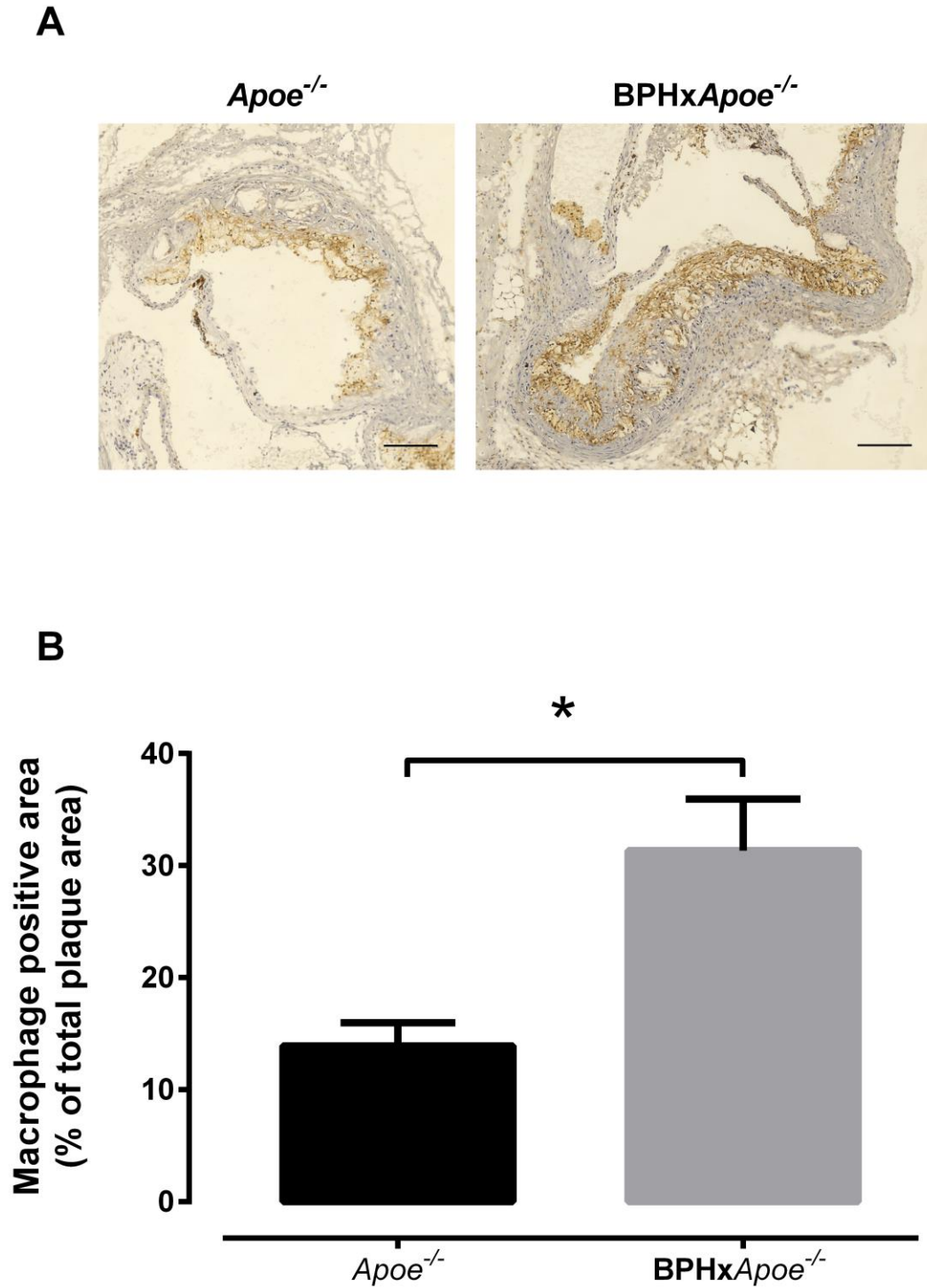
Figure 6.7 Macrophage content in aortic sinus. (**A**) Representative images of macrophage positive stained aortic sinus atherosclerotic lesions from *Apoe*$^{-/-}$ (black) and BPHx *Apoe*$^{-/-}$ (grey) mice fed a HFD and treated with saline. Scale bar = 150 μm. (**B**) Group data demonstrate macrophage positive stained area (%) (n=3-4). Data are presented as mean ± SEM. Data were analysed using an unpaired Student t-test where *P<0.05.
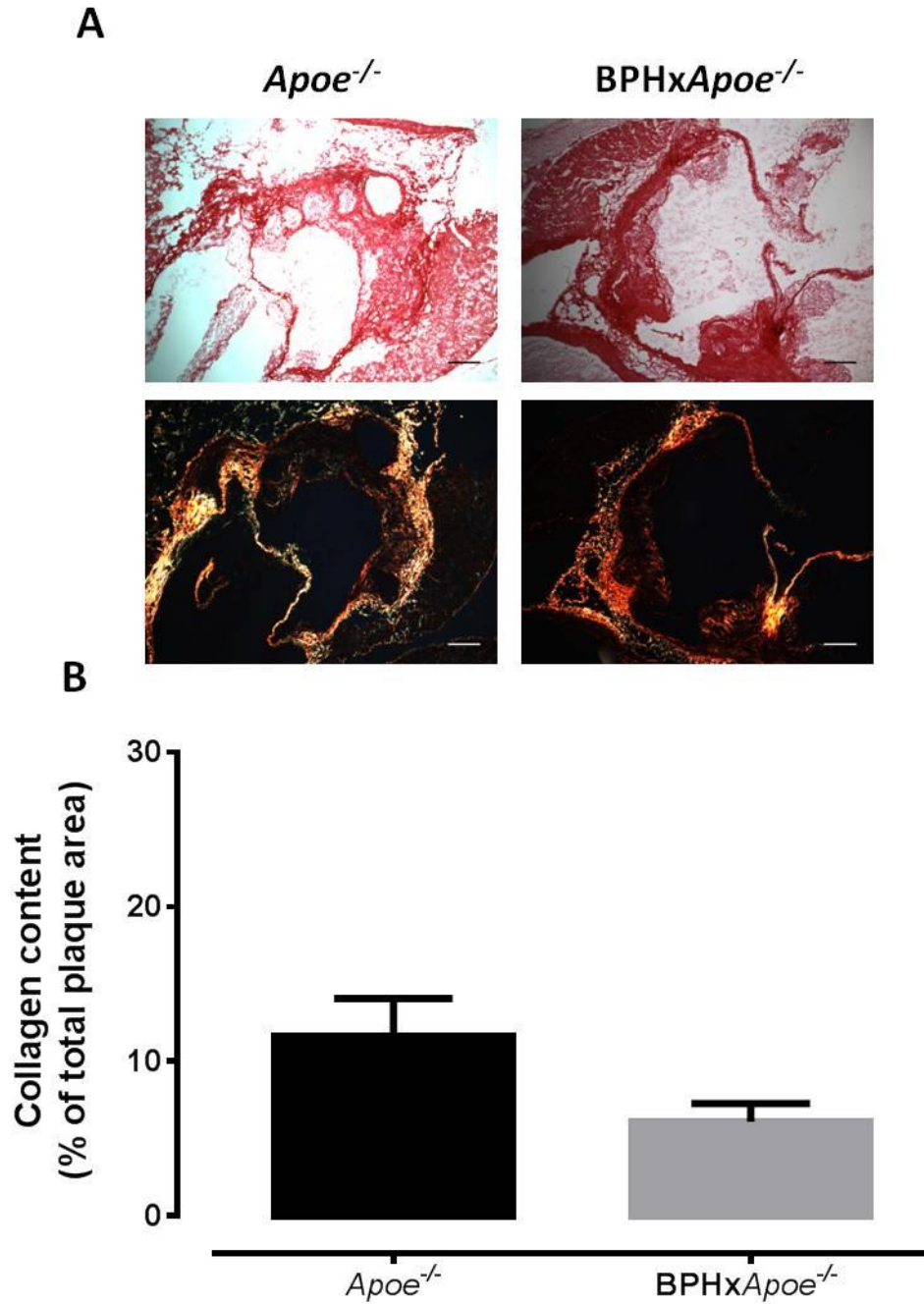
Figure 6.8 Collagen stained aortic sinus. (**A**) Representative images of collagen stained aortic sinus atherosclerotic lesions from *Apoe*$^{-/-}$ (black) and BPHx *Apoe*$^{-/-}$ (grey) mice fed a HFD and treated with saline. Scale bar = 150 μm. (**B**) Group data demonstrate collagen positive stained area (%) (n=3-4). Data are presented as mean ± SEM. Data were analysed using an unpaired Student t-test.

6.3.5 P-selectin may partially restore plaque vulnerability in BPHx*Apoe*$^{-/-}$ mice

To observe whether blocking vascular inflammation, and inhibiting leukocyte adhesion would reduce plaque progression in a chronic hypertensive animal model *Apoe*$^{-/-}$ and BPHx*Apoe*$^{-/-}$ mice were fed a high fat diet for 12 weeks and treated with either an isotype control antibody, a single injection of the P-selectin blocking antibody RB40.34 or two injections of RB40.34 2 weeks apart. Treatment with the isotype control antibody had no effect on weight again as the BPHx*Apoe*$^{-/-}$ mice still demonstrated greater weight change compared to *Apoe*$^{-/-}$ mice (7.6±0.7g vs. 12.2±1.4 g; n=10-11; *P*<0.01). Weight gain was also unaffected by P-selectin blockade (Fig 6.9 A&B).

P-selectin blockade did not affect total or regional plaque area as determined by Sudan IV staining (n=5-11; *P*>0.05; Fig 6.10A-D). Nor was there an effect on lipid deposition. Somewhat surprisingly there was no effect on macrophage content with the anti-P-selecin antibody in either strain (Fig 6.11A&B, Fig6.12A&B). Interestingly, while there was no change in collagen content in *Apoe*$^{-/-}$ mice (n=3-6; *P*>0.05; Fig 6.13A), the BPHx*Apoe*$^{-/-}$ demonstrated significantly increased collagen content with RB40.34 (Ctr: 5.1±1.0% vs. 2x100 µg RB40.34: 20.5±4.2%; n=4-5; *P*<0.01; Fig 6.13B). Plaque stability, as measured by the collagen/lipid ratio, was also improved with RB40.34 in the BPHx*Apoe*$^{-/-}$ mice (Ctr: 0.20±0.06 vs. 2x100 µg RB40.34: 0.93±0.20; n=4-5; *P*<0.01; Fig 6.14B) but not the *Apoe*$^{-/-}$ mice (Ctr: 0.62±0.20 vs. 2x100 µg RB40.34: 0.67±0.15; n=3-7; *P*>0.05; Fig 6.14A). Therefore, although P-selectin blockade did not affect total plaque area, lipid deposition or macrophage content, it did increase collagen deposition and consequently improved plaque stability.
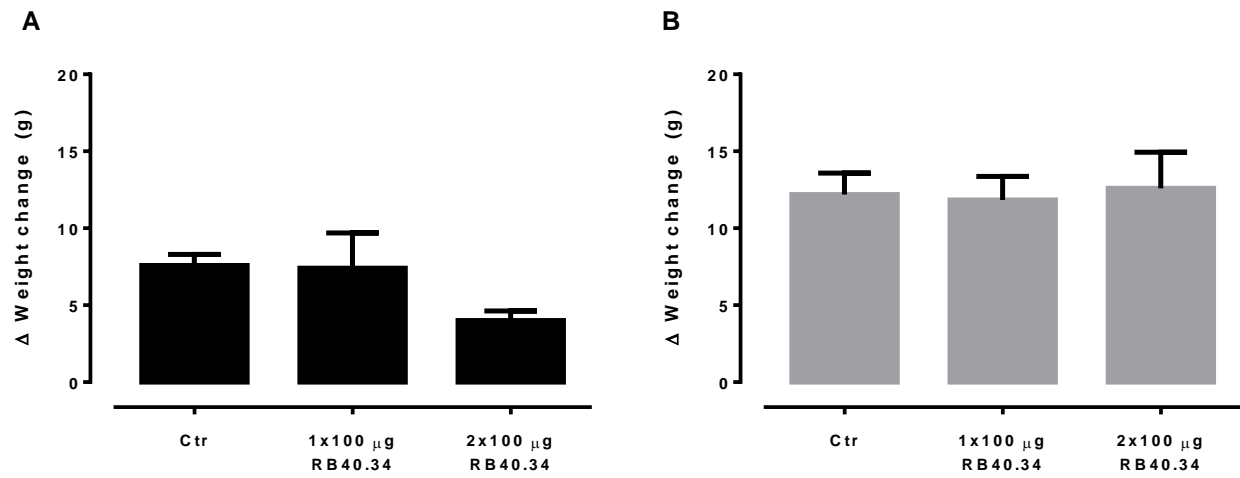
Figure 6.9 Change in weight following P-selectin blockade. (**A**) *Apoe*$^{-/-}$ (black) and (**B**) BPHx*Apoe*$^{-/-}$ (grey) mice weight change following a 12 week HFD and treatment with an isotype control (Ctr), one injection (1x100 µg) or two injections of RB40.34 (2x100 µg), n=5-6. Data are presented as mean ± SEM. Data were analysed using a one-way ANOVA.
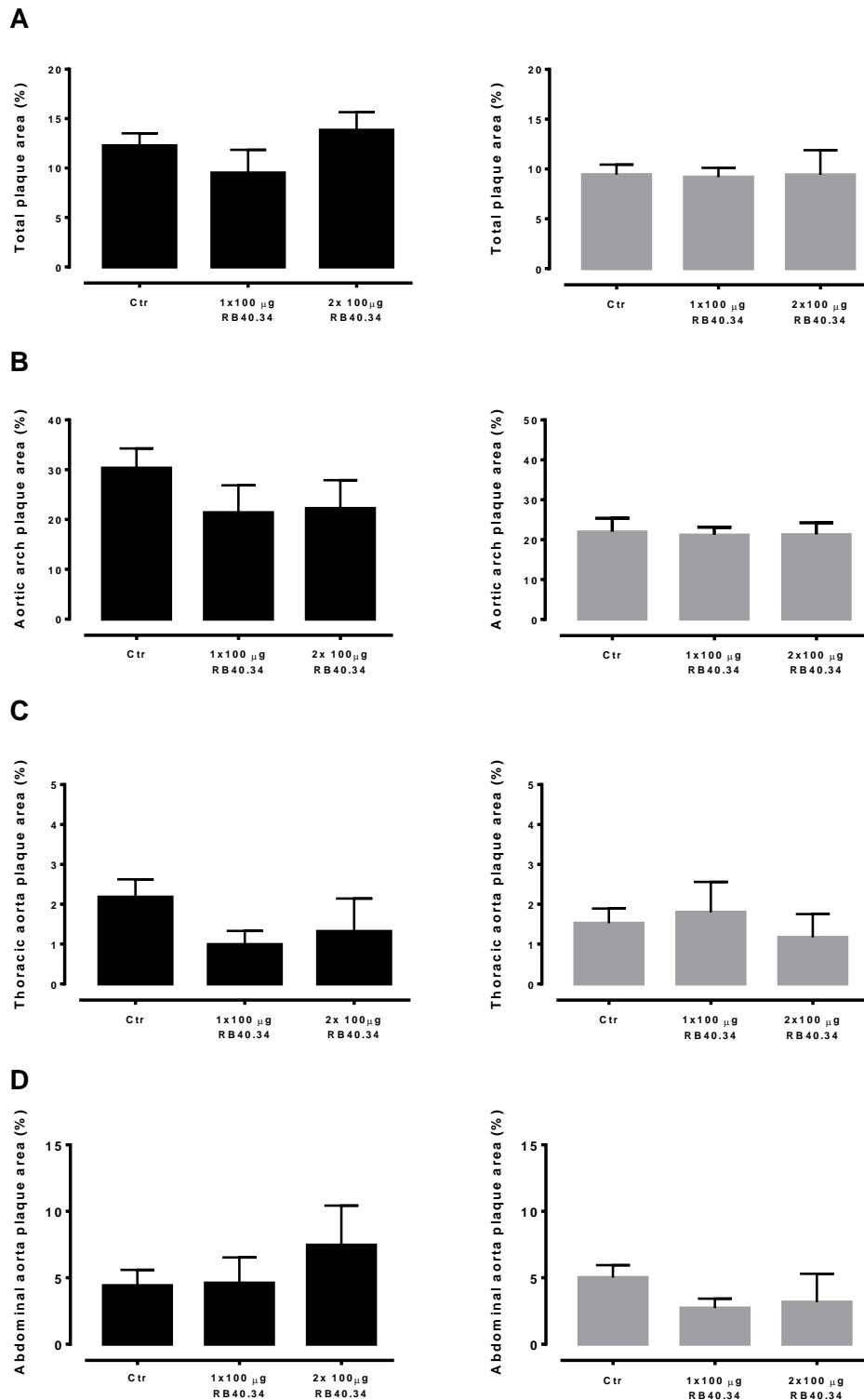
Figure 6.10 Effect of P-selectin blockade on plaque area. Sudan IV stained plaque area (%) in the (A) total, (B) arch, (C) thoracic and (D) abdominal aorta from *Apoe*^{-/-} (black) and BPHx*Apoe*^{-/-} (grey) mice following a 12 week HFD. Mice were treated with either isotype control (Ctr), one injection (1x100 µg) or two injections of RB40.34 (2x100 µg) (n=4-8). Data are presented as mean ± SEM. Data were analysed using a one-way ANOVA.
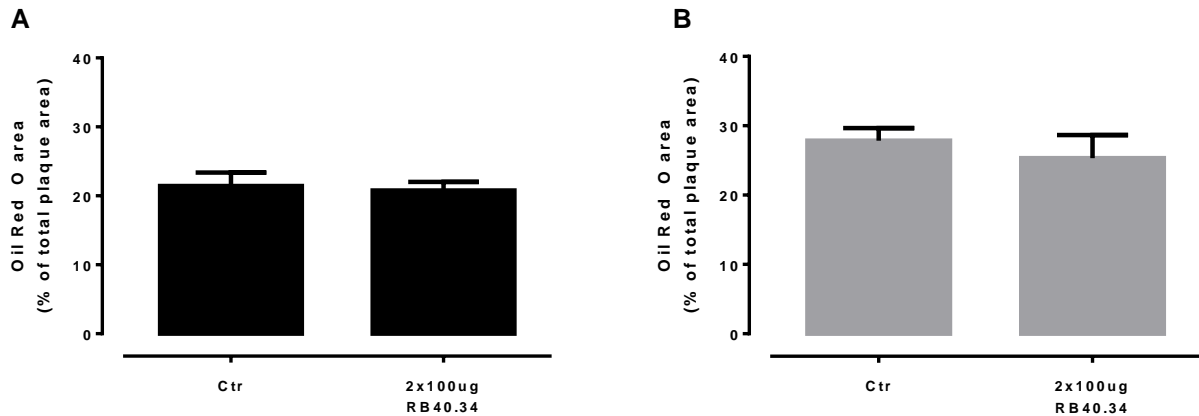
Figure 6.11 Effect of P-selectin blockade on Oil Red O stained aortic sinus. Oil Red O stained aortic sinus atherosclerotic lesions in (**A**) *Apoe*$^{-/-}$ (black) and (**B**) BPHx*Apoe*$^{-/-}$ (grey) mice fed a HFD and treated with isotype control (Ctr) or two injections of RB40.34 (2x100 µg) (n=4-5). Data are presented as mean ± SEM. Data were analysed with an unpaired Student's t-test.
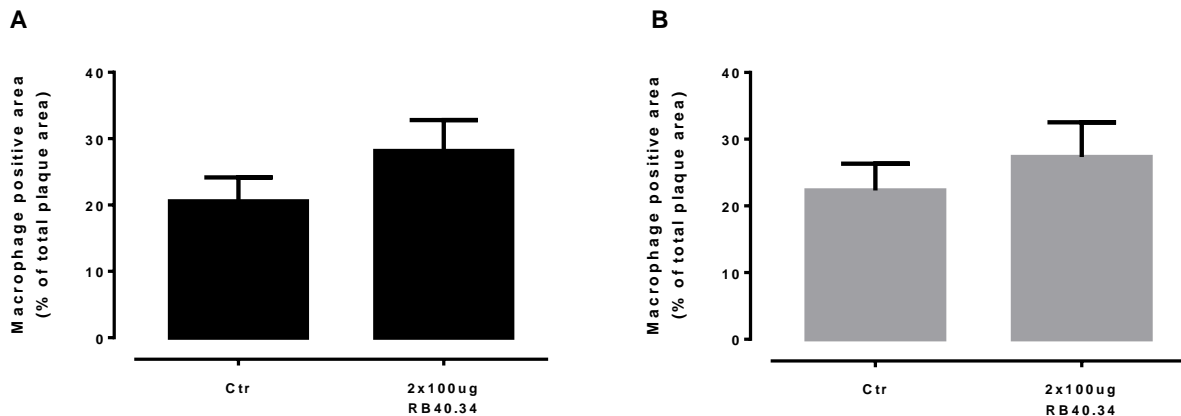
Figure 6.12 Effect of P-selectin blockade on macrophage content in the aortic sinus. Macrophage (CD68) positive stained aortic sinus atherosclerotic lesions in (**A**) *Apoe*$^{-/-}$ (black) and (**B**) BPHx*Apoe*$^{-/-}$ (grey) mice fed a HFD and treated with isotype control (Ctr) or two injections of RB40.34 (2x100 µg) (n=3-4). Data are presented as mean ± SEM. Data were analysed with an unpaired Student's t-test.
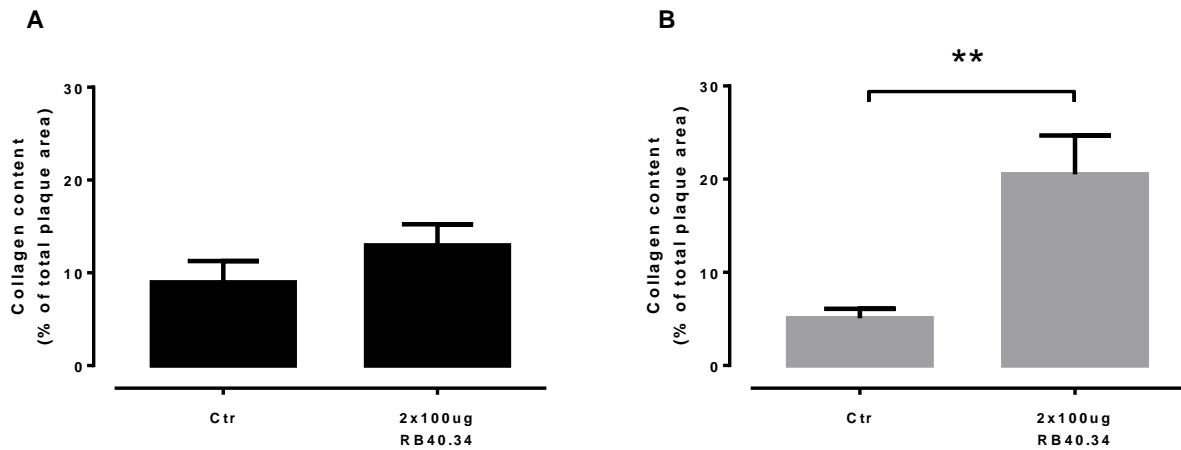
Figure 6.13 Effect of P-selectin blockade on collagen content in the aortic sinus. Collagen stained aortic sinus atherosclerotic lesions in (**A**) *Apoe*$^{-/-}$ (black) and (**B**) BPHx*Apoe*$^{-/-}$ (grey) mice fed a HFD and treated with isotype control (Ctr) or two injections of RB40.34 (2x100 µg) (n=3-6). Data are presented as mean ± SEM. Data were analysed using an unpaired Student t-test where **P<0.01.
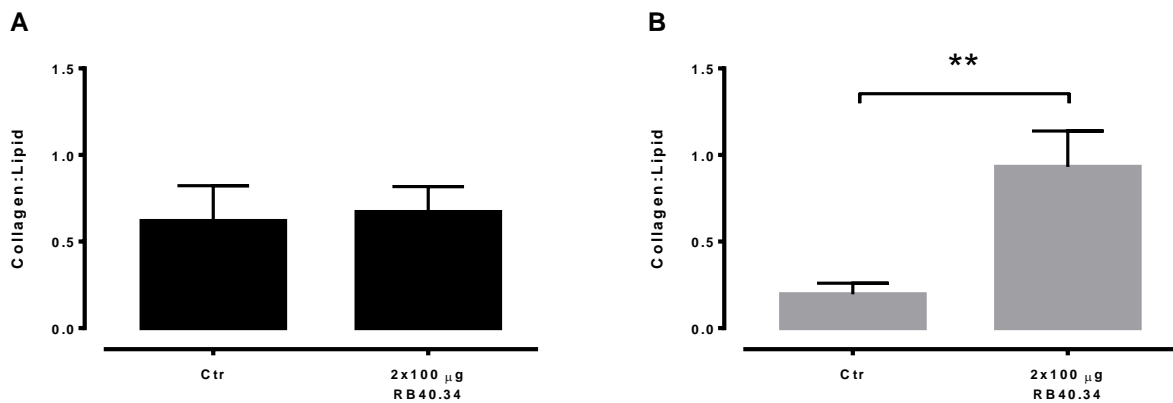
Figure 6.14 Effect of P-selectin blockade on plaque stability. Plaque stability, denoted by collagen/lipid ratio in aortic sinus atherosclerotic lesions, in (**A**) *Apoe*$^{-/-}$ (black) and (**B**) BPHx*Apoe*$^{-/-}$ (grey) fed a high-fat diet and treated with isotype control (Ctr) or two injections of RB40.34 (2x100 µg), n=3-7. Data are presented as mean ± SEM. Data were analysed using an unpaired Student t-test **P<0.01.

6.4 Discussion

This chapter details the development of a novel mouse model of chronic hypertension and atherosclerosis with the ultimate aim of elucidating the influence of high blood pressure on plaque composition and development in this model. Mice that have a neurogenic form of hypertension, Schlager (BPH/2J) mice, (Davern *et al.*, 2009), were crossed with the *Apoe*$^{-/-}$ atherosclerotic prone mouse to generate a new strain of mice the BPHx*Apoe*$^{-/-}$. They were placed on a HFD for 12 weeks to induce plaque development. On normal chow, BPHx*Apoe*$^{-/-}$ mice displayed a hypertensive phenotype. The results presented in this chapter show the successful creation of a mouse which is both hypertensive and prone to atherosclerotic lesion development. Furthermore, it appears that the BPHx*Apoe*$^{-/-}$ mice have more vulnerable plaques compared to *Apoe*$^{-/-}$ mice. We also demonstrate that treatment with the P-selectin antibody, RB40.34, may reduce this vulnerability suggesting a novel adjunct approach to treating those with hypertension.

The BPHx*Apoe*$^{-/-}$ mice displayed a hypertensive phenotype with increased SAP, DAP, MAP and HR. Schlager mice have been shown to have a pronounced hypertensive phenotype during the night-time or 'active' period (Davern *et al.*, 2009) as opposed to increased blood pressure during the day or 'inactive' phase as our results show. Since these mice are nocturnal this was an unexpected finding. Whether the neuronal activation of the BPHx*Apoe*$^{-/-}$ is the same as the BPH/2J (i.e. activation in the medial amygdala, Davern *et al.*, 2009) or whether the cross with the *Apoe*$^{-/-}$ strain has activated other neuronal regions, particularly those active during the daytime, remains to be determined. Regardless of the neuronal regions involved, BPH/2J mice (Davern *et al.*, 2009) presented with a greater increase in SAP compared to the BPHx*Apoe*$^{-/-}$ (139±1 vs. 119±2.0 mmHg, respectively) suggesting that the cross with *Apoe*$^{-/-}$ may have dampened the sympathetic activation under basal conditions. Nevertheless, the BPHx*Apoe*$^{-/-}$ mice did have significantly greater blood pressure, measured by telemetry, when compared to *Apoe*$^{-/-}$ mice.

When on a HFD, the hypertensive atherosclerotic BPHx*Apoe*$^{-/-}$ mice trended towards a greater weight gain compared to *Apoe*$^{-/-}$ mice. In the context of obesity and hypertension, many studies focus on obesity induced hypertension. Including the effect of increased renal sympathetic nerve activation (Armitage *et al.*, 2012; Lohmeier *et al.*, 2012), leptin resistance (Rahmouni *et al.*, 2002; Eikelis *et al.*, 2003), RAS activation and the production of the

adipocyte-derived angiotensinogen (Massiera *et al.*, 2001; Sharma, 2004), increased aldosterone and endothelial dysfunction that all result in vasoconstriction and increased sodium and water retention and ultimately increased blood pressure. The correlation of hypertension and obesity in this model suggests that the BPHx*Apoe*$^{-/-}$ mice may indeed be a model of metabolic syndrome. To determine if this is the case, further assessment of fat mass, insulin resistance, glucose tolerance and lipid levels will help to determine if this mouse is a novel model of metabolic syndrome.

Previous studies where blood pressure is increased demonstrate increased lesion formation in *Apoe*$^{-/-}$ via eNOS ablation (Knowles *et al.*, 2000a), which is RAS independent, aortic constriction (Wu *et al.*, 2002) and renal artery clamping (Mazzolai *et al.*, 2004), which are RAS dependent. In the current study we did not observe any influence of blood pressure-dependent total plaque area as measured by *en face* lesion area. BPHx*Apoe*$^{-/-}$ and *Apoe*$^{-/-}$ mice had similar plaque development (assessed with *en face* staining of the whole aorta with Sudan IV), particularly along the vascular tree most susceptible to various haemodynamic forces as discussed in the previous chapter. In contrast, plaque sections of the aortic sinus showed an increase in lipid deposition in the BPHx*Apoe*$^{-/-}$ compared to *Apoe*$^{-/-}$ mice suggesting that the increased blood pressure in the BPHx*Apoe*$^{-/-}$ mice may enhance lesion progression rather than contributing to plaque size *in vivo*. Significantly greater plaque macrophage content, as well as a trend towards reduced plaque collagen, was also seen in the hypertensive mice. Consequently, calculated plaque stability as measured by the collagen/lipid ratio (Naghavi *et al.*, 2003; Zeibig *et al.*, 2011) suggests increased plaque vulnerability in the BPHx*Apoe*$^{-/-}$ mice. These observations allude to an important role of hypertension on atherosclerotic plaque development as opposed to plaque initiation as seen in the previous chapters. Recently, Robbins *et al.*, (2013) demonstrated that macrophage accumulations in atherosclerotic lesions are predominantly from macrophage proliferation within the lesion as opposed to circulating monocyte infiltration. Further investigation, using fluorescent tagging with bromodeoxyuridine (a marker of cell proliferation), is required to definitely determine the influence of chronically elevated pressure on the amount of monocyte derived macrophages and self-renewing macrophages in atherosclerosis.

The progression of a stable plaque to an unstable plaque depends on not only on macrophage accumulation but also the lumen curvature (Steinman *et al.*, 2000), the

presence of a large lipid core (Libby *et al.*, 2002), increased apoptosis and cholesterol crystals (Suhalim *et al.*, 2012) and a reduced fibrous cap thickness (Li *et al.*, 2006). It is well accepted that plaques develop at areas of disturbed flow and low shear stress such as bifurcations and curvatures (Cheng, 2006; Chiu & Chien, 2011a) and, as stated in the previous chapter, hypertension has been associated with low shear flow in vessels. Therefore, it is possible that BPHx*Apoe*$^{-/-}$ mice may have lower shear flow resulting in increased vulnerability observed. Using a perivascular cast, Cheng *et al*., (2006) demonstrated low shear stress resulted in a reduced number of vascular smooth muscle cells, reduced collagen, and increased lipid deposition. More recently Chen *et al*., (2013) showed, via a tandem stenosis in the mouse carotid artery, that combining low shear stress and tensile stress elicited vulnerable plaques more closely resembling human atherosclerosis. These studies demonstrate a clear role for haemodynamic forces on plaque vulnerability and further examination of the exact shear forces using computational fluid dynamics will be beneficial in our BPHx*Apoe*$^{-/-}$ mice.

Following these findings we next examined the effect of inhibiting leukocyte recruitment in this chronic hypertensive atherosclerotic mouse model and determined if this could reduce plaque progression. In this study we used a monoclonal antibody, RB40.34, to transiently block P-selectin, which inhibits leukocyte adhesion to the activated endothelium acutely (Klintman *et al.*, 2004). One bolus injection of this antibody has been shown to reduce plaque progression in a carotid wire injury model (Phillips *et al.*, 2003). To the best of our knowledge, the current study is the first to assess chronic P-selectin blockade on atherosclerosis and we demonstrate variable results. Using one or two bolus injections of RB40.34 BPHx*Apoe*$^{-/-}$ mice demonstrated no improvement in plaque area or lipid content compared to isotype control treatment. However, since plaque stability was reduced in the BPHx*Apoe*$^{-/-}$ mice, further investigation of the effect of P-selectin inhibition on plaque composition was performed. Interestingly, although not statistically significant, *Apoe*$^{-/-}$ mice demonstrated an almost 50% reduction in weight change with two injections of RB40.34 treatment compared to control. This may underlie why no change in collagen content or plaque stability was seen in these animals but observed in the BPHx*Apoe*$^{-/-}$. However, if the RB40.34 did indeed improve weight gain in the *Apoe*$^{-/-}$, as the data suggest, one might expect to also see improved plaque stability as opposed to no change.

It has been shown that blockade of P-selectin inhibits monocyte recruitment and we therefore expected to see less macrophages in the plaques from mice treated with RB40.34. However, macrophage content was unchanged in plaques following P-selectin blockade in both strains of mice. This is in contrast to studies that have assessed the effect of RB40.34 acutely. Klintman *et al*., (2004) observed a reduction in leukocyte rolling and adhesion via intravital microscopy with a single injection of RB40.34 (40 μg i.p.) 6 hr prior to surgery. Phillips *et al*., (2003) also demonstrated reduced neointima formation and macrophage content 4 weeks after an injection of RB40.34 (100 or 200 μg i.p.). The current study quantified macrophage content 8-10 weeks post injection. Interestingly, Robbins et al., (2013) demonstrated macrophages within the atherosclerotic plaque start to turn over and proliferate after 4 weeks. Therefore, while RB40.34 may be effective acutely, it may not be as potent once macrophages start proliferating in advanced lesions. Phillips *et al*., (2003) demonstrated that following intraperitoneal injection, RB40.34 remained detectable for at least 7 days but had disappeared by 14 days. Therefore, two injections of RB40.34 at week 1 and week 3 may also not have been sufficient to produce a consistent long lasting effect.

As macrophage and lipid content were unchanged with RB40.34 it was somewhat surprising to see collagen content was improved. Vulnerable plaques are characterised as having a thin fibrous-cap with poor collagen content, whilst stable plaques tend to show thicker fibrous caps with greater collagen content (Aikawa & Libby, 2004). Therefore, while our results demonstrate blocking P-selectin did not alter lipid or macrophage content, it did improved collagen content and as a result, plaque stability. To date there are no reports of the effects of RB40.34 on collagen or fibrous cap content in a chronic setting. Dong *et al*., (2000) demonstrated *Apoe*$^{-/-}$/*P-selectin*$^{-/-}$ mice had reduced plaque progression with smaller necrotic cores, less fibrous tissue and less calcification compared to *Apoe*$^{-/-}$/*P-selectin*$^{+/+}$ mice after 15 months on a normal chow diet with 5% fat. They also showed less recruitment of monocytes and macrophages after 16 weeks. While Dong *et al.*, (2000) show genetically deficient Apoe/P-selectin mice have improved plaque stability, we show transiently blocking P-selectin with a monoclonal antibody only partially improved plaque stability. Assessing collagen synthesis and organisation in the BPHx*Apoe*$^{-/-}$ and in the presence of RB40.34 will help to determine the mechanisms behind this finding.

In summary, in this chapter we describe the development of a hypertensive atherosclerotic mouse model which presented with decreased plaque stability. We

hypothesised from our previous findings that hypertension would enhance plaque progression and that anti-inflammatory therapy *even in the continued presence of high blood pressure* would improve plaque stability. We showed that while chronic high blood pressure does not increase plaque size, plaque morphology in terms of stability/instability was worse in the setting of hypertension and atherosclerosis. This provides direct evidence that that high blood pressure contributes to the critical aspects of the disease, since plaque instability contributes to clinical end-points such as myocardial ischemia and death (Aikawa *et al.*, 2004). The finding that the P-selectin antibody partially improved plaque stability (evidenced by an increase in collagen content) is interesting, although the data is somewhat more difficult to interpret. Whether the partial restoration with P-selectin was due to insufficient dose or incorrect timing or whether in fact P-selectin is not the best target in the context of pressure-induced inflammation cannot be clearly determined with the current data set. Regardless, we can conclude that chronic high blood pressure promotes plaque instability and the anti-inflammatory therapy using a P-selectin antibody in the continued presence of high blood pressure can partially restore plaque stability.

From these results anti-P-selectin therapy may indeed be useful in stabilising plaques in those with atheroma. Immune cells localising to inflammatory sites is paramount in aiding in injury and infection. P-selectin is at the forefront of this mechanism where it can bind to Th1 and Th2 lymphocytes during injury (Bonder *et al.*, 2005), and is also involved in platelet recruitment and aggregation (Merten & Thiagarajan, 2000). While blocking P-selectin may reduce its ability to aide in preventing further injury, as with anti-platelet therapy the overall benefit may outweigh the side effects. Extensive toxicity testing will be vital for establishing this therapy. The recent clinical trial, SELECT-ACS (Tardif *et al*., 2013), provides promising results where they demonstrated reduced myocardial damage following percutaneous coronary intervention with anti-P-selectin therapy and of note demonstrated no significant difference in adverse advents between groups.

It is clear that the incidences of atherosclerotic plaques are greater in hypertensive patients compared to normotensive patients. We have demonstrated that elevated blood pressure exacerbates atherosclerosis progression via increased leukocyte recruitment. Importantly, this study demonstrates that treatment strategies targeted to prevent monocyte recruitment can improve plaque stability in the setting of hypertension. We

envisage that targeting these pathways would significantly improve the long-term management of atherosclerosis in hypertensive patients.

Chapter 7

General Discussion

The purpose of this thesis was to explore whether high blood pressure contributes to atherosclerosis by inducing vascular inflammation. Increased blood pressure is a global health burden and the number one biomedical risk factor for CVD. With a growing older population and an increased sedentary lifestyle, the percentage of the population at risk is on the rise. Clinically, hypertensive patients are treated with blood pressure lowering medications to reduce the risk of developing a cardiovascular event. Yet despite the widespread availability of antihypertensive medications, hypertension continues to be the single biggest contributor to the incidence and progression of atherosclerosis, the underlying cause of CAD and other CVDs.

As discussed in **Chapter 1**, environmental, lifestyle and genetic factors have all been shown to contribute to the development of hypertension. The physiological and cellular sequalae of these factors, such as increased sympathetic activity, and RAS and immune T cell activation are shown to not only influence the pathogenesis of hypertension but also the progression of atherosclerosis. It has therefore been difficult to clearly elucidate whether high intraluminal pressure *per se* has a direct contributory role to plaque development and progression. To examine this question, we used an *ex vivo* vessel chamber previously developed by our laboratory to study leukocyte adhesion in blood vessels in real time under physiological shear (Woollard *et al.*, 2008). By coupling the set up with a pressure system, we have been able to observe the direct effect of intraluminal pressure on leukocyte adhesion to the endothelium in real time (**Chapter 3**). Indeed, we have found that an acute pressure increase not only enhanced leukocyte adhesion but also increased adhesion molecules and endothelial microparticle production markers of endothelial activation and dysfunction (**Chapter 4**). From this clear and novel finding that high pressure *in itself* does induce endothelial activation, we then continued on as described in **Chapters 4 & 5,** to explore the various signalling pathways involved in this phenomenon (summarised in Fig 7.1).

7.1 Major pathways involved in pressure-induced inflammation
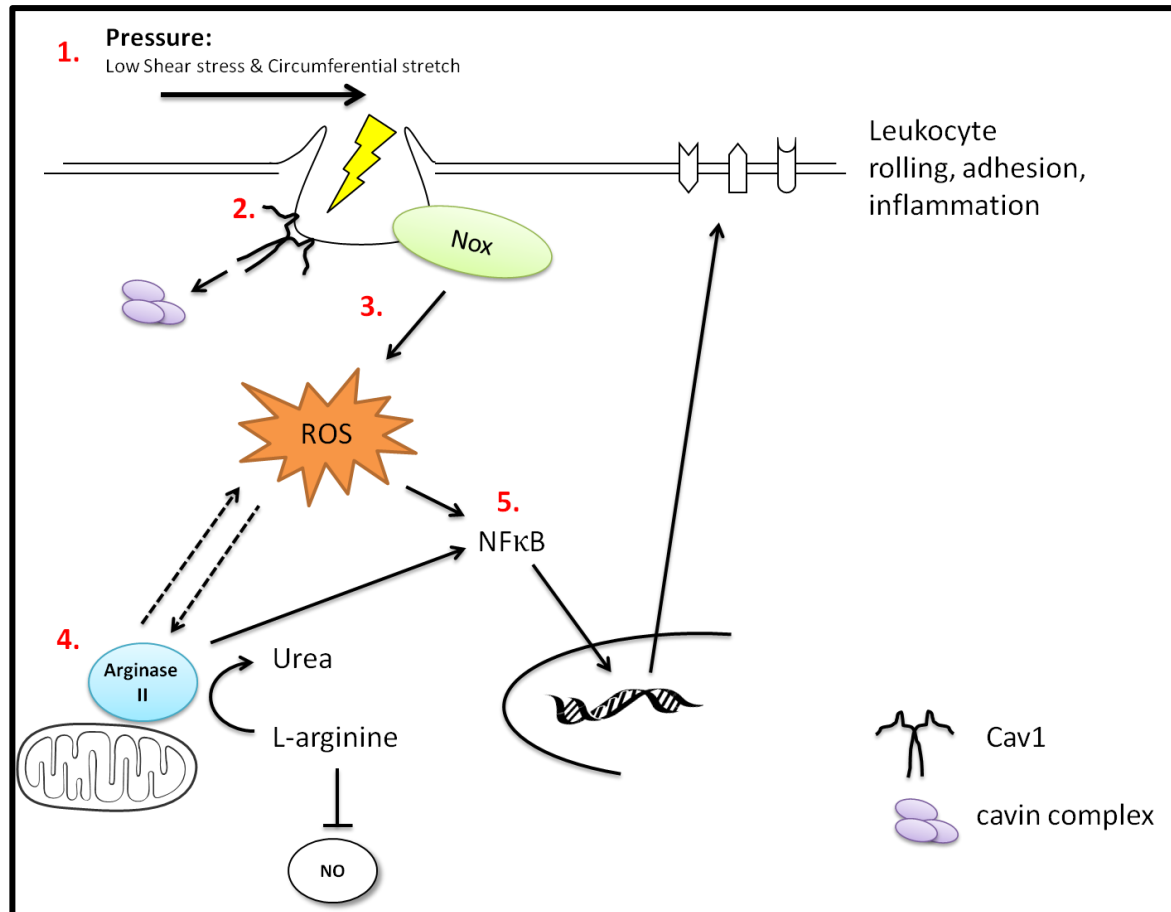
Fig 7.1 Pressure-induced inflammation. Acute high intraluminal pressure exerts both low shear stress and circumferential stretch (1), disassembling caveolae proteins Cav1 and cavins and causing flattening and reduction of caveolae (2). This disassembly and/or pressure exertion leads to an increase in Nox-dependent ROS production (3), which in turn results in an upregulation of arginase II activity and subsequently activating a feedback loop to further increase ROS production (4). The increase in arginase II and ROS causes a translocation of NFκB into the nucleus (5) resulting in increased gene and protein expression of adhesion molecules.

7.1.1 Low shear stress and circumferential stretch

Since endothelial cells line the innermost surface of blood vessels they are the first cells to sense changes in blood flow. To observe the effect of different shear rates on endothelial activation and inflammation, pressurised carotid arteries were exposed to high intraluminal pressure with varying rates of shear flow (**Chapter 5**). This led to the finding that LSS coupled with pressure (stretch) created the greatest insult on the vessel wall (Fig 5.1). Gene expression of MCP-1 was greater in vessels pressurised to 120 mmHg and subjected to LSS than those without pressure and subjected to low shear. Furthermore, leukocyte adhesion was greater in pressurised vessels with LSS and blunted in pressurised vessels subjected to high shear flow. These findings are consistent with previous i*n vivo* and clinical studies conducted in which adhesion and plaque formation are primarily seen along the vascular tree in areas of LSS (Chiu *et al.*, 2011b), and areas of high or laminar shear stress are instead associated with the release of NO and are consequently afforded cardio protection.

In **Chapters 3-5**, the acute effect of pressure on leukocyte adhesion was studied. This process forms an initial step in the chronic disease atherosclerosis and while in some atheroprone areas this can occur, leukocyte adhesion doesn't always necessarily lead to atherosclerosis. The purpose of these experiments was to examine whether pressure can cause increased adhesion and whether this may eventually lead to atherosclerosis. We were also keen to study what interventions can help diminish this response. Under the experimental conditions utilised in this thesis, 120 mmhHg at 1 hr was sufficient to observe changes in adhesion with increased pressure. It should be noted that the pressure used was constant and thus does not represent systolic blood pressure but more likely mean arterial pressure which in Sprague Dawley rats are normally reported to be ~100-110 mmHg. We therefore believe we are working above the normal range. While it would have been ideal to mimic overt hypertension in this setup the key objective was to observe the effect of acute increase in pressure on leukocyte adhesion and what interventions may aide in this. In addition, while it would be ideal for normal pressurised vessels to demonstrate no adhesion the vessels were still exposed to some amount of stretch at 60 and 80 mmHg and therefore generated some mechanotransduction and signalling and consequently a response.

Furthermore, we have shown in vessels exposed to 0 mmHg that no adhesion is observed suggesting that any adhesion observed is not due to experimental isolation or mounting.

The experiments described in this work have several limitations; firstly, that the 'high pressure' described is maximally at 120 mmHg. While it may be argued that this constant high pressure is reminiscent of mean arterial pressure and is thus pathophysiologically high, perhaps a better haemodynamic situation to study would have been to subject the vessels to pulsatile flow and pressure, mimicking the systole and diastole phases observed *in vivo*. As well, leukocyte adhesion under turbulent flow or oscillatory shear stress would be of great interest since disturbed flow can promote endothelial dysfunction and inflammation (Nam *et al.*, 2009). Furthermore, as we know that the geometry of the vascular tree is critical to the development of atherosclerosis so too would observing the effect of forces on bifurcations be of interest. All these features, however, were beyond the scope of this thesis, which focused on that first important step of altering a single variable.

As discussed previously, 1 hour was sufficient to induce various intracellular signalling molecules including NFκB and changes in adhesion molecule expression and consequently leukocyte adhesion. One explanation for the acute effects observed may be due to the altered activity and/or translocation of existing protein. Previous reports have shown cavin proteins can rapidly dissociate from caveolin proteins following osmotic swelling in cells (Sinha *et al.*, 2011) and superoxide generation as measured by spin-trap has shown to increase within 10 minutes in Sprague-Dawley rat aorta (Souza *et al.*, 2002). Furthermore, NFκB translocation has also been shown to increase with LPS stimulation in macrophages within 30 minutes (Noursadeghi *et al.*, 2008). Interestingly, Giri *et al.*, (2000) demonstrate increased expression of ICAM-1 and VCAM-1 within 1 hour as measured by ELISA in response to amyloid β-peptide. Therefore, it is still unclear if the increased adhesion is due to the increased transcription of adhesion molecules from the pathways mentioned or perhaps a more rapid response such as the sudden exposure of adhesion molecules from the flattened caveolae as these molecules are found to be co-localised with Cav-1 in endothelial cells (Fu *et al.*, 2010*).* For these reasons 1 hour duration may indeed be a limiting factor and a time course may help answer this question.

7.1.2 Caveolae

Various mechanosensors reside along the luminal membrane in place to respond to changes in flow and pressure. We demonstrate for the first time that caveolae number are reduced with increased pressure (Fig 5.7), and hypothesise that they may be flattening out to provide a membrane reservoir and activate signalling pathways. Indeed, Sinha *et al.*, (2011) reported that Cav1 and cavin-1 rapidly disassemble in response to osmotic swelling, which results in flattening out of caveolae. This process of disassembling is also likely to be an important step in the signalling response as TNFα-stimulated *Cav1$^{-/-}$* mice aorta and Cav1 KD cells show reduced gene expression of adhesion molecules, reduced monocyte adhesion *in vitro* and reduced leukocyte adhesion *ex vivo*. Furthermore, Cav1 KD cells demonstrated reduced gene expression of adhesion molecules compared to scrambled controls when pressurised (Fig 5.9), suggesting that the process of caveolae disassembling is key to the pressure-induced inflammation response. Chai *et al.*, (2013) demonstrate that caveolar integrity is essential for the generation of vasodilators such as NO. Furthermore, Fu et al., (2010) demonstrate that unstimulated ICAM-1 is mainly located in caveolae and that when stimulated, ICAM-1 translocates out of caveolae to increase adhesion. While we began to see changes with Cav1 and cavin-1 in our pressurised vessels (Fig 5.11) the findings were not conclusive and the methodology used requires further development.

Furthermore, while it was attempted vigorously, due to technical difficulties pressurizing and observing leukocyte adhesion in mouse carotids proved unachievable during this candidature. While this would have been ideal, caveolin knockout mouse aorta with TNFα without pressure was used to determine the role if any caveolae played in leukocyte adhesion alone. This technique is standard in our laboratory for determining the propensity of vascular inflammation in knockout mice. This then led us to pursue the role of caveolae in pressure and inflammation in specific knockdown cells along with observing caveolae number in pressurized rat carotid arteries.

The role of pressure and caveolae together is an exciting new area with many avenues warranting investigation in the future. Of particular note, the effect of chronic pressure on caveolae is largely unexplored. While chronic laminar shear has been shown to stimulate luminal caveolae formation in rat lung microvessels (Rizzo *et al.*, 2003) and bovine aortic endothelial cells (Boyd *et al.*, 2003), less is known about caveolae formation following

chronic increase in pressure. One study by Grayson *et al.*, (2007) demonstrates, via a microarray, that spontaneously hypertensive rats have greater gene expression of Cav1 in endothelial cells and smooth muscle cells compared to Wistar controls. They also demonstrate increased protein expression and caveolae number in these hypertensive animals, suggesting chronic pressure results in greater caveolae formation. From these studies, and those suggesting a role for T cells (Guzik *et al.*, 2007) and monocytes (Wenzel *et al.*, 2011), that caveolae are increased with chronic pressure suggest they may also have a role in the pathogenesis of hypertension. Pojoga *et al.*, (2010) demonstrate that *Cav1* $^{-/-}$ mice have reduced adverse cardiovascular responses to L-NAME and Ang II-induced hypertension. Furthermore, studies by Li *et al.*, (2011) reveal that *Cav1* $^{-/-}$ mice have an attenuated blood pressure response to Ang II and that this is likely due to the role of caveolae regulating the uptake of Ang II by the proximal tubules.

7.1.3 NADPH oxidase & reactive oxygen species

As discussed in **Chapter 1** (Section 1.10.4.3) caveolae may also regulate the production of ROS via Nox2. In **Chapter 4** we demonstrated that high pressure induces an upregulation of ROS, particularly hydrogen peroxide in HUVECs, which was attenuated with the Nox inhibitor apocynin. Furthermore, when rat carotid arteries were pressurised in the presence of various inhibitors in order to isolate the different sources of ROS generation it was found that leukocyte adhesion was reduced with apocynin as well as mitochondrial ROS blockade but not xanthine oxidase or cytochrome P450 blockade (Fig 4.6). These findings demonstrate an important role in the production of ROS following pressure stimulation. Interestingly, studies conducted by Yang and Rizzo (2007) and Han *et al.*, (2008) demonstrate Nox is inactive in caveolae and lipid rafts, and that upon disruption/activation, the p47^{phox} subunit is recruited to caveolae resulting in increased Nox activity and ROS production. Measuring Nox subunits in caveolae fractions via sucrose density ultracentrifugation, as demonstrated by Lobysheva *et al.*, (2011), would give further insight into our pressurised cells/vessels. Pressurising *Nox2* KD cells or *Nox2*$^{-/-}$ mice will also provide a greater understanding on the downstream signalling. While we have shown hydrogen peroxide is increased with pressure, other ROS products (superoxide, hydroxyl radical and peroxynitrite) also require further investigation.

7.1.4 Arginase

Oxidative stress is known to be a contributing factor of hypertension in which it reduces the actions of NO as well as inducing the uncoupling of eNOS, which can lead to even greater ROS production. Unexpectedly, we saw no alteration of eNOS with pressure i.e. eNOS gene expression was unchanged, nor was there any apparent uncoupling with increased pressure (**Chapter 4**). As mentioned previously evidence in the literature also show paradoxical results where increased eNOS can result in increased NO or superoxide. Further work investigating ADMA and BH$_4$ in the acute setting will hopefully shed light in the role of eNOS.

Interestingly, the endogenous enzyme arginase, which competes with eNOS for L-arginine, was found to be altered with increases in pressure. In rat carotid arteries pressurised to 120 mmHg, there was an upregulation of arginase II gene expression, increased arginase activity and a reduction in leukocyte adhesion with arginase inhibition (Fig 4.12). These results demonstrate a clear role for arginase II in the pressure-induced response. As previously discussed (Michell *et al.*, 2011a), while generally not a focus in hypertension-induced inflammation, arginase may have a more fundamental role than once thought. However, the exact mechanism by which arginase II acts is still unclear. Previous studies allude to a role of arginase as not only an early target of increased ROS (Thengchaisri *et al.*, 2006) but also a stimulator of ROS (Munzel *et al.*, 2005). Furthermore, that inhibition of Nox also reduces arginase activity (Matthiesen *et al.*, 2008) suggests that ROS and arginase are tightly connected. Assessing the pressure-induced inflammatory response and production of ROS in arginase I and II endothelial specific knockdown cells will therefore be valuable.

7.1.5 NFκB

In **Chapter 4** we demonstrated that NFκB is significantly increased in the nucleus of cells with acute high pressure. This is in line with previous studies by (Lemarie *et al.*, 2003; Riou *et al.*, 2007) demonstrating that pressure results in the degradation of IκBα and increased NFκB translocation to the nucleus. NFκB translocation is a key step in apoptosis

and inflammatory signalling pathways, propagating the upregulation of gene transcription and production of various inflammatory mediators. Although well known to be activated by LPS, inflammatory cytokines such as TNFα, and IL-1, as well as oxidative stress (Tak & Firestein, 2001), little is known about how pressure or mechanical forces induce activation. Leychenko *et al*., (2011) have previously demonstrated that cyclical stretch of cardiomyocytes can induce NFκB signalling, while Chaqour *et al*., (1999) showed that mechanical stretch increases platelet activation via NFκB. Here we show, for the first time, that pressure-dependent NFκB translocation is dependent on both arginase and Nox production (Fig 4.17). This is consistent with the findings of Ckless *et al*., (2007) who observed that arginase could regulate NFκB translocation via an NO-dependent pathway. Observing the effect of NFκB blockade via SN50 on leukocyte adhesion and adhesion molecule expression in pressurised cells/vessels will be beneficial to confirm these findings. Furthermore, examining NFκB production in *Cav1$^{-/-}$* models would further strengthen these observations.

7.2 In vivo approach

In **Chapters 4 & 5** we explored the effect of pressure on inflammation in an acute *ex vivo* setting. Therefore, to investigate the effect of chronic pressure on plaque development, in **Chapter 6** we crossed hypertensive schlager BPH/2J mice with *Apoe$^{-/-}$* to create a spontaneously hypertensive, diet-induced atherosclerotic model (BPHx *Apoe$^{-/-}$*). The major finding from this chapter was that, following a 12 week high fat diet, there was a worsening in plaque stability in the BPHx *Apoe$^{-/-}$* compared to *Apoe$^{-/-}$* mice (Fig 6.6-6.8), while plaque area, as measured by Sudan IV, was unchanged. BPHx *Apoe$^{-/-}$* mice demonstrated greater lipid deposition, macrophage content and lower collagen compared to *Apoe$^{-/-}$*. Furthermore, these mice also demonstrated greater weight gain, leading us to speculate that these mice are a potential model of metabolic syndrome, which warrants further investigation. One limitation with this study may be that *Apoe$^{-/-}$* mice were used as controls, therefore the more suitable BPHx*Apoe$^{-/-}$* normotensive littermate controls would be beneficial for future experiments.

Following the findings of Philips *et al.*, (2003), which demonstrate that blocking P-selectin acutely blunted plaque progression in a carotid wire injury model, we assessed the blockade of P-selectin in our chronic model. Unlike Philips *et al.*, (2003), we did not see a reduction in plaque area or lipid deposition, but greater collagen content was observed, suggesting a more stable plaque. These results demonstrate that P-selectin may partially improve plaque stability in the continued presence of high blood pressure. Further studies with increased doses/injections may be required to see a greater effect. Since the BPHx *Apoe*$^{-/-}$ mice have a neurogenic form of hypertension it will also be prudent to investigate whether there is increased sympathetic activity in these mice and whether it is affecting plaque development independent of blood pressure. In addition, P-selectin expression post antibody treatment was not assessed and would be beneficial to ensure RB40.34 was down-regulating P-selectin correctly.

This thesis focused predominantly on acute increases in pressure in an *ex vivo* system to carefully dissect out the mechanisms. **Chapter 6** discusses work conducted *in vivo* in a chronic hypertensive atherosclerotic model. As discussed, the chronic hypertensive atherosclerotic model demonstrated increased macrophage accumulation compared to the atherosclerotic mice demonstrating chronic increases in blood pressure may indeed promote leukocyte adhesion. While the pathways discussed in the acute setting are all known to be involved in atherosclerosis further work is required to determine if they relate to this particular chronic *in vivo* model.

7.3 Summary

In this thesis we have been able to establish fundamental pathways involved in how the mechanical forces exerted by high intraluminal pressure can alter cellular biological responses. We have novel evidence that high intraluminal pressure in itself, causes leukocyte to endothelial adhesion, a hallmark of vascular inflammation and the initial step in atherosclerosis. Further, we demonstrate the downstream inflammatory signalling events induced by high pressure and the involvement of caveolae as an essential intermediary link. Finally, we suggest that chronic high blood pressure worsens plaque instability and that

blocking inflammation may be useful adjunct therapy in the prevention of hypertension-induced myocardial infarction.

Chapter 8

References

(1987). Effects of enalapril on mortality in severe congestive heart failure. Results of the Cooperative North Scandinavian Enalapril Survival Study (CONSENSUS). The CONSENSUS Trial Study Group. *N Engl J Med* **316**(23)**:** 1429-1435.

(2011). High Blood Pressure Research 2011 Scientific Sessions Abstracts. *Hypertension* **58**(5)**:** e33-e183.

Aicher A, Rentsch M, Sasaki Ki, Ellwart JW, Fandrich F, Siebert R*, et al.* (2007). Nonbone marrow-derived circulating progenitor cells contribute to postnatal neovascularization following tissue ischemia. *Circulation Research* **100**(4)**:** 581-589.

Aikawa M, Libby P (2004). The vulnerable atherosclerotic plaque: pathogenesis and therapeutic approach. *Cardiovasc Pathol* **13**(3)**:** 125-138.

Aktan F (2004). iNOS-mediated nitric oxide production and its regulation. *Life Sciences* **75**(6)**:** 639-653.

Al-Solaiman Y, Jesri A, Mountford WK, Lackland DT, Zhao Y, Egan BM (2010). DASH lowers blood pressure in obese hypertensives beyond potassium, magnesium and fibre. *Journal of Human Hypertension* **24**(4)**:** 237-246.

Albinsson S, Shakirova Y, Rippe A, Baumgarten M, Rosengren BI, Rippe C*, et al.* (2007). Arterial remodeling and plasma volume expansion in caveolin-1-deficient mice. *American Journal of Physiology - Regulatory, Integrative and Comparative Physiology* **293**(3)**:** R1222-1231.

Alderton WK, Cooper CE, Knowles RG (2001). Nitric oxide synthases: structure, function and inhibition. *Biochemical Journal* **357**(Pt 3)**:** 593-615.

Allen AM (1998). Angiotensin AT1 receptor-mediated excitation of rat carotid body chemoreceptor afferent activity. *The Journal of Physiology* **510 (Pt 3):** 773-781.

Allen RG, Tresini M (2000). Oxidative stress and gene regulation. *Free Radical Biology and Medicine* **28**(3)**:** 463-499.

Alwan A (2011). *Global status report on noncommunicable diseases 2010*. Geneva: World Health Organization

Anderson JL, Adams CD, Antman EM, Bridges CR, Califf RM, Casey DE*, et al.* (2011). 2011 ACCF/AHA focused update incorporated into the ACC/AHA 2007 guidelines for the management of patients with unstable angina/non–ST-elevation myocardial infarction. *Circulation* **123**(18)**:** e426-e579.

Ando J, Yamamoto K (2009). Vascular mechanobiology: endothelial cell responses to fluid shear stress. *Circulation Journal* **73**(11)**:** 1983-1992.

Androulakis ES, Tousoulis D, Papageorgiou N, Tsioufis C, Kallikazaros I, Stefanadis C (2009). Essential hypertension: is there a role for inflammatory mechanisms? *Cardiol Rev* **17**(5)**:** 216-221.

Appel LJ, Moore TJ, Obarzanek E, Vollmer WM, Svetkey LP, Sacks FM*, et al.* (1997). A clinical trial of the effects of dietary patterns on blood pressure. DASH Collaborative Research Group. *N Eng J Med* **336**(16)**:** 1117-1124.

Aragay AM, Ruiz-Gomez A, Penela P, Sarnago S, Elorza A, Jimenez-Sainz MC*, et al.* (1998). G protein-coupled receptor kinase 2 (GRK2): mechanisms of regulation and physiological functions. *FEBS Letters* **430**(1-2)**:** 37-40.

Argaud L, Gateau-Roesch O, Chalabreysse L, Gomez L, Loufouat J, Thivolet-Béjui F, *et al*. (2004). Preconditioning delays Ca2+-induced mitochondrial permeability transition. *Cardiovasc Res* **61**(1): 115-122.

Armitage JA, Burke SL, Prior LJ, Barzel B, Eikelis N, Lim K*, et al.* (2012). Rapid onset of renal sympathetic nerve activation in rabbits fed a high-fat diet. *Hypertension* **60**(1)**:** 163-171.

Asahara T (1997). Isolation of Putative Progenitor Endothelial Cells for Angiogenesis. *Science* **275**(5302)**:** 964-966.

Atlas SA (2007). The renin-angiotensin aldosterone system: pathophysiological role and pharmacologic inhibition. *J Manag Care Pharm* **13**(8 Suppl B)**:** 9-20.

Bachetti T, Comini L, Curello S, Bastianon D, Palmieri M, Bresciani G*, et al.* (2004). Co-expression and modulation of neuronal and endothelial nitric oxide synthase in human endothelial cells. *J Mol Cell Cardiol* **37**(5)**:** 939-945.

Bagnost T, Ma L, da Silva RF, Rezakhaniha R, Houdayer C, Stergiopulos N*, et al.* (2010). Cardiovascular effects of arginase inhibition in spontaneously hypertensive rats with fully developed hypertension. *Cardiovascular Research* **87**(3)**:** 569-577.

Barhoumi T, Kasal DA, Li MW, Shbat L, Laurant P, Neves MF*, et al.* (2011). T regulatory lymphocytes prevent angiotensin II-induced hypertension and vascular injury. *Hypertension* **57**(3)**:** 469-476.

Bastiani M, Liu L, Hill MM, Jedrychowski MP, Nixon SJ, Lo HP*, et al.* (2009). MURC/Cavin-4 and cavin family members form tissue-specific caveolar complexes. *J Cell Biol* **185**(7)**:** 1259-1273.

Bastiani M, Parton RG (2010). Caveolae at a glance. *J Cell Sci* **123**(22)**:** 3831-3836.

Batandier C, Leverve X, Fontaine E (2004). Opening of the mitrochondrial permeability transition pore induces reactive oxygen species production at the level of the respiratory chain complex I. *J Biol Chem* **279**(17): 17197-17204.

Bauer PM, Yu J, Chen Y, Hickey R, Bernatchez PN, Looft-Wilson R*, et al.* (2005). Endothelial-specific expression of caveolin-1 impairs microvascular permeability and angiogenesis. *Proc Natl Acad Sci U S A* **102**(1)**:** 204-209.

Bauersachs J, Bouloumie A, Fraccarollo D, Hu K, Busse R, Ertl G (1998). Hydralazine prevents endothelial dysfunction, but not the increase in superoxide production in nitric oxide-deficient hypertension. *Eur J Pharmacol* **362**(1)**:** 77-81.

Beaumier L, Castillo L, Ajami AM, Young VR (1995). Urea cycle intermediate kinetics and nitrate excretion at normal and "therapeutic" intakes of arginine in humans. *Am J Physiol Endocrinol Metab* **269**(5 Pt 1)**:** E884-E896.

Berenson GS, Srinivasan SR, Bao W, Newman WP, Tracy RE, Wattigney WA (1998). Association between multiple cardiovascular risk factors and atherosclerosis in children and young adults. The Bogalusa Heart Study. *New Eng J Med* **338**(23)**:** 1650-1656.

Berk BC, Min W, Yan C, Surapisitchat J, Liu Y, Hoefen R (2002). Atheroprotective mechanisms activated by fluid shear stress in endothelial cells. *Drug News Perspect* **15**(3)**:** 133-139.

Berkowitz DE, White R, Li D, Minhas KM, Cernetich A, Kim S*, et al.* (2003). Arginase reciprocally regulates nitric oxide synthase activity and contributes to endothelial dysfunction in aging blood vessels. *Circ* **108**(16)**:** 2000-2006.

Bernatchez P, Sharma A, Bauer PM, Marin E, Sessa WC (2011). A noninhibitory mutant of the caveolin-1 scaffolding domain enhances eNOS-derived NO synthesis and vasodilation in mice. *J Clin Invest* **121**(9)**:** 3747-3755.

Bertuglia S, Ichimura H, Fossati G, Parthasarathi K, Leoni F, Modena D*, et al.* (2007). ITF1697, a stable Lys-Pro-containing peptide, inhibits weibel-palade body exocytosis induced by ischemia/reperfusion and pressure elevation. *Mol Med* **13**(11-12)**:** 615-624.

Blake GJ, Rifai N, Buring JE, Ridker PM (2003). Blood pressure, C-reactive protein, and risk of future cardiovascular events. *Circ* **108**(24)**:** 2993-2999.

Bode-Boger SM, Boger RH, Alfke H, Heinzel D, Tsikas D, Creutzig A*, et al.* (1996). L-arginine induces nitric oxide-dependent vasodilation in patients with critical limb ischemia. A randomized, controlled study. *Circ* **93**(1)**:** 85-90.

Boger RH, Bode-Boger SM, Szuba A, Tsao PS, Chan JR, Tangphao O*, et al.* (1998). Asymmetric dimethylarginine (ADMA): a novel risk factor for endothelial dysfunction: its role in hypercholesterolemia. *Circ* **98**(18)**:** 1842-1847.

Boos CJ, Lip GY (2006). Is hypertension an inflammatory process? *Curr Pharm Des* **12**(13)**:** 1623-1635.

Boulanger CM (2006). Circulating microparticles: a potential prognostic marker for atherosclerotic vascular disease. *Hypertension* **48**(2)**:** 180-186.

Boyd NL, Park H, Yi H, Boo YC, Sorescu GP, Sykes M*, et al.* (2003). Chronic shear induces caveolae formation and alters ERK and Akt responses in endothelial cells. *Am J Physiol Heart Circ Physiol* **285**(3)**:** H1113-1122.

Brandt MC, Reda S, Mahfoud F, Lenski M, Bohm M, Hoppe UC (2012). Effects of renal sympathetic denervation on arterial stiffness and central hemodynamics in patients with resistant hypertension. *J Am Coll Cardiol* **60**(19)**:** 1956-1965.

Brasier AR, Recinos A, 3rd, Eledrisi MS (2002). Vascular inflammation and the renin-angiotensin system. *Arterioscler Thromb Vasc Biol* **22**(8)**:** 1257-1266.

Braun-Menendez E, Page IH (1958). Suggested revision of nomenclature--Angiotensin. *Science* **127**(3292)**:** 242.

Bravo R, Somoza B, Ruiz-Gayo M, Gonzalez C, Ruilope LM, Fernandez-Alfonso MS (2001). Differential effect of chronic antihypertensive treatment on vascular smooth muscle cell phenotype in spontaneously hypertensive rats. *Hypertension* **37**(5)**:** E4-E10.

Brown MS, Goldstein JL (1979). Receptor-mediated endocytosis: insights from the lipoprotein receptor system. *Proc Nat Acad Sci USA* **76**(7)**:** 3330-3337.

Bucci M, Gratton JP, Rudic RD, Acevedo L, Roviezzo F, Cirino G*, et al.* (2000). In vivo delivery of the caveolin-1 scaffolding domain inhibits nitric oxide synthesis and reduces inflammation. *Nat Med* **6**(12)**:** 1362-1367.

Buemi M, Allegra A, Aloisi C, Corica F, Alonci A, Ruello A*, et al.* (1997). Cold pressor test raises serum concentrations of ICAM-1, VCAM-1, and E-selectin in normotensive and hypertensive patients. *Hypertension* **30**(4)**:** 845-847.

Burns J, Sivananthan MU, Ball SG, Mackintosh AF, Mary DA, Greenwood JP (2007). Relationship between central sympathetic drive and magnetic resonance imaging-determined left ventricular mass in essential hypertension. *Circ* **115**(15)**:** 1999-2005.

Butz GM, Davisson RL (2001). Long-term telemetric measurement of cardiovascular parameters in awake mice: a physiological genomics tool. *Physiol Genomics* **5**(2)**:** 89-97.

Cannon CP, Hand MH, Bahr R, Boden WE, Christenson R, Gibler WB*, et al.* (2002). Critical pathways for management of patients with acute coronary syndromes: an assessment by the National Heart Attack Alert Program. *Am Heart J* **143**(5)**:** 777-789.

Carman CV, Springer TA (2004). A transmigratory cup in leukocyte diapedesis both through individual vascular endothelial cells and between them. *J Cell Biol* **167**(2)**:** 377-388.

Carmody RJ, Chen YH (2007). Nuclear factor-kappaB: activation and regulation during toll-like receptor signaling. *Cell Mol Immunol* **4**(1)**:** 31-41.

Chabrashvili T, Tojo A, Onozato ML, Kitiyakara C, Quinn MT, Fujita T*, et al.* (2002). Expression and cellular localization of classic NADPH oxidase subunits in the spontaneously hypertensive rat kidney. *Hypertension* **39**(2)**:** 269-274.

Chae CU, Lee RT, Rifai N, Ridker PM (2001). Blood pressure and inflammation in apparently healthy men. *Hypertension* **38**(3)**:** 399-403.

Chai Q, Wang X-L, Zeldin DC, Lee H-C (2013). Role of caveolae in shear stress-mediated endothelium-dependent dilation in coronary arteries. *Cardiovas Res* **100**(151-159).

Chapman HA, Jr., Munger JS, Shi GP (1994). The role of thiol proteases in tissue injury and remodeling. *Am J Respir Crit Care Med* **150**(6 Pt 2)**:** S155-159.

Chaqour B, Howard PS, Richards CF, Macarak EJ (1999). Mechanical stretch induces platelet-activating factor receptor gene expression through the NF-kappaB transcription factor. *J Mol CellCardiol* **31**(7)**:** 1345-1355.

Chatzizisis YS, Coskun AU, Jonas M, Edelman ER, Feldman CL, Stone PH (2007). Role of endothelial shear stress in the natural history of coronary atherosclerosis and vascular remodeling: molecular, cellular, and vascular behavior. *J Am Coll Cardiol* **49**(25)**:** 2379-2393.

Chen J, Kuhlencordt PJ, Astern J, Gyurko R, Huang PL (2001a). Hypertension does not account for the accelerated atherosclerosis and development of aneurysms in male apolipoprotein e/endothelial nitric oxide synthase double knockout mice. *Circ* **104**(20)**:** 2391-2394.

Chen X, Touyz RM, Park JB, Schiffrin EL (2001b). Antioxidant effects of vitamins C and E are associated with altered activation of vascular NADPH oxidase and superoxide dismutase in stroke-prone SHR. *Hypertension* **38**(3)**:** 606-611.

Chen Y-C, Bui AV, Diesch J, Manasseh R, Hausding C, Rivera J*, et al.* (2013). A Novel Mouse Model of Atherosclerotic Plaque Instability for Drug Testing and Mechanistic/Therapeutic Discoveries Using Gene and MicroRNA Expression Profiling. *Circ Res* **113**(3)**:** 252-265.

Chen YT, Yang CC, Zhen YY, Wallace CG, Yang JL, Sun CK, *et al*. (2013). Cyclosporine-assisted adipose-derived mesenchymal stem cell therapy to mitigate acute kidney ischemia-reperfusion injury. *Stem Cell Res Ther* **4**(3): 62.

Cheng C (2006). Atherosclerotic Lesion Size and Vulnerability Are Determined by Patterns of Fluid Shear Stress. *Circ* **113**(23)**:** 2744-2753.

Cheng JJ, Wung BS, Chao YJ, Wang DL (1996). Cyclic strain enhances adhesion of monocytes to endothelial cells by increasing intercellular adhesion molecule-1 expression. *Hypertension* **28**(3)**:** 386-391.

Chernyak L, Tauber AI (1988). The birth of immunology: Metchnikoff, the embryologist. *Cell Immunol* **117**(1)**:** 218-233.

Chicoine LG, Paffett ML, Young TL, Nelin LD (2004). Arginase inhibition increases nitric oxide production in bovine pulmonary arterial endothelial cells. *Am J Physiol Lung Cell Mol Physiol* **287**(1)**:** L60-68.

Chiu JJ, Chien S (2011a). Effects of disturbed flow on vascular endothelium: pathophysiological basis and clinical perspectives. *Physiol Rev* **91**(1)**:** 327-387.

Chiu JJ, Usami S, Chien S (2009). Vascular endothelial responses to altered shear stress: pathologic implications for atherosclerosis. *Annal Med* **41**(1)**:** 19-28.

Chobanian AV (2009). The hypertension paradox — more uncontrolled disease despite improved therapy. *N Eng J Med* **361**(9)**:** 878-887.

Chomczynski P, Sacchi N (1987). Single-step method of RNA isolation by acid guanidinium thiocyanate-phenol-chloroform extraction. *Anal Biochem* **162**(1)**:** 156-159.

Chrysohoou C, Pitsavos C, Panagiotakos DB, Skoumas J, Stefanadis C (2004). Association between prehypertension status and inflammatory markers related to atherosclerotic disease: The ATTICA Study. *Am J Hypertens* **17**(7)**:** 568-573.

Church JE, Fulton D (2006). Differences in eNOS activity because of subcellular localization are dictated by phosphorylation state rather than the local calcium environment. *J Biol Chem* **281**(3)**:** 1477-1488.

Cirino G, Fiorucci S, Sessa WC (2003). Endothelial nitric oxide synthase: the Cinderella of inflammation? *Trends Pharmacol Sci* **24**(2)**:** 91-95.

Ckless K, van der Vliet A, Janssen-Heininger Y (2007). Oxidative-nitrosative stress and post-translational protein modifications: implications to lung structure-function relations. Arginase modulates NF-kappaB activity via a nitric oxide-dependent mechanism. *Am J Resp Cell Mol Biol* **36**(6)**:** 645-653.

Corraliza IM, Campo ML, Soler G, Modolell M (1994). Determination of arginase activity in macrophages: a micromethod. *J Immuno Methods* **174**(1-2)**:** 231-235.

Crowley SD, Song YS, Lin EE, Griffiths R, Kim HS, Ruiz P (2010). Lymphocyte responses exacerbate angiotensin II-dependent hypertension. *Am J Physiol Reg Integ Comp Physiol* **298**(4)**:** R1089-1097.

Cuspidi C, Macca G, Sampieri L, Michev I, Salerno M, Fusi V*, et al.* (2001). High prevalence of cardiac and extracardiac target organ damage in refractory hypertension. *J Hypertens* **19**(11)**:** 2063-2070.

Cybulsky MI, Iiyama K, Li H, Zhu S, Chen M, Iiyama M*, et al.* (2001). A major role for VCAM-1, but not ICAM-1, in early atherosclerosis. *J Clin Invest* **107**(10)**:** 1255-1262.

Cybulsky MI, Lichtman AH, Hajra L, Iiyama K (1999). Leukocyte adhesion molecules in atherogenesis. *Clinica Chimica Acta* **286**(1-2)**:** 207-218.

D'Alessio A, Al-Lamki RS, Bradley JR, Pober JS (2005). Caveolae participate in tumor necrosis factor receptor 1 signaling and internalization in a human endothelial cell line. *Am J Pathol* **166**(4)**:** 1273-1282.

Dahlof B, Devereux RB, Kjeldsen SE, Julius S, Beevers G, de Faire U*, et al.* (2002). Cardiovascular morbidity and mortality in the Losartan Intervention For Endpoint reduction in hypertension study (LIFE): a randomised trial against atenolol. *Lancet* **359**(9311)**:** 995-1003.

Dardik A, Chen L, Frattini J, Asada H, Aziz F, Kudo FA*, et al.* (2005). Differential effects of orbital and laminar shear stress on endothelial cells. *J of Vasc Surg* **41**(5)**:** 869-880.

Daugherty A, Manning MW, Cassis LA (2000). Angiotensin II promotes atherosclerotic lesions and aneurysms in apolipoprotein E-deficient mice. *J Clin Invest* **105**(11)**:** 1605-1612.

Davern PJ, Jackson KL, Nguyen-Huu TP, La Greca L, Head GA (2010). Cardiovascular reactivity and neuronal activation to stress in Schlager genetically hypertensive mice. *Neurosci* **170**(2)**:** 551-558.

Davern PJ, Nguyen-Huu TP, La Greca L, Abdelkader A, Head GA (2009). Role of the sympathetic nervous system in Schlager genetically hypertensive mice. *Hypertension* **54**(4)**:** 852-859.

Davies PF (2009). Hemodynamic shear stress and the endothelium in cardiovascular pathophysiology. *Nat Clin Prac Cardiovas Med* **6**(1)**:** 16-26.

De Ciuceis C, Amiri F, Brassard P, Endemann DH, Touyz RM, Schiffrin EL (2005). Reduced vascular remodeling, endothelial dysfunction, and oxidative stress in resistance arteries of angiotensin II-infused macrophage colony-stimulating factor-deficient mice: evidence for a role in inflammation in angiotensin-induced vascular injury. *Arterioscler Thromb Vasc Biol* **25**(10)**:** 2106-2113.

De Meirelles LR, Mendes-Ribeiro AC, Mendes MAP, Da Silva MNSB, John Clive Ellory JC, Mann GE*, et al.* (2008). Chronic exercise reduces platelet activation in hypertension: upregulation of the l-arginine-nitric oxide pathway. *Scand J Med Sci Sports* **19**(1)**:** 67-74.

Dejana E (2006). The transcellular railway: insights into leukocyte diapedesis. *Nature Cell Biology* **8**(2)**:** 105-107.

Delli Gatti C, Osto E, Kouroedov A, Eto M, Shaw S, Volpe M*, et al.* (2008). Pulsatile stretch induces release of angiotensin II and oxidative stress in human endothelial cells: effects of ACE inhibition and AT1 receptor antagonism. *Clin Exper Hypertens* **30**(7)**:** 616-627.

Demougeot C, Prigent-Tessier A, Bagnost T, Andre C, Guillaume Y, Bouhaddi M*, et al.* (2007a). Time course of vascular arginase expression and activity in spontaneously hypertensive rats. *Life Sci* **80**(12)**:** 1128-1134.

Demougeot C, Prigent-Tessier A, Bagnost T, André C, Guillaume Y, Bouhaddi M*, et al.* (2007b). Time course of vascular arginase expression and activity in spontaneously hypertensive rats. *Life Sci* **80**(12)**:** 1128-1134.

Demougeot C, Prigent-Tessier A, Marie C, Berthelot A (2005). Arginase inhibition reduces endothelial dysfunction and blood pressure rising in spontaneously hypertensive rats. *J Hypertens* **23**(5)**:** 971-978.

Desjardins F, Lobysheva I, Pelat M, Gallez B, Feron O, Dessy C*, et al.* (2008). Control of blood pressure variability in caveolin-1-deficient mice: role of nitric oxide identified in vivo through spectral analysis. *Cardiovas Res* **79**(3)**:** 527-536.

Dickinson BC, Peltier J, Stone D, Schaffer DV, Chang CJ (2011). Nox2 redox signaling maintains essential cell populations in the brain. *Nat Chem Biol* **7**(2)**:** 106-112.

Dignat-George F, Boulanger CM (2011). The many faces of endothelial microparticles. *Arterioscler Thromb Vasc Biol* **31**(1)**:** 27-33.

Dikalov SI, Nazarewicz RR (2013). Angiotensin II-induced production of mitochondrial reactive oxygen species: potential mechanisms and relevance for cardiovascular disease. *Antiox Redox Signal* **19**(10)**:** 1085-1094.

Dimmeler S, Fleming I, Fisslthaler B, Hermann C, Busse R, Zeiher AM (1999). Activation of nitric oxide synthase in endothelial cells by Akt-dependent phosphorylation. *Nature* **399**(6736)**:** 601-605.

Do TH, Chen Y, Nguyen VT, Phisitkul S (2010). Vaccines in the management of hypertension. *Exp Opin Biol Ther* **10**(7)**:** 1077-1087.

Dong ZM, Brown AA, Wagner DD (2000). Prominent role of P-selectin in the development of advanced atherosclerosis in ApoE-deficient mice. *Circ* **101**(19)**:** 2290-2295.

Drab M, Verkade P, Elger M, Kasper M, Lohn M, Lauterbach B*, et al.* (2001). Loss of caveolae, vascular dysfunction, and pulmonary defects in caveolin-1 gene-disrupted mice. *Science* **293**(5539)**:** 2449-2452.

Eikelis N, Schlaich M, Aggarwal A, Kaye D, Esler M (2003). Interactions between leptin and the human sympathetic nervous system. *Hypertension* **41**(5)**:** 1072-1079.

Engel D, Beckers L, Wijnands E, Seijkens T, Lievens D, Drechsler M*, et al.* (2011). Caveolin-1 deficiency decreases atherosclerosis by hampering leukocyte influx into the arterial wall and generating a regulatory T-cell response. *The FASEB Journal* **25**(11)**:** 3838-3848.

Engstrom G, Janzon L, Berglund G, Lind P, Stavenow L, Hedblad B*, et al.* (2002). Blood pressure increase and incidence of hypertension in relation to inflammation-sensitive plasma proteins. *Arterioscler Thromb Vasc Biol* **22**(12)**:** 2054-2058.

Eriksson EE, Xie X, Werr J, Thoren P, Lindbom L (2001). Direct viewing of atherosclerosis in vivo: plaque invasion by leukocytes is initiated by the endothelial selectins. *FASEB J* **15**(7)**:** 1149-1157.

Felder RB (2010). Mineralocorticoid receptors, inflammation and sympathetic drive in a rat model of systolic heart failure. *Exper Physiol* **95**(1)**:** 19-25.

Fernandez-Hernando C, Yu J, Davalos A, Prendergast J, Sessa WC (2010). Endothelial-specific overexpression of caveolin-1 accelerates atherosclerosis in apolipoprotein E-deficient mice. *Am J Pathol* **177**(2)**:** 998-1003.

Fernandez-Hernando C, Yu J, Suarez Y, Rahner C, Davalos A, Lasuncion MA*, et al.* (2009). Genetic evidence supporting a critical role of endothelial caveolin-1 during the progression of atherosclerosis. *Cell Metab* **10**(1)**:** 48-54.

Firuzi O, Miri R, Tavakkoli M, Saso L (2011). Antioxidant therapy: current status and future prospects. *Curr Med Chem* **18**(25): 3871-3888.

Forstermann U (2008). Oxidative stress in vascular disease: causes, defense mechanisms and potential therapies. *Nat Clin Prac Cardiovasc Med* **5**(6)**:** 338-349.

Fortuno A, Olivan S, Beloqui O, San Jose G, Moreno MU, Diez J*, et al.* (2004). Association of increased phagocytic NADPH oxidase-dependent superoxide production with diminished nitric oxide generation in essential hypertension. *J Hypertens* **22**(11)**:** 2169-2175.

Frank PG, Lee H, Park DS, Tandon NN, Scherer PE, Lisanti MP (2004). Genetic ablation of caveolin-1 confers protection against atherosclerosis. *Arterioscler Thromb Vasc Biol* **24**(1)**:** 98-105.

Frank PG, Pavlides S, Cheung MW, Daumer K, Lisanti MP (2008). Role of caveolin-1 in the regulation of lipoprotein metabolism. *Am J Physiol Cell Physiol* **295**(1)**:** C242-248.

Fu C, He J, Li C, Shyy JY-J, Zhu Y (2010). Cholesterol increases adhesion of monocytes to endothelium by moving adhesion molecules out of caveolae. *Biochim Biophys Acta* **1801**(7)**:** 702-710.

Fu Y, Moore XL, Lee MK, Fernandez-Rojo MA, Parat MO, Parton RG*, et al.* (2012). Caveolin-1 plays a critical role in the differentiation of monocytes into macrophages. *Arterioscler Thromb Vasc Biol* **32**(9)**:** e117-125.

Fulton D, Gratton JP, McCabe TJ, Fontana J, Fujio Y, Walsh K*, et al.* (1999). Regulation of endothelium-derived nitric oxide production by the protein kinase Akt. *Nature* **399**(6736)**:** 597-601.

Furchgott RF, Zawadzki JV (1980). The obligatory role of endothelial cells in the relaxation of arterial smooth muscle by acetylcholine. *Nature* **288**(5789)**:** 373-376.

Gabella G (1978). Inpocketings of the cell membrane (caveolae) in the rat myocardium. *J Ultrastruct Res* **65**(2)**:** 135-147.

Gaddam KK, Nishizaka MK, Pratt-Ubunama MN, Pimenta E, Aban I, Oparil S*, et al.* (2008). Characterization of resistant hypertension: association between resistant hypertension, aldosterone, and persistent intravascular volume expansion. *Arch Intern Med* **168**(11)**:** 1159-1164.

Gao S (2004). Docking of endothelial nitric oxide synthase (eNOS) to the mitochondrial outer membrane: a pentabasic amino acid sequence in the autoinhibitory domain of eNOS targets a proteinase K-cleavable peptide on the cytoplasmic face of mitochondria. *J Biol Chem* **279**(16)**:** 15968-15974.

Gao X, Xu X, Belmadani S, Park Y, Tang Z, Feldman AM*, et al.* (2007). TNF-α contributes to endothelial dysfunction by upregulating arginase in ischemia/reperfusion injury. *Arterioscler Thromb Vasc Biol* **27**(6)**:** 1269-1275.

Garlanda C, Parravicini C, Sironi M, De Rossi M, Wainstok de Calmanovici R, Carozzi F*, et al.* (1994). Progressive growth in immunodeficient mice and host cell recruitment by mouse endothelial cells transformed by polyoma middle-sized T antigen: implications for the pathogenesis of opportunistic vascular tumors. *Proc Natl Acad Sci U S A* **91**(15)**:** 7291-7295.

Ge S, Song L, Serwanski DR, Kuziel WA, Pachter JS (2008). Transcellular transport of CCL2 across brain microvascular endothelial cells. *J Neurochem* **104**(5)**:** 1219-1232.

Gheorghiade M, Albaghdadi M, Zannad F, Fonarow GC, Bohm M, Gimpelewicz C*, et al.* (2011). Rationale and design of the multicentre, randomized, double-blind, placebo-controlled Aliskiren Trial on Acute Heart Failure Outcomes (ASTRONAUT). *Eur J Heart Fail* **13**(1)**:** 100-106.

Ghitescu L, Fixman A, Simionescu M, Simionescu N (1986). Specific binding sites for albumin restricted to plasmalemmal vesicles of continuous capillary endothelium: receptor-mediated transcytosis. *J Cell Biol* **102**(4)**:** 1304-1311.

Giugliano D, Marfella R, Verrazzo G, Acampora R, Coppola L, Cozzolino D*, et al.* (1997). The vascular effects of L-Arginine in humans. The role of endogenous insulin. *J Clin Invest* **99**(3)**:** 433-438.

Glenney JR, Jr. (1989). Tyrosine phosphorylation of a 22-kDa protein is correlated with transformation by Rous sarcoma virus. *J Biol Chem* **264**(34)**:** 20163-20166.

Goh SY, Cooper ME (2008). The role of advanced glycation end products in progression and complications of diabetes. *J Clin Endocrinol Metab* **93**(4)**:** 1143-1152.

Goldblatt H, Lynch J, Hanzal RF, Summerville WW (1934). Studies on experimental hypertension : I. The production of persistent elevation of systolic blood pressure by means of renal ischemia. *J Exper Med* **59**(3)**:** 347-379.

Goret L, Tanguy S, Guiraud I, Dauzat M, Obert P (2008). Acute administration of l-arginine restores nitric oxide-mediated relaxation in isolated pulmonary arteries from pulmonary hypertensive exercise trained rats. *E J Pharmacol* **581**(1-2)**:** 148-156.

Grassi G (2007). Sympathetic activation in hypertension: what are the effects on vascular, endothelial, and metabolic function? *Dialog Cardiovasc Med* **12**(3)**:** 192-198.

Grassi G (2010). Sympathetic neural activity in hypertension and related diseases. *American J Hypertens* **23**(10)**:** 1052-1060.

Grassi G, Seravalle G, Stella ML, Turri C, Zanchetti A, Mancia G (2000). Sympathoexcitatory responses to the acute blood pressure fall induced by central or peripheral antihypertensive drugs. *Am J Hypertens* **13**(1 Pt 1)**:** 29-34.

Grassi G, Seravalle G, Turri C, Bolla G, Mancia G (2003). Short-versus long-term effects of different dihydropyridines on sympathetic and baroreflex function in hypertension. *Hypertension* **41**(3)**:** 558-562.

Grayson TH, Ohms SJ, Brackenbury TD, Meaney KR, Peng K, Pittelkow YE*, et al.* (2007). Vascular microarray profiling in two models of hypertension identifies Cav-1, Rgs2 and Rgs5 as antihypertensive targets. *BMC Genomics* **8**(1)**:** 404.

Greenberg S, Grinstein S (2002). Phagocytosis and innate immunity. *Curr Opin Immunol* **14**(1)**:** 136-145.

Greenwood JP, Scott EM, Stoker JB, Mary DA (2001). Hypertensive left ventricular hypertrophy: relation to peripheral sympathetic drive. *J Am Coll Cardiol* **38**(6)**:** 1711-1717.

Giri R, Shen Y, Stins M, Du Yan S, Schmidt AM, Stern D *et al*. (2000). beta-amyloid-induced migration of monocytes across human brain endothelial cells involves RAGE and PECAM-1. *Am J Physiol Cell Physiol* **279**(6): C1772-1781.

Griendling KK, Sorescu D, Ushio-Fukai M (2000). NAD(P)H oxidase: role in cardiovascular biology and disease. *Circ Res* **86**(5)**:** 494-501.

Griendling KK, Ushio-Fukai M, Lassegue B, Alexander RW (1997). Angiotensin II signaling in vascular smooth muscle. New concepts. *Hypertension* **29**(1 Pt 2)**:** 366-373.

Griffoni C, Spisni E, Santi S, Riccio M, Guarnieri T, Tomasi V (2000). Knockdown of caveolin-1 by antisense oligonucleotides impairs angiogenesis in vitro and in vivo. *Biochem Biophys Res Commun* **276**(2)**:** 756-761.

Groen HC, Gijsen FJ, van der Lugt A, Ferguson MS, Hatsukami TS, Yuan C*, et al.* (2008). High shear stress influences plaque vulnerability: Part of the data presented in this paper were published in Stroke 2007;38:2379-81. *Neth Heart J* **16**(7-8)**:** 280-283.

Gschwend S, Henning RH, Pinto YM, de Zeeuw D, van Gilst WH, Buikema H (2003). Myogenic constriction is increased in mesenteric resistance arteries from rats with chronic heart failure: instantaneous counteraction by acute AT1 receptor blockade. *Br J Pharmacol* **139**(7): 1317-1325.

Guillot FL, Audus KL, Raub TJ (1990). Fluid-phase endocytosis by primary cultures of bovine brain microvessel endothelial cell monolayers. *Microvasc Res* **39**(1)**:** 1-14.

Guzik TJ, Hoch NE, Brown KA, McCann LA, Rahman A, Dikalov S*, et al.* (2007). Role of the T cell in the genesis of angiotensin II induced hypertension and vascular dysfunction. *J Exp Med* **204**(10)**:** 2449-2460.

Haga JH, Li Y-SJ, Chien S (2007). Molecular basis of the effects of mechanical stretch on vascular smooth muscle cells. *J Biomech* **40**(5)**:** 947-960.

Hahn C, Schwartz MA (2009). Mechanotransduction in vascular physiology and atherogenesis. *Nat Rev Mol Cell Biol* **10**(1)**:** 53-62.

Halliwell B, Long LH, Yee TP, Lim S, Kelly R (2004). Establishing biomarkers of oxidative stress: the measurement of hydrogen peroxide in human urine. *Curr Med Chem* **11**(9): 1085-92.

Hamm CW, Bassand J-P, Agewall S, Bax J, Boersma E, Bueno H*, et al.* (2011). ESC Guidelines for the management of acute coronary syndromes in patients presenting without persistent ST-segment elevation: The Task Force for the management of acute coronary syndromes (ACS) in patients presenting without persistent ST-segment elevation of the European Society of Cardiology (ESC). Vol. 32, pp 2999-3054.

Han W, Li H, Villar VA, Pascua AM, Dajani MI, Wang X, *et al.* (2008). Lipid rafts keep NADPH oxidase in the inactive state in human renal proximal tubule cells. *Hypertension* **51**(2)**:** 481-487.

Hansen CG, Bright NA, Howard G, Nichols BJ (2009). SDPR induces membrane curvature and functions in the formation of caveolae. *Nat Cell Biol* **11**(7)**:** 807-814.

Hansen CG, Nichols BJ (2010). Exploring the caves: cavins, caveolins and caveolae. *Trends Cell Biol* **20**(4)**:** 177-186.

Hansson GK, Hermansson A (2011). The immune system in atherosclerosis. *Nat Immunol* **12**(3)**:** 204-212.

Harris MB, Ju H, Venema VJ, Liang H, Zou R, Michell BJ, *et al.* (2001). Reciprocal phosphorylation and regulation of endothelial nitric-oxide synthase in response to bradykinin stimulation. *J Biol Chem* **276**(19)**:** 16587-16591.

Harrison DG, Widder J, Grumbach I, Chen W, Weber M, Searles C (2006). Endothelial mechanotransduction, nitric oxide and vascular inflammation. *J Intern Med* **259**(4)**:** 351-363.

Hayer A, Stoeber M, Bissig C, Helenius A (2010a). Biogenesis of caveolae: stepwise assembly of large caveolin and cavin complexes. *Traffic* **11**(3)**:** 361-382.

Hayer A, Stoeber M, Ritz D, Engel S, Meyer HH, Helenius A (2010b). Caveolin-1 is ubiquitinated and targeted to intralumenal vesicles in endolysosomes for degradation. *The Journal of Cell Biology* **191**(3)**:** 615-629.

Head BP, Insel PA (2007). Do caveolins regulate cells by actions outside of caveolae? *Trends Cell Biol* **17**(2)**:** 51-57.

Head GA, Lukoshkova EV, Burke SL, Malpas SC, Lambert EA, Janssen BJ (2001). Comparing spectral and invasive estimates of baroreflex gain. *IEEE Eng Med Biol Mag* **20**(2)**:** 43-52.

Hein TW, Zhang C, Wang W, Chang CI, Thengchaisri N, Kuo L (2003). Ischemia-reperfusion selectively impairs nitric oxide-mediated dilation in coronary arterioles: counteracting role of arginase. *The FASEB Journal* **17**(15)**:** 2328-2330.

Hill MM, Bastiani M, Luetterforst R, Kirkham M, Kirkham A, Nixon SJ, *et al.* (2008). PTRF-Cavin, a conserved cytoplasmic protein required for caveola formation and function. *Cell* **132**(1)**:** 113-124.

Hobbs H, Brown M, Russel D, Davignon J, Goldstein J (1987). Deletion in the gene for the low-density-lipoprotein receptor in a majority of French Canadians with familial hypercholesterolemia. *N Engl J Med* **317**(12)**:** 734-737.

Holowatz LA, Kenney WL (2007). Up-regulation of arginase activity contributes to attenuated reflex cutaneous vasodilatation in hypertensive humans. *J Physiol* **581**(2)**:** 863-872.

Houston MC (2005). Nutraceuticals, vitamins, antioxidants, and minerals in the prevention and treatment of hypertension. *Prog Cardiovasc Dis* **47**(6)**:** 396-449.

Hu J, Ji M, Niu C, Aini A, Zhou Q, Zhang L*, et al.* (2012). Effects of renal sympathetic denervation on post-myocardial infarction cardiac remodeling in rats. *PLoS One* **7**(9)**:** e45986.

Huang Z, Huang PL, Ma J, Meng W, Ayata C, Fishman MC*, et al.* (1996). Enlarged infarcts in endothelial nitric oxide synthase knockout mice are attenuated by nitro-L-arginine. *J Cereb Blood Flow Metab* **16**(5)**:** 981-987.

Ibrahim J, Miyashiro JK, Berk BC (2003). Shear stress is differentially regulated among inbred rat strains. *Circ Res* **92**(9)**:** 1001-1009.

Ignarro LJ, Buga GM, Wood KS, Byrns RE, Chaudhuri G (1987). Endothelium-derived relaxing factor produced and released from artery and vein is nitric oxide. *Proc Natl Acad Sci U S A* **84**(24)**:** 9265-9269.

Insel PA, Patel HH (2007). Do studies in caveolin-knockouts teach us about physiology and pharmacology or instead, the ways mice compensate for 'lost proteins'? *Br J Pharmacol* **150**(3)**:** 251-254.

Jackson K, Head GA, Morris BJ, Chin-Dusting J, Jones E, La Greca L*, et al.* (2007). Reduced cardiovascular reactivity to stress but not feeding in renin enhancer knockout mice. *Am J Hypertens* **20**(8)**:** 893-899.

Jackson KL, Marques FZ, Watson AM, Palma-Rigo K, Nguyen-Huu TP, Morris BJ*, et al.* (2013). A Novel Interaction Between Sympathetic Overactivity and Aberrant Regulation of Renin by miR-181a in BPH/2J Genetically Hypertensive Mice. *Hypertension* **62**(4)**:** 775-781.

Jameson M, Dai FX, Luscher T, Skopec J, Diederich A, Diederich D (1993). Endothelium-derived contracting factors in resistance arteries of young spontaneously hypertensive rats before development of overt hypertension. *Hypertension* **21**(3)**:** 280-288.

Jiang F, Dusting G (2003). Natural phenolic compounds as cardiovascular therapeutics: potential role of their antiinflammatory effects. *Curr Vas Pharmacol* **1**(2)**:** 135-156.

Jiang Y, Kohara K, Hiwada K (1999). Low wall shear stress contributes to atherosclerosis of the carotid artery in hypertensive patients. *Hypertension Res* **22**(3)**:** 203-207.

Johansson PI, Ostrowski SR (2010). Acute coagulopathy of trauma: balancing progressive catecholamine induced endothelial activation and damage by fluid phase anticoagulation. *Medical Hypotheses* **75**(6)**:** 564-567.

Johnson FK, Johnson RA, Peyton KJ, Durante W (2005). Arginase inhibition restores arteriolar endothelial function in Dahl rats with salt-induced hypertension. *Am J Physiol Regul Integr Comp Physiol* **288**(4)**:** R1057-1062.

Ju H, Zou R, Venema VJ, Venema RC (1997). Direct interaction of endothelial nitric-oxide synthase and caveolin-1 inhibits synthase activity. *J Biol Chem* **272**(30)**:** 18522-18525.

Jung C, Gonon AT, Sjoquist PO, Lundberg JO, Pernow J (2010). Arginase inhibition mediates cardioprotection during ischaemia-reperfusion. *Cardiovas Res* **85**(1)**:** 147-154.

Kägi D, Ledermann B, Bürki K, Seiler P, Odermatt B, Olsen KJ*, et al.* (1994). Cytotoxicity mediated by T cells and natural killer cells is greatly impaired in perforin-deficient mice. *Nature* **369**(6475)**:** 31-37.

Kasal DA, Barhoumi T, Li MW, Yamamoto N, Zdanovich E, Rehman A*, et al.* (2012). T regulatory lymphocytes prevent aldosterone-induced vascular injury. *Hypertension* **59**(2)**:** 324-330.

Kashyap SR, Lara A, Zhang R, Park YM, DeFronzo RA (2008). Insulin reduces plasma arginase activity in type 2 diabetic patients. *Diab Care* **31**(1)**:** 134-139.

Katakam PV, Ujhelyi MR, Hoenig ME, Miller AW (1998). Endothelial dysfunction precedes hypertension in diet-induced insulin resistance. *Am J Physiol* **275**(3 Pt 2)**:** R788-792.

Kearney PM, Whelton M, Reynolds K, Muntner P, Whelton PK, He J (2005). Global burden of hypertension: analysis of worldwide data. *The Lancet* **365**(9455)**:** 217-223.

Khan NA, Hemmelgarn B, Herman RJ, Bell CM, Mahon JL, Leiter LA*, et al.* (2009). The 2009 Canadian Hypertension Education Program recommendations for the management of hypertension: Part 2--therapy. *Can J Cardiol* **25**(5)**:** 287-298.

Khder Y, Briancon S, Petermann R, Quilliot D, Stoltz JF, Drouin P*, et al.* (1998). Shear stress abnormalities contribute to endothelial dysfunction in hypertension but not in type II diabetes. *J Hypertens* **16**(11)**:** 1619-1625.

Kim SW, Jeong SJ, Munarriz R, Kim NN, Goldstein I, Traish AM (2003). Role of the nitric oxide-cyclic GMP pathway in regulation of vaginal blood flow. *Int J Impot Res* **15**(5)**:** 355-361.

King GL, Johnson SM (1985). Receptor-mediated transport of insulin across endothelial cells. *Science* **227**(4694)**:** 1583-1586.

Kisucka J, Chauhan AK, Patten IS, Yesilaltay A, Neumann C, Van Etten RA*, et al.* (2008). Peroxiredoxin1 prevents excessive endothelial activation and early atherosclerosis. *Circ Res* **103**(6)**:** 598-605.

Klintman D, Li X, Thorlacius H (2004). Important role of P-selectin for leukocyte recruitment, hepatocellular injury, and apoptosis in endotoxemic mice. *Clin Diagn Lab Immunol* **11**(1)**:** 56-62.

Knowles JW, Reddick RL, Jennette JC, Shesely EG, Smithies O, Maeda N (2000a). Enhanced atherosclerosis and kidney dysfunction in eNOS(-/-)Apoe(-/-) mice are ameliorated by enalapril treatment. *J Clin Invest* **105**(4)**:** 451-458.

Knowles JW, Reddick RL, Jennette JC, Shesely EG, Smithies O, Maeda N (2000b). Enhanced atherosclerosis and kidney dysfunction in eNOS(-/-)Apoe(-/-) mice are ameliorated by enalapril treatment. *J Clin Invest* **105**(4)**:** 451-458.

Koga H, Sugiyama S, Kugiyama K, Watanabe K, Fukushima H, Tanaka T*, et al.* (2005). Elevated levels of VE-cadherin-positive endothelial microparticles in patients with type 2 diabetes mellitus and coronary artery disease. *J Am Coll Cardiol* **45**(10)**:** 1622-1630.

Kohli R, Meininger CJ, Haynes TE, Yan W, Self JT, Wu G (2004). Dietary L-arginine supplementation enhances endothelial nitric oxide synthesis in streptozotocin-induced diabetic rats. *J Nutr* **134**(3)**:** 600-608.

Kono S, Kushiro T, Hirata Y, Hamada C, Takahashi A, Yoshida Y (2005). Class of antihypertensive drugs, blood pressure status, and risk of cardiovascular disease in hypertensive patients: a case-control study in Japan. *Hypertens Res* **28**(10)**:** 811-817.

Korn T, Bettelli E, Gao W, Awasthi A, Jäger A, Strom TB*, et al.* (2007). IL-21 initiates an alternative pathway to induce proinflammatory TH17 cells. *Nature* **448**(7152)**:** 484-487.

Krum H, Massie B, Abraham WT, Dickstein K, Kober L, McMurray JJ*, et al.* (2011). Direct renin inhibition in addition to or as an alternative to angiotensin converting enzyme inhibition in patients with chronic systolic heart failure: rationale and design of the Aliskiren Trial to Minimize OutcomeS in Patients with HEart failuRE (ATMOSPHERE) study. *Eur J Heart Fail* **13**(1)**:** 107-114.

Krum H, Schlaich M, Whitbourn R, Sobotka PA, Sadowski J, Bartus K*, et al.* (2009). Catheter-based renal sympathetic denervation for resistant hypertension: a multicentre safety and proof-of-principle cohort study. *Lancet* **373**(9671)**:** 1275-1281.

Kuang Y, Wu Y, Jiang H, Wu D (1996). Selective G protein coupling by C-C chemokine receptors. *J Biol Chem* **271**(8)**:** 3975-3978.

Kubes P, Suzuki M, Granger DN (1991). Nitric oxide: an endogenous modulator of leukocyte adhesion. *Proc Natl Acad Sci U S A* **88**(11)**:** 4651-4655.

Kunes J, Dobesova Z, Zicha J (2002). Altered balance of main vasopressor and vasodepressor systems in rats with genetic hypertension and hypertriglyceridaemia. *Clin Sci* **102**(3)**:** 269-277.

Kunes J, Hojna S, Kadlecova M, Dobesova Z, Rauchova H, Vokurkova M*, et al.* (2004). Altered balance of vasoactive systems in experimental hypertension: the role of relative NO deficiency. *Physiol Res* **53**: S23-34.

Lacolley P, Regnault V, Nicoletti A, Li Z, Michel JB (2012). The vascular smooth muscle cell in arterial pathology: a cell that can take on multiple roles. *Cardiovas Res* **95**(2)**:** 194-204.

Lacy F, Kailasam MT, O'Connor DT, Schmid-Schonbein GW, Parmer RJ (2000). Plasma hydrogen peroxide production in human essential hypertension: role of heredity, gender, and ethnicity. *Hypertension* **36**(5)**:** 878-884.

Lakka TA, Salonen R, Kaplan GA, Salonen JT (1999). Blood pressure and the progression of carotid atherosclerosis in middle-aged men. *Hypertension* **34**(1)**:** 51-56.

Langer HF, Chavakis T (2009). Leukocyte-endothelial interactions in inflammation. *J Cell Mol Med* **13**(7)**:** 1211-1220.

Langrish CL, Chen Y, Blumenschein WM, Mattson J, Basham B, Sedgwick JD*, et al.* (2005). IL-23 drives a pathogenic T cell population that induces autoimmune inflammation. *J Ex Med* **201**(2)**:** 233-240.

Lee MY, Wu CM, Yu KH, Chu CS, Lee KT, Sheu SH*, et al.* (2008). Association between hemodynamics in the common carotid artery and severity of carotid atherosclerosis in patients with essential hypertension. *Am J Hypertens* **21**(7)**:** 765-770.

Lee MY, Wu CM, Yu KH, Chu CS, Lee KT, Sheu SH*, et al.* (2009). Association between wall shear stress and carotid atherosclerosis in patients with never treated essential hypertension. *Am J Hypertens* **22**(7)**:** 705-710.

Lefer DJ, Jones SP, Girod WG, Baines A, Grisham MB, Cockrell AS*, et al.* (1999). Leukocyte-endothelial cell interactions in nitric oxide synthase-deficient mice. Am J Physiol **276**(6 Pt 2)**:** H1943-1950.

Lefort CT, Hyun Y-M, Schultz JB, Law F-Y, Waugh RE, Knauf PA*, et al.* (2009). Outside-in signal transmission by conformational changes in integrin Mac-1. *J Immunol* **183**(10)**:** 6460-6468.

Lemarie CA, Esposito B, Tedgui A, Lehoux S (2003). Pressure-induced vascular activation of nuclear factor-kappaB: role in cell survival. *Circ Res* **93**(3)**:** 207-212.

Levrand S, Pesse B, Feihl F, Waeber B, Pacher P, Rolli J*, et al.* (2005). Peroxynitrite is a potent inhibitor of NF-{kappa}B activation triggered by inflammatory stimuli in cardiac and endothelial cell lines. *Journal of Biological Chemistry* **280**(41)**:** 34878-34887.

Levy D, Ehret GB, Rice K, Verwoert GC, Launer LJ, Dehghan A*, et al.* (2009). Genome-wide association study of blood pressure and hypertension. *Nature Genetics* **41**(6)**:** 677-687.

Levy D, Larson MG, Vasan RS, Kannel WB, Ho KK (1996). The progression from hypertension to congestive heart failure. *JAMA* **275**(20)**:** 1557-1562.

Ley K, Laudanna C, Cybulsky MI, Nourshargh S (2007). Getting to the site of inflammation: the leukocyte adhesion cascade updated. *Nature Reviews Immunology* **7**(9)**:** 678-689.

Leychenko A, Konorev E, Jijiwa M, Matter ML (2011). Stretch-induced hypertrophy activates NFkB-mediated VEGF secretion in adult cardiomyocytes. *PLoS One* **6**(12)**:** e29055.

Li H, Forstermann U (2009). Prevention of atherosclerosis by interference with the vascular nitric oxide system. *Current Pharmaceutical Design* **15**(27)**:** 3133-3145.

Li XA, Everson WV, Smart EJ (2005a). Caveolae, lipid rafts, and vascular disease. *Trends in Cardiovascular Medicine* **15**(3)**:** 92-96.

Li Y-SJ, Haga JH, Chien S (2005b). Molecular basis of the effects of shear stress on vascular endothelial cells. *Journal of Biomechanics* **38**(10)**:** 1949-1971.

Li Z-Y, Howarth SPS, Tang T, Gillard JH (2006). How critical is fibrous cap thickness to carotid plaque stability? A flow-plaque interaction model. *Stroke* **37**(5)**:** 1195-1199.

Libby P (2013). Mechanisms of acute coronary syndromes and their implications for therapy. *New England Journal of Medicine* **368**(21)**:** 2004-2013.

Libby P, Ridker PM, Hansson GK (2011). Progress and challenges in translating the biology of atherosclerosis. *Nature* **473**(7347)**:** 317-325.

Libby P, Ridker PM, Maseri A (2002). Inflammation and Atherosclerosis. *Circulation*.

Lim HK, Ryoo S, Benjo A, Shuleri K, Miriel V, Baraban E*, et al.* (2007a). Mitochondrial arginase II constrains endothelial NOS-3 activity. *American Journal of Physiology - Heart and Circulatory Physiology* **293**(6)**:** H3317-3324.

Lim HK, Ryoo S, Benjo A, Shuleri K, Miriel V, Baraban E*, et al.* (2007b). Mitochondrial arginase II constrains endothelial NOS-3 activity. *American Journal of Physiology - Heart and Circulatory Physiology* **293**(6)**:** H3317-H3324.

Lindahl B (2013). Acute coronary syndrome - the present and future role of biomarkers. *Clinical chemistry and laboratory medicine : CCLM / FESCC***:** 1-8.

Lip GY, Blann AD, Zarifis J, Beevers M, Lip PL, Beevers DG (1995). Soluble adhesion molecule P-selectin and endothelial dysfunction in essential hypertension: implications for atherogenesis? A preliminary report. *Journal of Hypertension* **13**(12 Pt 2)**:** 1674-1678.

Liu L, Brown D, McKee M, Lebrasseur NK, Yang D, Albrecht KH*, et al.* (2008). Deletion of Cavin/PTRF causes global loss of caveolae, dyslipidemia, and glucose intolerance. *Cell Metabolism* **8**(4)**:** 310-317.

Lobysheva I, Rath G, Sekkali B, Bouzin C, Feron O, Gallez B*, et al.* (2011). Moderate caveolin-1 downregulation prevents NADPH oxidase-dependent endothelial nitric oxide synthase uncoupling by angiotensin II in endothelial cells. *Arteriosclerosis, Thrombosis, and Vascular Biology* **31**(9)**:** 2098-2105.

Lohmeier TE, Iliescu R, Liu B, Henegar JR, Maric-Bilkan C, Irwin ED (2012). Systemic and renal-specific sympathoinhibition in obesity hypertension. *Hypertension* **59**(2)**:** 331-338.

Lolis E, Bucala R (2003). Therapeutic approaches to innate immunity: severe sepsis and septic shock. *Nature Reviews Drug Discovery* **2**(8)**:** 635-645.

Lopez AD, Mathers CD, Ezzati M, Jamison DT, Murray CJ (2006). Global and regional burden of disease and risk factors, 2001: systematic analysis of population health data. *The Lancet* **367**(9524)**:** 1747-1757.

Lowry OH, Rosebrough NJ, Farr AL, Randall RJ (1951). Protein measurement with the Folin phenol reagent. *Journal of Biological Chemistry* **193**(1)**:** 265-275.

Luu NT, Rahman M, Stone PC, Rainger GE, Nash GB (2010a). Responses of endothelial cells from different vessels to inflammatory cytokines and shear stress: evidence for the pliability of endothelial phenotype. *Journal of Vascular Research* **47**(5)**:** 451-461.

Luu NT, Rahman M, Stone PC, Rainger GE, Nash GB (2010b). Responses of endothelial cells from different vessels to inflammatory cytokines and shear stress: evidence for the pliability of endothelial phenotype. *Journal of Vascular Research* **47**(5)**:** 451-461.

Lye S-H, Chahil JK, Bagali P, Alex L, Vadivelu J, Ahmad WAW*, et al.* (2013). Genetic polymorphisms in LDLR, APOB, PCSK9 and other lipid related genes associated with familial hypercholesterolemia in Malaysia. *PLoS ONE* **8**(4)**:** e60729.

MacAllister RJ, Calver AL, Collier J, Edwards CM, Herreros B, Nussey SS*, et al.* (1995). Vascular and hormonal responses to arginine: provision of substrate for nitric oxide or non-specific effect? *Clinical Science* **89**(2)**:** 183-190.

Makhmudov RM, Mamedov Ya D, Dolgov VV, Repin VS (1985). Catecholamine-mediated injury to endothelium in rabbit perfused aorta: a quantitative analysis by scanning electron microscopy. *Cor et Vasa* **27**(6)**:** 456-463.

Malek AM, Alper SL, Izumo S (1999). Hemodynamic shear stress and its role in atherosclerosis. *JAMA* **282**(21)**:** 2035-2042.

Marchesi C, Paradis P, Schiffrin EL (2008). Role of the renin-angiotensin system in vascular inflammation. *Trends in Pharmacological Sciences* **29**(7)**:** 367-374.

Marvar PJ, Thabet SR, Guzik TJ, Lob HE, McCann LA, Weyand C*, et al.* (2010). Central and peripheral mechanisms of T-lymphocyte activation and vascular inflammation produced by angiotensin II-induced hypertension. *Circulation Research* **107**(2)**:** 263-270.

Massiera F, Bloch-Faure M, Ceiler D, Murakami K, Fukamizu A, Gasc JM*, et al.* (2001). Adipose angiotensinogen is involved in adipose tissue growth and blood pressure regulation. *FASEB J* **15**(14)**:** 2727-2729.

Masuda H (2008). Significance of nitric oxide and its modulation mechanisms by endogenous nitric oxide synthase inhibitors and arginase in the micturition disorders and erectile dysfunction. *International Journal of Urology* **15**(2)**:** 128-134.

Matrougui K, Abd Elmageed Z, Kassan M, Choi S, Nair D, Gonzalez-Villalobos RA*, et al.* (2011). Natural regulatory T cells control coronary arteriolar endothelial dysfunction in hypertensive mice. *The American Journal of Pathology* **178**(1)**:** 434-441.

Matthiesen S, Lindemann D, Warnken M, Juergens UR, Racké K (2008). Inhibition of NADPH oxidase by apocynin inhibits lipopolysaccharide (LPS) induced up-regulation of arginase in rat alveolar macrophages. *European Journal of Pharmacology* **579**(1-3)**:** 403-410.

Mazzolai L, Duchosal MA, Korber M, Bouzourene K, Aubert JF, Hao H*, et al.* (2004). Endogenous angiotensin II induces atherosclerotic plaque vulnerability and elicits a Th1 response in ApoE-/- mice. *Hypertension* **44**(3)**:** 277-282.

McGuire JJ, Ding H, Triggle CR (2001). Endothelium-derived relaxing factors: a focus on endothelium-derived hyperpolarizing factor(s). *Canadian Journal of Physiology and Pharmacology* **79**(6)**:** 443-470.

McMahon KA, Zajicek H, Li WP, Peyton MJ, Minna JD, Hernandez VJ*, et al.* (2009). SRBC/cavin-3 is a caveolin adapter protein that regulates caveolae function. *The EMBO Journal* **28**(8)**:** 1001-1015.

Medina FA, Cohen AW, de Almeida CJ, Nagajyothi F, Braunstein VL, Teixeira MM*, et al.* (2007). Immune dysfunction in caveolin-1 null mice following infection with Trypanosoma cruzi (Tulahuen strain). *Microbes and Infection* **9**(3)**:** 325-333.

Medls S, Puska P, Norrving B (2011). *Global atlas on cardiovascular disease prevention and control*. Geneva: World Health Organization

Medzhitov R (2001). Toll-like receptors and innate immunity. *Nature Reviews Immunology* **1**(2)**:** 135-145.

Meier P, Franzen O, Lansky AJ (2013a). Almanac 2013: Novel non-coronary cardiac interventions. *Heart* **99**(18)**:** 1309-1316.

Meier P, Fröhlich GM, Lansky AJ (2013b). Bleeding complications in percutaneous coronary interventions. *Cardiology* **125**(4)**:** 213-216.

Meier P, Lansky AJ, Baumbach A (2013c). Almanac 2013: acute coronary syndromes. *Heart* **99**(20)**:** 1488-1493.

Meisel SR, Kutz I, Dayan KI, Pauzner H, Chetboun I, Arbel Y*, et al.* (1991). Effect of Iraqi missile war on incidence of acute myocardial infarction and sudden death in Israeli civilians. *Lancet* **338**(8768)**:** 660-661.

Merimee TJ, Rabinowitz D, Riggs L, Burgess JA, Rimoin DL, McKusick VA (1967). Plasma growth hormone after arginine infusion. Clinical experiences. *New England Journal of Medicine* **276**(8)**:** 434-439.

Michel JB, Feron O, Sacks D, Michel T (1997). Reciprocal regulation of endothelial nitric-oxide synthase by Ca2+-calmodulin and caveolin. *J Biol Chem* **272**(25)**:** 15583-15586.

Michell DL, Andrews KL, Chin-Dusting JP (2011a). Endothelial dysfunction in hypertension: the role of arginase. *Frontiers in Bioscience* **3:** 946-960.

Michell DL, Andrews KL, Woollard KJ, Chin-Dusting JP (2011b). Imaging leukocyte adhesion to the vascular endothelium at high intraluminal pressure. *Journal of Visualized Experiments : JoVE*(54).

Millan J, Hewlett L, Glyn M, Toomre D, Clark P, Ridley AJ (2006). Lymphocyte transcellular migration occurs through recruitment of endothelial ICAM-1 to caveola- and F-actin-rich domains. *Nature Cell Biology* **8**(2)**:** 113-123.

Milovanova T, Chatterjee S, Hawkins BJ, Hong N, Sorokina EM, Debolt K*, et al.* (2008). Caveolae are an essential component of the pathway for endothelial cell signaling associated with abrupt reduction of shear stress. *Biochimica et Biophysica Acta* **1783**(10)**:** 1866-1875.

Ming XF, Barandier C, Viswambharan H, Kwak BR, Mach F, Mazzolai L*, et al.* (2004). Thrombin stimulates human endothelial arginase enzymatic activity via RhoA/ROCK pathway: implications for atherosclerotic endothelial dysfunction. *Circulation* **110**(24)**:** 3708-3714.

Minuz P, Patrignani P, Gaino S, Degan M, Menapace L, Tommasoli R*, et al.* (2002). Increased oxidative stress and platelet activation in patients with hypertension and renovascular disease. *Circulation* **106**(22)**:** 2800-2805.

Miranville A (2004). Improvement of postnatal neovascularization by human adipose tissue-derived stem cells. *Circulation* **110**(3)**:** 349-355.

Miyawaki-Shimizu K, Predescu D, Shimizu J, Broman M, Predescu S, Malik AB (2006). siRNA-induced caveolin-1 knockdown in mice increases lung vascular permeability via the junctional pathway. *Am J Physiol Lung Cell Mol Physiol* **290**(2)**:** L405-413.

Mohan S, Koyoma K, Thangasamy A, Nakano H, Glickman RD, Mohan N (2007). Low shear stress preferentially enhances IKK activity through selective sources of ROS for persistent activation of NF-kappaB in endothelial cells. *Am J Physiol Cell Physiol* **292**(1)**:** C362-371.

Monier S, Parton RG, Vogel F, Behlke J, Henske A, Kurzchalia TV (1995). VIP21-caveolin, a membrane protein constituent of the caveolar coat, oligomerizes in vivo and in vitro. *Mol Biol Cell* **6**(7)**:** 911-927.

Morton J, Coles B, Wright K, Gallimore A, Morrow JD, Terry ES*, et al.* (2008). Circulating neutrophils maintain physiological blood pressure by suppressing bacteria and IFNgamma-dependent iNOS expression in the vasculature of healthy mice. *Blood* **111**(10)**:** 5187-5194.

Moss MB, Brunini TM, Soares De Moura R, Novaes Malagris LE, Roberts NB, Ellory JC*, et al.* (2004). Diminished L-arginine bioavailability in hypertension. *Clin Sci (Lond)* **107**(4)**:** 391-397.

Mowbray AL, Kang DH, Rhee SG, Kang SW, Jo H (2008). Laminar shear stress up-regulates peroxiredoxins (PRX) in endothelial cells: PRX 1 as a mechanosensitive antioxidant. *J Biol Chem* **283**(3)**:** 1622-1627.

Mullan BA, Young IS, Fee H, McCance DR (2002). Ascorbic acid reduces blood pressure and arterial stiffness in type 2 diabetes. *Hypertension* **40**(6)**:** 804-809.

Mungrue IN (2004). nNOS at a glance: implications for brain and brawn. *Journal of Cell Science* **117**(13)**:** 2627-2629.

Munzel T, Daiber A, Ullrich V, Mulsch A (2005). Vascular consequences of endothelial nitric oxide synthase uncoupling for the activity and expression of the soluble guanylyl cyclase and the cGMP-dependent protein kinase. *Arterioscler Thromb Vasc Biol* **25**(8)**:** 1551-1557.

Myung S-K, Ju W, Cho B, Oh S-W, Park SM, Koo B-K*, et al.* (2013). Efficacy of vitamin and antioxidant supplements in prevention of cardiovascular disease: systematic review and meta-analysis of randomised controlled trials. *BMJ* **346**: f10.

Nabha L, Garbern JC, Buller CL, Charpie JR (2005). Vascular oxidative stress precedes high blood pressure in spontaneously hypertensive rats. *Clin Exp Hypertens* **27**(1)**:** 71-82.

Naghavi M, Libby P, Falk E, Casscells SW, Litovsky S, Rumberger J*, et al.* (2003). From vulnerable plaque to vulnerable patient: a call for new definitions and risk assessment strategies: Part I. *Circulation* **108**(14)**:** 1664-1672.

Nam D, Ni C-W, Rezvan A, Suo J, Budzyn K, Llanos A*, et al.* (2009). Partial carotid ligation is a model of acutely induced disturbed flow, leading to rapid endothelial dysfunction and atherosclerosis. *AJP: Heart and Circulatory Physiology* **297**(4)**:** H1535-1543.

Napoli C, Armiento FP, Mancini FP, Postiglione A, Witztum JL, Palumbo G*, et al.* (1997). Fatty streak formation occurs in human fetal aortas and is greatly enhanced by maternal hypercholesterolemia. Intimal accumulation of low density lipoprotein and its oxidation precede monocyte recruitment into early atherosclerotic lesions. *Journal of Clinical Investigation* **100**(11)**:** 2680-2690.

Napoli C, Glass CK, Witztum JL, Deutsch R, D'Armiento FP, Palinski W (1999). Influence of maternal hypercholesterolaemia during pregnancy on progression of early atherosclerotic lesions in childhood: Fate of Early Lesions in Children (FELIC) study. *The Lancet* **354**(9186)**:** 1234-1241.

Neal B, MacMahon S, Chapman N, Blood Pressure Lowering Treatment Trialists C (2000). Effects of ACE inhibitors, calcium antagonists, and other blood-pressure-lowering drugs: results of prospectively designed overviews of randomised trials. Blood Pressure Lowering Treatment Trialists' Collaboration. *Lancet* **356**(9246)**:** 1955-1964.

Nematbakhsh M, Haghjooyjavanmard S, Mahmoodi F, Monajemi A (2008). The prevention of endothelial dysfunction through endothelial cell apoptosis inhibition in a hypercholesterolemic rabbit model: the effect of L-arginine supplementation. *Lipids in Health and Disease* **7**(1)**:** 27.

Nieminen M, Henttinen T, Merinen M, Marttila-Ichihara F, Eriksson JE, Jalkanen S (2006). Vimentin function in lymphocyte adhesion and transcellular migration. *Nature cell biology* **8**(2)**:** 156-162.

Nikitenko LL (2008). Vascular endothelium in cancer. *Cell and Tissue Research* **335**(1)**:** 223-240.

Noursadeghi M, Tsang J, Haustein T, Miller RF, Chain BM, Katz DR (2008). Quantitative imaging assay for NF-kappaB nuclear translocation in primary human macrophages. *J Immunol Methods* **39**(1-2): 194-200.

Nunes FC, Braga VA (2011). Chronic angiotensin II infusion modulates angiotensin II type I receptor expression in the subfornical organ and the rostral ventrolateral medulla in hypertensive rats. *J Renin Angiotensin Aldosterone Syst* **12**(4)**:** 440-445.

Ogata N, Yamamoto H, Kugiyama K, Yasue H, Miyamoto E (2000). Involvement of protein kinase C in superoxide anion-induced activation of nuclear factor-kappa B in human endothelial cells. *Cardiovasc Res* **45**(2)**:** 513-521.

Ostrowski SR, Pedersen SH, Jensen JS, Mogelvang R, Johansson PI (2013). Acute myocardial infarction is associated with endothelial glycocalyx and cell damage and a parallel increase in circulating catecholamines. *Crit Care* **17**(1)**:** R32.

Ou ZJ, Wei W, Huang DD, Luo W, Luo D, Wang ZP*, et al.* (2010). L-Arginine restores endothelial nitric oxide synthase-coupled activity and attenuates monocrotaline-induced pulmonary artery hypertension in rats. *AJP: Endocrinology and Metabolism* **298**(6)**:** E1131-E1139.

Ozaki M, Kawashima S, Hirase T, Yamashita T, Namiki M, Inoue N*, et al.* (2002). Overexpression of endothelial nitric oxide synthase in endothelial cells is protective against ischemia-reperfusion injury in mouse skeletal muscle. *Am J Pathol* **160**(4)**:** 1335-1344.

Palade GE (1953). An electron microscope study of the mitochondrial structure. *J Histochem Cytochem* **1**(4)**:** 188-211.

Palma-Rigo K, Jackson KL, Davern PJ, Nguyen-Huu TP, Elghozi JL, Head GA (2011). Renin-angiotensin and sympathetic nervous system contribution to high blood pressure in Schlager mice. *J Hypertens* **29**(11)**:** 2156-2166.

Pan S (2009). Molecular mechanisms responsible for the atheroprotective effects of laminar shear stress. *Antioxid Redox Signal* **11**(7)**:** 1669-1682.

Paravicini TM, Touyz RM (2008a). NADPH Oxidases, Reactive Oxygen Species, and Hypertension: Clinical implications and therapeutic possibilities. *Diabetes Care* **31**(Supplement_2)**:** S170-S180.

Paravicini TM, Touyz RM (2008b). NADPH oxidases, reactive oxygen species, and hypertension: clinical implications and therapeutic possibilities. *Diabetes Care* **31 Suppl 2:** S170-180.

Park H, Go YM, St John PL, Maland MC, Lisanti MP, Abrahamson DR*, et al.* (1998). Plasma membrane cholesterol is a key molecule in shear stress-dependent activation of extracellular signal-regulated kinase. *J Biol Chem* **273**(48)**:** 32304-32311.

Park JB, Touyz RM, Chen X, Schiffrin EL (2002). Chronic treatment with a superoxide dismutase mimetic prevents vascular remodeling and progression of hypertension in salt-loaded stroke-prone spontaneously hypertensive rats. *Am J Hypertens* **15**(1 Pt 1)**:** 78-84.

Parton RG, del Pozo MA (2013). Caveolae as plasma membrane sensors, protectors and organizers. *Nature Reviews Molecular Cell Biology* **14**(2)**:** 98-112.

Patel HH, Insel PA (2009). Lipid rafts and caveolae and their role in compartmentation of redox signaling. *Antioxid Redox Signal* **11**(6)**:** 1357-1372.

Perticone F, Sciacqua A, Maio R, Perticone M, Maas R, Boger RH*, et al.* (2005). Asymmetric Dimethylarginine, L-Arginine, and Endothelial Dysfunction in Essential Hypertension. *Journal of the American College of Cardiology* **46**(3)**:** 518-523.

Phillips JW, Barringhaus KG, Sanders JM, Hesselbacher SE, Czarnik AC, Manka D*, et al.* (2003). Single injection of P-selectin or P-selectin glycoprotein ligand-1 monoclonal antibody blocks neointima formation after arterial injury in apolipoprotein E-deficient mice. *Circulation* **107**(17)**:** 2244-2249.

Phillips MI, Kagiyama S (2002). Angiotensin II as a pro-inflammatory mediator. *Curr Opin Investig Drugs* **3**(4)**:** 569-577.

Phillips MI, Schmidt-Ott KM (1999). The Discovery of Renin 100 Years Ago. *News Physiol Sci* **14:** 271-274.

Pinaud F, Bocquet A, Dumont O, Retailleau K, Baufreton C, Andriantsitohaina R*, et al.* (2007). Paradoxical role of angiotensin II type 2 receptors in resistance arteries of old rats. *Hypertension* **50**(1)**:** 96-102.

Podjarny E (2004). Effect of chronic tetrahydrobiopterin supplementation on blood pressure and proteinuria in 5/6 nephrectomized rats. *Nephrology Dialysis Transplantation* **19**(9)**:** 2223-2227.

Pojoga LH, Romero JR, Yao TM, Loutraris P, Ricchiuti V, Coutinho P*, et al.* (2010). Caveolin-1 ablation reduces the adverse cardiovascular effects of N-omega-nitro-L-arginine methyl ester and angiotensin II. *Endocrinology* **151**(3)**:** 1236-1246.

Pol A, Martin S, Fernandez MA, Ingelmo-Torres M, Ferguson C, Enrich C*, et al.* (2005). Cholesterol and fatty acids regulate dynamic caveolin trafficking through the Golgi complex and between the cell surface and lipid bodies. *Mol Biol Cell* **16**(4)**:** 2091-2105.

Prado CM, Ramos SG, Alves-Filho JC, Elias J, Jr., Cunha FQ, Rossi MA (2006). Turbulent flow/low wall shear stress and stretch differentially affect aorta remodeling in rats. *J Hypertens* **24**(3)**:** 503-515.

Preston RA, Jy W, Jimenez JJ, Mauro LM, Horstman LL, Valle M*, et al.* (2003). Effects of severe hypertension on endothelial and platelet microparticles. *Hypertension* **41**(2)**:** 211-217.

Pries AR, Secomb TW, Gaehtgens P (2000). The endothelial surface layer. *Pflgers Archiv European Journal of Physiology* **440**(5)**:** 653-666.

Pueyo ME, Gonzalez W, Nicoletti A, Savoie F, Arnal JF, Michel JB (2000). Angiotensin II stimulates endothelial vascular cell adhesion molecule-1 via nuclear factor-kappaB activation induced by intracellular oxidative stress. *Arterioscler Thromb Vasc Biol* **20**(3)**:** 645-651.

Rahman A, Sward K (2009). The role of caveolin-1 in cardiovascular regulation. *Acta Physiol (Oxf)* **195**(2)**:** 231-245.

Rahmouni K, Haynes WG, Mark AL (2002). Cardiovascular and sympathetic effects of leptin. *Curr Hypertens Rep* **4**(2)**:** 119-125.

Rajagopalan S, Kurz S, Munzel T, Tarpey M, Freeman BA, Griendling KK*, et al.* (1996). Angiotensin II-mediated hypertension in the rat increases vascular superoxide production via membrane NADH/NADPH oxidase activation. Contribution to alterations of vasomotor tone. *J Clin Invest* **97**(8)**:** 1916-1923.

Ramkhelawon B, Vilar J, Rivas D, Mees B, de Crom R, Tedgui A*, et al.* (2009). Shear stress regulates angiotensin type 1 receptor expression in endothelial cells. *Circ Res* **105**(9)**:** 869-875.

Ramos CD, Canetti C, Souto JT, Silva JS, Hogaboam CM, Ferreira SH*, et al.* (2005). MIP-1alpha[CCL3] acting on the CCR1 receptor mediates neutrophil migration in immune inflammation via sequential release of TNF-alpha and LTB4. *J Leukoc Biol* **78**(1)**:** 167-177.

Ramos CL, Huo Y, Jung U, Ghosh S, Manka DR, Sarembock IJ*, et al.* (1999). Direct demonstration of P-selectin- and VCAM-1-dependent mononuclear cell rolling in early atherosclerotic lesions of apolipoprotein E-deficient mice. *Circ Res* **84**(11)**:** 1237-1244.

Ray R, Shah AM (2005). NADPH oxidase and endothelial cell function. *Clin Sci (Lond)* **109**(3)**:** 217-226.

Razani B, Engelman JA, Wang XB, Schubert W, Zhang XL, Marks CB*, et al.* (2001). Caveolin-1 null mice are viable but show evidence of hyperproliferative and vascular abnormalities. *J Biol Chem* **276**(41)**:** 38121-38138.

Razani B, Wang XB, Engelman JA, Battista M, Lagaud G, Zhang XL*, et al.* (2002). Caveolin-2-deficient mice show evidence of severe pulmonary dysfunction without disruption of caveolae. *Mol Cell Biol* **22**(7)**:** 2329-2344.

Reeves EP, Nagl M, Godovac-Zimmermann J, Segal AW (2003). Reassessment of the microbicidal activity of reactive oxygen species and hypochlorous acid with reference

to the phagocytic vacuole of the neutrophil granulocyte. *Journal of medical microbiology* **52**(Pt 8)**:** 643-651.

Riou S, Mees B, Esposito B, Merval R, Vilar J, Stengel D*, et al.* (2007). High Pressure Promotes Monocyte Adhesion to the Vascular Wall. *Circulation Research* **100**(8)**:** 1226-1233.

Rizzo V, McIntosh DP, Oh P, Schnitzer JE (1998). In situ flow activates endothelial nitric oxide synthase in luminal caveolae of endothelium with rapid caveolin dissociation and calmodulin association. *J Biol Chem* **273**(52)**:** 34724-34729.

Rizzo V, Morton C, DePaola N, Schnitzer JE, Davies PF (2003). Recruitment of endothelial caveolae into mechanotransduction pathways by flow conditioning in vitro. *American journal of physiology. Heart and circulatory physiology* **285**(4)**:** H1720-1729.

Rizzoni D, Agabiti-Rosei E (2012). Structural abnormalities of small resistance arteries in essential hypertension. *Internal and emergency medicine* **7**(3)**:** 205-212.

Robbins CS, Hilgendorf I, Weber GF, Theurl I, Iwamoto Y, Figueiredo J-L*, et al.* (2013). Local proliferation dominates lesional macrophage accumulation in atherosclerosis. *Nature medicine*.

Romero MJ, Platt DH, Tawfik HE, Labazi M, El-Remessy AB, Bartoli M*, et al.* (2008a). Diabetes-induced Coronary Vascular Dysfunction Involves Increased Arginase Activity. *Circulation Research* **102**(1)**:** 95-102.

Romero MJ, Platt DH, Tawfik HE, Labazi M, El-Remessy AB, Bartoli M*, et al.* (2008b). Diabetes-induced coronary vascular dysfunction involves increased arginase activity. *Circ Res* **102**(1)**:** 95-102.

Rompe F, Artuc M, Hallberg A, Alterman M, Stroder K, Thone-Reineke C*, et al.* (2010). Direct angiotensin II type 2 receptor stimulation acts anti-inflammatory through epoxyeicosatrienoic acid and inhibition of nuclear factor kappaB. *Hypertension* **55**(4)**:** 924-931.

Rondaij MG, Bierings R, Kragt A, van Mourik JA, Voorberg J (2006). Dynamics and plasticity of Weibel-Palade bodies in endothelial cells. *Arteriosclerosis, Thrombosis, and Vascular Biology* **26**(5)**:** 1002-1007.

Rossi R, Chiurlia E, Nuzzo A, Cioni E, Origliani G, Modena MG (2004). Flow-mediated vasodilation and the risk of developing hypertension in healthy postmenopausal women. *Journal of the American College of Cardiology* **44**(8)**:** 1636-1640.

Rouvier E, Luciani MF, Golstein P (1993). Fas involvement in Ca(2+)-independent T cell-mediated cytotoxicity. *The Journal of experimental medicine* **177**(1)**:** 195-200.

Rus H, Cudrici C, Niculescu F (2005). The Role of the Complement System in Innate Immunity. *Immunologic Research* **33**(2)**:** 103-112.

Ryoo S, Gupta G, Benjo A, Lim HK, Camara A, Sikka G*, et al.* (2008). Endothelial Arginase II: A Novel Target for the Treatment of Atherosclerosis. *Circulation Research* **102**(8)**:** 923-932.

Ryoo S, Lemmon CA, Soucy KG, Gupta G, White AR, Nyhan D*, et al.* (2006). Oxidized low-density lipoprotein-dependent endothelial arginase II activation contributes to impaired nitric oxide signaling. *Circ Res* **99**(9)**:** 951-960.

Sanchez FA (2006). Functional significance of differential eNOS translocation. *AJP: Heart and Circulatory Physiology* **291**(3)**:** H1058-H1064.

Sanz-Rosa D, Oubina MP, Cediel E, de Las Heras N, Vegazo O, Jimenez J*, et al.* (2005). Effect of AT1 receptor antagonism on vascular and circulating inflammatory mediators in SHR: role of NF-kappaB/IkappaB system. *Am J Physiol Heart Circ Physiol* **288**(1)**:** H111-115.

Sauer H, Wartenberg M, Hescheler J (2001). Reactive oxygen species as intracellular messengers during cell growth and differentiation. *Cell Physiol Biochem* **11**(4)**:** 173-186.

Savoia C, Schiffrin EL (2006). Inflammation in hypertension. *Curr Opin Nephrol Hypertens* **15**(2)**:** 152-158.

Schiffrin EL (2004). Remodeling of resistance arteries in essential hypertension and effects of antihypertensive treatment. *Am J Hypertens* **17**(12 Pt 1)**:** 1192-1200.

Schillaci G, Pirro M, Gemelli F, Pasqualini L, Vaudo G, Marchesi S*, et al.* (2003). Increased C-reactive protein concentrations in never-treated hypertension: the role of systolic and pulse pressures. *J Hypertens* **21**(10)**:** 1841-1846.

Schindelin J, Arganda-Carreras I, Frise E, Kaynig V, Longair M, Pietzsch T*, et al.* (2012). Fiji: an open-source platform for biological-image analysis. *Nat Methods* **9**(7)**:** 676-682.

Schlager G, Sides J (1997). Characterization of hypertensive and hypotensive inbred strains of mice. *Lab Anim Sci* **47**(3)**:** 288-292.

Schlaich MP (2004). Impaired L-Arginine Transport and Endothelial Function in Hypertensive and Genetically Predisposed Normotensive Subjects. *Circulation* **110**(24)**:** 3680-3686.

Schlaich MP, Kaye DM, Lambert E, Sommerville M, Socratous F, Esler MD (2003). Relation between cardiac sympathetic activity and hypertensive left ventricular hypertrophy. *Circulation* **108**(5)**:** 560-565.

Schlaich MP, Sobotka PA, Krum H, Lambert E, Esler MD (2009). Renal sympathetic-nerve ablation for uncontrolled hypertension. *N Engl J Med* **361**(9)**:** 932-934.

Schlormann W, Steiniger F, Richter W, Kaufmann R, Hause G, Lemke C*, et al.* (2010). The shape of caveolae is omega-like after glutaraldehyde fixation and cup-like after cryofixation. *Histochem Cell Biol* **133**(2)**:** 223-228.

Schmeisser A, Soehnlein O, Illmer T, Lorenz HM, Eskafi S, Roerick O*, et al.* (2004). ACE inhibition lowers angiotensin II-induced chemokine expression by reduction of NF-kappaB activity and AT1 receptor expression. *Biochem Biophys Res Commun* **325**(2)**:** 532-540.

Schmieder RE, Hilgers KF, Schlaich MP, Schmidt BM (2007). Renin-angiotensin system and cardiovascular risk. *Lancet* **369**(9568)**:** 1208-1219.

Selemidis S, Sobey CG, Wingler K, Schmidt HHHW, Drummond GR (2008). NADPH oxidases in the vasculature: Molecular features, roles in disease and pharmacological inhibition. *Pharmacology and Therapeutics* **120**(3)**:** 254-291.

Sens P, Turner MS (2006). Budded membrane microdomains as tension regulators. *Physical review. E, Statistical, nonlinear, and soft matter physics* **73**(3 Pt 1)**:** 031918.

Seravalle G, Cattaneo BM, Giannattasio C, Perondi R, Saino A, Grassi G*, et al.* (1993). RAA system and cardiovascular control in normal subjects, hypertensives and patients with congestive heart failure. *J Hum Hypertens* **7 Suppl 2:** S13-18.

Sharma AM (2004). Is there a rationale for angiotensin blockade in the management of obesity hypertension? *Hypertension* **44**(1)**:** 12-19.

Shaul PW (2002). R EGULATION OFE NDOTHELIALN ITRICO XIDES YNTHASE: Location, Location, Location. *Annual Review of Physiology* **64**(1)**:** 749-774.

Shaul PW, Smart EJ, Robinson LJ, German Z, Yuhanna IS, Ying Y*, et al.* (1996a). Acylation targets emdothelial nitric-oxide synthase to plasmalemmal caveolae. *J Biol Chem* **271**(11)**:** 6518-6522.

Shaul PW, Smart EJ, Robinson LJ, German Z, Yuhanna IS, Ying Y*, et al.* (1996b). Acylation targets emdothelial nitric-oxide synthase to plasmalemmal caveolae. *The Journal of biological chemistry* **271**(11)**:** 6518-6522.

Shesely EG, Maeda N, Kim HS, Desai KM, Krege JH, Laubach VE*, et al.* (1996). Elevated blood pressures in mice lacking endothelial nitric oxide synthase. *Proceedings of the National Academy of Sciences of the United States of America* **93**(23)**:** 13176-13181.

Shi P, Diez-Freire C, Jun JY, Qi Y, Katovich MJ, Li Q*, et al.* (2010). Brain microglial cytokines in neurogenic hypertension. *Hypertension* **56**(2)**:** 297-303.

Shimbo D, Muntner P, Mann D, Viera AJ, Homma S, Polak JF*, et al.* (2010). Endothelial Dysfunction and the Risk of Hypertension: The Multi-Ethnic Study of Atherosclerosis. *Hypertension* **55**(5)**:** 1210-1216.

Shimizu M, Wang QD, Sjöquist PO, Rydén L (1999). The angiotensin II AT1-receptor antagonist candesartan improves functional recovery and reduces the no-reflow area in reperfused ischemic rat hearts. *J Cardiovasc Pharmacol* **34**(1): 78-81.

Silva MT (2010). When two is better than one: macrophages and neutrophils work in concert in innate immunity as complementary and cooperative partners of a myeloid phagocyte system. *Journal of leukocyte biology* **87**(1)**:** 93-106.

Sinha B, Koster D, Ruez R, Gonnord P, Bastiani M, Abankwa D*, et al.* (2011). Cells respond to mechanical stress by rapid disassembly of caveolae. *Cell* **144**(3)**:** 402-413.

Skålén K, Gustafsson M, Rydberg EK, Hultén LM, Wiklund O, Innerarity TL*, et al.* (2002). Subendothelial retention of atherogenic lipoproteins in early atherosclerosis. *Nature* **417**(6890)**:** 750-754.

Smart EJ, Ying YS, Conrad PA, Anderson RG (1994). Caveolin moves from caveolae to the Golgi apparatus in response to cholesterol oxidation. *J Cell Biol* **127**(5)**:** 1185-1197.

Soda R, Tavassoli M (1984). Transendothelial transport (transcytosis) of iron-transferrin complex in the bone marrow. *J Ultrastruct Res* **88**(1)**:** 18-29.

Solomon SD, Zile M, Pieske B, Voors A, Shah A, Kraigher-Krainer E*, et al.* (2012). The angiotensin receptor neprilysin inhibitor LCZ696 in heart failure with preserved ejection fraction: a phase 2 double-blind randomised controlled trial. *Lancet* **380**(9851)**:** 1387-1395.

SoRelle R (1998). Nobel prize awarded to scientists for nitric oxide discoveries. *Circ* **98**: 2365-2366.

Souza HP, Liu X, Samouilov A, Kuppusamy P, Laurindo FR, Zweier JL (2002). Quantitation of superoxide generation and substrate utilization by vascular NAD(P)H oxidase. *Am J Physiol Heart Circ Physiol* **282**(2): H466-474.

Sowa G (2012). Caveolae, caveolins, cavins, and endothelial cell function: new insights. *Front Physiol* **2:** 120.

Stahlhut M, van Deurs B (2000). Identification of filamin as a novel ligand for caveolin-1: evidence for the organization of caveolin-1-associated membrane domains by the actin cytoskeleton. *Mol Biol Cell* **11**(1): 325-337.

Steinman DA, Poepping TL, Tambasco M, Rankin RN, Holdsworth DW (2000). Flow patterns at the stenosed carotid bifurcation: effect of concentric versus eccentric stenosis. *Annals of biomedical engineering* **28**(4)**:** 415-423.

Stossel TP (1974). Phagocytosis (first of three parts). *N Engl J Med* **290**(13)**:** 717-723.

Suhalim JL, Chung C-Y, Lilledahl MB, Lim RS, Levi M, Tromberg BJ, *et al.* (2012). Characterization of cholesterol crystals in atherosclerotic plaques using stimulated Raman scattering and second-harmonic generation microscopy. *Biophysical journal* **102**(8)**:** 1988-1995.

Sumagin R, Prizant H, Lomakina E, Waugh RE, Sarelius IH (2010). LFA-1 and Mac-1 define characteristically different intralumenal crawling and emigration patterns for monocytes and neutrophils in situ. *J Immunol* **185**(11)**:** 7057-7066.

Suzuki S, Sakamoto S, Miki T, Matsuo T (1995). Hanshin-Awaji earthquake and acute myocardial infarction. *Lancet* **345**(8955)**:** 981.

Sverdlov M, Shinin V, Place AT, Castellon M, Minshall RD (2009). Filamin A regulates caveolae internalization and trafficking in endothelial cells. *Mol Biol Cell* **20**(21)**:** 4531-4540.

Tadzic R, Mihalj M, Vcev A, Ennen J, Tadzic A, Drenjancevic I (2013). The effects of arterial blood pressure reduction on endocan and soluble endothelial cell adhesion molecules (CAMs) and CAMs ligands expression in hypertensive patients on Ca-channel blocker therapy. *Kidney Blood Press Res* **37**(2-3)**:** 103-115.

Tagawa A, Mezzacasa A, Hayer A, Longatti A, Pelkmans L, Helenius A (2005). Assembly and trafficking of caveolar domains in the cell: caveolae as stable, cargo-triggered, vesicular transporters. *J Cell Biol* **170**(5)**:** 769-779.

Tagawa M, Ueyama T, Ogata T, Takehara N, Nakajima N, Isodono K, *et al.* (2008). MURC, a muscle-restricted coiled-coil protein, is involved in the regulation of skeletal myogenesis. *Am J Physiol Cell Physiol* **295**(2)**:** C490-498.

Tak PP, Firestein GS (2001). NF-kappaB: a key role in inflammatory diseases. *J Clin Invest* **107**(1)**:** 7-11.

Takimoto E, Champion HC, Li M, Ren S, Rodriguez ER, Tavazzi B, *et al.* (2005). Oxidant stress from nitric oxide synthase-3 uncoupling stimulates cardiac pathologic remodeling from chronic pressure load. *J Clin Invest* **115**(5)**:** 1221-1231.

Tang BT, Pickard SS, Chan FP, Tsao PS, Taylor CA, Feinstein JA (2012). Wall shear stress is decreased in the pulmonary arteries of patients with pulmonary arterial hypertension: An image-based, computational fluid dynamics study. *Pulm Circ* **2**(4)**:** 470-476.

Tangphao O, Chalon S, Moreno H, Jr., Hoffman BB, Blaschke TF (1999). Pharmacokinetics of L-arginine during chronic administration to patients with hypercholesterolaemia. *Clin Sci (Lond)* **96**(2)**:** 199-207.

Tardif JC, Tanguay JF, Wright SS, Duchatelle V, Petroni T, Gregoire JC, *et al.* (2013). Effects of the P-selectin antagonist inclacumab on myocardial damage after percutaneous

coronary intervention for non-ST-segment elevation myocardial infarction: results of the SELECT-ACS trial. *J Am Coll Cardiol* **61**(20)**:** 2048-2055.

Thannickal VJ, Fanburg BL (2000). Reactive oxygen species in cell signaling. *Am J Physiol Lung Cell Mol Physiol* **279**(6)**:** L1005-1028.

Thatcher SE, Zhang X, Howatt DA, Lu H, Gurley SB, Daugherty A*, et al.* (2011). Angiotensin-converting enzyme 2 deficiency in whole body or bone marrow-derived cells increases atherosclerosis in low-density lipoprotein receptor-/- mice. *Arterioscler Thromb Vasc Biol* **31**(4)**:** 758-765.

Thengchaisri N (2006). Upregulation of Arginase by H2O2 Impairs Endothelium-Dependent Nitric Oxide-Mediated Dilation of Coronary Arterioles. *Arteriosclerosis, Thrombosis, and Vascular Biology* **26**(9)**:** 2035-2042.

Thengchaisri N, Hein TW, Wang W, Xu X, Li Z, Fossum TW*, et al.* (2006). Upregulation of arginase by H2O2 impairs endothelium-dependent nitric oxide-mediated dilation of coronary arterioles. *Arterioscler Thromb Vasc Biol* **26**(9)**:** 2035-2042.

Thery C, Amigorena S (2001). The cell biology of antigen presentation in dendritic cells. *Curr Opin Immunol* **13**(1)**:** 45-51.

Thomas MC, Pickering RJ, Tsorotes D, Koitka A, Sheehy K, Bernardi S*, et al.* (2010). Genetic Ace2 deficiency accentuates vascular inflammation and atherosclerosis in the ApoE knockout mouse. *Circ Res* **107**(7)**:** 888-897.

Thomas SR, Witting PK, Drummond GR (2008). Redox Control of Endothelial Function and Dysfunction: Molecular Mechanisms and Therapeutic Opportunities. *Antioxidants & Redox Signaling* **10**(10)**:** 1713-1766.

Thorn H, Stenkula KG, Karlsson M, Ortegren U, Nystrom FH, Gustavsson J*, et al.* (2003). Cell surface orifices of caveolae and localization of caveolin to the necks of caveolae in adipocytes. *Mol Biol Cell* **14**(10)**:** 3967-3976.

Thuraisingham RC, Roberts NB, Wilkes M, New DI, Mendes-Ribeiro AC, Dodd SM*, et al.* (2002). Altered L-arginine metabolism results in increased nitric oxide release from uraemic endothelial cells. *Clin Sci (Lond)* **103**(1)**:** 31-41.

Thymiakou E, Episkopou V (2011). Detection of signaling effector-complexes downstream of bmp4 using PLA, a proximity ligation assay. *J Vis Exp*(49).

Tinken TM, Thijssen DH, Hopkins N, Dawson EA, Cable NT, Green DJ (2010). Shear stress mediates endothelial adaptations to exercise training in humans. *Hypertension* **55**(2)**:** 312-318.

Tofts PS, Chevassut T, Cutajar M, Dowell NG, Peters AM (2011). Doubts concerning the recently reported human neutrophil lifespan of 5.4 days. *Blood* **117**(22)**:** 6050-6052; author reply 6053-6054.

Torok J (2008). Participation of nitric oxide in different models of experimental hypertension. *Physiol Res* **57**(6)**:** 813-825.

Tousoulis D, Boger RH, Antoniades C, Siasos G, Stefanadi E, Stefanadis C (2007). Mechanisms of Disease: L-arginine in coronary atherosclerosis—a clinical perspective. *Nature Clinical Practice Cardiovascular Medicine* **4**(5)**:** 274-283.

Touyz RM (2004). Reactive oxygen species, vascular oxidative stress, and redox signaling in hypertension: what is the clinical significance? *Hypertension* **44**(3)**:** 248-252.

Touyz RM (2005). Intracellular mechanisms involved in vascular remodelling of resistance arteries in hypertension: role of angiotensin II. *Experimental physiology* **90**(4)**:** 449-455.

Touyz RM, Schiffrin EL (2004). Reactive oxygen species in vascular biology: implications in hypertension. *Histochem Cell Biol* **122**(4)**:** 339-352.

Tropea BI, Huie P, Cooke JP, Tsao PS, Sibley RK, Zarins CK (1996). Hypertension-enhanced monocyte adhesion in experimental atherosclerosis. *J Vasc Surg* **23**(4)**:** 596-605.

Tuttolomondo A, Di Raimondo D, Pecoraro R, Arnao V, Pinto A, Licata G (2012). Atherosclerosis as an inflammatory disease. *Curr Pharm Des* **18**(28)**:** 4266-4288.

Uddin M, Yang H, Shi M, Polley-Mandal M, Guo Z (2003). Elevation of oxidative stress in the aorta of genetically hypertensive mice. *Mech Ageing Dev* **124**(7)**:** 811-817.

Unger BS, Patil BM (2009). Apocynin improves endothelial function and prevents the development of hypertension in fructose fed rat. *Indian J Pharmacol* **41**(5)**:** 208-212.

Ungvari Z, Orosz Z, Labinskyy N, Rivera A, Xiangmin Z, Smith K*, et al.* (2007). Increased mitochondrial H2O2 production promotes endothelial NF-kappaB activation in aged rat arteries. *Am J Physiol Heart Circ Physiol* **293**(1)**:** H37-47.

Utsuyama M, Hirokawa K (2002). Differential expression of various cytokine receptors in the brain after stimulation with LPS in young and old mice. *Exp Gerontol* **37**(2-3)**:** 411-420.

Van den Hoogen PC, Seidell JC, Menotti A, Kromhout D (2000). Blood pressure and long-term coronary heart disease mortality in the Seven Countries study: implications for clinical practice and public health. *Eur Heart J* **21**(20)**:** 1639-1642.

Viel EC, Benkirane K, Javeshghani D, Touyz RM, Schiffrin EL (2008). Xanthine oxidase and mitochondria contribute to vascular superoxide anion generation in DOCA-salt hypertensive rats. *AJP: Heart and Circulatory Physiology* **295**(1)**:** H281-H288.

Virdis A, Neves MF, Amiri F, Touyz RM, Schiffrin EL (2004). Role of NAD(P)H oxidase on vascular alterations in angiotensin II-infused mice. *J Hypertens* **22**(3)**:** 535-542.

Vivekanathan DP, Penn MS, Sapp SK, Hsu A, Topol EJ (2003). Use of antioxidant vitamins for the prevention of cardiovascular disease: meta-analysis of randomised trials. *Lancet* **361**: 2017-23.

Volonte D, Galbiati F (2011). Polymerase I and transcript release factor (PTRF)/cavin-1 is a novel regulator of stress-induced premature senescence. *J Biol Chem* **286**(33)**:** 28657-28661.

von Kanel R, Dimsdale JE (2000). Effects of sympathetic activation by adrenergic infusions on hemostasis in vivo. *Eur J Haematol* **65**(6)**:** 357-369.

von Lueder TG, Krum H (2013). RAAS inhibitors and cardiovascular protection in large scale trials. *Cardiovasc Drugs Ther* **27**(2)**:** 171-179.

von Offenberg Sweeney N, Cummins PM, Birney YA, Cullen JP, Redmond EM, Cahill PA (2004). Cyclic strain-mediated regulation of endothelial matrix metalloproteinase-2 expression and activity. *Cardiovasc Res* **63**(4)**:** 625-634.

Waki H, Liu B, Miyake M, Katahira K, Murphy D, Kasparov S*, et al.* (2007). Junctional adhesion molecule-1 is upregulated in spontaneously hypertensive rats: evidence for a prohypertensive role within the brain stem. *Hypertension* **49**(6)**:** 1321-1327.

Wallin BG, Sundlof G, Stromgren E, Aberg H (1984). Sympathetic outflow to muscles during treatment of hypertension with metoprolol. *Hypertension* **6**(4)**:** 557-562.

Walpola PL, Gotlieb AI, Cybulsky MI, Langille BL (1995). Expression of ICAM-1 and VCAM-1 and monocyte adherence in arteries exposed to altered shear stress. *Arterioscler Thromb Vasc Biol* **15**(1)**:** 2-10.

Wang H, Nawata J, Kakudo N, Sugimura K, Suzuki J, Sakuma M*, et al.* (2004). The upregulation of ICAM-1 and P-selectin requires high blood pressure but not circulating renin???angiotensin system in vivo. *Journal of Hypertension* **22**(7)**:** 1323-1332.

Watanabe T, Fan J (1998). Atherosclerosis and inflammation mononuclear cell recruitment and adhesion molecules with reference to the implication of ICAM-1/LFA-1 pathway in atherogenesis. *Int J Cardiol* **66 Suppl 1:** S45-53; discussion S55.

Weiss D, Kools JJ, Taylor WR (2001). Angiotensin II-induced hypertension accelerates the development of atherosclerosis in apoE-deficient mice. *Circulation* **103**(3)**:** 448-454.

Weiss D, Taylor WR (2008). Deoxycorticosterone acetate salt hypertension in apolipoprotein E-/- mice results in accelerated atherosclerosis: the role of angiotensin II. *Hypertension* **51**(2)**:** 218-224.

Wenzel P, Knorr M, Kossmann S, Stratmann J, Hausding M, Schuhmacher S*, et al.* (2011). Lysozyme M-positive monocytes mediate angiotensin II-induced arterial hypertension and vascular dysfunction. *Circulation* **124**(12)**:** 1370-1381.

White FN, Grollman A (1964). Autoimmune Factors Associated with Infarction of the Kidney. *Nephron* **1:** 93-102.

Widdop RE, Jones ES, Hannan RE, Gaspari TA (2003). Angiotensin AT2 receptors: cardiovascular hope or hype? *Br J Pharmacol* **140**(5)**:** 809-824.

Wilbert-Lampen U, Leistner D, Greven S, Pohl T, Sper S, Volker C*, et al.* (2008). Cardiovascular events during World Cup soccer. *N Engl J Med* **358**(5)**:** 475-483.

Willmot M, Gray L, Gibson C, Murphy S, Bath PMW (2005). A systematic review of nitric oxide donors and l-arginine in experimental stroke; effects on infarct size and cerebral blood flow. *Nitric Oxide* **12**(3)**:** 141-149.

Woodman SE, Park DS, Cohen AW, Cheung MW, Chandra M, Shirani J*, et al.* (2002). Caveolin-3 knock-out mice develop a progressive cardiomyopathy and show hyperactivation of the p42/44 MAPK cascade. *J Biol Chem* **277**(41)**:** 38988-38997.

Woodward JJ, Chang MM, Martin NI, Marletta MA (2009). The Second Step of the Nitric Oxide Synthase Reaction: Evidence for Ferric-Peroxo as the Active Oxidant. *Journal of the American Chemical Society* **131**(1)**:** 297-305.

Woollard KJ, Suhartoyo A, Harris EE, Eisenhardt SU, Jackson SP, Peter K*, et al.* (2008). Pathophysiological levels of soluble P-selectin mediate adhesion of leukocytes to the endothelium through Mac-1 activation. *Circ Res* **103**(10)**:** 1128-1138.

Wu CC, Wang SH, Kuan, II, Tseng WK, Chen MF, Wu JC*, et al.* (2009). OxLDL upregulates caveolin-1 expression in macrophages: Role for caveolin-1 in the adhesion of oxLDL-treated macrophages to endothelium. *J Cell Biochem* **107**(3)**:** 460-472.

Wu JH, Hagaman J, Kim S, Reddick RL, Maeda N (2002). Aortic constriction exacerbates atherosclerosis and induces cardiac dysfunction in mice lacking apolipoprotein E. *Arterioscler Thromb Vasc Biol* **22**(3)**:** 469-475.

Xiong Y, Hu Z, Han X, Jiang B, Zhang R, Zhang X*, et al.* (2013). Hypertensive stretch regulates endothelial exocytosis of Weibel-Palade bodies through VEGF receptor 2 signaling pathways. *Cell Res* **23**(6)**:** 820-834.

Xu W, Kaneko FT, Zheng S, Comhair SA, Janocha AJ, Goggans T*, et al.* (2004). Increased arginase II and decreased NO synthesis in endothelial cells of patients with pulmonary arterial hypertension. *FASEB J* **18**(14)**:** 1746-1748.

Yamawaki H, Lehoux S, Berk BC (2003). Chronic physiological shear stress inhibits tumor necrosis factor-induced proinflammatory responses in rabbit aorta perfused ex vivo. *Circulation* **108**(13)**:** 1619-1625.

Yang B, Rizzo V (2007). TNF-alpha potentiates protein-tyrosine nitration through activation of NADPH oxidase and eNOS localized in membrane rafts and caveolae of bovine aortic endothelial cells. *Am J Physiol Heart Circ Physiol* **292**(2)**:** H954-962.

Yu J, Bergaya S, Murata T, Alp IF, Bauer MP, Lin MI*, et al.* (2006). Direct evidence for the role of caveolin-1 and caveolae in mechanotransduction and remodeling of blood vessels. *J Clin Invest* **116**(5)**:** 1284-1291.

Yuen CM, Sun CK, Lin YC, Chang LT, Kao YH, Yen CH, *et al*. (2011). Combination of cyclosporine and erythropoietin improves brain infarct size and neurological function in rats after ischemic stroke. *J Transl Med* **9**: 141.

Yun JK, Anderson JM, Ziats NP (1999). Cyclic-strain-induced endothelial cell expression of adhesion molecules and their roles in monocyte-endothelial interaction. *J Biomed Mater Res* **44**(1)**:** 87-97.

Zalba G, José GS, Moreno MU, Fortuño MA, Fortuño A, Beaumont FJ*, et al.* (2001). Oxidative Stress in Arterial Hypertension.

Zaman MA, Oparil S, Calhoun DA (2002). Drugs targeting the renin-angiotensin-aldosterone system. *Nat Rev Drug Discov* **1**(8)**:** 621-636.

Zeibig S, Li Z, Wagner S, Holthoff HP, Ungerer M, Bultmann A*, et al.* (2011). Effect of the oxLDL binding protein Fc-CD68 on plaque extension and vulnerability in atherosclerosis. *Circ Res* **108**(6)**:** 695-703.

Zhang C, Hein TW, Wang W, Miller MW, Fossum TW, McDonald MM*, et al.* (2004). Upregulation of vascular arginase in hypertension decreases nitric oxide-mediated dilation of coronary arterioles. *Hypertension* **44**(6)**:** 935-943.

Zhang J, Chu W, Crandall I (2008). Lipoprotein binding preference of CD36 is altered by filipin treatment. *Lipids Health Dis* **7:** 23.

Zhao YY, Liu Y, Stan RV, Fan L, Gu Y, Dalton N*, et al.* (2002). Defects in caveolin-1 cause dilated cardiomyopathy and pulmonary hypertension in knockout mice. *Proc Natl Acad Sci U S A* **99**(17)**:** 11375-11380.

Zhao YY, Zhao YD, Mirza MK, Huang JH, Potula HH, Vogel SM*, et al.* (2009). Persistent eNOS activation secondary to caveolin-1 deficiency induces pulmonary hypertension in mice and humans through PKG nitration. *J Clin Invest* **119**(7)**:** 2009-2018.

Zhou X, Bohlen HG, Miller SJ, Unthank JL (2008). NAD(P)H oxidase-derived peroxide mediates elevated basal and impaired flow-induced NO production in SHR mesenteric arteries in vivo. *Am J Physiol Heart Circ Physiol* **295**(3)**:** H1008-H1016.

Zou Y, Akazawa H, Qin Y, Sano M, Takano H, Minamino T*, et al.* (2004). Mechanical stress activates angiotensin II type 1 receptor without the involvement of angiotensin II. *Nat Cell Biol* **6**(6)**:** 499-506.

Zubcevic J, Waki H, Raizada MK, Paton JF (2011). Autonomic-immune-vascular interaction: an emerging concept for neurogenic hypertension. *Hypertension* **57**(6)**:** 1026-1033.

Chapter 9

Appendices

Appendix I: *'Endothelial dysfunction in hypertension: The role of arginase'*

Endothelial dysfunction in hypertension: The role of arginase

Danielle L Michell[1,2], Karen L Andrews[1], Jaye PF Chin-Dusting[1]

[1]Baker IDI Heart and Diabetes Institute, Melbourne, Victoria, Australia. [2]Department of Medicine Alfred Hospital, Monash University, Melbourne, Victoria, Australia

TABLE OF CONTENTS

1. ABSTRACT

Essential hypertension is the leading risk factor for mortality worldwide, accountable for 13% of deaths globally. Despite numerous therapies available uncontrolled hypertension is still very prevalent today and a large subset are shown to have treatment resistant hypertension. Several cardiovascular diseases including hypertension result in endothelial dysfunction and inflammation. Once thought of as a passive barrier between blood flow and tissue the endothelium is now considered a main hub for maintaining vascular tone, structure and haemostasis. Several pathways occur in the endothelium that can result in dysfunction and altered vascular stasis. Such pathways include the impairment of the vasodilator nitric oxide (NO), increases in pro-inflammatory pathways such as ROS (reactive oxygen species) production and also recent reports suggest that the enzyme arginase, associated with the L-arginine-urea cycle, may be an important factor that is increased in hypertension. These pathways may offer alternative mechanisms to treat the complications associated with hypertension rather than the conventional therapies that aim to lower blood pressure.

2. INTRODUCTION

Vascular endothelial cells play a key role in the initiation, development and progression of many cardiovascular diseases particularly hypertension. As the major risk factor for mortality worldwide much research has gone into the pathways, causes and possible pharmacotherapy's involved in hypertension. Despite growing therapies to reduce blood pressure uncontrolled hypertension is still very prevalent today. Mechanical, functional and structural changes in the vasculature such as turbulent blood flow, fluid shear stress, and vascular remodelling results in endothelial dysfunction, which further increases these changes and are also commonly associated with increases in blood pressure. Inflammatory mechanisms are also gaining interest in the context of hypertension and hypertension related vascular complications however the exact pathways involved are not yet fully understood. This review discusses current findings on the pathophysiological pathways of endothelial dysfunction and inflammation and their contribution to hypertension induced cardiovascular complications.

Endothelial dysfunction in hypertension: The role of arginase

3. HYPERTENSION

In the 2009 WHO Global Health Risks Report hypertension is identified as the leading risk factor for mortality worldwide (1). Accountable for 13% of deaths globally it is also listed in the top five causes of disability-adjusted life years. Hypertension is defined as persistently elevated systolic blood pressure (SBP) over 140 mmHg and diastolic blood pressure (DBP) over 90 mmHg. The prevalence of elevated blood pressure is estimated to be ~23% of the adult population and by 2025 this global burden is predicted to increase to 29% (2). With age and obesity identified as two major risk factors for hypertension, it will continue to be an even greater risk as longevity and weight gain of populations increase. Other risk factors include genetic, environmental, central nervous system, cardiac, renal, gastrointestinal and endocrine factors. With its strong association with inheritability, genome-wide association studies have been conducted to assess a genetic background with raised blood pressure. Several single-nucleotide polymorphisms and various genes have found to be associated with SBP (Chr 10, 11, 12), DBP (Chr 10, 12, 15) as well as hypertension (Chr 12) (3). Co-morbidities such as diabetes mellitus, dyslipidemia, coronary heart disease, and hypercholesterolemia all correlate with increases in blood pressure. Other factors such as stress and increased sympathetic nervous system activity stimulates the cardiovascular and renal systems to increase heart rate, cardiac output, insulin resistance, platelet activation, sodium retention, and augment vascular reactivity and vascular function leading to elevations in blood pressure and the progression of atherosclerosis.

Essential or idiopathic hypertension, the most common type, involves increased peripheral resistance to blood flow particularly in small resistance arteries. In these arteries vascular remodelling can occur and changes in structural, functional and mechanical mechanisms in these vessels leads to reduced lumen diameter and increased intimal thickening. This hypertrophic phenotype coupled with altered myogenic tone results in cardiovascular complications and damaging effects to target organs. Therefore it is not surprising that hypertension is the single biggest risk factor for incidence, development and progression of coronary heart disease, stroke, chronic heart failure and chronic kidney disease (4, 5). Furthermore with each 10 increments in blood pressure the risk for developing a cardiovascular event increases (6). Several lifestyle and drug treatments provide excellent therapy in the management of hypertension. Lifestyle recommendations include physical exercise, healthy body weight, and reduced alcohol consumption. Following the DASH study (Dietary Approaches to Stop Hypertension) (7) dietary recommendations involve reduced sodium intake and increased grains, vegetables, fruits and nuts, which have found to lower blood pressure. In obese patients undertaking the DASH diet, blood pressure was lower compared to those taking potassium, magnesium and fibre supplements (8). First-line pharmaceutical treatments include thiazide diuretics, beta-blockers, ACE (angiotensin converting enzyme) inhibitors, long-acting calcium channel blockers, or angiotensin receptor blockers (ARB) (9).

Ideally, these drugs are used on their own but when optimal blood pressure levels are not reached these agents are used concomitantly. While no one class of antihypertensive treatment appears superior in reducing the risk of cardiovascular disease (10) some agents are more suitable in certain cardiovascular complications. For example, ACE inhibitors and ARB are recommended for chronic renal disease to control hypertension (11). Despite many effective antihypertensive agents and the recent developments of vaccines (particularly targeting the rennin-angiotensin aldosterone system) (12) uncontrolled blood pressure and its severe effects remains an ongoing issue today. Furthermore, while some antihypertensive treatments are effective in lowering blood pressure they may not be sufficient in helping target the vascular dysfunction or remodelling (13). Therefore targeting another aspect in the progression of hypertension may help to reduce cardiovascular morbidity particularly for those difficult to treat with current antihypertensive treatments.

4. RESISTANT HYPERTENSION

Resistant hypertension (RH), also termed 'refractory hypertension' or 'treatment-resistant hypertension', describes a subset of hypertensive patients that despite the use of 3 or more antihypertensive treatments usually including a diuretic, remain persistently above their goal blood pressure. RH also encompasses those patients that have controlled blood pressure but require 4 or more pharmacological treatments. However, RH should not be confused with uncontrolled elevated blood pressure, which is commonly misdiagnosed as RH and thus termed 'pseudo-resistant hypertension'. Uncontrolled hypertension is a broad term for all hypertensive patients who cannot maintain their high blood pressure, this can be due to therapeutic inertia, poor compliance to the treatments, inappropriate or inadequate treatments prescribed, undiagnosed hypertension, or the white coat effect, which is the differences seen between clinical and home blood pressure measurements. Of these, poor adherence from the patient and therapeutic inertia that involves poor management from the physician appear to be the most common problems of uncontrolled hypertension. However, RH generally stems from those that are older, have increased adiposity, are diabetic (14) and have a history of uncontrolled elevated blood pressure.

To date the prevalence of treatment resistance hypertension has not yet been defined. Recent large antihypertensive trials with criteria including dose titration and monitored adherence provide the best estimation for determining prevalence (Table 1). The ALLHAT trial (Antihypertensive and Lipid-Lowering Treatment to Prevent Heart Attack Trial) (15) with 33,000 participants and a 5 year follow-up demonstrated a third of participants still presented with uncontrolled blood pressure even with on average 2 antihypertensive medications. The proportion with elevated blood pressure despite 3 or more antihypertensive treatments was 27%. They show that DBP was a lot easier to control with ~92% demonstrating opitmal levels at the 5 year follow-up. The LIFE trial (Losartan Intervention For Endpoint reduction) (16) with

947

Endothelial dysfunction in hypertension: The role of arginase

Table 1. Uncontrolled blood pressure results from recent clinical trials

Trial	Mean follow up	No. of participants	No. of anti-hypertensive drugs administered	Participants with uncontrolled BP at end of trial	Participants on greater than 3 anti-hypertensive drugs at end of trial	Reference
ALLHAT (Antihypertensive and Lipid-Lowering Treatment to Prevent Heart Attack Trial)	5 years	33,357	1 or more	34.4 %	27.3 %	Cushman *et al.* (15)
LIFE (Losartan Intervention for Endpoint Reduction in Hypetension)	4.8 years	9,193	1 or more	53.5 %	24 %	Dahlof *et al.* (16)
INVEST (International Verapamil-Trandolapril Study)	2.7 years	22,576	2 or more	28.8 %	51.6 %	Pepine *et al.* (17)
CONVINCE (Controlled Onset Verapamil Investigation of Cardiovascular Endpoints)	3 years	16,602	1 or more	34.3 %	39.6 %	Black *et al.* (18)
ACCOMPLISH (Avoiding Cardiovascular Events Through Combination Therapy in Patients Living with Systolic Hypertension)	3 years	11,506	2 or more	26.1 %	--	Jamerson *et al.* (19)
HYVET (Hypertension in the Very Elderly Trial)	1.8 years	3,845	1-2	52 %	--	Beckett *et al.* (135)

just over 9000 participants demonstrated much higher incidence of uncontrolled blood pressure with those taking Losartan (an angiotensin-II receptor type 1 antagonist) where only 49% and 89% showed optimal SBP and DBP, respectively. Similarly of patients taking atenolol (beta blocker) only 46% and 89% demonstrated optimal levels. In a trial with 22,000+ participants specifically looking at hypertensive coronary artery disease, the INVEST trial (International Verapamil-Trandolapril Study) (17) compared a thiazide diuretic with a beta blocker to a calcium channel blocker with an ACE inhibitor. At 12 and 24 months half the participants in each group were still on 3 or more antihypertensive drugs and neither group was superior in lowering blood pressure. Similar results can found in the CONVINCE trial (Controlled Onset Verapamil Investigation of Cardiovascular End Points) (18) with 33% uncontrolled at 3 year follow-up and 18% with 3 or more antihypertensive agents; and more recently the ACCOMPLISH trial (Avoiding Cardiovascular Events Through Combination Therapy in Patients Living With Systolic Hypertension) (19), while demonstrating that by 6 months combination therapy is effective and safe, 20% still remained above goal.

Patients with RH are found to have a higher risk of target organ damage (20), increased left ventricular hypertrophy, increased carotid intima-media thickening, and a greater propensity of plaque development (21). Furthermore, aortic stiffening, sleep apnoea, and chronic kidney disease are all found to contribute to the risk of becoming resistant to treatment. Studies also suggest that primary aldosteronism may be a common cause of RH (20, 22, 23) with one study demonstrating 20% of RH patients presented with increased aldosterone (24). Generally, overproduction of aldosterone leads to sodium and water reabsorption and potassium excretion causing increased blood volume and hypertension. However hyperaldosteronism also results in leukocyte infiltration (25), increased expression of pro-inflammatory cytokines

(26) and the production of reactive oxygen species leading to vascular fibrosis and remodelling.

5. ENDOTHELIAL STRUCTURE AND FUNCTION

Endothelial cells (EC) line the vasculature to form the endothelium, which acts as a semi-permeable monolayer between the lumen and the vessel wall. Their structure and integrity are essential in maintaining vascular tone and haemostasis. Prenatally these cells originate from same precursor as haematopoietic cells, the hemangioblast (CD34$^+$), which can differentiate into endothelial precursor cells (VEGFR3$^+$) to become vascular endothelial cells (VEGF-R3$^+$, podoplanin$^-$, PAL-E$^+$). Recent studies have shown that vasculogenesis also occurs postnatally with endothelial progenitor cells found to mobilize from the bone marrow (27) and other sites in the body including the peripheral blood, liver (28), and adipose tissue (29) to help repair and regenerate vessel walls in adults.

Despite the total mass of the endothelium only weighing between 100 – 500 g the amount of surface area exposed to blood flow is thought to be highly active and up to 350 m^2 (30). Through its paracrine, endocrine and autocrine functions the endothelium helps to regulate various cardiovascular processes. Blood wall exchanges occur through the abundant ion channels (K$^+$, Ca^{2+}, Na$^+$, Cl$^-$), G-proteins, caveolae and tyrosine kinase receptors in the plasma membrane lipid bilayer of the endothelium. Such exchanges include the release of vasomotor factors such nitric oxide (NO) or prostacyclin (PGI$_2$) that inhibit platelet aggregation and cause relaxation as well as release of endothelium-derived hyperpolarizing factor (EDHF) that leads to activation of outward K$^+$ currents causing vascular smooth muscle cell hyperpolarization (31). These responses result from stimuli such as thrombin, bradykinin, ADP or changes in blood flow or pressure. Conversely, vasoconstriction factors such as thromboxane A$_2$, endothelin-1, angiotensin-II (AngII), prostaglandins,

948

Endothelial dysfunction in hypertension: The role of arginase

reactive oxygen species, free radicals, pro-coagulant, pro-thrombotic factors and pro-inflammatory mediators are stimulated during disease states leading to impaired endothelium-derived vasodilatation or endothelial dysfunction (ED).

Under basal conditions fluid shear stress and pulsatile stretch results in continuous release of compensatory vasoactive substances. The magnitude of endothelial shear flow in vessels is dependent on the velocity of blood flow, direction, obstructions along the vessel as well as the location of flow in the vascular tree. Under physiological conditions flow of blood along straight vessels, also known as undisturbed laminar flow, results in high shear stress (HSS) values $(15 - 70 \text{ dyn/cm}^2)$ and several cardioprotective properties. Indeed, cultured endothelial cells from different human vessels demonstrated reduced inflammation following exposure to high shear stress compared to static conditions (32). Physiological shear stress conditions have also shown to lead to anti-inflammatory effects with reduced TNF-alpha induced adhesion molecule expression (33). However conflicting reports exist, where one study has shown that using MRI technology, one patient was found to develop plaque ulceration at the location with the highest shear stress (34). This suggests HSS may not be protective in areas of vulnerable plaques. However, it is well established that sites in the vascular tree most vulnerable to atherosclerotic plaques include the inner curve of vessels as well as at bifurcations and branches. At these sites disturbed laminar flow is shown to be the most prominent (35, 36) and presents in two forms: unidirectional which results in low shear stress (LSS) values $(<12 \text{ dyne/cm}^2)$ or bidirectional that leads to oscillatory shear stress (OSS) or turbulent flow. LSS and OSS has been found to be associated with decreased NO bioavailability, upregulation of LDL, degradation of the ECM, apoptosis, promotion of oxidative stress, inflammation as well as vascular and plaque remodelling (37).

6. ENDOTHELIAL DYSFUNCTION IN HYPERTENSION

6.1. Characteristics and measurements

Under physiological conditions damage to the vasculature leads to several haemostatic processes signalled by the endothelium to reduce blood flow. These include vasoconstriction, formation of a haemostatic plug, initiation of the coagulation cascade, repair of the damaged site via endothelial progenitor cells, local endothelial cells and smooth muscle cells and finally fibrinolysis. However, under pathological conditions such as hypertension, atherosclerosis, diabetes, and coronary heart disease endothelial dysfunction occurs and the endothelium is unable to help regulate these processes. In 1980 the seminal paper, Furchgott and Zawadzki (38) demonstrated that damage to the integrity of the endothelium led to impaired relaxation when stimulated with acetylcholine (ACh) compared to vessels where the endothelium was preserved. They further demonstrated that the vasorelaxation observed was mediated by the release of an endothelium derived relaxing factor (EDRF), later identified by Ignarro and

colleagues as NO (39). Endothelial dysfunction is generally defined as impaired endothelium-dependent vasodilatation to specific stimuli and characterised by an imbalance between vasoconstriction and vasodilatation factors, predominantly NO. However, there is growing literature to support that endothelial dysfunction also involves pro-inflammatory states, which will be discussed later. It is recognised that ED is the initial and reversible step in the pathological process of cardiovascular diseases such as hypertension and diabetes mellitus but is also implicated to be essential in the progression of many infections and autoimmune diseases due to its angiogenic properties the pathogenesis of certain cancers (40).

Assessing ED can be based on a variety of biomarkers, cellular markers and gross vasoreactivity techniques. Serum concentration of ICAM, VCAM, E-selectin, P-selectin as well as von Willebrand Factor and microalbuminuria have been used as biomarkers due to their expression on vascular endothelial cells during dysfunction and their consequent release into the bloodstream. Despite the current controversy in determining specific surface markers for endothelial progenitor cells, typically CD34+/KDR+/CD133+, a vast amount of literature demonstrate that these cells are found to inversely correlate with endothelial dysfunction in patients with coronary artery disease, diabetes and other CVD risk factors and co-morbidities. Increases in mature circulating endothelial cells, which are products of endothelial wall turnover and apoptosis during endothelial damage are another cellular marker implicated in cardiovascular diseases. Emerging evidence also suggests increased endothelial microparticles, which are continually shed blebbings of endothelial cells into the bloodstream, are elevated in CVD (41). Non-invasive tests of endothelial function include flow-mediated dilatation (FMD) of the brachial artery, which measures change in diameter of the brachial artery via an ultrasound, laser Doppler examination, pulse wave analysis, and pulse amplitude tonometry. While more invasive techniques include venous occlusion plethysmography that is used to assess change in forearm blood flow and arterial stiffness via infusion of various vasorelaxants. Cardiac catherization is the most invasive and expensive and assesses changes in epicardial diameter and blood flow.

Despite the various techniques available it is still unclear whether endothelial dysfunction is a cause or a consequence of hypertension. In hypertensive animal models, rats fed on a fructose-rich diet were found to have impaired endothelial-mediated vasodilatation 10 days before the rats were shown to have increased blood pressure (42), a similar result is also seen in eNOS knockout mice. However, many other models demonstrate chronic hypertension can lead to damaging effects on the endothelium (43, 44). Clinical studies also show confounding results where a study conducted by Rossi and colleagues (45) using 952 normotensive post-menopausal women demonstrate that each decrease in flow-mediated dilation predicted an increased risk in the development of hypertension during a 3.5 year follow-up even when a adjusted for multiple factors This suggests impaired

949

Chapter 9 Appendicies

Endothelial dysfunction in hypertension: The role of arginase

endothelial-mediated vasodilatation precedes future development of hypertension in this cohort. In a recent report from the MESA (Multi Ethnic Study of Atherosclerosis) looking at FMD and hypertension in 3500 participants they demonstrate a different finding over a 4.8 year follow-up (46). While at baseline reduced FMD correlated with increased prevalence in blood pressure but when adjusted for various factors such as age, sex, ethnicity, BMI, cholesterol levels and other metabolic factors the association was not found. Therefore they suggest that endothelial dysfunction is a consequence of hypertension not a cause.

6.2. Impaired NO

The most widely studied biological mechanism of endothelial dysfunction in hypertension is the decreased bioavailability of nitric oxide (NO). NO is not only a potent vasodilator and essential in regulating vascular tone and blood pressure but it also contributes to the regulation of haemostasis, platelet and leukocyte adhesion as well as vascular smooth muscle cell proliferation. NO is a very small lipid soluble molecule with a half-life of just a few seconds before it is converted into nitrates and nitrites that are ultimately excreted. In the various systems NO can act in many ways such as a neurotransmitter (nervous system), a vasodilator (cardiovascular system) and an inhibitor of viral replication (immune system).

Nitric oxide synthase (NOS), a family of P450 mono-oxygenase-like enzymes, catalyses the production of NO and exists in three distinct isoforms; NOS-1, NOS-2, NOS-3. They differ not only in their genetic origin (47, 48) but also their location. NOS-1 or neuronal NOS (nNOS) is found in the central and peripheral nervous system but also skeletal muscle, pancreas and endometrium and has role in neurotransmission and glomerular interactions (49). NOS-2 or inducible NOS (iNOS) is found in activated macrophages, heart, liver, smooth muscle and the endothelium and has a role in inflammation (50, 51). Finally NOS-3 or endothelial NOS (eNOS) is found predominantly in the endothelium but also in the brain and epithelial cells. eNOS is involved in vascular relaxation, regulating platelet adhesion/aggregation and angiogenesis (52, 53). The process of NO synthesis involves firstly the oxidation of arginine to N^G-hydroxy-$_L$-arginine (NHA) using NADPH (nicotinamide adenine dinucleotide phosphate) and O_2 catalyzed by the nitric oxide synthases (NOS), a family of P450 mono-oxygenase-like enzymes (54). The second step involves the production of NO when NHA is converted to $_L$-citrulline via NOS. Actions of NOS are accelerated by the cofactors flavin adenine dinucleotide (FAD), flavin mononucleotide (FMN) and tetrahydrobioptern (BH$_4$). In the endothelium eNOS is localized in the plasma membrane and more specifically in highly rich lipid invaginations or caveolae (55) where it is bound in an 'inactive' state to the coat protein caveolin-1 (Cav-1). Besides NO production, caveolae, caveolins and cavins (regulators of caveolins) are involved in the regulation of various signaling cascades involved in vascular remodeling, intracellular calcium (Ca^{2+}), and microvascular permeability. Activation of eNOS also involves heat shock protein 90, calmodulin binding,

phosphorylation of Ser1179 and dephosphorylation of Thr497 domains and subcellular localization. Under normal shear flow there is an influx of Ca^{2+} causing calmodulin to bind to eNOS and causing its subcellular localization to either the cytosol or the Golgi (56) or possibly to the mitochondria (57) which ultimately results in activation. Once NO is produced it can then stimulate soluble guanylate cyclase (sGC) in vascular smooth muscle cells (VSMC) to increase cyclic GMP (cGMP) that leads to relaxation and reduced Ca^{2+}. Impaired NO bioavailability commonly seen in various cardiovascular diseases including hypertension can be due to either impaired production or increased degradation of NO. Given the already established pathway of NO synthesis, impaired production may be a result of reduced eNOS activity, substrate and cofactor availability and the localization of eNOS or the presence of endogenous inhibitors.

Since the works of Huang and colleagues (58) and Shesely and colleagues (59) demonstrated a hypertensive phenotype in eNOS knockout models studies have been utilizing these models extensively and have demonstrated am essential role of eNOS in the vasculature. In animal models, supplementation with the eNOS substrate L-arginine leads to enhanced NO synthesis in diabetic (60) and pulmonary hypertensive rats (61, 62) as well as reduced atherosclerotic lesions in rabbits (63) and cerebral infarcts in various experimental models of stroke (64). More importantly, clinical studies have also shown supplementation increases NO synthesis and enhances vascular reactivity. Indeed, hypertensive patients have paradoxically high levels of L-arginine in their plasma (65) yet display impaired L-arginine transport in platelets, red blood cells (66) and endothelial cells and are therefore unable to adequately produce optimum NO. Consequently, L-arginine activity may be rate-limiting for NO production and this is seen even in normotensive patients with a family history of hypertension (67). Increased transport can be seen in various studies to improve vascular function where De Meirelles and collegues (68) demonstrated hypertensive patients undergoing 12 weeks of aerobic exercise had significantly improved L-arginine transport as well as NOS activity as well as reductions in fibrinogen and C-reactive protein.

Against this backdrop, it is thus of little surprise that L-arginine supplementation has been reported to improve endothelial function. Certainly, supplementation of L-arginine in humans has been delivered via several modes, including intra-arterially, intravenously and oral supplementation and in high risk patients it has been shown to increase NO production and decrease leukocyte adhesion, platelet aggregation and hyperplasia of the intimal layer (69). Despite this, owing to the diverse role of L-arginine, its supplementation is likely to result in increased metabolism via pathways other than NO synthesis, such as those that increase ornithine, polyamines, creatine, proline and spermine (70). It is thus important to note that although L-arginine therapy can produce its effects via NO dependent mechanisms, effects independent of NO may also play a functional role. L-arginine is also a potent hormone secretagogue. It has long been used for the

- 226 -- 226 -

Endothelial dysfunction in hypertension: The role of arginase

assessment of growth hormone release by the pituitary gland (71) and L-arginine administration results in an approximate twofold increase in plasma growth hormone, insulin and glucagons release (72), (73). L-arginine also releases prolactin (74) and insulin either directly or indirectly (by the release of other endothelium dependent agents such as muscarinic agonists) (73). The mechanisms regulating the endocrine secretagogue effect on various hormones in response to L-arginine remains largely unknown. However, the secretagogue effect is of important consideration when evaluating the role of L-arginine on the vasculature, since many of these resultant hormones have been independently reported to act on vascular smooth muscle cells. Apart from its complex metabolism and potent secretagogue effects, dietary L-arginine supplementation is also less than ideal since it is an amino acid that undergoes considerable first pass metabolism. Ingestion of L-arginine may not have large physiological effects due to its low bioavailability, reported to be as low as 21% through to 67% (75), (76).

Another cause of L-arginine reductions may involve the eNOS inhibitor ADMA (asymmetric dimethylarginine) an endogenous analogues of L-arginine, which is not only increased essential hypertension but also inversely correlated with forearm blood flow (65). The enzyme arginase (discussed later) may also be another determinant of reduced cytosolic L-arginine and impaired NO production.

Reduced L-arginine, increased ADMA or BH_4 deficiency can also lead to uncoupling or dysfunction of eNOS and other NOS isoforms. eNOS contains two dimers with an N-terminal oxygenase domain that binds BH_4, L-arginine, iron, and calmodulin ions as well as a C-terminal reductase domain that binds FAD, FMN and NADPH. In the pathological setting, BH_4 is oxidised to BH_2 causing altered electron flow from FMN and FAD to L-arginine and the uncoupling of eNOS dimers. This results in free radical production particularly superoxide from O_2 in replace of NO. Studies show in hypertension there is a downregulation of BH_4 and in a animal nephrectomy model BH_4 supplementation normalised SBP levels (77). Other mechanisms causing uncoupling of eNOS include impaired Akt kinase phosphorylation of the serine (Ser^{1179}) domain (78), (79) or increased phosphorylation of the theronine (Thr^{497}) domain via protein kinase C (80), (81). In pulmonary hypertension it is suggested that the tight binding of Cav-1 and eNOS may play a major role leading to reduced angiogenesis and increased cell proliferation. While the binding of Cav-1 is generally shown to suppress eNOS activity, $Cav-1^{-/-}$ mice in response to vascular shear stress demonstrate reduced blood flow but no change in lumen diameter and an increase in vessel wall thickness and cellular proliferation compared to controls (82). This study then showed that reconstituting Cav-1 into the vessels the effects were then ablated, suggesting in these knockout mice eNOS is unable to localize in the caveolae causing impaired response to shear stress. Therefore Cav-1 is found to not only regulate eNOS activation but also is essential in its localization. While eNOS is found to produce more NO when bound to the membrane compared to cytosolic eNOS it appears that the location is more important (52). Sanchez *et al* (56) suggest that eNOS translocation from the caveolae to the Golgi via acetylcholine may correspond to a vasodilation pathway whereas they show with platelet-activating factor (PAF), which is an inflammatory marker and vasoconstrictor causes eNOS to locate to the cytosol. Therefore cytosolic relocation of eNOS, and particularly mitochondrial bound eNOS (57) may relate to an inflammatory response. Indeed, arginase II is known to compete with eNOS for L-arginine and is found to be not only bound to the mitochondria but is also shown to regulate eNOS activity (83).

Production of reactive oxygen species (ROS) are another set of molecules that may result from and cause eNOS uncoupling, decreased NO production and increased NO degradation. While essential for cell metabolism and signaling when there is an imbalance in the production of oxidants or ROS to antioxidants in blood vessels this leads to a pro-oxidant state and the pathogenesis of oxidative stress causing endothelial dysfunction, increased contractility, vascular smooth muscle cell growth and apoptosis, monocyte migration, lipid peroxidation, inflammation and increased deposition of extracellular matrix proteins. Furthermore, ROS has been shown to activate signal transduction pathways and induce gene expression and growth factors (84, 85). As reviewed extensively endothelial dysfunction in hypertension and many cardiovascular diseases is due in part to an increase in ROS production (43), (86)-(87). ROS are produced from the mitochondria and subcellular sources such as the mitochondrial electron transport chain, NADPH oxidase, xanthine oxidase, cytochrome P450, cyclooxygenase, lipoxygenase, and uncoupled eNOS. Initial formation begins with the reduction in one electron of molecular oxygen causing formation of superoxide anions ($\cdot O_2^-$). Superoxide can then go on to produce hydroxyl radical (OH^-), hydrogen peroxide (H_2O_2) via superoxide dismutase (SOD), and peroxynitrite ($ONOO^-$) from scavenging NO.

Experimental models of hypertension including DOCA-salt rats (88), spontaneous hypertensive rats (89), L-NAME hypertensive rats (90), and hypertriglyceridaemic rats (91) all demonstrate increases in ROS production. In some models, increases in ROS is found to precede hypertension suggesting that production of ROS may contribute to the initiation and the progression of hypertension (92). Furthermore, treatment with antioxidants improves vascular function and structure, prevents target-organ damage, and reduces blood pressure in animal models of hypertension (92, 93). However, clinical studies have been less conclusive. Indeed, ROS levels are enhanced in hypertensive patients with reports of increased levels of H_2O_2 (94) and upregulation of vascular NADPH (95). However most clinical trials demonstrate no beneficial effects on blood pressure (96). Of the many toxic affects excess ROS has on the vasculature, inflammation appears to be the greatest and is involved in the initiation and development of atherosclerotic plaques commonly associated with hypertension and various cardiovascular diseases.

6.3. Endothelial inflammation

Recent reports suggest that hypertension induced endothelial dysfunction involves low-grade inflammation

951

Endothelial dysfunction in hypertension: The role of arginase

that can progress into hypertension induced atherosclerosis and several cardiovascular complications. This comes as no surprise as these conditions are commonly correlated and both have similar risk factors (age, obesity, diet, diabetes, smoking) and result in vascular remodeling and dysfunction. Indeed, inflammatory markers that are reportedly upregulated in hypertensive patients include tumor necrosis factor-alpha (TNF-α), C-reactive protein (CRP) (97), interleukin (IL)-6, IL-1b and angiotensin II (AngII) (98-100). Many of these inflammatory markers are involved in the initial step in atherosclerotic plaque development, the adhesion cascade. Some animal studies have shown a relationship exists between high intraluminal pressure and plaque development. Indeed, in ApoE knockout mice with induced hypertension via either eNOS ablation (101), renal artery clamping (102), or aortic constriction (103) increases in atherosclerosis and expression of adhesion molecules were seen including intracellular cell adhesion molecule-1 (ICAM-1), vascular cell adhesion molecule-1 (VCAM-1), and E-selectin. This effect is also seen in clinical studies where essential hypertensive patients demonstrate increases in ICAM-1, VCAM-1 and E-selectin in their serum following a cold pressor test (104). Furthermore, studies show that when an aortic stenosis is administered to rabbits, hypertension causes monocyte adhesion to be increased only in the proximal region to the stenosis (105) which is where the highest oscillatory shear stress occurs. While it is clear that high intraluminal pressure results in leukocyte adhesion and atherosclerotic development, the exact mechanisms and pathways are still unclear. Several studies have implicated various factors including ROS production, NF-kB activation, endothelin-1 (ET-1), and the rennin-angiotensin-aldosterone system (RAAS).

ROS production as previously stated is important in the progression of inflammation and atherosclerotic plaques. They are involved in the gene expression of many adhesion molecules such as ICAM-1, VCAM-1, E-selectin and monocyte chemoattractant protein-1 (MCP-1) (106) and in disease states such as hypertension play a role in regulating the inflammatory response to shear stress. Ang II a well-regarded mediator of the RAAS and well characterized in hypertension and vascular dysfunction is shown to stimulate leukocyte adhesion through angiotensin type 1 (AT$_1$) and 2 (AT$_2$) receptors. However, it is also shown Ang II acts on ROS production and proinflammatory transcription factors. For example, rats perfused with Ang II and an NADPH oxidase inhibitor present with reduced ICAM-1 expression and macrophage infiltration compared to those perfused with Ang II alone and this was shown to be independent of blood pressure changes (107). Suggesting that Ang II induced inflammation is mediated via NADPH oxidase and ROS production.

The proinflammatory transcription factors NF-kB aand enodthelin-1 (ET-1) also correlate with increases in Ang II resulting in increases in proinflammatory genes, cytokines and signaling pathways (108). RAAS independent inflammatory pathways have also been implicated where increases in shear flow and pressure has shown to increase NF-kB binding to DNA in cells (109) and upregulate expression in vessels (110). Furthermore, when pressurized vessels were incubated with an NF-kB inhibitor this dramatically reduced the number of adhered monocytes to the endothelium and the expression of adhesion molecule (111). This study also showed that addition of Ang II to vessels at various pressures was not sufficient to increased adhesion. This suggests that upregulation of the adhesion cascade may result from more mechanical factors such as intraluminal pressure and stretch independent of Ang II. Indeed, this effect is also seen in studies with rats undergoing aortic constriction in which they demonstrate that increased blood pressure and not RAAS upregulated the adhesion molecules ICAM-1 and P-selectin (112). This is also seen in terms of ROS production where NADPH oxidase deficient mice demonstrated lower blood pressure compared to controls and this was not increased with Ang II was administered (113). Therefore these results suggest antoher pathway may be involved in endothelial inflammation in hypertension.

6.4. Role of arginase

The enzyme arginase may be one factor involved in an alternative pathway involved in endothelial dysfunction and inflammation in hypertension (Figure 1). Arginase is a fundamental manganese metalloenzyme in the hepatic urea cycle that hydrolyses L-arginine to urea and L-ornithine. Arginase exists in two distinct isoforms (I and II) where they differ in intracellular, gene and tissue expression, gene transcription and transduction regulators as well as metabolism. While both enzymes are found throughout the body arginase I or hepatic arginase is a cytosolic enzyme found abundantly in the liver but also in red blood cells whereas arginase II or extra-hepatic arginase is a mitochondrial enzyme expressed more widely and is seen in the kidney, brain, gastrointestinal tract, prostate and the vasculature. It has been shown vascular endothelial cells and smooth muscle cells express both isoforms, but it appears that the distribution is vessel and species dependent (114-116). In particular arginase II appears to be the predominant isoform in human endothelial cells (115). Arginase isoforms share ~59% homology, with arginase I composed of 322 amino acide residues, 11.5 kbp long and 8 exons on chromosome 6q23, where arginase II appears to have 344 amino acid residues and 8 exons but is on chromosome 14q24.1-q24.3. Products of arginine hydrolysis involve increased urea production and L-ornithine leading to increases in polyamines, proline, and glutamate (involved in cell growth and proliferation) as well as a reduction in NO.

Initially the role of arginase in the body was mainly thought of as disposing excess nitrogen via amino acid and nucleotide metabolism. Recently studies suggest an important role for arginase in the vasculature. In the endothelium arginase is now regarded to help regulate NO levels by competing with eNOS for L-arginine. Arginase is also thought to modulate eNOS (117) and this is most likely to occur when eNOS is translocated from the caveolae to the cytosol and perhaps even the mitochondria under proinflammatory states. As such increased arginase activity/expression has been implicated in many vascular

952

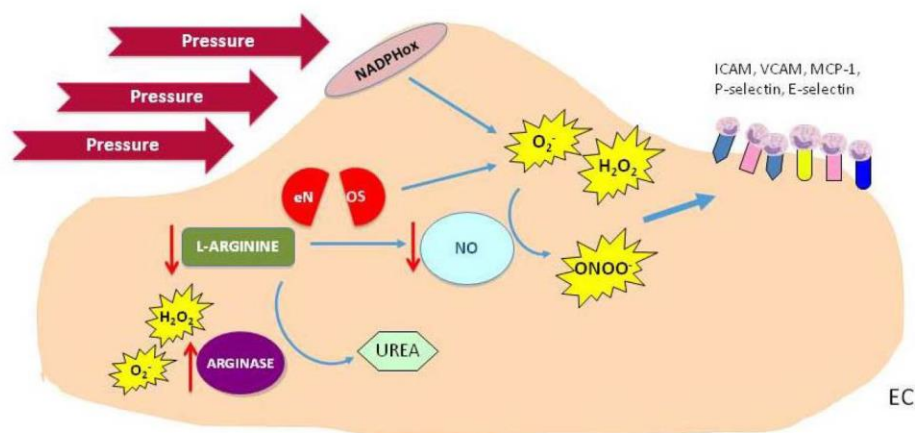Endothelial dysfunction in hypertension: The role of arginase

Figure 1. Our hypothesis is that high blood pressure induces an increase in reactive oxygen species (ROS) production in endothelial cells (EC) possibly via NADPH oxidase (NADPHox) which causes an increase in endothelial arginase expression and/or activity which decreases available L-arginine, this increases endothelial nitric oxide synthase (eNOS) expression and/or activity and the 'uncoupled' eNOS produces superoxide ($\cdot O_2^-$) over NO resulting in the production of hydrogen peroxide (H_2O_2) and peroxynitrite ($ONOO^-$) and pro-inflammatory factors leading to the expression of adhesion molecules.

pathologies including hypertension (118, 119), ischaemia-repurfusion (120), uremia (121), aging (117), sexual arousal (122, 123), diabetes (124, 125) and atherosclerosis (115), (126). In hypertension arginase activity and expression studies demonstrate increased arginase activity reduces NO mediated dilation in hypertensive pigs, which was then normalized using an arginase inhibitor (116). These results area also seen in other models of hypertension including Dahl rats with salt induced hypertension (127) and in bovine pulmonary arterial endothelial cells where NO production was increased and urea was decreased when both L-arginine and L-valine were used to inhibit arginase activity (128). And in a model of chronic hypertension treatment with an arginase inhibitor for 10 weeks in older aged spontaneous hypertensive rats decreased blood pressure and cardiac fibrosis and improved vascular function (129). In one small clinical study assessing attenuated reflex cutaneous vasodilatation in essential hypertension increased NO-dependent vasolation was found when arginase was inhibited and not with L-arginine supplementation (130). Interestingly, it has also been reported that arginase expression of both isoforms is increased in spontaneous hypertensive rats before overt hypertension develops and is positively correlated to systolic blood pressure in these rats (131). Therefore these results suggest that in genetic hypertension vessels have the propensity to develop endothelial dysfunction before established hypertension is even developed. This may also occur before inflammatory mechanisms take place, as increased inflammatory markers are not seen till these rats are adults (131, 132), suggesting underlying molecular/transcriptional mechanisms, possibly via NF-kB pathway.

Despite these recent findings it is still unclear the exact mechanisms/pathways that induces arginase upregulation in hypertension. Several studies have examined a possible link with ROS production that may help link hypertension induced endothelial dysfunction and inflammation. Ryoo and colleagues (126) demonstrate that in atherogenic prone ApoE$^{-/-}$ when arginase II activity was reduced via either inhibition or gene deletion NO bioavailability was increased and ROS production was reduced, resulting in improved endothelial function and reduced vascular stiffness. They also show that plaque area, thickness and foam cells were all reduced in thoracic aora treated with the arginase inhibitor BEC, S-(2-boronoethyl)-L-cysteine. The ROS/arginase link is may also be reciprocal where intraluminal H_2O_2 is found to upregulate arginase expression and impair NO-mediated dilation in porcine coronary arteries and these affects were attenuated when arginase inhibitors DFMO or nor-NOHA reduced H_2O_2 and increased vascular function. Inflammatory cytokine TNF-a has also shown to upregulate arginase in ischemia-repurfusion resulting in reduced bioavailability of L-arginine and the uncoupling of eNOS producing increased superoxide production (133). This action may be via NADPH oxidase. Where one study has demonstrated that in alveolar macrophages treated with apocynin, NADPH oxidase inhibitor, arginase is also attenuated (134).

7. SUMMARY

Endothelial dysfunction plays a significant role in the initiation and development of hypertension and its progression to cardiovascular related diseases. Impaired

953

Endothelial dysfunction in hypertension: The role of arginase

NO production is a strong indicator of endothelial dysfunction and continues to be an essential component when measuring vascular impairment. Recently, reports suggest that inflammatory mechanisms in the vasculature may also be an important factor determining dysfunction in the endothelium. While it is still unclear the exact pathways involved in the progression of essential hypertension to cardiovascular diseases there is increasing interest in the role of arginase and reactive oxygen species play in the inflammatory progression of hypertension.

8. ACKNOWLEDGMENTS

9. REFERENCES

1. Global health risks: mortality and burden of disease attributable to selected major risks. In: World Health Organization, Geneva (2009)

2. P. M. Kearney, M. Whelton, K. Reynolds, P. Muntner, P. K. Whelton and J. He: Global burden of hypertension: analysis of worldwide data. *Lancet*, 365(9455), 217-23 (2005)

3. D. Levy, G. B. Ehret, K. Rice, G. C. Verwoert, L. J. Launer, A. Dehghan, N. L. Glazer, A. C. Morrison, A. D. Johnson, T. Aspelund, Y. Aulchenko, T. Lumley, A. Kottgen, R. S. Vasan, F. Rivadeneira, G. Eiriksdottir, X. Guo, D. E. Arking, G. F. Mitchell, F. U. Mattace-Raso, A. V. Smith, K. Taylor, R. B. Scharpf, S. J. Hwang, E. J. Sijbrands, J. Bis, T. B. Harris, S. K. Ganesh, C. J. O'Donnell, A. Hofman, J. I. Rotter, J. Coresh, E. J. Benjamin, A. G. Uitterlinden, G. Heiss, C. S. Fox, J. C. Witteman, E. Boerwinkle, T. J. Wang, V. Gudnason, M. G. Larson, A. Chakravarti, B. M. Psaty and C. M. van Duijn: Genome-wide association study of blood pressure and hypertension. *Nat Genet* (2009)

4. D. Levy, M. G. Larson, R. S. Vasan, W. B. Kannel and K. K. Ho: The progression from hypertension to congestive heart failure. *JAMA*, 275(20), 1557-62 (1996)

5. A. D. Lopez, C. D. Mathers, M. Ezzati, D. T. Jamison and C. J. Murray: Global and regional burden of disease and risk factors, 2001: systematic analysis of population health data. *Lancet*, 367(9524), 1747-57 (2006)

6. P. C. van den Hoogen, E. J. Feskens, N. J. Nagelkerke, A. Menotti, A. Nissinen and D. Kromhout: The relation between blood pressure and mortality due to coronary heart disease among men in different parts of the world. Seven Countries Study Research Group. *N Engl J Med*, 342(1), 1-8 (2000)

7. L. J. Appel, T. J. Moore, E. Obarzanek, W. M. Vollmer, L. P. Svetkey, F. M. Sacks, G. A. Bray, T. M. Vogt, J. A. Cutler, M. M. Windhauser, P. H. Lin and N. Karanja: A clinical trial of the effects of dietary patterns on blood pressure. DASH Collaborative Research Group. *N Engl J Med*, 336(16), 1117-24 (1997)

8. Y. Al-Solaiman, A. Jesri, W. K. Mountford, D. T. Lackland, Y. Zhao and B. M. Egan: DASH lowers blood pressure in obese hypertensives beyond potassium, magnesium and fibre. *J Hum Hypertens*, 24(4), 237-46 (2010)

9. N. A. Khan, B. Hemmelgarn, R. J. Herman, C. M. Bell, J. L. Mahon, L. A. Leiter, S. W. Rabkin, M. D. Hill, R. Padwal, R. M. Touyz, P. Larochelle, R. D. Feldman, E. L. Schiffrin, N. R. Campbell, G. Moe, R. Prasad, M. O. Arnold, T. S. Campbell, A. Milot, J. A. Stone, C. Jones, R. I Ogilvie, P. Hamet, G. Fodor, G. Carruthers, K. D. Burns, M. Ruzicka, J. DeChamplain, G. Pylypchuk, R. Petrella, J. M. Boulanger, L. Trudeau, R. A. Hegele, V. Woo, P. McFarlane, M. Vallee, J. Howlett, S. L. Bacon, P. Lindsay, R. E. Gilbert, R. Z. Lewanczuk and S. Tobe: The 2009 Canadian Hypertension Education Program recommendations for the management of hypertension: Part 2--therapy. *Can J Cardiol*, 25(5), 287-98 (2009)

10. S. Kono, T. Kushiro, Y. Hirata, C. Hamada, A. Takahashi and Y. Yoshida: Class of antihypertensive drugs, blood pressure status, and risk of cardiovascular disease in hypertensive patients: a case-control study in Japan. *Hypertens Res*, 28(10), 811-7 (2005)

11. A. V. Chobanian: Shattuck Lecture. The hypertension paradox--more uncontrolled disease despite improved therapy. *N Engl J Med*, 361(9), 878-87 (2009)

12. T. H. Do, Y. Chen, V. T. Nguyen and S. Phisitkul: Vaccines in the management of hypertension. *Expert Opin Biol Ther*, 10(7), 1077-87 (2010)

13. R. Bravo, B. Somoza, M. Ruiz-Gayo, C. Gonzalez, L. M. Ruilope and M. S. Fernandez-Alfonso: Differential effect of chronic antihypertensive treatment on vascular smooth muscle cell phenotype in spontaneously hypertensive rats. *Hypertension*, 37(5), E4-E10 (2001)

14. K. Jamerson, G. L. Bakris, B. Dahlof, B. Pitt, E. Velazquez, J. Gupte, M. Lefkowitz, A. Hester, V. Shi, S. E. Kjeldsen, W. Cushman, V. Papademetriou and M. Weber: Exceptional early blood pressure control rates: the ACCOMPLISH trial. *Blood Press*, 16(2), 80-6 (2007)

15. W. C. Cushman, C. E. Ford, J. A. Cutler, K. L. Margolis, B. R. Davis, R. H. Grimm, H. R. Black, B. P. Hamilton, J. Holland, C. Nwachuku, V. Papademetriou, J. Probstfield, J. T. Wright, Jr., M. H. Alderman, R. J. Weiss, L. Piller, J. Bettencourt and S. M. Walsh: Success and predictors of blood pressure control in diverse North American settings: the antihypertensive and lipid-lowering treatment to prevent heart attack trial (ALLHAT). *J Clin Hypertens (Greenwich)*, 4(6), 393-404 (2002)

16. B. Dahlof, R. B. Devereux, S. E. Kjeldsen, S. Julius, G. Beevers, U. de Faire, F. Fyhrquist, H. Ibsen, K. Kristiansson, O. Lederballe-Pedersen, L. H. Lindholm, M.

954

Endothelial dysfunction in hypertension: The role of arginase

S. Nieminen, P. Omvik, S. Oparil and H. Wedel: Cardiovascular morbidity and mortality in the Losartan Intervention For Endpoint reduction in hypertension study (LIFE): a randomised trial against atenolol. *Lancet*, 359(9311), 995-1003 (2002)

17. C. J. Pepine, E. M. Handberg, R. M. Cooper-DeHoff, R. G. Marks, P. Kowey, F. H. Messerli, G. Mancia, J. L. Cangiano, D. Garcia-Barreto, M. Keltai, S. Erdine, H. A. Bristol, H. R. Kolb, G. L. Bakris, J. D. Cohen and W. W. Parmley: A calcium antagonist vs a non-calcium antagonist hypertension treatment strategy for patients with coronary artery disease. The International Verapamil-Trandolapril Study (INVEST): a randomized controlled trial. *JAMA*, 290(21), 2805-16 (2003)

18. H. R. Black, W. J. Elliott, G. Grandits, P. Grambsch, T. Lucente, W. B. White, J. D. Neaton, R. H. Grimm, Jr., L. Hansson, Y. Lacourciere, J. Muller, P. Sleight, M. A. Weber, G. Williams, J. Wittes, A. Zanchetti and R. J. Anders: Principal results of the Controlled Onset Verapamil Investigation of Cardiovascular End Points (CONVINCE) trial. *JAMA*, 289(16), 2073-82 (2003)

19. K. Jamerson, M. A. Weber, G. L. Bakris, B. Dahlof, B. Pitt, V. Shi, A. Hester, J. Gupte, M. Gatlin and E. J. Velazquez: Benazepril plus amlodipine or hydrochlorothiazide for hypertension in high-risk patients. *N Engl J Med*, 359(23), 2417-28 (2008)

20. K. K. Gaddam, M. K. Nishizaka, M. N. Pratt-Ubunama, E. Pimenta, I. Aban, S. Oparil and D. A. Calhoun: Characterization of resistant hypertension: association between resistant hypertension, aldosterone, and persistent intravascular volume expansion. *Arch Intern Med*, 168(11), 1159-64 (2008)

21. C. Cuspidi, G. Macca, L. Sampieri, I. Michev, M. Salerno, V. Fusi, B. Severgnini, S. Meani, F. Magrini and A. Zanchetti: High prevalence of cardiac and extracardiac target organ damage in refractory hypertension. *J Hypertens*, 19(11), 2063-70 (2001)

22. M. Epstein and D. A. Calhoun: The role of aldosterone in resistant hypertension: implications for pathogenesis and therapy. *Curr Hypertens Rep*, 9(2), 98-105 (2007)

23. D. A. Calhoun, D. Jones, S. Textor, D. C. Goff, T. P. Murphy, R. D. Toto, A. White, W. C. Cushman, W. White, D. Sica, K. Ferdinand, T. D. Giles, B. Falkner and R. M. Carey: Resistant hypertension: diagnosis, evaluation, and treatment: a scientific statement from the American Heart Association Professional Education Committee of the Council for High Blood Pressure Research. *Circulation*, 117(25), e510-26 (2008)

24. D. A. Calhoun, M. K. Nishizaka, M. A. Zaman, R. B. Thakkar and P. Weissmann: Hyperaldosteronism among black and white subjects with resistant hypertension. *Hypertension*, 40(6), 892-6 (2002)

25. K. Yoshida, S. Kim-Mitsuyama, R. Wake, Y. Izumiya, Y. Izumi, T. Yukimura, M. Ueda, M. Yoshiyama and H. Iwao: Excess aldosterone under normal salt diet induces cardiac hypertrophy and infiltration via oxidative stress. *Hypertens Res*, 28(5), 447-55 (2005)

26. E. R. Blasi, R. Rocha, A. E. Rudolph, E. A. Blomme, M. L. Polly and E. G. McMahon: Aldosterone/salt induces renal inflammation and fibrosis in hypertensive rats. *Kidney Int*, 63(5), 1791-800 (2003)

27. T. Asahara, T. Murohara, A. Sullivan, M. Silver, R. van der Zee, T. Li, B. Witzenbichler, G. Schatteman and J. M. Isner: Isolation of putative progenitor endothelial cells for angiogenesis. *Science*, 275(5302), 964-7 (1997)

28. A. Aicher, M. Rentsch, K. Sasaki, J. W. Ellwart, F. Fandrich, R. Siebert, J. P. Cooke, S. Dimmeler and C. Heeschen: Nonbone marrow-derived circulating progenitor cells contribute to postnatal neovascularization following tissue ischemia. *Circ Res*, 100(4), 581-9 (2007)

29. A. Miranville, C. Heeschen, C. Sengenes, C. A. Curat, R. Busse and A. Bouloumie: Improvement of postnatal neovascularization by human adipose tissue-derived stem cells. *Circulation*, 110(3), 349-55 (2004)

30. A. R. Pries, T. W. Secomb and P. Gaehtgens: The endothelial surface layer. *Pflugers Arch*, 440(5), 653-66 (2000)

31. J. J. McGuire, H. Ding and C. R. Triggle: Endothelium-derived relaxing factors: a focus on endothelium-derived hyperpolarizing factor(s). *Can J Physiol Pharmacol*, 79(6), 443-70 (2001)

32. N. T. Luu, M. Rahman, P. C. Stone, G. E. Rainger and G. B. Nash: Responses of endothelial cells from different vessels to inflammatory cytokines and shear stress: evidence for the pliability of endothelial phenotype. *J Vasc Res*, 47(5), 451-61 (2010)

33. H. Yamawaki, S. Lehoux and B. C. Berk: Chronic physiological shear stress inhibits tumor necrosis factor-induced proinflammatory responses in rabbit aorta perfused ex vivo. *Circulation*, 108(13), 1619-25 (2003)

34. H. C. Groen, F. J. Gijsen, A. van der Lugt, M. S. Ferguson, T. S. Hatsukami, C. Yuan, A. F. van der Steen and J. J. Wentzel: High shear stress influences plaque vulnerability Part of the data presented in this paper were published in Stroke 2007;38:2379-81. *Neth Heart J*, 16(7-8), 280-3 (2008)

35. Y. S. Chatzizisis, A. U. Coskun, M. Jonas, E. R. Edelman, C. L. Feldman and P. H. Stone: Role of endothelial shear stress in the natural history of coronary atherosclerosis and vascular remodeling: molecular, cellular, and vascular behavior. *J Am Coll Cardiol*, 49(25), 2379-93 (2007)

955

Endothelial dysfunction in hypertension: The role of arginase

36. J. J. Chiu, S. Usami and S. Chien: Vascular endothelial responses to altered shear stress: pathologic implications for atherosclerosis. *Ann Med*, 41(1), 19-28 (2009)

37. A. Dardik, L. Chen, J. Frattini, H. Asada, F. Aziz, F. A. Kudo and B. E. Sumpio: Differential effects of orbital and laminar shear stress on endothelial cells. *J Vasc Surg*, 41(5), 869-80 (2005)

38. R. F. Furchgott and J. V. Zawadzki: The obligatory role of endothelial cells in the relaxation of arterial smooth muscle by acetylcholine. *Nature*, 288(5789), 373-6 (1980)

39. L. J. Ignarro, R. E. Byrns, G. M. Buga and K. S. Wood: Endothelium-derived relaxing factor from pulmonary artery and vein possesses pharmacologic and chemical properties identical to those of nitric oxide radical. *Circ Res*, 61(6), 866-79 (1987)

40. L. L. Nikitenko: Vascular endothelium in cancer. *Cell Tissue Res*, 335(1), 223-40 (2009)

41. C. M. Boulanger, N. Amabile and A. Tedgui: Circulating microparticles: a potential prognostic marker for atherosclerotic vascular disease. *Hypertension*, 48(2), 180-6 (2006)

42. P. V. Katakam, M. R. Ujhelyi, M. E. Hoenig and A. W. Miller: Endothelial dysfunction precedes hypertension in diet-induced insulin resistance. *Am J Physiol*, 275(3 Pt 2), R788-92 (1998)

43. J. Kunes, S. Hojna, M. Kadlecova, Z. Dobesova, H. Rauchova, M. Vokurkova, J. Loukotova, O. Pechanova and J. Zicha: Altered balance of vasoactive systems in experimental hypertension: the role of relative NO deficiency. *Physiol Res*, 53 Suppl 1, S23-34 (2004)

44. J. Torok: Participation of nitric oxide in different models of experimental hypertension. *Physiol Res*, 57(6), 813-25 (2008)

45. R. Rossi, E. Chiurlia, A. Nuzzo, E. Cioni, G. Origliani and M. G. Modena: Flow-mediated vasodilation and the risk of developing hypertension in healthy postmenopausal women. *J Am Coll Cardiol*, 44(8), 1636-40 (2004)

46. D. Shimbo, P. Muntner, D. Mann, A. J. Viera, S. Homma, J. F. Polak, R. G. Barr, D. Herrington and S. Shea: Endothelial dysfunction and the risk of hypertension: the multi-ethnic study of atherosclerosis. *Hypertension*, 55(5), 1210-6 (2010)

47. P. L. Huang and M. C. Fishman: Genetic analysis of nitric oxide synthase isoforms: targeted mutation in mice. *J Mol Med*, 74(8), 415-21 (1996)

48. W. K. Alderton, C. E. Cooper and R. G. Knowles: Nitric oxide synthases: structure, function and inhibition. *Biochem J*, 357(Pt 3), 593-615 (2001)

49. I. N. Mungrue and D. S. Bredt: nNOS at a glance: implications for brain and brawn. *J Cell Sci*, 117(Pt 13), 2627-9 (2004)

50. F. Aktan: iNOS-mediated nitric oxide production and its regulation. *Life Sci*, 75(6), 639-53 (2004)

51. H. Li and U. Forstermann: Prevention of atherosclerosis by interference with the vascular nitric oxide system. *Curr Pharm Des*, 15(27), 3133-45 (2009)

52. P. W. Shaul: Regulation of endothelial nitric oxide synthase: location, location, location. *Annu Rev Physiol*, 64, 749-74 (2002)

53. G. Cirino, S. Fiorucci and W. C. Sessa: Endothelial nitric oxide synthase: the Cinderella of inflammation? *Trends Pharmacol Sci*, 24(2), 91-5 (2003)

54. J. J. Woodward, M. M. Chang, N. I. Martin and M. A. Marletta: The second step of the nitric oxide synthase reaction: evidence for ferric-peroxo as the active oxidant. *J Am Chem Soc*, 131(1), 297-305 (2009)

55. P. W. Shaul, E. J. Smart, L. J. Robinson, Z. German, I. S. Yuhanna, Y. Ying, R. G. Anderson and T. Michel: Acylation targets endothelial nitric-oxide synthase to plasmalemmal caveolae. *J Biol Chem*, 271(11), 6518-22 (1996)

56. F. A. Sanchez, N. B. Savalia, R. G. Duran, B. K. Lal, M. P. Boric and W. N. Duran: Functional significance of differential eNOS translocation. *Am J Physiol Heart Circ Physiol*, 291(3), H1058-64 (2006)

57. S. Gao, J. Chen, S. V. Brodsky, H. Huang, S. Adler, J. H. Lee, N. Dhadwal, L. Cohen-Gould, S. S. Gross and M. S. Goligorsky: Docking of endothelial nitric oxide synthase (eNOS) to the mitochondrial outer membrane: a pentabasic amino acid sequence in the autoinhibitory domain of eNOS targets a proteinase K-cleavable peptide on the cytoplasmic face of mitochondria. *J Biol Chem*, 279(16), 15968-74 (2004)

58. P. L. Huang, Z. Huang, H. Mashimo, K. D. Bloch, M. A. Moskowitz, J. A. Bevan and M. C. Fishman: Hypertension in mice lacking the gene for endothelial nitric oxide synthase. *Nature*, 377(6546), 239-42 (1995)

59. E. G. Shesely, N. Maeda, H. S. Kim, K. M. Desai, J. H. Krege, V. E. Laubach, P. A. Sherman, W. C. Sessa and O. Smithies: Elevated blood pressures in mice lacking endothelial nitric oxide synthase. *Proc Natl Acad Sci U S A*, 93(23), 13176-81 (1996)

60. R. Kohli, C. J. Meininger, T. E. Haynes, W. Yan, J. T. Self and G. Wu: Dietary L-arginine supplementation enhances endothelial nitric oxide synthesis in streptozotocin-induced diabetic rats. *J Nutr*, 134(3), 600-8 (2004)

956

Endothelial dysfunction in hypertension: The role of arginase

61.   L. Goret, S. Tanguy, I. Guiraud, M. Dauzat and P. Obert: Acute administration of l-arginine restores nitric oxide-mediated relaxation in isolated pulmonary arteries from pulmonary hypertensive exercise trained rats. *Eur J Pharmacol*, 581(1-2), 148-56 (2008)

62.   Z. J. Ou, W. Wei, D. D. Huang, W. Luo, D. Luo, Z. P. Wang, X. Zhang and J. S. Ou: L-arginine restores endothelial nitric oxide synthase-coupled activity and attenuates monocrotaline-induced pulmonary artery hypertension in rats. *Am J Physiol Endocrinol Metab*, 298(6), E1131-9 (2010)

63.   M. Nematbakhsh, S. Haghjooyjavanmard, F. Mahmoodi and A. R. Monajemi: The prevention of endothelial dysfunction through endothelial cell apoptosis inhibition in a hypercholesterolemic rabbit model: the effect of L-arginine supplementation. *Lipids Health Dis*, 7, 27 (2008)

64.   M. Willmot, L. Gray, C. Gibson, S. Murphy and P. M. Bath: A systematic review of nitric oxide donors and L-arginine in experimental stroke; effects on infarct size and cerebral blood flow. *Nitric Oxide*, 12(3), 141-9 (2005)

65.   F. Perticone, A. Sciacqua, R. Maio, M. Perticone, R. Maas, R. H. Boger, G. Tripepi, G. Sesti and C. Zoccali: Asymmetric dimethylarginine, L-arginine, and endothelial dysfunction in essential hypertension. *J Am Coll Cardiol*, 46(3), 518-23 (2005)

66.   M. B. Moss, T. M. Brunini, R. Soares De Moura, L. E. Novaes Malagris, N. B. Roberts, J. C. Ellory, G. E. Mann and A. C. Mendes Ribeiro: Diminished L-arginine bioavailability in hypertension. *Clin Sci (Lond)*, 107(4), 391-7 (2004)

67.   M. P. Schlaich, M. M. Parnell, B. A. Ahlers, S. Finch, T. Marshall, W. Z. Zhang and D. M. Kaye: Impaired L-arginine transport and endothelial function in hypertensive and genetically predisposed normotensive subjects. *Circulation*, 110(24), 3680-6 (2004)

68.   L. R. de Meirelles, A. C. Mendes-Ribeiro, M. A. Mendes, M. N. da Silva, J. C. Ellory, G. E. Mann and T. M. Brunini: Chronic exercise reduces platelet activation in hypertension: upregulation of the L-arginine-nitric oxide pathway. *Scand J Med Sci Sports*, 19(1), 67-74 (2009)

69.   D. Tousoulis, R. H. Boger, C. Antoniades, G. Siasos, E. Stefanadi and C. Stefanadis: Mechanisms of disease: L-arginine in coronary atherosclerosis--a clinical perspective. *Nat Clin Pract Cardiovasc Med*, 4(5), 274-83 (2007)

70.   L. Beaumier, L. Castillo, A. M. Ajami and V. R. Young: Urea cycle intermediate kinetics and nitrate excretion at normal and "therapeutic" intakes of arginine in humans. *Am J Physiol*, 269(5 Pt 1), E884-96 (1995)

71.   T. J. Merimee, D. Rabinowitz, L. Riggs, J. A. Burgess, D. L. Rimoin and V. A. McKusick: Plasma growth hormone after arginine infusion. Clinical experiences. *N Engl J Med*, 276(8), 434-9 (1967)

72.   S. M. Bode-Boger, R. H. Boger, H. Alfke, D. Heinzel, D. Tsikas, A. Creutzig, K. Alexander and J. C. Frolich: L-arginine induces nitric oxide-dependent vasodilation in patients with critical limb ischemia. A randomized, controlled study. *Circulation*, 93(1), 85-90 (1996)

73.   D. Giugliano, R. Marfella, G. Verrazzo, R. Acampora, L. Coppola, D. Cozzolino and F. D'Onofrio: The vascular effects of L-Arginine in humans. The role of endogenous insulin. *J Clin Invest*, 99(3), 433-8 (1997)

74.   R. J. MacAllister, A. L. Calver, J. Collier, C. M. Edwards, B. Herreros, S. S. Nussey and P. Vallance: Vascular and hormonal responses to arginine: provision of substrate for nitric oxide or non-specific effect? *Clin Sci (Lond)*, 89(2), 183-90 (1995)

75.   O. Tangphao, S. Chalon, H. Moreno, Jr., B. B. Hoffman and T. F. Blaschke: Pharmacokinetics of L-arginine during chronic administration to patients with hypercholesterolaemia. *Clin Sci (Lond)*, 96(2), 199-207 (1999)

76.   R. H. Boger, S. M. Bode-Boger, A. Szuba, P. S. Tsao, J. R. Chan, O. Tangphao, T. F. Blaschke and J. P. Cooke: Asymmetric dimethylarginine (ADMA): a novel risk factor for endothelial dysfunction: its role in hypercholesterolemia. *Circulation*, 98(18), 1842-7 (1998)

77.   E. Podjarny, G. Hasdan, J. Bernheim, G. Rashid, J. Green and Z. Korzets: Effect of chronic tetrahydrobiopterin supplementation on blood pressure and proteinuria in 5/6 nephrectomized rats. *Nephrol Dial Transplant*, 19(9), 2223-7 (2004)

78.   D. Fulton, J. P. Gratton, T. J. McCabe, J. Fontana, Y. Fujio, K. Walsh, T. F. Franke, A. Papapetropoulos and W. C. Sessa: Regulation of endothelium-derived nitric oxide production by the protein kinase Akt. *Nature*, 399(6736), 597-601 (1999)

79.   S. Dimmeler, I. Fleming, B. Fisslthaler, C. Hermann, R. Busse and A. M. Zeiher: Activation of nitric oxide synthase in endothelial cells by Akt-dependent phosphorylation. *Nature*, 399(6736), 601-5 (1999)

80.   M. B. Harris, H. Ju, V. J. Venema, H. Liang, R. Zou, B. J. Michell, Z. P. Chen, B. E. Kemp and R. C. Venema: Reciprocal phosphorylation and regulation of endothelial nitric-oxide synthase in response to bradykinin stimulation. *J Biol Chem*, 276(19), 16587-91 (2001)

81.   J. E. Church and D. Fulton: Differences in eNOS activity because of subcellular localization are dictated by phosphorylation state rather than the local calcium environment. *J Biol Chem*, 281(3), 1477-88 (2006)

82.   J. Yu, S. Bergaya, T. Murata, I. F. Alp, M. P. Bauer, M. I. Lin, M. Drab, T. V. Kurzchalia, R. V. Stan and W. C.

957

Endothelial dysfunction in hypertension: The role of arginase

Sessa: Direct evidence for the role of caveolin-1 and caveolae in mechanotransduction and remodeling of blood vessels. *J Clin Invest*, 116(5), 1284-91 (2006)

83. H. K. Lim, S. Ryoo, A. Benjo, K. Shuleri, V. Miriel, E. Baraban, A. Camara, K. Soucy, D. Nyhan, A. Shoukas and D. E. Berkowitz: Mitochondrial arginase II constrains endothelial NOS-3 activity. *Am J Physiol Heart Circ Physiol*, 293(6), H3317-24 (2007)

84. R. G. Allen and M. Tresini: Oxidative stress and gene regulation. *Free Radic Biol Med*, 28(3), 463-99 (2000)

85. H. Sauer, M. Wartenberg and J. Hescheler: Reactive oxygen species as intracellular messengers during cell growth and differentiation. *Cell Physiol Biochem*, 11(4), 173-86 (2001)

86. E. L. Schiffrin: Remodeling of resistance arteries in essential hypertension and effects of antihypertensive treatment. *Am J Hypertens*, 17(12 Pt 1), 1192-200 (2004)

87. S. R. Thomas, P. K. Witting and G. R. Drummond: Redox control of endothelial function and dysfunction: molecular mechanisms and therapeutic opportunities. *Antioxid Redox Signal*, 10(10), 1713-65 (2008)

88. E. C. Viel, K. Benkirane, D. Javeshghani, R. M. Touyz and E. L. Schiffrin: Xanthine oxidase and mitochondria contribute to vascular superoxide anion generation in DOCA-salt hypertensive rats. *Am J Physiol Heart Circ Physiol*, 295(1), H281-8 (2008)

89. X. Zhou, H. G. Bohlen, S. J. Miller and J. L. Unthank: NAD(P)H oxidase-derived peroxide mediates elevated basal and impaired flow-induced NO production in SHR mesenteric arteries *in vivo*. *Am J Physiol Heart Circ Physiol*, 295(3), H1008-H1016 (2008)

90. J. Bauersachs, A. Bouloumie, D. Fraccarollo, K. Hu, R. Busse and G. Ertl: Hydralazine prevents endothelial dysfunction, but not the increase in superoxide production in nitric oxide-deficient hypertension. *Eur J Pharmacol*, 362(1), 77-81 (1998)

91. J. Kunes, Z. Dobesova and J. Zicha: Altered balance of main vasopressor and vasodepressor systems in rats with genetic hypertension and hypertriglyceridaemia. *Clin Sci (Lond)*, 102(3), 269-77 (2002)

92. M. C. Houston: Nutraceuticals, vitamins, antioxidants, and minerals in the prevention and treatment of hypertension. *Prog Cardiovasc Dis*, 47(6), 396-449 (2005)

93. X. Chen, R. M. Touyz, J. B. Park and E. L. Schiffrin: Antioxidant effects of vitamins C and E are associated with altered activation of vascular NADPH oxidase and superoxide dismutase in stroke-prone SHR. *Hypertension*, 38(3 Pt 2), 606-11 (2001)

94. F. Lacy, M. T. Kailasam, D. T. O'Connor, G. W. Schmid-Schonbein and R. J. Parmer: Plasma hydrogen peroxide production in human essential hypertension: role of heredity, gender, and ethnicity. *Hypertension*, 36(5), 878-84 (2000)

95. A. Fortuno, S. Olivan, O. Beloqui, G. San Jose, M. U. Moreno, J. Diez and G. Zalba: Association of increased phagocytic NADPH oxidase-dependent superoxide production with diminished nitric oxide generation in essential hypertension. *J Hypertens*, 22(11), 2169-75 (2004)

96. T. M. Paravicini and R. M. Touyz: NADPH oxidases, reactive oxygen species, and hypertension: clinical implications and therapeutic possibilities. *Diabetes Care*, 31 Suppl 2, S170-80 (2008)

97. G. Schillaci, M. Pirro, F. Gemelli, L. Pasqualini, G. Vaudo, S. Marchesi, D. Siepi, F. Bagaglia and E. Mannarino: Increased C-reactive protein concentrations in never-treated hypertension: the role of systolic and pulse pressures. *J Hypertens*, 21(10), 1841-6 (2003)

98. C. J. Boos and G. Y. Lip: Is hypertension an inflammatory process? *Curr Pharm Des*, 12(13), 1623-35 (2006)

99. C. Savoia and E. L. Schiffrin: Inflammation in hypertension. *Curr Opin Nephrol Hypertens*, 15(2), 152-8 (2006)

100. E. S. Androulakis, D. Tousoulis, N. Papageorgiou, C. Tsioufis, I. Kallikazaros and C. Stefanadis: Essential hypertension: is there a role for inflammatory mechanisms? *Cardiol Rev*, 17(5), 216-21 (2009)

101. J. W. Knowles, R. L. Reddick, J. C. Jennette, E. G. Shesely, O. Smithies and N. Maeda: Enhanced atherosclerosis and kidney dysfunction in eNOS(-/-)Apoe(-/-) mice are ameliorated by enalapril treatment. *J Clin Invest*, 105(4), 451-8 (2000)

102. L. Mazzolai, M. A. Duchosal, M. Korber, K. Bouzourene, J. F. Aubert, H. Hao, V. Vallet, H. R. Brunner, J. Nussberger, G. Gabbiani and D. Hayoz: Endogenous angiotensin II induces atherosclerotic plaque vulnerability and elicits a Th1 response in ApoE-/- mice. *Hypertension*, 44(3), 277-82 (2004)

103. J. H. Wu, J. Hagaman, S. Kim, R. L. Reddick and N. Maeda: Aortic constriction exacerbates atherosclerosis and induces cardiac dysfunction in mice lacking apolipoprotein E. *Arterioscler Thromb Vasc Biol*, 22(3), 469-75 (2002)

104. M. Buemi, A. Allegra, C. Aloisi, F. Corica, A. Alonci, A. Ruello, G. Montalto and N. Frisina: Cold pressor test raises serum concentrations of ICAM-1, VCAM-1, and E-selectin in normotensive and hypertensive patients. *Hypertension*, 30(4), 845-7 (1997)

105. B. I. Tropea, P. Huie, J. P. Cooke, P. S. Tsao, R. K. Sibley and C. K. Zarins: Hypertension-enhanced monocyte adhesion in experimental atherosclerosis. *J Vasc Surg*, 23(4), 596-605 (1996)

958

Endothelial dysfunction in hypertension: The role of arginase

106. C. Kunsch and R. M. Medford: Oxidative stress as a regulator of gene expression in the vasculature. *Circ Res*, 85(8), 753-66 (1999)

107. J. Liu, F. Yang, X. P. Yang, M. Jankowski and P. J. Pagano: NAD(P)H oxidase mediates angiotensin II-induced vascular macrophage infiltration and medial hypertrophy. *Arterioscler Thromb Vasc Biol*, 23(5), 776-82 (2003)

108. C. Marchesi, P. Paradis and E. L. Schiffrin: Role of the renin-angiotensin system in vascular inflammation. *Trends Pharmacol Sci*, 29(7), 367-74 (2008)

109. Q. Lan, K. O. Mercurius and P. F. Davies: Stimulation of transcription factors NF kappa B and AP1 in endothelial cells subjected to shear stress. *Biochem Biophys Res Commun*, 201(2), 950-6 (1994)

110. C. A. Lemarie, B. Esposito, A. Tedgui and S. Lehoux: Pressure-induced vascular activation of nuclear factor-kappaB: role in cell survival. *Circ Res*, 93(3), 207-12 (2003)

111. S. Riou, B. Mees, B. Esposito, R. Merval, J. Vilar, D. Stengel, E. Ninio, R. van Haperen, R. de Crom, A. Tedgui and S. Lehoux: High pressure promotes monocyte adhesion to the vascular wall. *Circ Res*, 100(8), 1226-33 (2007)

112. H. Wang, J. Nawata, N. Kakudo, K. Sugimura, J. Suzuki, M. Sakuma, J. Ikeda and K. Shirato: The upregulation of ICAM-1 and P-selectin requires high blood pressure but not circulating renin-angiotensin system *in vivo*. *J Hypertens*, 22(7), 1323-32 (2004)

113. J. K. Bendall, A. C. Cave, C. Heymes, N. Gall and A. M. Shah: Pivotal role of a gp91(phox)-containing NADPH oxidase in angiotensin II-induced cardiac hypertrophy in mice. *Circulation*, 105(3), 293-6 (2002)

114. T. Bachetti, L. Comini, S. Curello, D. Bastianon, M. Palmieri, G. Bresciani, F. Callea and R. Ferrari: Co-expression and modulation of neuronal and endothelial nitric oxide synthase in human endothelial cells. *J Mol Cell Cardiol*, 37(5), 939-45 (2004)

115. X. F. Ming, C. Barandier, H. Viswambharan, B. R. Kwak, F. Mach, L. Mazzolai, D. Hayoz, J. Ruffieux, S. Rusconi, J. P. Montani and Z. Yang: Thrombin stimulates human endothelial arginase enzymatic activity via RhoA/ROCK pathway: implications for atherosclerotic endothelial dysfunction. *Circulation*, 110(24), 3708-14 (2004)

116. C. Zhang, T. W. Hein, W. Wang, M. W. Miller, T. W. Fossum, M. M. McDonald, J. D. Humphrey and L. Kuo: Upregulation of vascular arginase in hypertension decreases nitric oxide-mediated dilation of coronary arterioles. *Hypertension*, 44(6), 935-43 (2004)

117. D. E. Berkowitz, R. White, D. Li, K. M. Minhas, A. Cernetich, S. Kim, S. Burke, A. A. Shoukas, D. Nyhan, H. C. Champion and J. M. Hare: Arginase reciprocally regulates nitric oxide synthase activity and contributes to endothelial dysfunction in aging blood vessels. *Circulation*, 108(16), 2000-6 (2003)

118. W. Xu, F. T. Kaneko, S. Zheng, S. A. Comhair, A. J. Janocha, T. Goggans, F. B. Thunnissen, C. Farver, S. L. Hazen, C. Jennings, R. A. Dweik, A. C. Arroliga and S. C. Erzurum: Increased arginase II and decreased NO synthesis in endothelial cells of patients with pulmonary arterial hypertension. *FASEB J*, 18(14), 1746-8 (2004)

119. C. Demougeot, A. Prigent-Tessier, C. Marie and A. Berthelot: Arginase inhibition reduces endothelial dysfunction and blood pressure rising in spontaneously hypertensive rats. *J Hypertens*, 23(5), 971-8 (2005)

120. T. W. Hein, C. Zhang, W. Wang, C. I. Chang, N. Thengchaisri and L. Kuo: Ischemia-reperfusion selectively impairs nitric oxide-mediated dilation in coronary arterioles: counteracting role of arginase. *FASEB J*, 17(15), 2328-30 (2003)

121. R. C. Thuraisingham, N. B. Roberts, M. Wilkes, D. I. New, A. C. Mendes-Ribeiro, S. M. Dodd and M. M. Yaqoob: Altered L-arginine metabolism results in increased nitric oxide release from uraemic endothelial cells. *Clin Sci (Lond)*, 103(1), 31-41 (2002)

122. S. W. Kim, S. J. Jeong, R. Munarriz, N. N. Kim, I. Goldstein and A. M. Traish: Role of the nitric oxide-cyclic GMP pathway in regulation of vaginal blood flow. *Int J Impot Res*, 15(5), 355-61 (2003)

123. H. Masuda: Significance of nitric oxide and its modulation mechanisms by endogenous nitric oxide synthase inhibitors and arginase in the micturition disorders and erectile dysfunction. *Int J Urol*, 15(2), 128-34 (2008)

124. S. R. Kashyap, A. Lara, R. Zhang, Y. M. Park and R. A. DeFronzo: Insulin reduces plasma arginase activity in type 2 diabetic patients. *Diabetes Care*, 31(1), 134-9 (2008)

125. M. J. Romero, D. H. Platt, H. E. Tawfik, M. Labazi, A. B. El-Remessy, M. Bartoli, R. B. Caldwell and R. W. Caldwell: Diabetes-induced coronary vascular dysfunction involves increased arginase activity. *Circ Res*, 102(1), 95-102 (2008)

126. S. Ryoo, G. Gupta, A. Benjo, H. K. Lim, A. Camara, G. Sikka, J. Sohi, L. Santhanam, K. Soucy, E. Tuday, E. Baraban, M. Ilies, G. Gerstenblith, D. Nyhan, A. Shoukas, D. W. Christianson, N. J. Alp, H. C. Champion, D. Huso and D. E. Berkowitz: Endothelial arginase II: a novel target for the treatment of atherosclerosis. *Circ Res*, 102(8), 923-32 (2008)

127. F. K. Johnson, R. A. Johnson, K. J. Peyton and W. Durante: Arginase inhibition restores arteriolar endothelial function in Dahl rats with salt-induced hypertension. *Am J Physiol Regul Integr Comp Physiol*, 288(4), R1057-62 (2005)

959

Endothelial dysfunction in hypertension: The role of arginase

128. L. G. Chicoine, M. L. Paffett, T. L. Young and L. D. Nelin: Arginase inhibition increases nitric oxide production in bovine pulmonary arterial endothelial cells. *Am J Physiol Lung Cell Mol Physiol*, 287(1), L60-8 (2004)

129. T. Bagnost, L. Ma, R. F. da Silva, R. Rezakhaniha, C. Houdayer, N. Stergiopulos, C. Andre, Y. Guillaume, A. Berthelot and C. Demougeot: Cardiovascular effects of arginase inhibition in spontaneously hypertensive rats with fully developed hypertension. *Cardiovasc Res*, 87(3), 569-77 (2010)

130. L. A. Holowatz and W. L. Kenney: Up-regulation of arginase activity contributes to attenuated reflex cutaneous vasodilatation in hypertensive humans. *J Physiol*, 581(Pt 2), 863-72 (2007)

131. C. Demougeot, A. Prigent-Tessier, T. Bagnost, C. Andre, Y. Guillaume, M. Bouhaddi, C. Marie and A. Berthelot: Time course of vascular arginase expression and activity in spontaneously hypertensive rats. *Life Sci*, 80(12), 1128-34 (2007)

132. D. Sanz-Rosa, M. P. Oubina, E. Cediel, N. de Las Heras, O. Vegazo, J. Jimenez, V. Lahera and V. Cachofeiro: Effect of AT1 receptor antagonism on vascular and circulating inflammatory mediators in SHR: role of NF-kappaB/IkappaB system. *Am J Physiol Heart Circ Physiol*, 288(1), H111-5 (2005)

133. X. Gao, X. Xu, S. Belmadani, Y. Park, Z. Tang, A. M. Feldman, W. M. Chilian and C. Zhang: TNF-alpha contributes to endothelial dysfunction by upregulating arginase in ischemia/reperfusion injury. *Arterioscler Thromb Vasc Biol*, 27(6), 1269-75 (2007)

134. S. Matthiesen, D. Lindemann, M. Warnken, U. R. Juergens and K. Racke: Inhibition of NADPH oxidase by apocynin inhibits lipopolysaccharide (LPS) induced up-regulation of arginase in rat alveolar macrophages. *Eur J Pharmacol*, 579(1-3), 403-10 (2008)

135. N. S. Beckett, R. Peters, A. E. Fletcher, J. A. Staessen, L. Liu, D. Dumitrascu, V. Stoyanovsky, R. L. Antikainen, Y. Nikitin, C. Anderson, A. Belhani, F. Forette, C. Rajkumar, L. Thijs, W. Banya and C. J. Bulpitt: Treatment of hypertension in patients 80 years of age or older. *N Engl J Med*, 358(18), 1887-98 (2008)

Abbreviations: RH: resistant hypertension; HSS: high shear stress; LSS: low shear stress; OSS: oscillatory shear stress; NO: nitric oxide; ED: endothelial dysfunction; ROS: reactive oxygen species; $\cdot O_2^-$: superoxide; H_2O_2: hydrogen peroxide; $ONOO^-$: peroxynitrite; OH^-: hydroxyl radical; eNOS: endothelial nitric oxide synthase; Cav-1: caveolin-1; ICAM: intracellular adhesion molecule; VCAM: vascular cell adhesion molecule.

Key Words: Hypertension, Resistant Hypertension, Endothelial Dysfunction, Inflammation, Arginase, Reactive Oxygen Species, Nitric Oxide, Endothelial Nitric Oxide Synthase, Review

Send correspondence to: Karen L Andrews, Vascular Pharmacology, Baker IDI Heart and Diabetes Institute, PO Box 6492, St Kilda Rd Central, Victoria 8008, Australia, Tel: 61-3-8532-1294, Fax: 61-3-8532-1100, E-mail: Karen.Andrews@bakeridi.edu.au

http://www.bioscience.org/current/vol3S.htm

Appendix II: *'Arginase II inhibition prevents nitrate tolerance'*

RESEARCH PAPER

Arginase II inhibition prevents nitrate tolerance

SML Khong[1], KL Andrews[1], NN Huynh[1], K Venardos[1], A Aprico[1], DL Michell[1], M Zarei[2], KT Moe[1,3], GJ Dusting[4], DM Kaye[1] and JPF Chin-Dusting[1]

[1]*Baker IDI Heart and Diabetes Institute, Melbourne, Australia*, [2]*Department of Physiology, Faculty of Medicine, Hamadan University of Medical Sciences, Hamadan, Iran*, [3]*Research and Development Unit, National Heart Centre, Singapore, Singapore*, and [4]*Bernard O'Brien Institute of Microsurgery, Melbourne, Australia*

BACKGROUND AND PURPOSE

Nitrate tolerance, the loss of vascular responsiveness with continued use of nitrates, remains incompletely understood and is a limitation of these therapeutic agents. Vascular superoxide, generated by uncoupled endothelial NOS (eNOS), may play a role. As arginase competes with eNOS for L-arginine and may exacerbate the production of reactive oxygen species (ROS), we hypothesized that arginase inhibition might reduce nitrate tolerance.

EXPERIMENTAL APPROACH

Vasodilator responses were measured in aorta from C57Bl/6 and arginase II knockout (argII –/–) mice using myography. Uncoupling of eNOS, determined as eNOS monomer : dimer ratio, was assessed using low-temperature SDS-PAGE and ROS levels were measured using L-012 and lucigenin-enhanced chemiluminescence.

KEY RESULTS

Repeated application of glyceryl trinitrate (GTN) on aorta isolated from C57Bl/6 mice produced a 32-fold rightward shift of the concentration–response curve. However this rightward shift (or resultant tolerance) was not observed in the presence of the arginase inhibitor (s)-(2-boronethyl)-L-cysteine HCl (BEC; 100 μM) nor in aorta isolated from argII –/– mice. Similar findings were obtained after inducing nitrate tolerance *in vivo*. Repeated administration of GTN in human umbilical vein endothelial cells induced uncoupling of eNOS from its dimeric state and increased ROS levels, which were reduced with arginase inhibition and exogenous L-arginine. Aortae from GTN tolerant C57Bl/6 mice exhibited increased arginase activity and ROS production, whereas vessels from argII –/– mice did not.

CONCLUSION AND IMPLICATIONS

Arginase II removal prevents nitrate tolerance. This may be due to decreased uncoupling of eNOS and consequent ROS production.

Abbreviations

ALDH-2, aldehyde dehydrogenase 2; argII –/–, arginase II knockout; BEC, (s)-(2-boronethyl)-L-cysteine HCl; DEA/NO, diethylamine NONOate; eNOS, endothelial NOS; GTN, glyceryl trinitrate; HUVEC, human umbilical vein endothelial cell; KPSS, potassium depolarizing solution; ROS, reactive oxygen species

Introduction

Nitrate tolerance describes the loss of vessel responsiveness to the continued use of drugs, which actions mimic the endothelial endogenous vasodilator NO. It is a serious limitation in an otherwise highly useful class of drugs, collectively referred to as nitrates, in the treatment of ischaemia and angina. Although these compounds have been used for well over a century, the mechanisms underlying the phenomenon of tolerance remain incompletely understood. One of the best-studied and most widely accepted postulates involves the production of reactive oxygen species (ROS). The essential

SML Khong et al.

hypothesis is that nitrate tolerance results from an increase in vascular superoxide due to uncoupled endothelial NOS (eNOS) and increased activity of NADPH oxidase(s) (Münzel *et al.*, 1995). As well, there are studies that demonstrate abnormalities in the biotransformation and in particular, the de-nitrification of nitrates by the enzyme aldehyde dehydrogenase (ALDH-2) within the mitochondria (Sage *et al.*, 2000; Chen *et al.*, 2002). Importantly, the problem of mitochondrial de-nitrification has since been linked with increased mitochondrial free radical bioavailability during sustained nitrate therapy (Sydow *et al.*, 2004).

Pertaining to the L-arginine-NO pathway, the enzyme arginase, originally identified for its role in the hepatic urea cycle, has been found in the vasculature (see Morris, 2009). Now known to exist in at least two isoforms, arginase I and II, up-regulation of this enzyme suppresses NO synthesis in endothelial cells (Li *et al.*, 2001; Berkowitz *et al.*, 2003; Chicoine *et al.*, 2004; White *et al.*, 2006), most likely by depleting L-arginine stores in competition with eNOS. Arginase II, in particular, appears to be the predominant form in endothelial cells (Gerzanich *et al.*, 2003; Bachetti *et al.*, 2004; Ming *et al.*, 2004) and is confined to the mitochondria where it modulates eNOS activity by regulating intracellular L-arginine levels (Lim *et al.*, 2007). Here, we have hypothesized that, as arginase contributes to the depletion of intracellular L-arginine stores and to downstream events including eNOS uncoupling and ROS production, inhibition of arginase, and specifically of arginase II, might prevent nitrate tolerance.

Methods

Animals and treatments
All animal care and experimental procedures were approved by the AMREP Institutional Animal Ethics Committee (Approval #E/0665/2008/B), which adheres to the US National Institutes of Health Guide for the Care and Use of Laboratory Animals. Arginase II knockout (argII –/–) mice on a C57BL/6 (WT) background [a gift from Prof William O'Brien (Shi *et al.*, 2001)] and WT mice were studied at 10 and 15 weeks old. Animals were housed under standard laboratory conditions and food and water was available *ad libitum*. Mice were killed by asphyxiation in 80% CO_2 and 20% O_2.

Vascular reactivity studies
Thoracic aorta from 10 and 15 week old WT and argII –/– mice were isolated and placed in ice-cold carbogenated (95% O_2; 5% CO_2) Krebs solution (composition in mM: NaCl 119, KCl 4.7, $MgSO_4$ 1.17, $NaHCO_3$ 25, KH_2PO_4 1.18, $CaCl_2$ 2.5 and glucose 11 and EDTA 0.03); and subsequently cleared of connective tissue and mounted in Mulvany myographs bubbled with carbogen (95% O_2 and 5% CO_2.) at 37°C (model 610 M, JP Trading), for isometric tension recording as described previously (Kimura *et al.*, 2003). Vessel viability was assessed by maximally contracting the aorta with a K+-depolarizing solution (KPSS; composition in mM: KCl 123, $MgSO_4$ 1.17, KH_2PO_4 1.18, $CaCl_2$ 2.5 and glucose 11 and EDTA 0.03).

In vitro *tolerance model*
Full concentration response curves to glyceryl trinitrate (GTN; 0.1 nM–10 μM) were obtained in vessels preconstricted

to approximately 50% of the KPSS maximum with phenylephrine (0.1–1 μM). A repeat curve was constructed 30 min later in the absence (control) or presence of the arginase inhibitor (s)-(2-boronethyl-L-cysteine) HCl (BEC; 100 μM). Repeat responses to GTN were also obtained in vessels from argII –/– mice. Relaxation responses are expressed as a percentage reversal of the PE precontraction. Individual relaxation curves were fitted to a sigmoidal logistic equation (GraphPad Prism 5.0, GraphPad Software, Inc., San Diego, CA, USA) and the corresponding negative log EC_{50} values (pEC_{50}) calculated.

In vivo *tolerance model*
In vivo tolerance to GTN was induced by subcutaneous injections of GTN (20 mg·kg^{-1}) three times a day (0700, 1500, 2300 h) for 3 days (total 60 mg·kg^{-1}·day^{-1}) (Wang *et al.*, 2002). Control animals received vehicle (5% glucose) diluted in saline over the same period. At the end of the 72 h period on day 4 mice were killed and the thoracic aorta removed for further study. These studies were performed in both WT and argII –/– mice.

Determination of ROS
In endothelial cells. Human umbilical vein endothelial cells (HUVECs) were seeded onto white 96 well plates and grown to confluence. 24 h prior to experimentation, cells were serum-starved and either treated with GTN (0.5 mM; diluted in Krebs-HEPES; composition in mM: NaCl 111.2, D-glucose 11.1, $NaHCO_3$ 25.0, HEPES 10.1, MgSO$_4$·7H20 1.3, $CaCl_2$ 2.5, KH_2PO_4 1.2 and KCl 4.8) or vehicle (Krebs-HEPES) as previously described (Dikalov *et al.*, 1998). Cells were washed and serum-free media was replaced with pre-warmed Krebs-HEPES and treated with GTN (0.5 mM) for a total of 60 min. 30 min from the start of GTN treatment, cells were treated with L-arginine (100 μM), BEC (100 μM) or tempol (1 mM) for a total of 30 min, after which L-012 (100 μM) was added to each well and fluorescence measurements obtained at 37°C (excitation 485 nm, emission 520 nm) and expressed as relative light units per second (RLU·s^{-1}) as previously described (Sohn *et al.*, 1999; Daiber *et al.*, 2004).

In intact vessels. Superoxide formation in thoracic aortae from 15 week-old argII –/– and WT mice was measured using NADPH (100 μM)-driven lucigenin-enhanced chemiluminescence (5 μM) using a luminometer as previously described (Ritchie *et al.*, 2007). Aortae were incubated at 37°C in the dark for 1 h either in the absence (control) or presence of GTN (100 μM). For vessels obtained from animals receiving GTN (or vehicle) *in vivo* only baseline superoxide formation was obtained. Background luminescence was subtracted from an average of 10 readings and each measurement was expressed as counts per mg per second (counts·mg^{-1}·s^{-1}).

eNOS monomer/dimer detection by Western blot analysis
Aortic lysates were obtained by homogenization in a glass homogenizer in cold lysis buffer while HUVECs were sonicated in ice-cold lysis buffer, and both were centrifuged at 13 000× *g* for 10 min to remove unlysed cells and cell fragments. Protein content was measured by the Lowry method

(Lowry *et al.*, 1951). 20 µg of protein per sample were dissolved in 0.225 M Tris-HCl (pH 6.8), 50% glycerol, 5% SDS, and 0.05% bromophenol blue; and loaded onto a 6% gel. Low-temperature SDS-PAGE (LT-PAGE) was performed using previously reported methods (Klatt *et al.*, 1996; Yang *et al.*, 2009). Gels and buffers were kept at 4°C prior to and during electrophoresis. Following LT-PAGE, gels were transferred on to a PVDF membrane at 4°C and the blots were probed as routine Western blots for eNOS monomer and dimer (both BD Transduction, Franklin Lakes, NJ, USA; 1:10 000) and β-tubulin (as the loading control; Bio-Rad, Hercules, CA, USA, 1:1000). Densitometry was used to quantitate the bands and the dimer/monomer calculated.

L-arginine uptake

Cellular ^{3}H-L-arginine uptake was measured as previously described (Chin-Dusting *et al.*, 2003; Parnell *et al.*, 2004; Zhang *et al.*, 2006). Briefly, EA.hy926 cells were plated in 24-well, flat bottom, tissue culture plates and grown to ≈ 90% confluence at 37 °C in 5% CO_2. Two hours prior to treatment, cells were deprived of L-arginine by washing cells twice and replacing media with pre-warmed (37 °C) phosphate buffered saline (PBS, composition in mM; $CaCl_2$ 0.901, $MgCl_2$ 0.495, KCl 2.97, KH_2PO_4 1.47, NaCl 137.93, Na_2HPO_4 8.10). Cells were treated with GTN (100nM) for 30 min after an initial 30 min pre-treatment period with L-arginine (200µM), L-NOHA (10µM), BEC (100µM) or an untreated control. Treatments remained present throughout the remainder of the experiment. Cells were then incubated in 500µl of total uptake solution containing ^{3}H-L-arginine (100nM) and unlabelled L-arginine (100 nM) prepared in Locke's buffer (composition in mM: NaCl 154, KCl 5.6, $CaCl_2$ 1, $MgCl_2$ 1, HEPES 10, $NaHCO_3$ 3.6 and D-glucose 5.6) or non-specific uptake solution which comprised of the total uptake solution with additional unlabelled L-arginine (10mM) for 20 min at 37 °C in triplicate. At the conclusion of the incubation period, each culture well was washed twice with ice cold PBS and then lysed in the endothelial cell lysis buffer [0.2% sodium dodecyl sulphate (SDS) and 0.2 N NaOH] at room temperature for 1 hour. Counts were then obtained by liquid scintillation spectroscopy, whereby 400 µl of the lysate was added to 4 ml of scintillation fluid and ^{3}H was counted for 2 min on the Liquid Scintillation analyzer. The remaining 100µl, containing ^{3}H-L-arginine, was used for determination of protein content. Specific arginine uptake over 20 min was calculated by subtracting averaged counts of the non-specific from total uptake mixture. All counts (specific ^{3}H-L-arginine uptake) were normalised as dpm per mg total cellular proteins and normalised to the control (% control dpm.mg^{-1} of protein).

Determination of arginase activity in intact vessels

Arginase activity was determined in aortic lysates following GTN (or vehicle) treatment *in vivo* using a previously reported method (Corraliza *et al.*, 1994). Briefly, aortas were homogenized in ice-cold lysis buffer and the homogenate (100 µL) added to Tris-HCl (50 mM, pH 7.5, 150 µL), which contained 10 mM $MnCl_2$. To activate arginase, samples were heated to 56°C for 10 min, L-arginine (100 µL of 0.5 mM) was added and samples incubated at 37°C for a further

60 min. To halt the reaction, a mixture of acids (H_2SO_4 (17.8M): H_3PO_4 (14.6M): H_2O = 1:3:7; 800 µL) was added. α-Isonitrosopropriophenone (50 µL, 9% in absolute ethanol, w/v) was added and the samples heated at 100°C for 45 min followed by 10 min in darkness at room temperature. The colorimetric determination of urea was achieved spectrophotometrically at an absorbance of 550 nm. Urea production was calculated from a standard curve and expressed as pmol of urea per minute per milligram of tissue.

Statistical analysis

Results are expressed as mean ± SEM. A two way ANOVA with Bonferroni *post hoc* analysis was used to compare all vascular reactivity responses. Where more than two groups were studied, a one-way ANOVA with Bonferroni's multiple comparisons *post hoc* analysis in GraphPad Prism (v 5.0) was used, where $P < 0.05$ was considered statistically significant. For experiments using mice, n refers to the number of animals and for cell experiments n refers to independent experiments.

Materials

The following suppliers were used: [^{3}H]L-arginine from Perkin Elmer Life Sciences, Boston, USA; BEC and L-NOHA from Calbiochem, USA; Tempol and α-isonitrosopropriophenone from Sigma, USA; L-012 from Wako Pure Chemicals, USA.

Results

Arginase inhibition or arginase II deletion abolishes in vitro nitrate tolerance

A significant rightward shift was evident in the repeated concentration response curve to GTN (Figure 1A pEC_{50} 1st vs. 2nd curve: 7.5 ± 0.1 vs. 6.0 ± 0.4 $n = 8$, $P < 0.01$; these values represent about 30-fold difference in molar concentrations), establishing that tolerance had occurred. Non-specific arginase inhibition by BEC prevented tolerance (Figure 1B). GTN ($pEC_{50} = 7.7 ± 0.1$ M, Rmax = 91 ± 3% relaxation) caused concentration-dependent relaxation responses in aorta from argII –/– mice (Figure 1C) comparable with that observed on aorta from WT mice (Figure 1A). However, unlike aorta from WT mice, subsequent administration of GTN after a 30 min washout period did not result in the development of tolerance ($n = 5$–8; $P > 0.05$).

In vivo tolerance to GTN was not evident in aorta from argII –/– mice

Aorta isolated from WT mice treated with GTN *in vivo* showed a significant rightward shift compared to vehicle-treated animals confirming that nitrate tolerance had occurred (Figure 2A: vehicle vs. GTN treated: $pEC_{50} = 8.2 ± 0.3$ vs. 7.4 ± 0.3, $n = 9$–11; $P < 0.01$). Tolerance however was not apparent in aorta from argII –/– mice (Figure 2B: vehicle vs. GTN treated: $pEC_{50} = 7.9 ± 0.2$ vs. 7.4 ± 0.2 M, $n = 7$–9, $P > 0.05$), nor was there any significant differences in GTN-induced relaxation between vehicle-treated WT and argII –/– mice ($P > 0.05$). Cross-tolerance between nitrates is well established (see Münzel *et al.*, 2005a). Diethylamine NONOate (DEA/NO), like GTN, is an exogenous NO donor. In aorta from WT mice
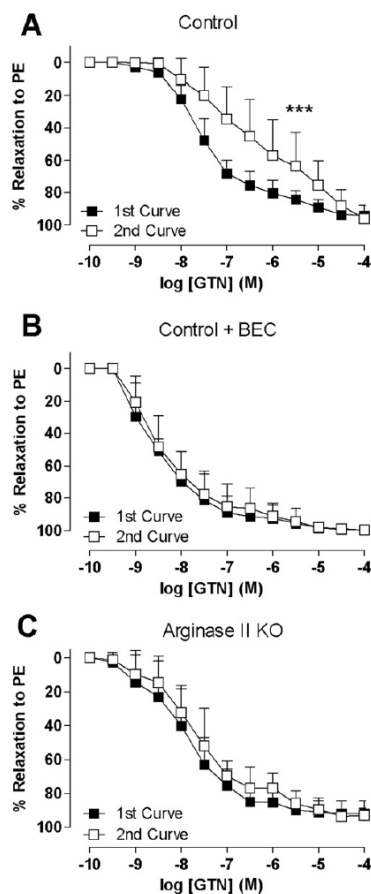
BJP SML Khong et al.

Figure 1

Two concentration response curves were obtained 30 min apart in aorta from WT mice (A, B) and argII –/– mice (C) to GTN either (A, C) alone or in the presence of (B) BEC (100 μM). The aorta was pre-contracted by phenylephrine (PE). Data are presented as mean ± SEM; n = 5–8 mice. ***P < 0.001, significant difference between curves; two-way ANOVA with Bonferroni *post hoc* analysis.

(Figure 2C), a significant shift to the right to DEA/NO is seen in GTN tolerant vessels (pEC$_{50}$ = 7.8 ± 0.1, n = 5) compared with vehicle-treated non-tolerant vessels (pEC$_{50}$ = 8.2 ± 0.1, n = 8; P < 0.001). Cross-tolerance was not observed in aorta from argII –/– mice (Figure 2D; vehicle vs. GTN treated: pEC$_{50}$ = 8.1 ± 0.1 vs. 8.4 ± 0.2, n = 6–8; P > 0.05).

GTN induces ROS production in HUVECs and in intact vessels

Recent findings show that GTN can induce both increased ROS production and eNOS uncoupling (Sage *et al*., 2000;

Chen *et al*., 2002; Münzel *et al*., 2005b), particularly when the endothelium is in an L-arginine-deprived state (Abou-Mohamed *et al*., 2000). The effect of GTN tolerance on acute ROS generation was investigated in the presence of exogenously added L-arginine, superoxide scavenging with tempol and arginase inhibiton with BEC. Addition of L-arginine and BEC by themselves did not significantly affect basal ROS production (Figure 3A), compared with control. Addition of the antioxidant tempol did reduce basal ROS levels (Figure 3A). GTN significantly increased ROS generation (Figure 3B), which was significantly reduced by pre-treatment of the endothelial cells with BEC, L-arginine and tempol (Figure 3C).

ROS production in aorta from WT mice treated with GTN *in vivo* was significantly higher compared with vessels from vehicle-treated WT mice (Figure 3D). ROS production in aorta from argII –/– mice treated with GTN *in vivo* was not different from vehicle-treated argII –/– mice nor WT mice (Figure 3E).

GTN induces eNOS uncoupling

HUVECs, tolerant to GTN, showed a significant increase in eNOS present in the monomeric compared with dimeric state when compared with control non-tolerant cells (Figure 4A). Similarly, WT aorta tolerant to GTN show a trend towards an increase in monomer : dimer ratio (Figure 4C), whereas GTN and vehicle-treated argII –/– mice were not different (Figure 4C), but significantly lower than that observed in WT aorta tolerant to GTN.

L-arginine uptake is increased with L-arginine and reduced by arginase inhibition

Using radioactively labelled L-arginine, exogenous L-arginine significantly increased L-arginine uptake into endothelial cells (Figure 4B) whereas BEC significantly reduced basal L-arginine uptake.

Arginase activity is increased in WT aorta after *in vivo* induction of nitrate tolerance

The arginase activity of aorta from tolerant WT mice was increased by 330% above that observed in non-tolerant WT aorta (Figure 5A). In contrast there was no significant increase in arginase activity in GTN-treated aorta from argII –/– mice compared with vehicle-treated aorta from the same strain (Figure 5B), nor was there any significant differences in aortic arginase activity between vehicle-treated WT and argII –/– mice (Figure 5). BEC (100 μM) significantly reduced arginase activity in WT vehicle-treated aorta (control = 7095 ± 1208 vs. +BEC = 0 ± 0 pmol·mg^{-1}·min^{-1}; n = 3–6; P < 0.05) suggesting specificity for arginase.

Discussion and conclusions

Our major new finding is that inhibition of arginase, and specifically of arginase II, prevents nitrate tolerance. We showed that increased arginase activity together with excessive ROS production and uncoupled eNOS was induced by repeated exposure to nitrates and propose that arginase inhibition prevents nitrate tolerance by reducing ROS production
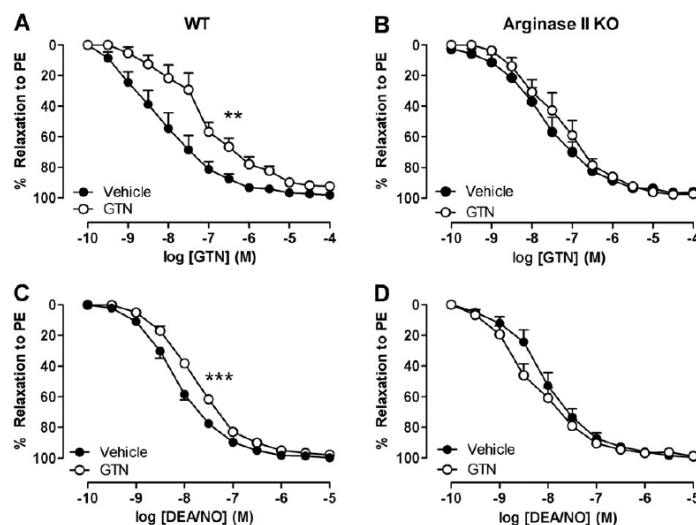
Arginase II inhibition prevents nitrate tolerance **BJP**

Figure 2

Concentration response curves to (A and B) GTN and (C and D) DEA/NO obtained from aorta from (A and C) WT and (B and D) argII –/– mice after *in vivo* treatment with GTN or vehicle for 3 days. The aorta was pre-contracted by phenylephrine (PE). Data are presented as mean ± SEM, n = 5–8. **$P < 0.01$ ***$P < 0.001$, significant difference between curves; two-way ANOVA with Bonferroni *post hoc* analysis.

possibly through increasing intracellular L-arginine (Chicoine *et al.*, 2004; White *et al.*, 2006). Our finding is consistent with previous work and is the first to show that arginase inhibition has the beneficial, functional result of preventing nitrate tolerance.

In the current study we demonstrated a reduction in responsiveness upon repeated application of the organic nitrate GTN in an *in vitro* model of tolerance. Importantly, pharmacological blockade of arginase using the non-specific arginase inhibitor BEC prevented tolerance to GTN. In endothelial cells, inhibition of arginase stimulates NO production (Chicoine *et al.*, 2004), whereas overexpression of arginase I or II decreases intracellular L-arginine concentrations and suppresses NO synthesis (Li *et al.*, 2001). It has recently been proposed that arginase II is confined to the mitochondria where it regulates eNOS and therefore NO bioavailability (Lim *et al.*, 2007). Although eNOS is predominantly localized to the caveolae, microdomains located in the plasma membrane, internalization of eNOS from the caveolae to the cytoplasm is now thought to regulate its function. Indeed, in HUVECs eNOS has been reported to be co-localized with the mitochondria (Gao *et al.*, 2004), rendering a direct modulation of eNOS via arginase likely. Of interest in this context, and particularly as the arginase II isoform is located in the mitochondria, is that mitochondrial de-nitrification abnormalities and increased mitochondrial ROS have previously been identified in previous studies of nitrate tolerance (Chen *et al.*, 2002; Sydow *et al.*, 2004) suggesting potential advantages of arginase inhibition, related to cellular compartmentalization.

As such we examined whether arginase II inhibition may be particularly effective in preventing nitrate tolerance. As there are no selective inhibitors of the different enzyme isoforms, we also studied nitrate tolerance in argII –/– mice. Nitrate tolerance was not observed in aortae from argII –/– mice. We thus speculate that inhibition of arginase II may be particularly effective in the prevention of nitrate tolerance, due at least in part to its subcellular localization concurrently enabling mitochondrial eNOS stabilization as well as preventing mitochondrial ROS production, which has a key role in the de-nitrification process.

To confirm the key finding that elimination of arginase II prevents nitrate tolerance and as *in vitro* induction of tolerance has been reported to lack certain physiological features such as the activation of the renin-angiotensin system, these studies were repeated *in vivo*. Using the commonly reported model of inducing tolerance by repeated *in vivo* application of GTN (Wang *et al.*, 2002) we observed a shift to the right of the concentration response curve to GTN of similar magnitude to that reported in mice previously (Wang *et al.*, 2002). Further, we confirmed that elimination of arginase II not only prevented tolerance to GTN but also to DEA/NO indicating that cross-tolerance, the phenomenon of tolerance to other nitrovasodilators, did not develop in the absence of arginase.

Under conditions of reduced L-arginine or co-factors such as tetrahydrobiopterin, eNOS is 'uncoupled' from its dimeric state and, rather than producing NO, the superoxide anion •O_2^- is formed (Vasquez-Vivar *et al.*, 1998; Ozaki *et al.*, 2002; Münzel *et al.*, 2005b). Increased eNOS expression and uncoupling of eNOS have been reported to contribute to nitrate
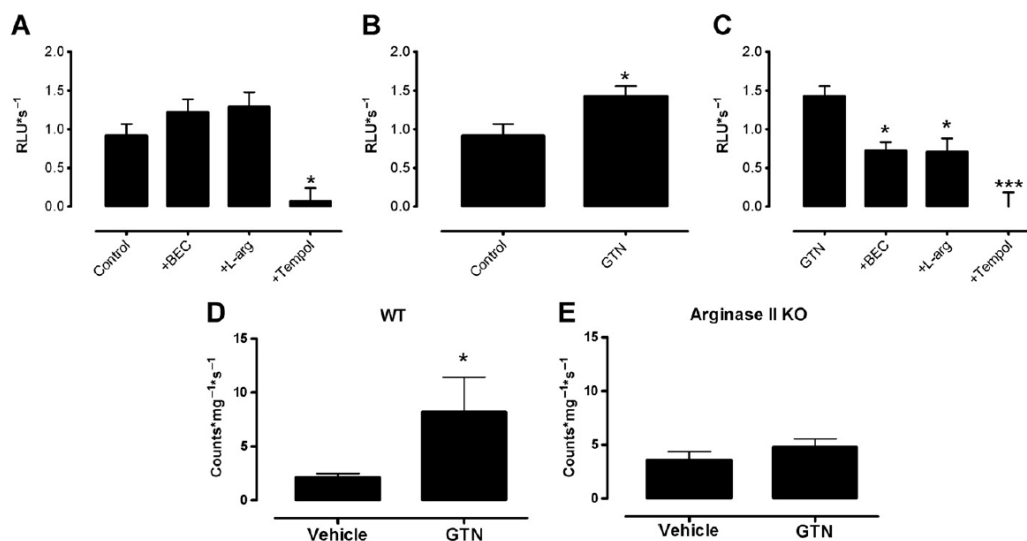
Figure 3

Basal levels of superoxide production were measured in HUVECs using a L-012-enhanced chemiluminescence assay receiving either (A) no treatment (control) or pretreatment with the arginase inhibitor BEC (100 μM), L-arginine (L-arg, 100 μM) or tempol (1 mM) or (B) no treatment or the NO donor, GTN (0.5 mM) or (C) GTN in the presence of either L-arginine, BEC or tempol. Superoxide levels were measured using a lucigenin-enhanced chemiluminescence assay in aorta from (D) WT and (E) argII –/– mice after *in vivo* treatment with GTN or vehicle for 3 days. Data are presented as mean ± SEM, n = 5–10. Data analysis used either (A, C) one-way ANOVA with Bonferroni's *post hoc* analysis or (B, D, E) Student's *t*-test. *P < 0.05, ***P < 0.001, significantly different from (A, B, D) control or (C) from GTN alone.
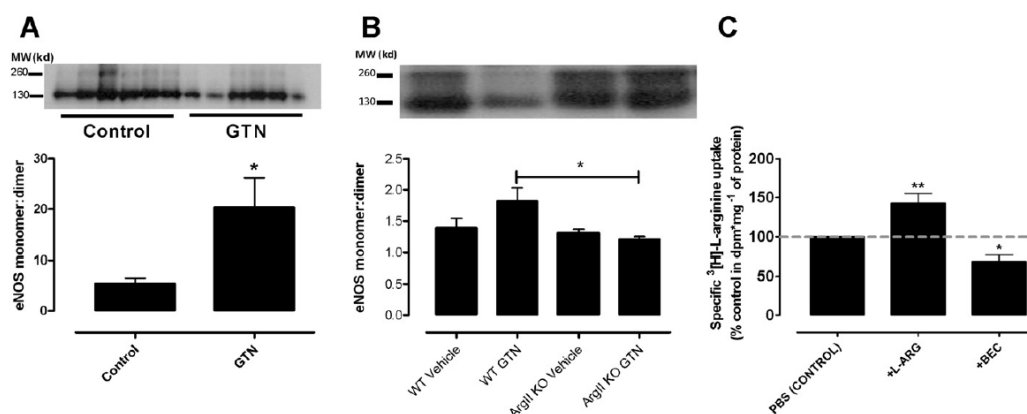
Figure 4

Ratios of eNOS dimer: monomer in tolerant and non-tolerant HUVECS (A) and aorta (B) was assessed by Western blotting and the densitometric ratio of eNOS monomer and dimer expression were normalized to β-tubulin expression. Data are presented as mean ± SEM, n = 3–6. *P < 0.05, significantly different from control; Student's *t*-test. (C) Basal levels of L-arginine uptake were measured in EA.hy926 cells receiving either no treatment (control) or pre-treatment with L-arginine (L-arg, 200 μM) or the arginase inhibitor, BEC (100 μM). Data are presented as % control uptake (mean ± SEM; n = 5–6 experiments, each performed in triplicate). *P < 0.05; **P < 0.01, significantly different from control; one-way ANOVA with Bonferroni's *post hoc* analysis.
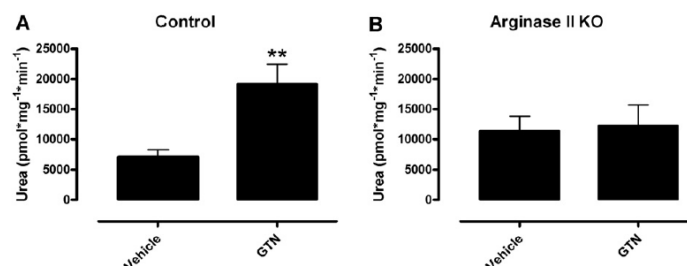
Arginase II inhibition prevents nitrate tolerance

BJP

Figure 5

Arginase activity levels were measured in aorta of (A) WT and (B) argII –/– mice after *in vivo* treatment with GTN or vehicle for 3 days. Data are presented as mean ± SEM, n = 5–7. **P < 0.01, significantly different from vehicle; Student's *t*-test.

tolerance in several studies (Abou-Mohamed *et al.*, 2000; Kaesemeyer *et al.*, 2000; Münzel *et al.*, 2000; Gori *et al.*, 2001a,b) and although inhibition of eNOS has been shown to decrease ROS (Münzel *et al.*, 2000), a definitive role is still somewhat controversial. As our findings were consistent with the hypothesis (Caramori *et al.*, 1998; Gori *et al.*, 2001b) that GTN uncouples NOS causing an increase in ROS production and that arginase activity appears to further contribute to the phenomenon, the monomer : dimer ratio of eNOS and ROS production were determined in the setting of tolerance. Similar to previous reports (Kaesemeyer *et al.*, 2000; Schmidt *et al.*, 2010), we also showed that GTN uncoupled eNOS and increased ROS production in cultured endothelial cells and in aortae made tolerant *in vivo*. In addition, this increase in ROS was prevented by treatment with the arginase inhibitor BEC and L-arginine supplementation. ROS was increased in vessels from WT mice treated with repeated doses of GTN over 3 days but was not increased in vessels from arg II –/– mice, consistent with studies by others showing a reduction in GTN tolerance in the presence of an antioxidant (Münzel *et al.*, 2000; Abou-Mohamed *et al.* 2004). It has been shown that *in vitro* and *in vivo* tolerances to GTN have different underlying mechanisms, where only *in vivo* tolerant aorta display increased production of superoxide (Münzel *et al.*, 1999). In the current paper, the concentration of GTN used in the *in vitro* cell experiments, although similar to those previously reported by Dikalov *et al.* 1998, were higher than those used in the vascular reactivity studies. Similarly incubation periods differed under the two conditions. Although providing some mechanistic insight, direct comparison between these studies thus need to be viewed with some caution.

In our study, exogenous L-arginine supplementation increased cellular L-arginine uptake. This is as expected as one of the main factors in the regulation of L-arginine transport is intracellular substrate availability. In addition BEC reduced L-arginine uptake in endothelial cells. Although BEC can be postulated to increase intracellular L-arginine levels, whether this increase was sufficient to saturate NOS activity is not known. An alternative postulate might be that BEC has direct interaction with cationic amino acid transporters as has been reported for NOS inhibitors (Bogle *et al.*, 1992).

Finally, the arginase activity in WT and argII –/– mice treated with GTN for 3 days was investigated. The aorta from GTN tolerant mice had significantly increased arginase activity. However, arginase activity in argII –/– mice (presumably due to arginase I) was not increased in aortic homogenates from mice treated with GTN, providing further evidence that arginase II was the isoform involved in tolerance to GTN. Increased arginase activity has been reported in many vascular pathologies involving endothelial dysfunction including atherosclerosis, hypertension, diabetes and ageing (Berkowitz *et al.*, 2003; Johnson *et al.*, 2005; Romero *et al.*, 2008; Ryoo *et al.*, 2008). Further, inhibition of arginase has been shown to be highly beneficial in treating *in vitro* endothelial dysfunction (Huynh *et al.*, 2009) and can also restore NOS coupling and reduce the production of ROS from uncoupled eNOS (Ryoo *et al.*, 2008; Kim *et al.*, 2009; Zhang *et al.*, 2009). Increased mitochondrial and NADPH oxidase produced ROS have been consistently reported in tolerant vessels (Münzel *et al.*, 1995; Sydow *et al.*, 2004; Szöcs *et al.*, 2007) and this is also true in disease states where there is increased arginase activity (Romero *et al.*, 2008; Ryoo *et al.*, 2008). Indeed, ROS can mediate the induction of arginase in the vasculature after only 1 h of treatment (Thengchaisri *et al.*, 2006) and reduce L-arginine levels (Gao *et al.*, 2007) suggesting that arginase may be an early target of increased ROS. However, NO has also been shown to activate arginase by the nitrosylation of Cys^{303}, stabilizing the arginase trimer and increasing its activity (Santhanam *et al.*, 2007) and subsequently leading to a decrease in L-arginine, the uncoupling of eNOS and increased ROS production. From the current studies, it is not possible to explain exactly how arginase activity is increased in tolerant vessels, although such an increase is clearly demonstrable.

In summary, we confirm the hypothesis that nitrate tolerance is at least in part due to increased ROS production. It is likely that this occurs due to increased arginase activity limiting cellular L-arginine and causing an uncoupling of eNOS. We show for the first time that arginase, and more specifically arginase II, can influence nitrate tolerance and that inhibition of this enzyme increases L-arginine levels, diminishes ROS production and ameliorates tolerance. As such we suggest that arginase inhibition should be investigated for possible prevention of nitrate tolerance in man.

BJP SML Khong et al.

Acknowledgements

Conflict of interest

None declared.

References

Abou-Mohamed G, Kaesemeyer WH, Caldwell RB, Caldwell RW (2000). Role of L-arginine in the vascular actions and development of tolerance to nitroglycerin. Br J Pharmacol 130: 211–218.

Abou-Mohamed G, Johnson JA, Jin L, El-Remessy AD, Do K, Kaesemeyer WH et al. (2004). Roles of superoxide, peroxynitrite, and protein kinase C in the development of tolerance to nitroglycerin. J Pharmacol Exp Ther 308: 289–299.

Bachetti T, Comini L, Francolini G, Bastianon D, Valetti B, Cadei M et al. (2004). Arginase pathway in human endothelial cells in pathophysiological conditions. J Mol Cell Cardiol 37: 515–523.

Berkowitz DE, White R, Li D, Minhas KM, Cernetich A, Kim S et al. (2003). Arginase reciprocally regulates nitric oxide synthase activity and contributes to endothelial dysfunction in aging blood vessels. Circulation 108: 2000–2006.

Bogle RG, Moncada S, Pearson JD, Mann GE (1992). Identification of inhibitors of nitric oxide synthase that do not interact with the endothelial cell L-arginine transporter. Br J Pharmacol 105: 768–770.

Caramori PR, Adelman AG, Azevedo ER, Newton GE, Parker AB, Parker JD (1998). Therapy with nitroglycerin increases coronary vasoconstriction in response to acetylcholine. J Am Coll Cardiol 32: 1969–1974.

Chen Z, Zhang J, Stamler JS (2002). Identification of the enzymatic mechanism of nitroglycerin bioactivation. Proc Natl Acad Sci USA 99: 8306–8311.

Chicoine LG, Paffett ML, Young TL, Nelin LD (2004). Arginase inhibition increases nitric oxide production in bovine pulmonary arterial endothelial cells. Am J Physiol Lung Cell Mol Physiol 287: L60–L68.

Chin-Dusting JP, Ahlers BA, Kaye DM, Kelly JJ, Whitworth JA (2003). L-arginine transport in humans with cortisol-induced hypertension. Hypertension 41: 1336–1340.

Corraliza IM, Campo ML, Soler G, Modolell M (1994). Determination of arginase activity in macrophages: a micromethod. J Immunol Methods 174: 231–235.

Daiber A, Oelze M, August M, Wendt M, Sydow K, Wieboldt H et al. (2004). Detection of superoxide and peroxynitrite in model systems and mitochondria by the luminol analogue L-012. Free Radic Res 38: 259–269.

Dikalov S, Fink B, Skatchkov M, Stalleicken D, Bassenge E (1998). Formation of reactive oxygen species by pentaerithrityltetranitrate and glyceryl trinitrate *in vitro* and development of nitrate tolerance. J Pharmacol Exp Ther 286: 938–944.

Gao S, Chen J, Brodsky SV, Huang H, Adler S, Lee JH et al. (2004). Docking of endothelial nitric oxide synthase (eNOS) to the mitochondrial outer membrane: a pentabasic amino acid sequence in the autoinhibitory domain of eNOS targets a proteinase K-cleavable peptide on the cytoplasmic face of mitochondria. J Biol Chem 279: 15968–15974.

Gao X, Xu X, Belmadani S, Park Y, Tang Z, Feldman AM et al. (2007). TNF-alpha contributes to endothelial dysfunction by upregulating arginase in ischemia/reperfusion injury. Arterioscler Thromb Vasc Biol 27: 1269–1275.

Gerzanich V, Ivanov A, Ivanova S, Yang JB, Zhou H, Dong Y et al. (2003). Alternative splicing of cGMP-dependent protein kinase I in angiotensin-hypertension: novel mechanism for nitrate tolerance in vascular smooth muscle. Circ Res 93: 805–812.

Gori T, Burstein JM, Ahmed S, Miner SE, Al-Hesayen A, Kelly S et al. (2001a). Folic acid prevents nitroglycerin-induced nitric oxide synthase dysfunction and nitrate tolerance: a human in vivo study. Circulation 104: 1119–1123.

Gori T, Mak SS, Kelly S, Parker JD (2001b). Evidence supporting abnormalities in nitric oxide synthase function induced by nitroglycerin in humans. J Am Coll Cardiol 38: 1096–1101.

Huynh NN, Harris EE, Chin-Dusting JFP, Andrews KL (2009). The vascular effects of different arginase inhibitors in rat isolated aorta and mesenteric arteries. Br J Pharmacol 156: 84–93.

Johnson FK, Johnson RA, Peyton KJ, Durante W (2005). Arginase inhibition restores arteriolar endothelial function in Dahl rats with salt-induced hypertension. Am J Physiol Regul Integr Comp Physiol 288: R1057–R1062.

Kaesemeyer WH, Ogonowski AA, Jin L, Caldwell RB, Caldwell RW (2000). Endothelial nitric oxide synthase is a site of superoxide synthesis in endothelial cells treated with glyceryl trinitrate. Br J Pharmacol 131: 1019–1023.

Kim JH, Bugaj LJ, Oh YJ, Bivalacqua TJ, Ryoo S, Soucy KG et al. (2009). Arginase inhibition restores NOS coupling and reverses endothelial dysfunction and vascular stiffness in old rats. J Appl Physiol 107: 1249–1257.

Kimura M, Sudhir K, Jones M, Simpson E, Jefferis AM, Chin-Dusting JP (2003). Impaired acetylcholine-induced release of nitric oxide in the aorta of male aromatase-knockout mice: regulation of nitric oxide production by endogenous sex hormones in males. Circ Res 93: 1267–1271.

Klatt P, Schmidt K, Werner ER, Mayer B (1996). Determination of nitric oxide synthase cofactors: heme, FAD, FMN, and tetrahydrobiopterin. Methods Enzymol 268: 358–365.

Li H, Meininger CJ, Hawker JR, Jr, Haynes TE, Kepka-Lenhart D, Mistry SK et al. (2001). Regulatory role of arginase I and II in nitric oxide, polyamine, and proline syntheses in endothelial cells. Am J Physiol Endocrinol Metab 280: E75–E82.

Lim HK, Lim HK, Ryoo S, Benjo A, Shuleri K, Miriel V et al. (2007). Mitochondrial arginase II constrains endothelial NOS-3 activity. Am J Physiol Heart Circ Physiol 293: H3317–H3324.

Lowry OH, Rosebrough NJ, Farr AL, Randall RJ (1951). Protein measurement with the Folin phenol reagent. J Biol Chem 193: 265–275.

Arginase II inhibition prevents nitrate tolerance

Ming X-F, Barandier C, Viswambharan H, Kwak BR, Mach F, Mazzolai L *et al.* (2004). Thrombin stimulates human endothelial arginase enzymatic activity via RhoA/ROCK pathway: implications for atherosclerotic endothelial dysfunction. Circulation 110: 3708–3714.

Morris SM, Jr (2009). Recent advances in arginine metabolism: roles and regulation of the arginases. Br J Pharmacol 157: 922–930.

Münzel T, Sayegh H, Freeman BA, Tarpey MM, Harrison DG (1995). Evidence for enhanced vascular superoxide anion production in nitrate tolerance. A novel mechanism underlying tolerance and cross-tolerance. J Clin Invest 95: 187–194.

Münzel T, Hink U, Yigit H, Macharzina R, Harrison DG, Mulsch A (1999). Role of superoxide dismutase in in vivo and in vitro nitrate tolerance. Br J Pharmacol 127: 1224–1230.

Münzel T, Li H, Mollnau H, Hink U, Matheis E, Hartmann M *et al.* (2000). Effects of long-term nitroglycerin treatment on endothelial nitric oxide synthase (NOS III) gene expression, NOS III-mediated superoxide production, and vascular NO bioavailability. Circ Res 86: E7–E12.

Münzel T, Daiber A, Mülsch A (2005a). Explaining the phenomenon of nitrate tolerance. Circ Res 97: 618–628.

Münzel T, Daiber A, Ullrich V, Mulsch A (2005b). Vascular consequences of endothelial nitric oxide synthase uncoupling for the activity and expression of the soluble guanylyl cyclase and the cGMP-dependent protein kinase. Arterioscler Thromb Vasc Biol 25: 1551–1557.

Ozaki M, Kawashima S, Yamashita T, Hirase T, Namiki M, Inoue N *et al.* (2002). Overexpression of endothelial nitric oxide synthase accelerates atherosclerotic lesion formation in apoE-deficient mice. J Clin Invest 110: 331–340.

Parnell MM, Chin-Dusting JP, Starr J, Kaye DM (2004). In vivo and in vitro evidence for ACh-stimulated L-arginine uptake. Am J Physiol Heart Circ Physiol 287: H395–H400.

Ritchie RH, Quinn JM, Cao AH, Drummond GR, Kaye DM, Favaloro JM *et al.* (2007). The antioxidant tempol inhibits cardiac hypertrophy in the insulin-resistant GLUT4-deficient mouse in vivo. J Mol Cell Cardiol 42: 1119–1128.

Romero MJ, Platt DH, Tawfik HE, Labazi M, El-Remessy AB, Bartoli M *et al.* (2008). Diabetes-induced coronary vascular dysfunction involves increased arginase activity. Circ Res 102: 95–102.

Ryoo S, Gupta G, Benjo A, Lim HK, Camara A, Sikka G *et al.* (2008). Endothelial arginase II: a novel target for the treatment of atherosclerosis. Circ Res 102: 923–932.

Sage PR, de la Lande IS, Stafford I, Bennett CL, Phillipov G, Stubberfield J *et al.* (2000). Nitroglycerin tolerance in human vessels: evidence for impaired nitroglycerin bioconversion. Circulation 102: 2810–2815.

Santhanam L, Lim HK, Lim HK, Miriel V, Brown T, Patel M *et al.* (2007). Inducible NO synthase dependent S-nitrosylation and activation of arginase1 contribute to age-related endothelial dysfunction. Circ Res 101: 692–702.

Schmidt K, Rehn M, Stessel H, Wolkart G, Mayer B (2010). Evidence against tetrahydrobiopterin depletion of vascular tissue exposed to nitric oxide/superoxide or nitroglycerin. Free Radic Biol Med 48: 145–152.

Shi O, Morris SM, Jr, Zoghbi H, Porter CW, O'Brien WE (2001). Generation of a mouse model for arginase II deficiency by targeted disruption of the arginase II gene. Mol Cell Biol 21: 811–813.

Sohn HY, Gloe T, Keller M, Schoenafinger K, Pohl U (1999). Sensitive superoxide detection in vascular cells by the new chemiluminescence dye L-012. J Vasc Res 36: 456–464.

Sydow K, Daiber A, Oelze M, Chen Z, August M, Wendt M *et al.* (2004). Central role of mitochondrial aldehyde dehydrogenase and reactive oxygen species in nitroglycerin tolerance and cross-tolerance. J Clin Invest 113: 482–489.

Szöcs K, Lassègue B, Wenzel P, Wendt M, Daiber A, Oelze M *et al.* (2007). Increased superoxide production in nitrate tolerance is associated with NAD(P)H oxidase and aldehyde dehydrogenase 2 downregulation. J Mol Cell Cardiol 42: 1111–1118.

Thengchaisri N, Hein TW, Wang W, Xu X, Li Z, Fossum TW *et al.* (2006). Upregulation of arginase by H2O2 impairs endothelium-dependent nitric oxide-mediated dilation of coronary arterioles. Arterioscler Thromb Vasc Biol 26: 2035–2042.

Vasquez-Vivar J, Kalyanaraman B, Martasek P, Hogg N, Masters BS, Karoui H *et al.* (1998). Superoxide generation by endothelial nitric oxide synthase: the influence of cofactors. Proc Natl Acad Sci USA 95: 9220–9225.

Wang EQ, Lee W-I, Fung H-L (2002). Lack of critical involvement of endothelial nitric oxide synthase in vascular nitrate tolerance in mice. Br J Pharmacol 135: 299–302.

White AR, Ryoo S, Li D, Champion HC, Steppan J, Wang D *et al.* (2006). Knockdown of arginase I restores NO signaling in the vasculature of old rats. Hypertension 47: 245–251.

Yang Y-M, Huang A, Kaley G, Sun D (2009). eNOS uncoupling and endothelial dysfunction in aged vessels. Am J Physiol Heart Circ Physiol 297: H1829–H1836.

Zhang DX, Mendoza SA, Bubolz AH, Mizuno A, Ge ZD, Li R *et al.* (2009). Transient receptor potential vanilloid type 4-deficient mice exhibit impaired endothelium-dependent relaxation induced by acetylcholine *in vitro* and *in vivo*. Hypertension 53: 532–538.

Zhang WZ, Venardos K, Chin-Dusting J, Kaye DM (2006). Adverse effects of cigarette smoke on NO bioavailability: role of arginine metabolism and oxidative stress. Hypertension 48: 278–285.

Appendix III: '*Increased carotid intima-media thickness and reduced distensibility in human class III obesity: independent and* differential influe*nces of adiposity and blood pressure on the vasculature'*

Increased Carotid Intima-Media Thickness and Reduced Distensibility in Human Class III Obesity: Independent and Differential Influences of Adiposity and Blood Pressure on the Vasculature

Xiao L. Moore[1], Danielle Michell[1], Sabrina Lee[1], Michael R. Skilton[2], Rajesh Nair[1,4], John B. Dixon[1,3], Anthony M. Dart[1,4*], Jaye Chin-Dusting[1]

1 Baker IDI Heart and Diabetes Institute, Melbourne, Victoria, Australia, 2 The Boden Institute of Obesity, Nutrition, Exercise & Eating Disorders, The University of Sydney, Camperdown, New South Wales, Australia, 3 Obesity Research Unit, Department of General Practise, Monash University, Clayton, Victoria, Australia, 4 Alfred Heart Centre, Alfred Hospital, Prahran, Victoria, Australia

Abstract

Carotid intima-media-thickness (cIMT) and carotid distensibility (distensibility), structural and functional properties of carotid arteries respectively, are early markers, as well as strong predictors of cardiovascular disease (CVD). The characteristic of these two parameters in individuals with BMI>40.0 kg/m^2 (Class III obesity), however, are largely unknown. The present study was designed to document cIMT and distensibility in this population and to relate these to other factors with established association with CVD in obesity. The study included 96 subjects (65 with BMI>40.0 kg/m^2 and 31, age- and gender-matched, with BMI of 18.5 to 30.0 kg/m^2). cIMT and distensibility were measured by non-invasive high resolution ultrasonography, circulatory CD133$^+$/KDR$^+$ angiogenic cells and endothelial microparticles (EMP) by flow cytometry, and plasma levels of adipokines, growth factors and cytokines by Luminex immunoassay kits. The study results demonstrated increased cIMT (0.62±0.11 mm *vs.* 0.54±0.08 mm, *P = 0.0002*) and reduced distensibility (22.52±10.79 10^{-3}kpa^{-1} *vs.* 29.91±12.37 10^{-3}kpa^{-1}, *P<0.05*) in individuals with BMI>40.0 kg/m^2. Both cIMT and distensibility were significantly associated with traditional CVD risk factors, adiposity/adipokines and inflammatory markers but had no association with circulating angiogenic cells. We also demonstrated, for the first time, elevated plasma EMP levels in individuals with BMI>40.0 kg/m^2. In conclusion, cIMT is increased and distensibility reduced in Class III obesity with the changes predominantly related to conventional CVD risk factors present in this condition, demonstrating that both cIMT and distensibility remain as CVD markers in Class III obesity.

Introduction

Carotid intima-media-thickness (cIMT) and carotid distensibility (distensibility) represent structural and functional properties of carotid arteries respectively. Both increased cIMT, a noninvasive measure of subclinical atherosclerosis, and reduced distensibility, an indicator of regional artery stiffness, are independent predictors of future cardiovascular events [1,2]. Importantly, a combined assessment of the two allows for a better analysis of the individual atherosclerotic burden and improved prediction of aortic atherosclerosis [3].

Increased cIMT or decreased distensibility has been linked to hypertension [4], diabetes mellitus [5] and obesity [6–10], determinant risk factors for cardiovascular disease (CVD) [11–14]. The occurrence of these three co-morbidities is linked with chronic low-grade inflammation. Furthermore insulin resistance present in obesity is believed to be a principal contributor to this link. The inter-relation between adipogenesis, inflammation, insulin resistance, hypertension and diabetes mellitus remains a current focus of obesity research. Nevertheless higher CVD incidences are evident in hypertensive and/or diabetic obese compared to non-obese counterparts. The prevalence of obesity is rising at an alarming rate worldwide. Moreover the prevalence of Class III obesity, defined as BMI≥40.0 kg/m^2, is increasing at an even steeper rate [15,16]. cIMT and distensibility in Class III obesity, however, are largely undocumented with only two papers providing both cIMT and distensibility data in people with BMI≥40.0 kg/m^2 [17,18]. Similarly, little information is available in Class III obesity on novel biomarkers of CVD, such as circulatory angiogenic cells [19] or endothelial microparticles [20].

The main objective of this study was therefore to document cIMT and distensibility in Class III obese subjects compared with a non-obese cohort, and to examine and compare traditional CVD risk factors (CVRF) and novel CVD biomarkers between the two populations. We hypothesized that cIMT and distensibility remain useful as CVD markers in the severely obese population despite technical difficulties that may be encountered and verified this by determining the association of cIMT and distensibility with other established CVRF in Class III obesity.

Materials and Methods

Ethics Statement

The study protocol was approved by the institutional ethics committee of Alfred Healthcare (#158/06), and informed written consent was obtained from each participant.

Study Population and Design

A total of 96 subjects (31 non-obese controls: BMI 18.5 to 30.0 kg/m^2 and 65 class III obesity: BMI>40.0 kg/m^2) were included in the study. Class III obesity subjects were recruited via the Obesity Research Groups at Monash University while the age- and gender-matched non obese were from the Baker IDI BioBank database. Exclusion criteria were known coronary artery disease, cardiac failure, vascular brain disease, peripheral obstructive artery disease, significant renal or hepatic dysfunction and pregnancy. Subjects with current or past history of multiple myeloma, blood dyscrasia or any form of leukemia or lymphoma were also excluded.

All individuals underwent a physical examination and had their medical histories recorded. In brief, participants were measured for height, weight, waist and hip circumferences and blood pressure. 30 ml of peripheral blood was drawn for routine blood tests following a 12 hr fast and also analyzed for levels of plasma adipokines, growth factors and cytokines, circulating angiogenic cells (CD133$^+$/KDR$^+$ PBMCs & Hill-CFU) and endothelial microparticles (EMP). Routine blood tests were performed by the Alfred Pathology Department including a full blood count, hsCRP, glucose and a lipid profile (HDL, LDL, total cholesterol and triglycerides). cIMT and distensibility were examined using non-invasive high resolution ultrasonography.

The measurement of cIMT and distensibility were compared between the two groups. The associations of cIMT or distensibility with traditional CVRF (age, gender, BP, glucose and lipids etc) and adiposity/adipokines (BMI, waist:hip, adiponectin and leptin) were examined, as were their respective associations with inflammatory markers and circulating angiogenic cells. Plasma levels of EMP were measured in randomly selected subpopulations including both males and females (Class III obese = 15 and non-obese = 16) to determine vascular inflammation and integrity.

Carotid Imaging and Measurement

The left and right common carotid arteries proximal to the carotid bifurcation were imaged through non-invasive high resolution ultrasonography using a Philips iE33 ultrasound system (Philips, Bothell, WA, USA) with a 11–3 MHz linear array transducer while the subject was at rest in a supine position. Briefly, the carotid arteries were imaged in longitudinal sections, 0–2 cm proximal to the carotid artery bifurcation, focusing on the far wall of the vessel. Two 10-second loops were captured for each of the left and right arteries and stored for offline analysis. cIMT was defined as the distance between the intima-lumen interface and the media-adventitia interface, and measured at end diastole (as determined from the simultaneous electrocardiogram record-

ings) over a 10 mm long portion of the vessel wall between 0–1 cm proximal to the carotid bulb. Diastolic and systolic diameters, for distensibility calculation, were determined as the smallest and largest diameter values during a cardiac cycle. An average of three measurements from consecutive cardiac cycles from each of the left and the right carotid artery was made, and the average of the left and right arteries was used for the final analysis. All measurements were conducted independently using an automatic edge detection system (Philips QLAB version 7.0) by two observers blinded to all participant information.

Carotid distensibility was calculated as $(2\Delta d/ds)/\Delta P$ in $10^{-3}\cdot kPa^{-1}$, where Δd is carotid internal diameter change between systole and diastole, ds is carotid systolic diameter and ΔP is pulse pressure [21].

Determination of Plasma Adipokines and Cytokines

Plasma samples were collected and stored at $-80°C$ until use. Plasma levels of adiponectin, leptin, IL-10 and SDF-1 were measured using Luminex immunoassay kits (Millipore, USA) as per manufacturer's instruction. Briefly, the appropriate adipokines or cytokine standards, plasma samples (25 μL), and fluorescent conjugated, antibody-immobilized beads were added to wells of a pre-wet filtered plate and then incubated in dark overnight at 4°C. The following day, the plate was washed twice with wash buffer and then incubated with secondary detection antibody for 1 hr, followed by subsequent incubation with streptavidin-PE for 30 min. After the plate was washed twice again with wash buffer, it was run on the Luminex system (BioRad) with the addition of sheath fluid. Concentrations of different analytes in the plasma samples were determined by using respective standard curves generated in the assays.

Measurement of Circulating Angiogenic Cells

Enumeration of peripheral blood CD133$^+$/KDR$^+$ PBMCs by flow cytometry. Peripheral blood mononuclear cells (PBMCs), isolated from fresh venous blood by ficoll-gradient centrifugation, were used to quantitate the number of CD133$^+$/KDR$^+$ PBMCs by flow cytometry. In brief, 100 μl of PBMCs (1.5×10^7/ml) was incubated with Fc-γ receptor blocking agent followed by 30 min incubation on ice with antibodies against human CD133 (PE-conjugated, Miltenyi Biotec, Germany) and VEGFR-2 (KDR) (APC-conjugated, R&D Systems, USA). PE- and APC-conjugated mouse IgG from the same manufacturers served as isotype controls. Following incubation, cells were washed with PBS and then fixed in 1% paraformaldehyde. Flow cytometry acquisition was performed on BD FACSCalibur^{TM} using appropriate settings excluding debris and platelets as shown in Figure 1-A1 & Figure 1-B1. 10^6 events per sample were collected within the R1 monocyte gates. Cells positive for both CD133 and KDR (upper right quadrants of the FL2-FL4 plots as shown in Figure 1-A2 & Figure 1-B2) were characterized as angiogenic cells. Results were expressed as percentage of CD133$^+$KDR$^+$PBMCs/PBMCs. Analysis was carried out by a blinded randomized approach in regard to patient profiles using the FlowJo software (Tree Star Inc, USA).

Hill-CFU assay. The ability to clonally expand and generate colonies in an endothelial-specific medium is considered a key functional feature of angiogenic cells. The Hill-CFU assay was performed using the commercially available kit, EndoCult^{TM} liquid medium Kit (Stem cells Technologies, USA) and used as per the manufacturer's instructions. In brief, 5×10^6 ficoll-isolated PMNCs were resuspended with 2 ml EndoCult medium and plated in a well of fibronectin-coated 6-well plates (BD Biosciences, USA), which were incubated for two days at 37°C, 5% CO$_2$ with
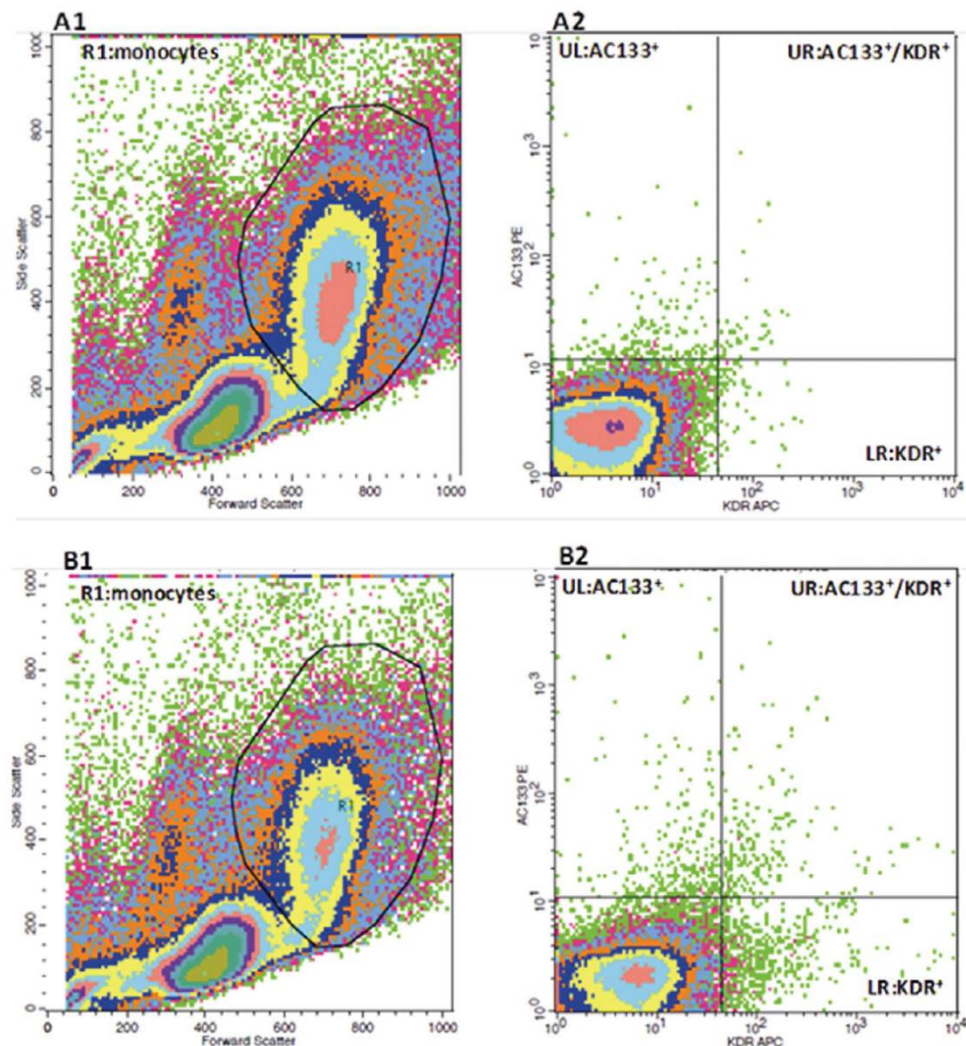
Figure 1. Illustration of FACS gating analysis of angiogenic cells (AC133⁺/KDR⁺PBMCs). Representative flow cytometric density plots demonstrating the gating protocol used to identify angiogenic cells: **A)** PBMCs stained with PE-conjugated and APC-conjugated mouse IgG (isotype controls) for non-specific fluorescent signals; **B)** PBMCs stained with antibodies against human CD133 (AC133) (PE-conjugated) and VEGFR-2 (KDR) (APC-conjugated) for AC133⁺/KDR⁺PBMCs; **A1, B1)** FSC-SSC density dot plots of Ficoll-isolated PBMCs and R1 was gated for monocytes; **A2, B2)** FL2 (PE)-FL4 (APC) density dot plots of R1-gated monocytes. Angiogenic cells = cells in B2 upper-right quadrant – cells in A2 upper-right quadrant.
doi:10.1371/journal.pone.0053972.g001

≥95% humidity. After two days the non-adherent cells were harvested, counted and plated as at a density of 1×10^6 cells per well onto a 24-well fibronectin-coated plate, which was then incubated at 37°C for another 3 days. Hill-CFUs, characterized by a central cellular cluster surrounded by emerging spindle-shaped cells were counted at day 5 in 24-well plates in a minimum of 3 wells per subject and the average count was recorded. Results were expressed as number of colony per well.

cIMT and Distensibility in Human Class III Obesity
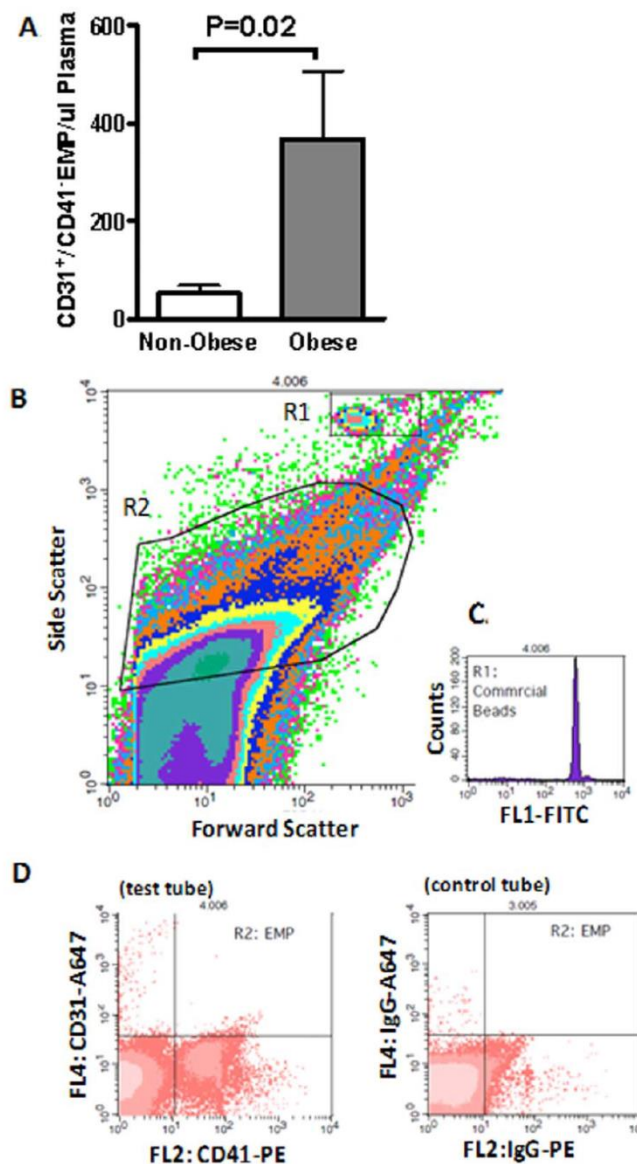
Figure 2. Elevated levels of circulating CD31$^+$/CD41$^-$ EMP in obesity. A) Quantification of circulating EMP levels in plasma. Data presented as mean±SEM. **B)** Representative flow cytometric density plots demonstrating the gating protocol used to identify EMP (R2) and bead populations (R1); **C)** Representative flow cytometric histogram of commercial beads; **D)** Representative flow cytometric dot plots demonstrating EMP population with a negative staining of CD41-PE but positive staining of CD31-Alexa 647 and its corresponding staining of isotype-controls.
doi:10.1371/journal.pone.0053972.g002

Isolation and Identification of Circulating EMPs

EMPs are defined as CD31$^+$/CD41$^-$ particles sized between 0.1–1 μm in platelet-depleted plasma. They were determined by the analysis for the expression of surface antigens by flow cytometry. In brief, 500 μl of completely thawed plasma was centrifuged at 16000 g for 5 min at 4°C to deplete platelets or any cell debris. The top 450 μl of plasma was transferred into a fresh tube, which was centrifuged again at 16000 g for 30 min at 4°C. The top 250 μl plasma was carefully removed and the remaining 200 μl vortexed and used for FACS analysis. Following a 15 min incubation with 50 μl Fc-γ receptor blocking agent (Miltenyi Biotec, Germany) at room temperature to reduce non-specific binding, half of the treated plasma was incubated with antibodies against human CD31 (Alexa647-conjugated, BD Biosciences, USA) and CD41 (PE-conjugated, BD Biosciences, USA). The other half was incubated with Alexa647- and PE-conjugated mouse IgG from the same manufacturer served as isotype controls. At the end of 20 min incubation, 300 μl of double filtered 1% Formaldehyde/0.2% FBS/PBS (filtered through a 0.2 and then a 0.1 μm membrane filter before use) was added for fixation and 50 μl of diluted calibration beads (BD Biosciences, USA) was added for EMP calculation and size reference. Each sample and its corresponding control were counted on BD FACSCalibur^{TM} (BD Biosciences, USA) for 5 min.

For flow cytometry counting, EMP gate (R2 as shown in Figure 2-B) was pre-defined using commercial beads sized at 0.1 and 1 μm (Sigma-Aldrich, USA). Only events included within this gate were further analysed for fluorescence signal as shown in Figure 2-D. For EMP enumeration, a formula was used based on the concentration of the added calibration beads [22], which discriminated themselves from the EMP population on the FSC-SSC cytogram (R1 as shown in Figure 2-B and Figure 2-C). All
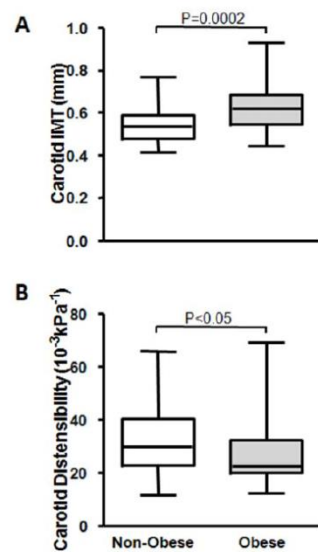

Figure 3. Increased cIMT (A) and reduced distensibility (B) in obesity. Median, minimum and maximum values of cIMT and distensibility.
doi:10.1371/journal.pone.0053972.g003

Table 1. Anthropometric, clinical and biochemical characteristics.

	Non-obese (n = 31)	Severely Obese (n = 65)	P
Age, y	48.13±11.16	46.44±8.73	0.42
Male sex, %	48	52	0.72
Smoking, %	52	52	0.97
Systolic blood pressure, mmHg	120.47±16.78	139.9±17.59	<0.0001
Diastolic blood pressure, mmHg	73.75±10.98	85.88±11.22	<0.0001
Mean arterial pressure, mmHg	88.43±11.98	103.06±11.82	<0.0001
Pulse pressure, mmHg	46.72 (42.6, 50.8)	54.03 (50.4, 57.6)	0.014
Hypertension, %	26	60	0.001
Blood Pressure-Medication, %	13	50	<0.0001
Fasting glucose, mmol/L	4.82 (4.7, 5.0)	6.33 (5.7, 7.0)	<0.0001
Type 2 Diabetes, %	7	56	<0.0001
Total cholesterol, mmol/L	5.28 (4.9, 5.7)	5.18 (5.7, 7.0)	0.70
HDL cholesterol, mmol/L	1.56 (1.4, 1.8)	1.17 (1.1, 1.2)	<0.0001
LDL cholesterol, mmol/L	3.25±0.87	3.17±0.99	0.69
Triglycerides, mmol/L	1.02 (0.9, 1.2)	1.88 (1.7, 2.1)	<0.0001
Body mass index (BMI), kg/m^2	25.51±2.61	45.46±5.47	<0.0001
Waist:Hip	0.85±0.09	0.97±0.09	<0.0001
Leptin, ng/ml	11.46 (7.2, 15.7)	41.0 (33.8, 48.1)	<0.0001
Adiponectin, μg/ml	48.90 (39.4, 58.4)	14.6 (9.8, 19.5)	<0.0001
White blood cells (WBC), 10^9/L	5.47±1.19	7.58±1.83	<0.0001
hsCRP, mg/L	1.19 (0.8, 1.5)	6.41 (5.6, 7.2)	<0.0001
Interleukin-10 (IL-10), pg/ml	30.45 (13.7, 47.2)	6.7 (4.1, 9.3)	0.007
CD133$^+$KDR$^+$ PBMC, %	0.34 (0.32, 0.35)	0.34 (0.32, 0.36)	0.91
Hill-colony forming units	4.06 (1.7, 6.4)	11.7 (7.0, 16.4)	0.005
SDF-1, pg/ml	2929.83±2387.46	1492.31±554.09	<0.0001

Data are expressed as means± SD (non-transformed data) or geometric means (95% CI) (transformed data). HDL indicates high-density lipoprotein; LDL, low-density lipoprotein; hsCRP, high-sensitivity C-reactive protein; PBMC, peripheral blood mononuclear cells; SDF-1, stromal cell-derived factor-1.
doi:10.1371/journal.pone.0053972.t001

Table 2. Bivariate correlation between BMI, Waist:Hip, SBP, cIMT and CD with other covariates.

	BMI		Waist/Hip		SBP		cIMT		CD	
	r	p-value	r	p-value	r	p-value	r	p-value	R	p-value
Age	−0.080	0.48	−0.056	0.60	0.084	0.43	**0.291**	**0.005**	**−0.323**	**0.002**
Gender	0.123	0.28	**0.654**	**<0.0001**	0.143	0.17	0.065	0.54	−0.115	0.29
Smoking	0.062	0.59	0.193	0.09	0.114	0.32	0.128	0.27	−0.127	0.28
SBP	**0.587**	**<0.0001**	**0.409**	**<0.0001**	–	–	**0.323**	**0.002**	**−0.643**	**<0.0001**
Hypertension	**0.397**	**<0.0001**	**0.332**	**0.001**	**0.593**	**<0.0001**	**0.246**	**0.020**	**−0.383**	**<0.0001**
BP-Med	**0.359**	**0.001**	**0.406**	**0.024**	**0.254**	**0.024**	0.213	0.06	**−0.256**	**0.029**
Type 2 Diabetes	**0.434**	**<0.0001**	**0.372**	**0.001**	**0.385**	**<0.0001**	**0.307**	**0.005**	**−0.305**	**0.007**
Fasting glucose	**0.338**	**0.003**	**0.314**	**0.003**	**0.236**	**0.025**	**0.343**	**0.001**	**−0.267**	**0.015**
HDL cholesterol	**−0.472**	**<0.0001**	**−0.540**	**<0.0001**	−0.158	0.13	−0.143	0.18	0.026	0.81
LDL cholesterol	0.014	0.91	0.140	0.19	0.144	0.17	0.107	0.32	0.019	0.86
Triglycerides	**0.533**	**<0.0001**	**0.448**	**<0.0001**	**0.278**	**0.014**	**0.256**	**0.026**	−0.221	0.06
BMI	–	–	**0.633**	**<0.0001**	**0.580**	**<0.0001**	**0.422**	**<0.0001**	**−0.379**	**0.001**
Waist:Hip	**0.633**	**<0.0001**	–	–	**0.409**	**<0.0001**	**0.385**	**<0.0001**	**−0.289**	**0.008**
Adiponectin	**−0.601**	**<0.0001**	**−0.460**	**<0.0001**	**−0.403**	**<0.0001**	−0.181	0.12	**0.301**	**0.010**
Leptin	**0.733**	**<0.0001**	**0.301**	**0.008**	**0.383**	**0.001**	0.220	0.056	**−0.282**	**0.015**
hsCRP	**0.808**	**<0.0001**	**0.530**	**<0.0001**	**0.432**	**<0.0001**	**0.335**	**0.003**	**−0.337**	**0.004**
IL-10	**−0.467**	**<0.0001**	**−0.316**	**0.005**	**−0.265**	**0.019**	−0.168	0.15	0.079	0.51
WBC	**0.550**	**<0.0001**	**0.429**	**<0.0001**	0.216	0.051	0.170	0.13	−0.115	0.32
CD133$^+$KDR$^+$PBMC,%	−0.003	0.98	0.026	0.81	0.120	0.25	0.128	0.23	0.19	0.87
Hill-colony forming units	0.141	0.28	0.145	0.22	0.116	0.33	−0.116	0.33	0.023	0.85
SDF-1	**0.309**	**0.006**	0.110	0.34	0.198	0.08	0.126	0.28	−0.096	0.42

BP-Med indicates blood pressure related medication, SBP, systolic blood pressure.
doi:10.1371/journal.pone.0053972.t002

counting data were then processed with a blinded randomized approach using BD CellQuest Pro (BD Biosciences, USA). Results are presented as number of CD31$^+$/CD41$^-$ EMP per µl of plasma.

Statistical Analysis

Logarithmic transformations were applied if appropriate to skewed data following histogram analyses and Kolmogorov-Smirnov test. Transformed data are expressed as geometric mean (95% CI) and non-transformed data are expressed as mean ± SD. Comparisons between the non-obese and Class III obese groups were performed by two tailed Student's t-test. Bivariate correlation analysis of adiposity (BMI and waist:hip), carotid variables (cIMT and distensibility) and blood pressure (SBP) was performed to define each crude association with other variables measured. Multivariable linear regression models were then constructed with the use of important covariates concluded from correlation analysis ($P<0.1$), in a hierarchal fashion, to elucidate independent determinants of cIMT and distensibility. Model 1 was adjusted for traditional CVRF (age, SBP, BP-med, fasting glucose and triglycerides), while Model 2 for traditional CVRF and adiposity/adipokines (BMI, adiponectin and leptin), and Model 3 for traditional CVRF, adiposity/adipokines and inflammatory markers (hsCRP, IL10 and WBC). Multivariable analysis was also repeated with no BP adjustment to further assess reliability of independent association between SBP and distensibility, since distensibility is a derivative parameter related to pulse pressure. For the same purpose, multivariable analysis of distensibility was again carried out separately in non-hypertensive and hypertensive subjects. In addition, multivariable analysis of SBP was performed as well. All statistical analyses were performed with SPSS version 12.0 for Windows and a probability value $P<0.05$ was considered statistically significant.

Results

The demographic, anthropometric, clinic and laboratory characteristics of the 96 subjects included in the study are shown in Table 1. Except for age, gender and smoking history, the 31 non-obese and 65 Class III obese subjects presented as two distinctive phenotypes in respective to all parameters related to traditional CVRF, adiposity, and plasma levels of circulating adipokines as well as inflammatory markers. All traditional CVRF measured were significantly worse in the Class III obese group. The heavier atherosclerotic burden in the Class III obese subjects was demonstrated both through increased cIMT ($P = 0.0002$) and reduced distensibility ($P<0.05$) in comparison to their age- and gender-matched non-obese counterparts (Figure 3-A & Figure 3-B). Furthermore, significantly higher levels of circulating EMP ($P = 0.02$) indicated vascular inflammation and a compromised integrity of vascular endothelium in Class III obese subjects (Figure 2-A).

As expected, significantly elevated plasma leptin and suppressed adiponectin, a typical adipokine phenotype of obesity, were shown in Class III obese subjects (Table 1), as was the inflammatory profile of much higher levels of plasma hsCRP but lower IL10. Both measures of adiposity, BMI and waist:hip, closely correlated to status of metabolic syndromes (blood pressure, glucose, type 2 diabetes, HDL and triglycerides) and inflammation (Table 2).

Table 3. Multivariable linear Regression Analyses.

	cIMT		CD	
Model	β	p-value	β	p-value
SBP adjusted-Model 1				
Age	0.271	0.017	−0.351	<0.0001
SBP	0.199	0.08	−0.585	<0.0001
Model 2				
Age	0.313	0.009	−0.418	<0.0001
SBP	0.031	0.81	−0.619	<0.0001
BP-med	0.065	0.56	−0.202	0.020
BMI	0.520	0.020	−0.372	0.026
Adiponectin	0.004	0.98	0.308	0.010
Model 3				
Age	0.359	0.006	−0.421	<0.0001
SBP	−0.015	0.91	−0.592	<0.0001
BP-Med	0.042	0.72	−0.215	0.018
BMI	0.723	0.013	−0.300	0.16
Adiponectin	−0.076	0.66	0.378	0.004
No BP adjustment-Model 1				
Age	0.288	0.013	−0.424	<0.0001
Model 2				
Age	0.329	0.005	−0.536	<0.0001
BMI	0.329	0.004	−0.096	0.58
Adiponectin	0.000	0.999	0.400	0.008
Model 3				
Age	0.364	0.004	−0.568	<0.0001
BMI	0.661	0.003	−0.322	0.12
Adiponectin	−0.061	0.72	0.552	0.001

Model 1 was adjusted for traditional CVRF (age, SBP, BP-med, fasting glucose and triglycerides), while Model 2 for traditional CVRF and adiposity/adipokines (BMI, adiponectin and leptin), and Model 3 for traditional CVRF, adiposity/adipokines and inflammatory markers (hsCRP, IL10 and WBC). Results are expressed as standardized β and only factors showing significant association are listed.
doi:10.1371/journal.pone.0053972.t003

On the other hand, there was no difference in the number of circulatory angiogenic cells ($CD133^+KDR^+PBMC$) between obese and non-obese populations, despite significantly higher colony-forming capacities (Hill-CFU) in Class III obese subjects (Table 1). Plasma levels of SDF-1, a critical cytokine mobilizing angiogenic cells, were nearly doubled ($P = 0.003$) in subjects with $BMI > 40$ kg/m^2.

cIMT significantly correlated with age, BMI, waist:hip ratio, hsCRP, and status of the metabolic syndrome (Table 2). These correlations were also true for distensibility. As well, distensibility was also linked to BP-medication and plasma levels of leptin and adiponectin.

Subjects with hypertension were defined, in this study, for those who either presented with elevated blood pressure ($\geq 140/90$ mmHg) at the time of BP measurement or were taking antihypertensive medications (BP-med) or had a history of hypertension. Blood pressure was significantly elevated in Class III obese subjects, and multivariate regression analysis revealed that SBP was independently associated with BMI ($\beta = 0.879$, $P < 0.0001$) and plasma levels of adiponectin ($\beta = -0.304$, $P = 0.049$) in this cohort. Multivariate regression analysis of cIMT

and distensibility, therefore, was performed with and without BP adjustment (Table 3). The results showed that age and BMI were independently associated with cIMT regardless of BP adjustment (Table 3). In contrast, carotid distensibility was independently associated with age, BP-medication and plasma levels of adiponectin when adjusted for SBP, which was also associated with distensibility, but only with age and plasma adiponectin when not adjusted for BP. In further regression analysis for distensibility stratified by hypertensive status, age (non-hypertensive: $\beta = -0.562$, $P < 0.0001$; hypertensive: $\beta = -0.465$, $P = 0.007$) and plasma adiponectin (non-hypertensive: $\beta = 0.527$, $P = 0.001$; hypertensive: $\beta = 0.518$, $P = 0.023$) were independently associated with distensibility in non-hypertensive and hypertensive groups, in addition to SBP in the hypertensive group ($\beta = -0.465$, $P = 0.007$).

Discussion

The present study demonstrates that increased cIMT and reduced distensibility is observed in Class III obese subjects with no overt CVD conditions when compared to their age- and gender-matched non-obese counterparts. Changes in both cIMT and distensibility corresponded well with elevated traditional CVRF in this cohort. We also show that cIMT and distensibility are significantly associated with adiposity, adipokines and inflammatory markers, however, none had any connection with circulatory angiogenic cells.

Since obesity, and in particular abdominal obesity, is a major risk factor for CVD [23], tools to screen, monitor and predict CVD in this population can be very useful clinically. cIMT and distensibility, structural and functional parameters of carotid arteries, are early markers as well as strong predictors of CVD [1,2]. While previous studies have demonstrated a strong association of increased cIMT and/or reduced distensibility with obesity [6–9], documentation of these two parameters of carotid artery in individuals with BMI>40 kg/m^2 is lacking. Our finding that cIMT is increased and distensibility reduced in the Class III obese is consistent with the only other published studies that documented increased cIMT in 64 subjects with BMI of 42.3 ± 4.3 kg/m^2 [17,18] and increased cIMT and decreased distensibility in 13 obese subjects with average BMI of 40.5 ± 7 kg/m^2 [18]. In addition, we show that cIMT is positively associated with age, adiposity, blood pressure, type-2 diabetes, hyperglycemia, dyslipidemia and hsCRP, while distensibility demonstrates negative associations with these covariates. These demonstrated associations verify that cIMT and distensiblity remain as CVD markers in Class III obesity.

Obesity is highly associated with the metabolic syndrome (MS), which is closely linked to cardiovascular morbidity and mortality [24]. Two of the most widely accepted MS criteria have been respectively promulgated by the World Health Organization (WHO) and the National Cholesterol Education Program (NCEP-ATP III). The principal distinction between the two is that the NCEP-ATP III emphasizes CVD risks whereas the WHO focus on insulin resistance [25]. We used NCEP-ATP III criteria for this study. Based on the MS criteria defined by the NCEP-ATP III [25], about 86% of our Class III obese subjects had MS: dyslipidemia, hyperglycemia (diabetes), hypertension, or central obesity. This extremely high prevalence of MS was highly associated with BMI in our cohort as evidenced by the close association of BMI with various measures of MS status (Table 2). It is thus not surprising that BMI and/or plasma adiponectin was found to be independently linked to cIMT and distensibility, besides age which is a strong predictor of arterial remodeling [26,27].

Hypertension and diabetes mellitus are common in obesity, which is also evident in this study. 60% and 56% of our Class III obese subjects were, respectively, hypertensive or diabetic in comparison to 20% and 7% in the non-obese group. Indeed in our obese subjects only 14% were free of both diabetes and hypertension. As both hypertension and diabetes are important in development of CVD, it is therefore difficult to apportion relative contributions to hypertension, diabetes or obesity per se. Further, artery stiffness and blood pressure are two closely related factors and distensibility is a derivative parameter of pulse pressure. Indeed, distensibility was revealed to independently associate with SBP and BP-medication besides age and plasma adiponectin when BP was adjusted in its multivariate regression analysis. The fact that an independent link between distensibility and plasma adiponectin stands regardless of the adjustment of BP demonstrates the essential role of adiposity in development of CVD suggesting the paramount importance of weight control in prevention and reduction of CVD. Obesity is also known to be characterized by a chronic systemic inflammatory state [28]. This was reflected by elevated plasma levels of CRP in our study. Plasma levels of CRP were strongly correlated with all important measures, cIMT, distensibility, BMI/waist:hip and as well as SBP, demonstrating a crucial role of inflammation in the development of obesity and obesity associated CVD. To further directly assess vascular inflammation and integrity, plasma endothelial micro-particles (EMP) were examined and compared in randomly selected subpopulations including both genders from both groups. EMP are small membrane vesicles, 0.1–1 μm in diameter, which are released from the endothelium following endothelial cell activation or injury by a process of exocytotic budding of the plasma membrane [29] sometimes referred to as endothelial blebbing. Increased plasma EMP levels can be detected by FACS [30] and have been reported in various CVD conditions [29,31]. In patients presenting a characterized endothelial dysfunction, levels of circulating EMP are inversely correlated with the amplitude of flow-mediated dilatation, independent of age and pressure [31,32]. EMP has thus been suggested as a novel surrogate marker of endothelial injury, which precedes CVD, and hence a novel potential biomarker of CVD [20]. To our knowledge, this is the first report measuring EMPs in the Class III obese population and we show, for the first time, that circulating levels of EMP are significantly elevated in obesity.

In addition, we also examined plasma levels of angiogenic cells, an established cellular biomarker of CVD, and their associated cytokine SDF-1, a potent stimulator to mobilize angiogenic cells [33]. Decreased circulating levels of endothelial progenitor cells (EPC) have been used as an indicator of higher CVD risk [19]. We measured angiogenic cells in our study as $CD133^+/KDR^+$ peripheral blood mononuclear cells (PBMCs) by FACS. In comparison to EPC, commonly defined as $CD34^+/KDR^+$ PBMCs, $CD133^+/KDR^+$ PBMCs are earlier endothelial progenitors [34]. The role of EPC or angiogenic cells in obesity, and particularly in the Class III obese is largely unknown albeit there

have been some studies which demonstrate low circulating levels of EPC in obesity with suggestions of the potential to predict CVD prevalence in this population [35], although contrary reports have also been observed [36]. In the current study, circulating levels of angiogenic cells were unchanged. This result might relate to the difference of angiogenic cells carrying different surface markers. We suggest, however, that the difference, at least partly, is the outcome of the contradicting processes occurring with inflammation suppressing the generation and mobilization of bone marrow-derived EPC [37] and highly activated adipogenesis promoting increased release of EPC from adipose tissue [38]. The latter is supported with the finding that SDF-1, secreted by adipose stromal cells [39], was significantly increased in the obese cohort. Intriguingly, the functional capacity of angiogenic cells measured as CFU-Hill colonies was significantly increased in the Class III obese group. The finding of a recent report by Hirschi *et al.* might explain this dichotomy. It reported that CFU-Hill colonies comprise primarily of monocytes and macrophages [40], and indeed what we are observing in the current study with increased CFU-Hill may simply reflect the activated inflammatory status in Class III obesity, in line with hsCRP. Our result of no correlation between cIMT or distensibility with angiogenic cells indicates that these cells may not be a cellular biomarker of CVD in Class III obesity.

It is a limitation of this study that only BMI or waist:hip ratio, but not direct measurement of body fat or body composition, was measured to reflect adiposity. Also neither insulin levels nor insulin resistance were evaluated. Further, this is a cross-sectional study, from which no casual relationship can be further explored. A future study in a cohort of subjects with BMI>40 kg/m^2 with no overt CVD and also free of MS, *esp.* hypertension and diabetes mellitus, would be extremely useful to delineate the complexity of CVD pathophysiology in this population. Such individuals, however, are uncommon and thus difficult to identify.

In conclusion, we document in the current study that increased cIMT and reduced distensibility are present in Class III obesity. cIMT and distensibility correlate closely with traditional CVRF, adiposity and inflammatory markers, confirming the validity of these two important parameters in CVD detection in individuals with BMI>40 kg/m^2. We also demonstrate, for the first time, elevated plasma EMP levels and unchanged circulatory $CD133^+/KDR^+$ angiogenic cells in Class III obesity.

Acknowledgments

Author Contributions

Conceived and designed the experiments: XLM RN AMD JCD. Performed the experiments: DM SL XLM MRS. Analyzed the data: XLM MRS DM SL. Contributed reagents/materials/analysis tools: RN JBD AMD JCD. Wrote the paper: XLM AMD JCD.

References

1. Polak JF, Pencina MJ, Pencina KM, O'Donnell CJ, Wolf PA, et al. (2011) Carotid-wall intima-media thickness and cardiovascular events. N Engl J Med 365: 213–221.
2. Blaha MJ, Budoff MJ, Rivera JJ, Katz R, O'Leary DH, et al. (2009) Relationship of carotid distensibility and thoracic aorta calcification: multi-ethnic study of atherosclerosis. Hypertension 54: 1408–1415.
3. Harloff A, Strecker C, Reinhard M, Kollum M, Handke M, et al. (2006) Combined measurement of carotid stiffness and intima-media thickness improves prediction of complex aortic plaques in patients with ischemic stroke. Stroke 37: 2708–2712.
4. Peralta CA, Adeney KL, Shlipak MG, Jacobs D Jr, Duprez D, et al. (2010) Structural and functional vascular alterations and incident hypertension in normotensive adults: the Multi-Ethnic Study of Atherosclerosis. Am J Epidemiol 171: 63–71.
5. Tentolouris N, Liatis S, Moyssakis I, Tsapogas P, Psallas M, et al. (2003) Aortic distensibility is reduced in subjects with type 2 diabetes and cardiac autonomic neuropathy. Eur J Clin Invest 33: 1075–1083.
6. Burke GL, Bertoni AG, Shea S, Tracy R, Watson KE, et al. (2008) The impact of obesity on cardiovascular disease risk factors and subclinical vascular disease: the Multi-Ethnic Study of Atherosclerosis. Arch Intern Med 168: 928–935.

7. Tounian P, Aggoun Y, Dubern B, Varille V, Guy-Grand B, et al. (2001) Presence of increased stiffness of the common carotid artery and endothelial dysfunction in severely obese children: a prospective study. Lancet 358: 1400–1404.

8. Recio-Rodriguez JI, Gomez-Marcos MA, Patino-Alonso MC, Agudo-Conde C, Rodriguez-Sanchez E, et al. (2012) Abdominal obesity vs general obesity for identifying arterial stiffness, subclinical atherosclerosis and wave reflection in healthy, diabetics and hypertensive. BMC Cardiovasc Disord 12: 3.

9. Elkiran O, Yilmaz E, Koc M, Kamanli A, Ustundag B, et al. (2011) The association between intima media thickness, central obesity and diastolic blood pressure in obese and overweight children: A cross-sectional school-based study. Int J Cardiol [Epub ahead of print].

10. Skilton MR, Sieveking DP, Harmer JA, Franklin J, Loughnan G, et al. (2008) The effects of obesity and non-pharmacological weight loss on vascular and ventricular function and structure. Diabetes Obes Metab 10: 874–884.

11. Rosendorff C (2007) Hypertension and coronary artery disease: a summary of the American Heart Association scientific statement. J Clin Hypertens (Greenwich) 9: 790–795.

12. Laakso M (2010) Cardiovascular disease in type 2 diabetes from population to man to mechanisms: the Kelly West Award Lecture 2008. Diabetes Care 33: 442–449.

13. Loehr LR, Rosamond WD, Poole C, McNeill AM, Chang PP, et al. (2009) Association of multiple anthropometrics of overweight and obesity with incident heart failure: the Atherosclerosis Risk in Communities study. Circ Heart Fail 2: 18–24.

14. Cheriyath P, Duan Y, Qian Z, Nambiar L, Liao D (2010) Obesity, physical activity and the development of metabolic syndrome: the Atherosclerosis Risk in Communities study. Eur J Cardiovasc Prev Rehabil 17: 309–313.

15. Sturm R (2007) Increases in morbid obesity in the USA: 2000–2005. Public Health 121: 492–496.

16. Lavie CJ, Milani RV, Ventura HO (2009) Obesity and cardiovascular disease: risk factor, paradox, and impact of weight loss. J Am Coll Cardiol 53: 1925–1932.

17. Sturm W, Sandhofer A, Engl J, Laimer M, Molnar C, et al. (2009) Influence of visceral obesity and liver fat on vascular structure and function in obese subjects. Obesity (Silver Spring) 17: 1783–1788.

18. Ketel IJ, Stehouwer CD, Henry RM, Seme EH, Hompes P, et al. (2010) Greater arterial stiffness in polycystic ovary syndrome (PCOS) is an obesity–but not a PCOS-associated phenomenon. J Clin Endocrinol Metab 95: 4566–4575.

19. Sen S, McDonald SP, Coates PT, Bonder CS (2011) Endothelial progenitor cells: novel biomarker and promising cell therapy for cardiovascular disease. Clin Sci (Lond), 120: 263–283.

20. Nozaki T, Sugiyama S, Sugamura K, Ohba K, Matsuzawa Y, et al. (2010) Prognostic value of endothelial microparticles in patients with heart failure. Eur J Heart Fail 12: 1223–1228.

21. Liang YL, Teede H, Kotsopoulos D, Shiel L, Cameron JD, et al. (1998) Non-invasive measurements of arterial structure and function: repeatability, interrelationships and trial sample size. Clin Sci (Lond) 95: 669–679.

22. Montes M, Jaensson EA, Orozco AF, Lewis DE, Corry DB (2006) A general method for bead-enhanced quantitation by flow cytometry. J Immunol Methods 317: 45–55.

23. Folsom AR, Kushi LH, Anderson KE, Mink PJ, Olson JE, et al. (2000) Associations of general and abdominal obesity with multiple health outcomes in older women: the Iowa Women's Health Study. Arch Intern Med 160: 2117–2128.

24. Potenza MV, Mechanick JI (2009) The metabolic syndrome: definition, global impact, and pathophysiology. Nutr Clin Pract 24: 560–577.

25. Fonseca VA (2005) The metabolic syndrome, hyperlipidemia, and insulin resistance. Clin Cornerstone 7: 61–72.

26. Juonala M, Kahonen M, Laitinen T, Hutri-Kahonen N, Jokinen E, et al. (2008) Effect of age and sex on carotid intima-media thickness, elasticity and brachial endothelial function in healthy adults: the cardiovascular risk in Young Finns Study. Eur Heart J 29: 1198–1206.

27. Noon JP, Trischuk TC, Gaucher SA, Galante S, Scott RL (2008) The effect of age and gender on arterial stiffness in healthy Caucasian Canadians. J Clin Nurs 17: 2311–2317.

28. Clement K, Langin D (2007) Regulation of inflammation-related genes in human adipose tissue. J Intern Med 262: 422–430.

29. Chironi GN, Boulanger CM, Simon A, Dignat-George F, Freyssinet JM, et al. (2009) Endothelial microparticles in diseases. Cell Tissue Res 335: 143–151.

30. Enjeti AK, Lincz LF, Seldon M (2007) Detection and measurement of microparticles: an evolving research tool for vascular biology. Semin Thromb Hemost 33: 771–779.

31. Feng B, Chen Y, Luo Y, Chen M, Li X, et al. (2010) Circulating level of microparticles and their correlation with arterial elasticity and endothelium-dependent dilation in patients with type 2 diabetes mellitus. Atherosclerosis 208: 264–269.

32. Esposito K, Ciotola M, Schisano B, Gualdiero R, Sardelli L, et al. (2006) Endothelial microparticles correlate with endothelial dysfunction in obese women. J Clin Endocrinol Metab 91: 3676–3679.

33. De Falco E, Porcelli D, Torella AR, Straino S, Iachininoto MG, et al. (2004) SDF-1 involvement in endothelial phenotype and ischemia-induced recruitment of bone marrow progenitor cells. Blood 104: 3472–3482.

34. Rustemeyer P, Wittkowski W, Greve B, Stehling M (2007) Flow-cytometric identification, enumeration, purification, and expansion of CD133+ and VEGF-R2+ endothelial progenitor cells from peripheral blood. J Immunoassay Immunochem 28: 13–23.

35. Muller-Ehmsen J, Braun D, Schneider T, Pfister R, Worm N, et al. (2008) Decreased number of circulating progenitor cells in obesity: beneficial effects of weight reduction. Eur Heart J 29: 1560–1568.

36. Bellows CF, Zhan Y, Simmons PJ, Khalsa AS, Kolonin MG (2011) Influence of BMI on Level of Circulating Progenitor Cells. Obesity (Silver Spring) 19: 1722–1726.

37. Grisar J, Aletaha D, Steiner C W, Kapral T, Steiner S, et al. (2005) Depletion of endothelial progenitor cells in the peripheral blood of patients with rheumatoid arthritis. Circulation 111: 204–211.

38. Martinez-Estrada OM, Munoz-Santos Y, Julve J, Reina M, Vilaro S (2005) Human adipose tissue as a source of Flk-1+ cells: new method of differentiation and expansion. Cardiovasc Res 65: 328–333.

39. Zhao BC, Zhao B, Han JG, Ma HC, Wang ZJ (2010) Adipose-derived stem cells promote gastric cancer cell growth, migration and invasion through SDF-1/CXCR4 axis. Hepatogastroenterology 57: 1382–1389.

40. Hirschi KK, Ingram DA, Yoder MC (2008) Assessing identity, phenotype, and fate of endothelial progenitor cells. Arterioscler Thromb Vasc Biol 28: 1584–1595.